THE UNIVERSITY
of EDINBURGH

Identifying new shared substrates of Aurora kinases at the mitotic apparatus

Jovana Deretic

A thesis presented for the degree of Doctor of Philosophy

The University of Edinburgh

August 2017

Declaration

I declare that I composed this thesis and that the work presented is my own, except where work has formed part of jointly-authored publication. I confirm that appropriate credit has been given within the thesis where reference has been made to the work of others.

The jointly-authored work was published in Current Biology (2015) as 'Aurora A kinase contributes to a pole-based error correction pathway'. Authors of the work are Ye AA, **Deretic J**, Hoel CM, Hinman AW, Cimini D, Welburn JP and Maresca TJ. I obtained permission of other authors to present the published material in my thesis. My work from the publication is included in the Chapter 2 of the thesis: Aurora A kinase phosphorylates HEC1/Ndc80 contributing to the correction of mal-oriented chromosomes near the spindle poles.

The work presented in this thesis has not been submitted for any other degree or professional qualification.

Jovana Deretic

Acknowledgements

I would first and foremost like to thank Dr Julie Welburn for being a supportive supervisor and giving me a chance to complete an experimental part of my PhD in her lab. Throughout these four years, I learnt a multitude of experimental techniques and methods that helped me establish myself as a scientist, which would not have been possible without her.

I am very grateful to the Darwin Trust of Edinburgh for a financial support throughout my PhD. Without this organisation, I would have not been able to come to Edinburgh and spend a wonderful four years here. I am also grateful for a given opportunity to share my work on the Darwin Trust Symposiums and meet fellow colleagues.

Very special thanks to Dr Alastair Kerr for a selfless help and tremendous support with the bioinformatics and statistics. I am very grateful to Dr David Kelly for all the invaluable help with the microscopy and for being a very pleasant and funny collaborator.

Thanks to my wonderful lab mates (both past and present members of the Welburn lab) for their friendship and support in hard times. I am especially grateful to amazing Agata Głuszek-Kustusz for being there for me and spending a great deal of her free time reviewing my thesis. Thanks to Sandeep Talapatra, Sarah Young, Bethany Harker, Thibault Legal, Toni McHugh and Heather Johnston for making a PhD life so much more fun and enjoyable. I would also like to thank the members of the JP lab for their time and help with so many protocols and reagents, Maria Alba Abad Fernandez, Bethan Medina-Pritchard, Tanmay Gupta, and Frances Spiller. Thanks to good friends and colleagues for making this PhD such a valuable experience, especially Rafal Czapiewski, Andrea Rizzoto and Kim Webb. Thank you for being there for me in both good and bad times!

Thanks to my family for all their support, especially my mum and dad for their unconditional love. Tata, iako znam da više nisi tu sa nama i da nećeš ovo pročitati, želim da znaš da te volim najviše na svetu. Beskrajno ti hvala, ovo nikad ne

bih postigla bez tvoje nepokolebljive vere u mene. Znaj da ću večno stremiti ka tome da budem tako dobra i tako puna ljubavi kao što si ti uvek bio.

I am especially grateful to have Nikola Petkovic in my life. Nikola is my partner, my love, my support, my everything! Volim te!

Lay summary

New cells are generated through the process of cell division. Cell division must be highly regulated to ensure that the new cells are healthy. Aurora kinases, Aurora A and B, are crucial regulators of cell division, acting at different steps of the process. Aurora kinases modify other proteins to enable their function in cell division. Although many of Auroras target proteins have been identified, there are indications that there are still a few unknown proteins that are modified by these kinases. Identification of these targets, and the precise roles of the modifications by Auroras, are important for comprehensive understanding of cell division, and these were the aims of my research.

Both Auroras reside in different locations within the division apparatus. However, previous studies suggested that Aurora A and B always modify very similar regions within their target proteins. I hypothesised that both Auroras modify the same proteins but in different cellular locations. In my study, I showed that a known target of Aurora B is also a target of Aurora A kinase. I revealed a new and crucial role of Aurora A in cell division.

Based on the presence of the specific targeting region for Auroras and several features of cell division, I developed a tool which enabled me to search protein databases to identify new potential targets of Auroras. Using this approach, I found a previously unknown target which has a role in cell division.

In summary, I proved that Auroras share their protein targets, and the use of a shared targeting region in combination with other division features is a successful tool to identify new Aurora target proteins.

Abstract

Aurora A and B are the major kinases that control key events in mitosis, such as centrosome function, spindle assembly, chromosome segregation and cytokinesis, through phosphorylation of multiple proteins. These kinases share identical consensus target motifs, so the substrate specificity is determined by distinctive sub-cellular localization of the Auroras. Many proteins have been identified as targets of either Aurora A, or Aurora B, or both kinases by mass spectrometry studies. However, only a few of the identified phosphorylation sites in these targets have a characterized function *in vivo*. Therefore, the molecular mechanisms underlying the regulation of certain mitotic events by Aurora kinases remain unclear.

The objective of my work was to develop a tool for identifying new substrates of both Aurora kinases. More specifically, I aimed to identify the molecular targets of Aurora A at the kinetochores, and determine how Aurora A contributes to the error correction near spindle poles.

I first demonstrated that the outer kinetochore protein HEC1/Ndc80, phosphorylated by Aurora B at kinetochores, can also be phosphorylated by Aurora A close to the centrosomes (Chapter 2). My finding showed that Aurora kinases can share substrates in the cells and revealed the mechanism by which Aurora A contributes to the error-correction near spindle poles.

To identify and characterise novel substrates of Aurora kinases, I developed a bioinformatic approach in collaboration with the Centre Bioinformatician, Alastair Kerr. This bioinformatic method uses the Auroras' shared consensus motifs combined with several parameters that control the substrate specificity of Aurora kinases. I tested the phosphorylation of the chosen candidates *in vitro* using radiolabelled kinase assays. In my study, five proteins were validated - SPICE1, TTLL4, AHCTF1, CLASP2 and an uncharacterized protein KIAA1468 - as *in vitro* substrates of Aurora A and Aurora B kinases (Chapter 3).

I then focussed on the Aurora kinases-dependent regulation of spindle and centriole-associated protein, SPICE1, in cells (Chapter 4). Using either site-directed mutagenesis of SPICE1 or inhibition of Aurora kinases with small molecule inhibitors, I found that the predicted phosphorylation of the SPICE1 C terminus had the function in cells of directing the SPICE1 localization on the spindle MTs.

My results demonstrate the high accuracy of this genome-wide bioinformatics approach. By complementing mass spectrometry studies, here lies a potential for the identification of other unknown substrates, which is important for the general understanding of how Aurora kinases regulate the mitotic apparatus.

Table of Contents

List of figures

List of tables

Abbreviations

+TIP plus-end tracking protein

γ-TURC γ-tubulin ring complex

A alanine

APC anaphase promoting complex

APS ammonium persulfate

Ark Aurora-related kinase

ATP adenosine triphosphate

BME β-mercaptoethanol

Bub budding uninhibited by benzimidazole

Bub R1 budding uninhibited by benzimidazole related 1

C. elegans *Caenorhabditis elegans*

CCAN constitutive centromere associated network

CDK cyclin-dependent kinase

cDNA complementary DNA

CENP centromere associated protein

CEP120 centrosomal protein of 120 kDa

CID centromere identifier protein

CLASP cytoplasmic linker-associated protein

CLIPs cytoplasmic linker proteins

CPAP centrosomal P4.1-associated protein

CPC chromosome passenger complex

Cse4 chromosome segregation protein 4

D.melanogaster *Drosophila melanogaster*

Da dalton

Dam1 DUO1 and MPS1-interacting protein 1

DAPI 4’, 6-diamidino-2-phenylindole

DMSO dimethyl sulfoxide

DNA deoxyribonucleic acid

dNTPs deoxyribonucleotides

TACC3 transforming acidic coiled-coil-containing protein 3

EB1 end binding 1

EDTA ethylenediaminetetraacetic acid

EGTA ethylene glycol-bis(β-aminoethyl ether)-N,N,N',N'-tetraacetic acid

Eg5 Egg5

ELYS embryonic large molecule derived from yolk sac

F phenylalanine

G1/2 growth phase 1/2

GAP GTPase activating protein

GCP γ-tubulin complex protein

GDP guanine diphosphate

GEF guanine nucleotide exchange factor

GFP green fluorescent protein

GSK3 glycogen synthase kinase 3

GST glutathione S-transferase

GTP guanosine-5’-triphosphate

H hour

HAUS human Augmin proteins

HEAT Huntingtin, elongation factor 3 (EF3), protein phosphatase 2A (PP2A), and the yeast kinase TOR1

HEC1 highly expressed in cancer 1

HEPES 4-(2-hydroxyethyl)-1-piperazineethanesulfonic acid

HP1 heterochromatin protein 1

HURP hepatoma upregulated protein

I isoleucine

INCENP Inner Centromere Protein

Ipl1 increase in ploidy 1

IPTG isopropyl β-D-1-thiogalactopyranoside

K lysine

K-fibers kinetochore fibers

KMN Knl-1, Mis12 and Ndc80

KNL kinetochore null

KO knockout

L leucine

LATS2 large tumor suppressor homolog 2

LB lysogeny broth

M methionine

Mad mitotic arrest deficient

MAPs microtubule associated proteins

MCAK mitotic centromere-associated protein

Min minute

Mis12 missegregation 12

MKLP mitotic kinesin like protein

Mps1 monopolar spindle protein 1

MTOCs microtubule organizing centres

MTs microtubules

Ndc80 nuclear division cycle 80

NEB nuclear envelope breakdown

Nek2A never in mitosis A-related kinase 2

NEDD neural precursor cell expressed developmentally down-regulated

Ni-NTA nickel-nitrilotriacetic acid

Nuf2 nuclear filamentous 2

NuMa nuclear mitotic apparatus

Nup nuclear pore complex

P proline

PBS phosphate buffered saline

PCM pericentriolar material

PCR polymerase chain reaction

PEF polar ejection force

PFA paraformaldehyde

PIPES piperazine-N,N'-bis(2-ethanesulfonic acid)

PLK Polo-like kinase

PMSF phenylmethane sulfonyl fluoride

PP1 protein phosphatase 1

Rac Ras-related C3 botulinum toxin substrate 1

Ran Ras-related nuclear

MgcRacGap male germ cell Rac GTPase-activating protein

RanGAP Ran GTPase activating protein

RNAi ribonucleic acid intereference

Rod rough deal

RZZ Rod-ZW10-Zwilch complex

S serine

S phase synthesis phase

S. cerevisiae *Saccharomyces cerevisiae*

S. pombe *Schizosaccharomyces pombe*

SAC spindle assembly checkpoint

SDS-PAGE sodium dodecyl sulfate polyacrylamide gel electrophoresis

Sec second

siRNA small interfering ribonucleic acid

SKA spindle and kinetochore associated

SPB spindle pole body

SPICE1 spindle and centriole-associated protein 1

SPC spindle pole component

T threonine

TACC3 transforming acidic coiled-coil-containing protein 3

TBS tris buffered saline

TEMED tetramethylethylenediamine

TPX2 targeting protein for Xklp2

Tris base tris(hydroxymethyl)aminomethane

V valine

X.leavis *Xenopus leavis*

Xklp2 *Xenopus* kinesin-like protein 2

XMAP215 *Xenopus* microtubule assembly protein 215

ZW10 zeste white 10

1 Chapter 1: Introduction

Genetic material is transferred to new cells through the process of cell division. Mitosis is a type of cell division that occurs in somatic cells and leads to the generation of genetically identical progeny cells, while meiosis leads to the formation of gametes, which are genetically diverse from the parental cell. Distribution of genetic material, into daughter cells occurs in multiple stages including duplication of chromosomes, generation of the division apparatus, attachment of the division apparatus to chromosomes, segregation of chromosomes and exit from the division through cytokinesis. All these processes must be precisely regulated to avoid errors in chromosome distribution, which may lead to an abnormal number of chromosomes in daughter cells, called aneuploidy. In mitosis, aneuploidy is associated with the majority of tumour cancers (Lengauer et al., 1997; Beroukhim et al., 2010; Gordon et al., 2012).

Despite increasing understanding of regulation of cell division, knowledge about its key components and mechanisms is still incomplete. In this work, I studied the regulation of the division apparatus in mitosis through phosphorylation.

1.1 General mitotic division apparatus

The complex machinery of mitotic division apparatus consists firstly of the spindle, made up of microtubules, which creates the forces required to organise and separate chromosomes. Also important are the structures from which the spindle originates, called microtubule organizing centres, and kinetochores, macromolecular structures on the chromosomes that enables chromosome-microtubule interaction.

1.1.1 The spindle

The spindle is a highly organized, dynamic cytoskeletal structure, composed of microtubules (MTs). MTs are hollow tubes, 25 nm in diameter, formed by lateral interaction of thirteen protofilaments (Tilney et al., 1973; Evans et al., 1985). Each protofilament is formed by head-to-tail interaction of α-/β-tubulin heterodimers

(Ludueña et al., 1977). This results in MT polarity with one end of the polymer exposing β-tubulin, the plus end of MT, and the other end exposing α-tubulin, the minus end (Mitchison, 1993; Figure 1.1).

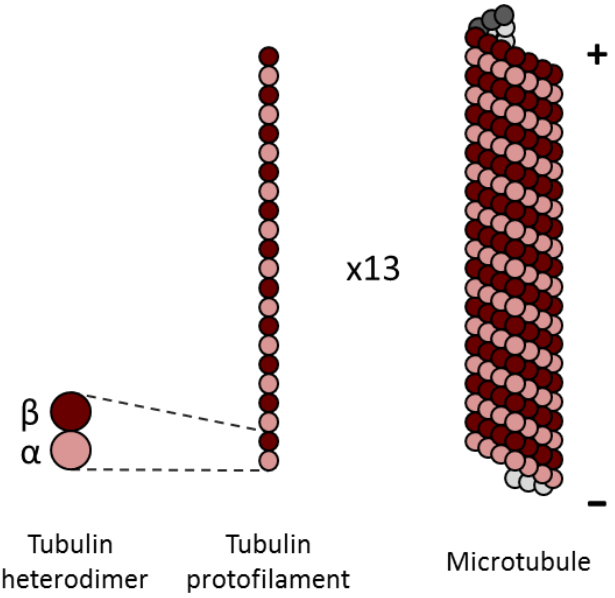

Figure 1.1: Microtubule structure. Three structures are presented here, α-/β-heterodimer are presented as red and pink circles and 13 marks the number of protofilaments that assemble into MT. Plus and minus are marking the MT polarity.

MTs are dynamic polymers. They stochastically switch between phases of growth and shrinkage, termed rescue and catastrophe, respectively (Desai and Mitchison, 1997). This property of MTs is referred to as dynamic instability (Mitchison and Kirschner, 1984), and it is based on GTP to GDP hydrolysis. Tubulin contain two nucleotide binding sites, one on the α/β interface and one on the exposed end of β-tubulin. MTs grow by addition of GTP bound α-/β-tubulin heterodimers. This newly arriving tubulin dimer catalyses the hydrolysis of the GTP molecule on the β-tubulin that is already incorporated into the MT lattice (Kobayashi, 1975; Weisenberg et al., 1976; Nogales et al., 1998). Therefore, the lattice of growing MTs is mainly composed by GDP-tubulin while the growing end contains GTP-bound β-tubulin, and this GTP-tubulin forms a stabilizing cap at the MT tip (Drechsel and Kirschner, 1994). Fast shrinkage of MTs is a result of loss of

this stabilising cap due to faster GTP hydrolysis than tubulin incorporation at the MT tip (Alushin et al., 2014).

In addition to the intrinsic dynamic properties of MTs, MT dynamicity can be regulated by MT-associated proteins (MAPs). Many MAPs regulate MT dynamics through stabilizing or destabilizing activity. Some MAPs affect MT dynamics through interactions with other proteins. MAPs can promote the active addition of tubulin dimer to the MT plus ends, or they can act as capping proteins, dampening growth or shrinkage (Komarova et al., 2002; Tirnauer et al., 2002; Brouhard et al., 2008; Du et al., 2010; Al-Bassam et al., 2010). There are also MAPs that actively depolymerize MTs, sequester free tubulin or severe MTs (Walczak et al., 1996; Desai et al., 1999; Sharp and Ross, 2012). MT dynamics are crucial for chromosome segregation during cell division. Attachment of chromosomes to polymerizing or depolymerizing ends of MTs allows for their positioning at the spindle equator and then generation of the pulling forces required for chromosome migration to the cell poles.

MAPs also contribute to the structure of the spindle. They can bundle MTs in a parallel or anti-parallel fashion and some MAPs use motor activity to move one MT relative to another (Cai et al., 2009; Sharp et al., 2000; van den Wildenberg et al., 2008). Subpopulations of MTs in a bipolar spindle can be divided into three groups: (a) kinetochore fibers (K-fibers) composed of parallel MT bundles; (b) interpolar MTs formed from bundled antiparallel MTs originating from opposite poles; (c) astral MTs.

Kinetochore MTs connect the spindle MTs with chromosomes. Interpolar MTs overlap at the spindle equator and generate pushing force for spindle poles separation at the mitosis onset and push chromosomes apart during segregation. Astral MTs emanate from the centrosomes and interact with the cell cortex to position the spindle within a cell (Figure 1.2).

During anaphase, the central spindle forms from interpolar MTs and de novo synthesis of MTs (Uehara and Goshima, 2010). In cytokinesis, a dense bundle of MTs embedded in electron dense material forms the midbody.

Spindle dynamics and organization, crucial to the chromosome segregation, are highly regulated through post-translational modification of MAPs (See 1.2. and 1.3.).

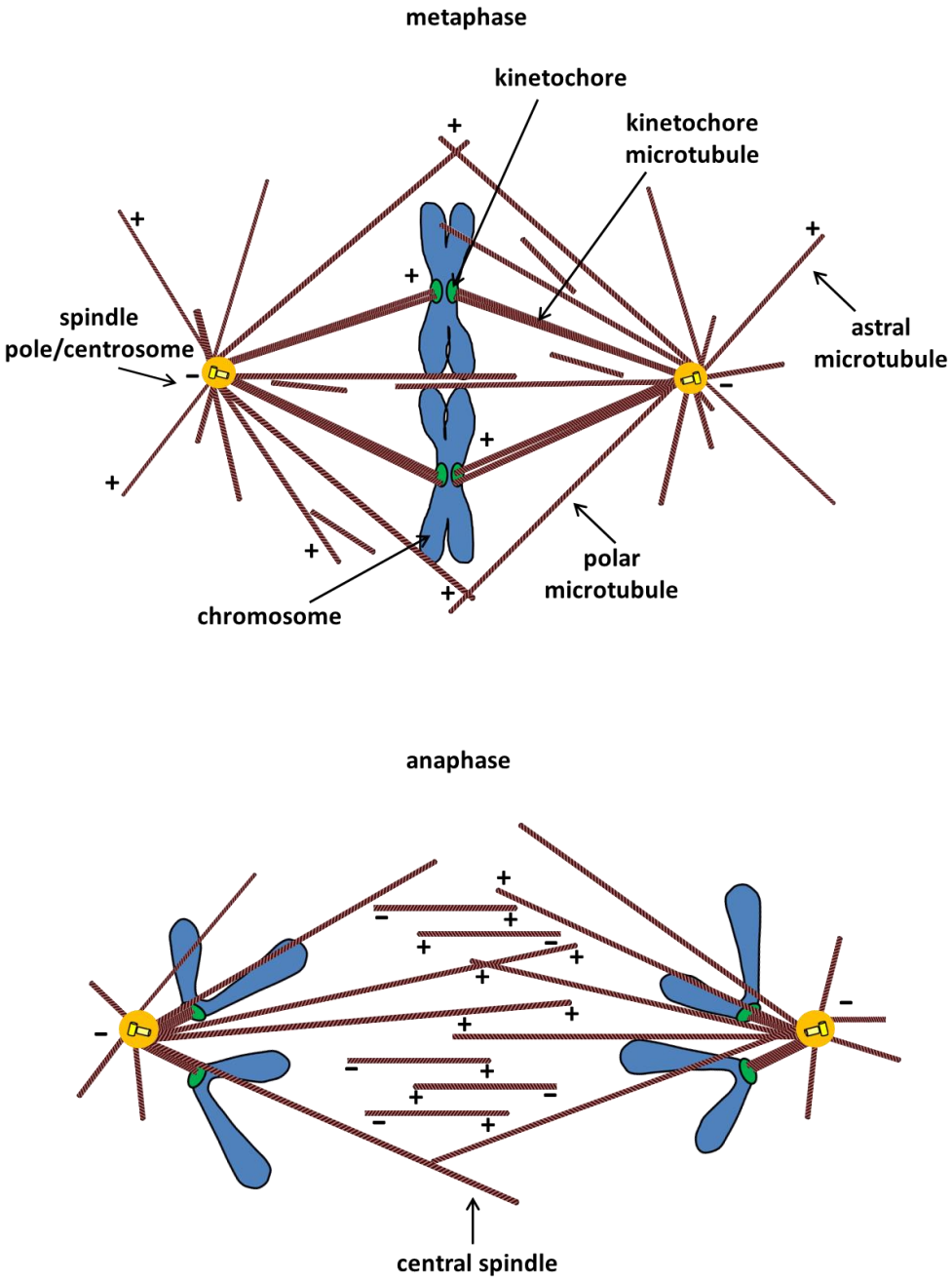

Figure 1.2: Organization of the spindle MTs during metaphase and anaphase. Different spindle structures and subpopulation of MTs are presented with labelled plus and minus ends. Chromosomes are drawn in blue, MTs in red, kinetochores in green and centrosomes/centrioles are yellow.

1.1.2 **Spindle microtubule organizing centres**

In cells, MT formation does not occur spontaneously due to the low concentration of tubulin, but MTs nucleate at specific foci, referred to as MT organising centres (MTOCs). MTOCs can be classified as either non-centrosomal or centrosomal. MTOCs always contain γ-tubulin, another member of the tubulin family, which is conserved in all eukaryotes (Weil et al., 1986; Oakley and Oakley, 1989; Stearns et al., 1991). MT nucleation requires multiple copies of γ-tubulin and five γ-tubulin complex proteins (GCPs), which together form a γ-tubulin ring complex (γ-TuRC). This complex serves as a template for α-/β-tubulin dimer addition and MT polymerization (Teixidó-Travesa et al., 2010; Kollman et al., 2011).

Most animal cells have centrosomes which are the dominant MTOCs. Centrosomes are spherical structures, composed of two centrioles, which are surrounded by pericentriolar material (PCM), a proteinaceous structure. The centrioles within a centrosome have a defined size and a barrel-like shape with a nine-fold symmetrically arranged array of MT structures, usually organized as MTs triplets (Winey and O'Toole, 2014). The nine-fold symmetry of centrioles is in part provided by the cartwheel structure that displays this symmetry and one of the first structures to assemble during centriole biogenesis (Nakazawa et al., 2007). The older centriole called the mother contains additional appendages and is functionally different form the daughter centriole. Centrosomes duplicate in S phase (Synthesis phase), when each centriole serves as a template for a new daughter centriole. These procentrioles elongate during S and G2 phase (Gap phase 2) reaching a defined length. Duplicated centrosomes, which were previously connected with a protein linker, split before NEB (Bettencourt-Dias and Glover, 2007; Figure 1.3).

Centrosomes have the ability to form and anchor MTs, thus organizing them into two MT arrays. An important process in centrosome biogenesis is centrosome maturation, which is recruitment of PCM component by centrioles. The PCM is a scaffold important for docking MT stabilization factors and nucleation factors, such as the γ-TuRC (Piehl et al., 2004; Khodjakov and Rieder, 1999).

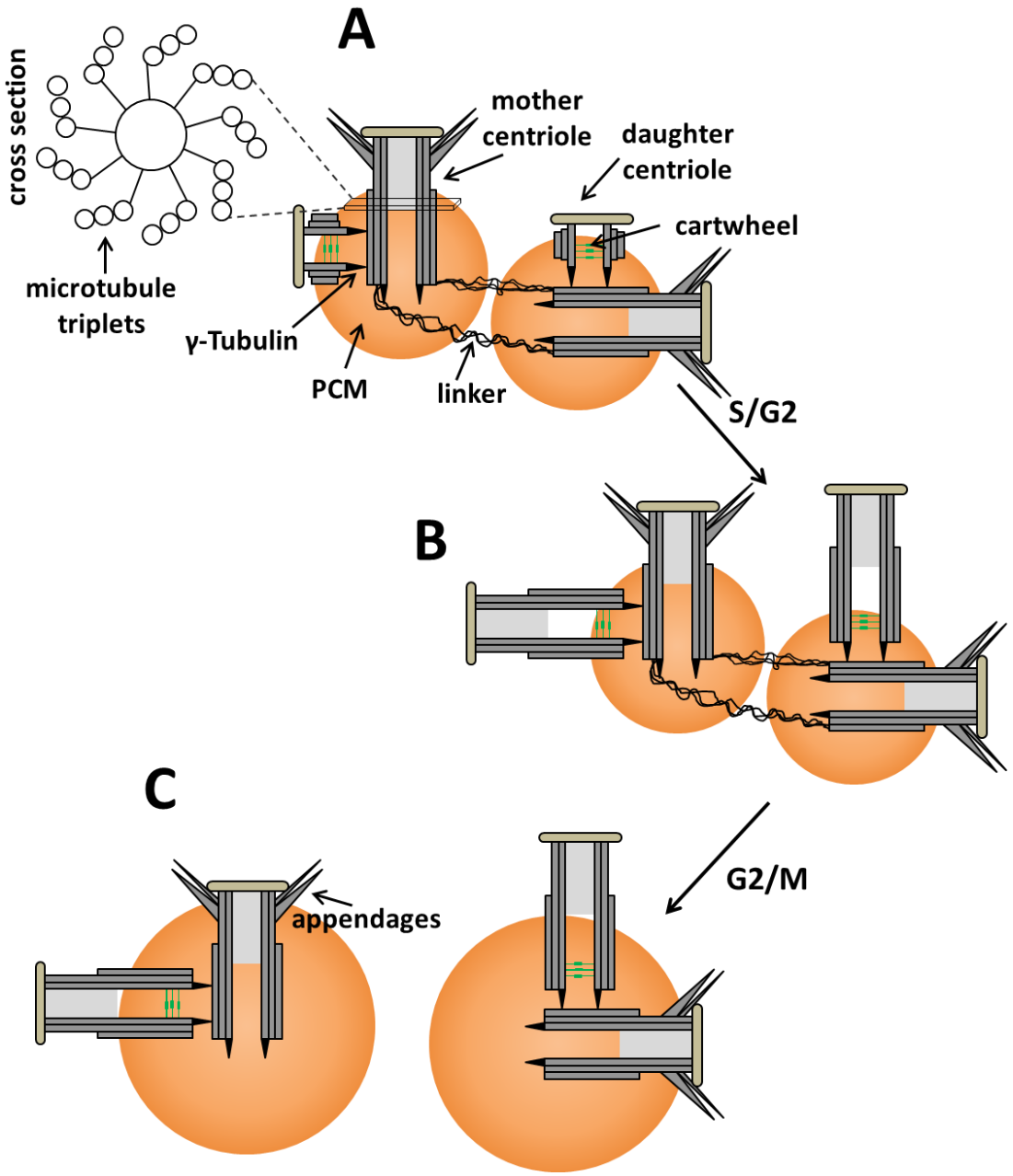

Figure 1.3: Centrosome structure and biogenesis. Duplication of centrioles is presented in A, centriole elongation is presented in B and centrosome separation and maturation is presented in C. Depicted is a longitudinal section of the mother and daughter centrioles with cross section of one centriole on the top left. MT triplets are drawn in grey and cartwheel structure in green. γ-tubulin is represented with black triangle (adapted from Firat-Karalar and Stearns, 2014).

Regulation of centrosome assembly, number and function is important for mitosis in animal cells. Anomalies in centrosome and centriole numbers are often observed in different cancers (Ganem et al., 2009; Nigg and Raff, 2009).

Interestingly, removal or mutational loss of centrosomes from mitotic animal cells shows that centrosomes are not essential for the bipolar spindle assembly (Khodjakov et al., 2002; Hinchcliffe et al., 2001; Basto et al., 2006). Plant cells and animals female oocytes do not have centrosomes and use alternative pathaways of MT nucleation, while budding yeast contains specialized structures, spindle pole bodies (SPB).

The non-centrosomal MT nucleation pathway involves nucleation in the vicinity of chromosomes (Karsenti et al., 1984; Heald et al., 1996). The underlying mechanism is based on the RanGTP gradient formed around chromosomes. Ran is a small GTPase that can exist in two forms, RanGTP and RanGDP. The nucleotide state is determined via the activity of guanosine exchange factor (GEF) or activating protein (GAP). The highest concentration of RanGTP is centered around chromosomes due to the activity of GEFs (Carazo-Salas et al., 1999). The RanGTP gradient activates many factors important for spindle assembly. MTs can nucleate in the vicinity of chromatin or in the region of the kinetochores (Carazo-Salas et al., 1999, Carazo-Salas et al., 2001; Kalab et al., 1999; Kalab et al., 2002; De Brabander et al., 1981; Khodjakov et al., 2003; Maiato et al., 2004; Mishra et al., 2010). Another MT-nucleating pathway is the Augmin pathway, which occurs at sites on pre-formed MTs. The augmin complex binds the lattice of pre-existing spindle MTs, and recruits γ-TuRCs and promotes nucleation (Goshima et al., 2008; Petry et al., 2011; Kamasaki et al., 2013).

1.1.3 **The kinetochore**

The kinetochore is a structure assembled on chromosomes, which is the site of MT attachment. The kinetochores form on the surface of chromosomes at the site of primary constriction, called the centromere. The site of the centromere is determined by the presence of distinct nucleosomes, consisting of a conserved histone H3 variant, called CENP-A in humans (Centromere Associated Protein-A;

Cse4 in budding yeast, CID in Drosophila; Earnshaw and Rothfield, 1985; Palmer et al., 1987; Allshire and Karpen, 2008). CENP-A is critical to kinetochore assembly. It serves as a platform upon which kinetochore proteins assemble.

Electron microscopy revealed the laminar structure of the kinetochore with distinct planes of the inner and outer plate (Maiato et al., 2006). The constitutive centromere associated network (CCAN) comprises the inner kinetochore. CCAN contains sixteen members identified so far through many studies, and they are divided in subgroups, based on their interaction and reciprocal dependencies: CENP-C, CENP-N/L, CENP-T/W/S/X, middle part of kinetochore CENP-H/I/K/M, CENP-O/P/R/Q/U (McAinsh and Meraldi, 2011; Perpelescu and Fukagawa, 2011; Nishino et al., 2012; Figure 1.4).

The outer kinetochore components assemble onto the inner kinetochore in a process that is cell cycle regulated, occurring in G2 phase or at specific time during division (Cheeseman and Desai, 2008). The core of the outer kinetochore is the KMN network, which contains KNL1 (kinetochore null protein 1, also known as Blinkin and CASC5) and two complexes: Mis12 complex (missegregation 12) and Ndc80 complex (nuclear division cycle 80; Cheeseman and Desai, 2008). These complexes play an essential role in the formation of end-on attachments with MTs. The human Mis12 complex consists of the Nnf1, Mis12, Dsn1 and Nsl1 proteins (Kline et al., 2006; Cheeseman and Desai, 2008; Petrovic et al., 2010). The Mis12 complex is important for connecting the KMN network with the inner kinetochore through interaction with CENP-C (Screpanti et al., 2011; Richter et al., 2016), and also interacts with both the Ndc80 complex and KNL1 (Maskell et al., 2010; Welburn and Cheeseman, 2008; Hornung et al., 2011; Petrovic et al., 2010). In humans, KNL1 does not direct the Ndc80 complex to the kinetochores (Cheeseman et al., 2008). CENP-T directly interacts with Ndc80 complex (Gascoigne et al., 2011; Hori et al., 2008).

The Ndc80 complex is tetramer, consisting of Ndc80 (also known as HEC1 in humans) and Nuf2 (nuclear filamentous 2) heterodimer, which interacts with Spc24 and Spc25 heterodimer (spindle pole component 24 and 25; Ciferri et al., 2005). The

Spc24/Spc25 heterodimer interacts with Mis12 complex, while HEC1/Ndc80/Nuf2 heterodimer faces the MTs. It has been established that the Ndc80 complex binds MTs through the N terminus of Ndc80, and more precisely through tail domain of the N terminus, which contains positively charged residues that interact with the negatively charged interface between α-/β-tubulin (Cheeseman et al., 2006; Ciferri et al., 2008; Alushin et al., 2010). Additionally, Ndc80 forms interactions with the acidic C terminus of each tubulin monomer, so called E-hooks (Wei et al., 2007; Ciferri et al., 2008; Alushin et al., 2010). Dam1 in yeast and the Ska1 complex in humans, were shown to interact with Ndc80 and stabilize the interaction with MTs (Maure et al., 2011; Kim et al., 2017; Janczyk et al., 2017; Cheerambathur et al., 2017).

Kinetochore-MT attachments are highly regulated. The unattached kinetochores activate a specific control mechanism, called the spindle assembly checkpoint (SAC). The best known components of SAC are Mad1, Mad2, Mad3/BubR1, Bub1, Bub3 and Mps1 (Musacchio and Salmon, 2007). Additionally, proteins CENP-E and the RZZ complex (containing Zwint, ZW10 and Rod) were shown to play role in SAC signalling (Karess, 2005; Musacchio and Salmon, 2007). The activated SAC at the kinetochores prevents anaphase until all chromosomes are properly attached via inhibition of the anaphase promoting complex (APC/C). SAC proteins at the unattached kinetochores generate a diffusible inhibitor of APC/C, which is called mitotic checkpoint complex (MCC). The MCC consist of Mad2, Mad3/BubR1 and Bub3 that together bind Cdc20 (cell division cycle 20), preventing Cdc20 from binding and activating APC/C (Sudakin et al., 2001). MCC can inhibit the second Cdc20 molecule that has already bound and activated APC/C (Izawa and Pines, 2014), and this stable interaction of MCC and APC/C is required for functional SAC (Hein and Nilsson, 2014). Monitoring kinetochore-MT attachments is strictly regulated, to prevent chromosome mis-segregation. This will be discussed in Chapter 2.

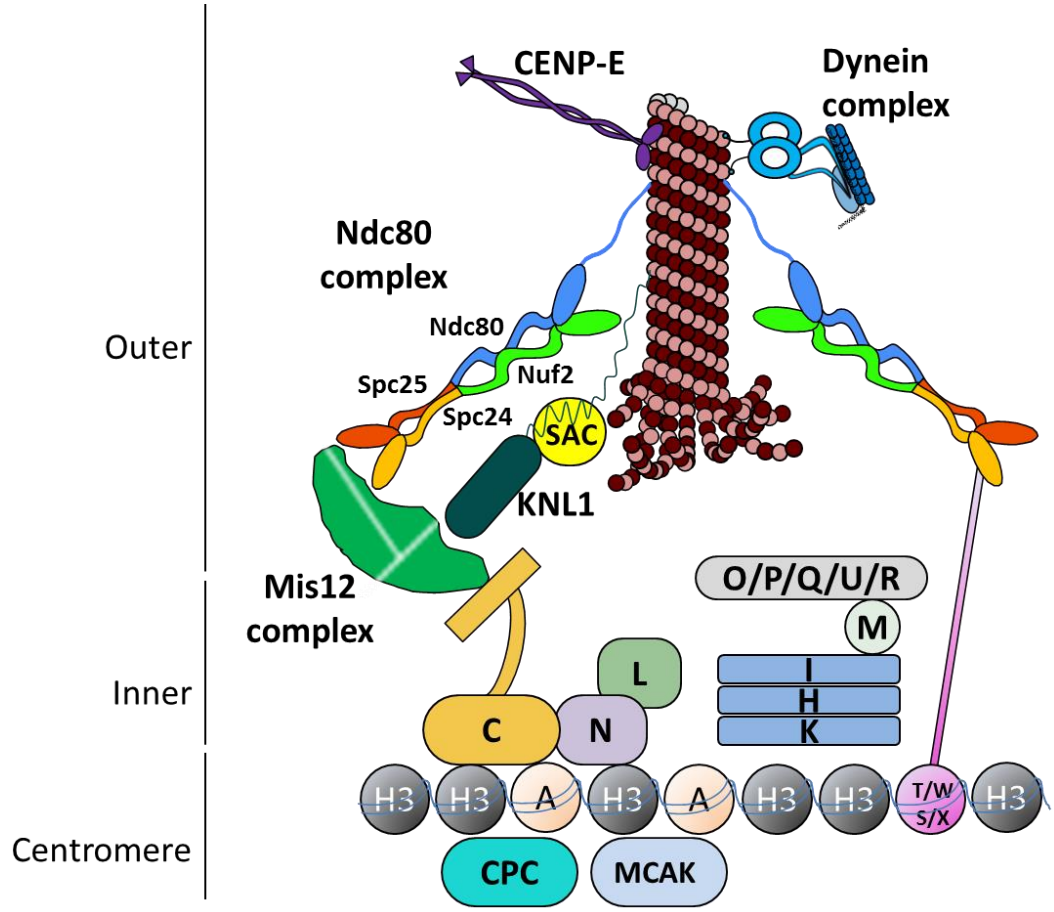

Figure 1.4: Kinetochore structure in vertebrates. Schematic diagram of vertebrate kinetochores is adapted from Maiato et al., 2004. Centromere proteins and the nucleosomes containing CENP-A and histone H3 are depicted with single letter. CPC represents chromosome passenger complex, MCAK is mitotic centromere-associated kinesin.

1.2 Regulation of mitosis through post-translational modification of proteins

Regulation of mitosis is largely driven by posttranslational modifications of proteins rather than transcriptional changes. Protein modification can control enzymatic activity, protein conformation, protein-protein interactions, protein degradation and cellular localization (Olsen et al., 2006). Protein modifications, such as phosphorylation, ubiquitination, sumoylation, acetylation and methylation, affect the mitotic division apparatus and mitotic progression (Dephoure et al., 2008; Malik et al., 2009; Merbl and Kirschner, 2009; Yang and Seto, 2008; Zencheck et al., 2012).

Protein ubiquitination and sumoylation are modifications that involve covalent binding of multiple ubiquitin or the ubiquitin-like molecule, SUMO, to the target proteins. The modified proteins are then usually targeted for proteolytic degradation. These modifications may also affect other aspects of protein function and localization (Teixeira and Reed, 2013; Fournane et al., 2012; Wang and Dasso, 2009). The most known protein E3 ubiquitin ligase is APC/C. The APC/C is essential for the metaphase to anaphase transition via ubiquitylation and the subsequent degradation of cyclin B and securin, which are important for inactivation of Cyclin-dependent kinase 1 (CDK1) and activation of the protein separase, respectively. The APC/C is also important for mitotic exit as it targets many factors active in late stages of mitosis for degradation, among them are most of the enzymes responsible for mitotic phosphorylation (Teixeira and Reed, 2013).

Additionally, tubulin modification can guide mitosis. Post-translational modifications of the unstructured C terminus of α- and β-tubulin regulate the interaction of MTs and MAPs, this is termed the "tubulin code" (Garnham and Roll-Mecak, 2012). Tubulin detyrosination/tyrosination, which is removal or addition of tyrosine residue from α-tubulin C terminus, regulates the stability of MT plus ends (Peris et al., 2009; Gupta et al., 2010; Sirajuddin et al., 2014), as well as chromosome congression (Barisic et al., 2015). Acetylation/deacetylation and polyglutamylation regulate MT-binding of MAPs, and polyglutamylation is important for centriole maturation. Polyglycylation is essential in Tetrahymena for cytokinesis, regulating MT severing (Westermann and Weber, 2003). Further investigation is needed to elucidate how these post-translational modifications of tubulin regulate mitosis.

1.2.1 **The role of phosphorylation in mitosis**

The most abundant post-translational modification in cells is phosphorylation, since the one-third of proteins in cells is phosphorylated at any stage in the cell cycle (Olsen et al., 2010). In mitosis, phosphorylation is even more prominent than in interphase (Dephoure et al., 2008; Malik et al., 2009; Olsen et al., 2010). Phosphorylation modulates protein activity (inactivating or activating) by

regulating interactions with other proteins, influencing the tertiary and quaternary structure of a protein (conformational change), controlling subcellular distribution, or targeting proteins for degradation (Olsen et al., 2010). Protein phosphorylation is the addition of phosphate groups, originating from ATP, to amino acid side chains of target proteins and is mediated by protein kinases. Phosphorylation is reversible, and the equally important process of dephosphorylation is mediated by protein phosphatases (Figure 1.5). Both processes are highly controlled by various intracellular and extracellular stimuli.

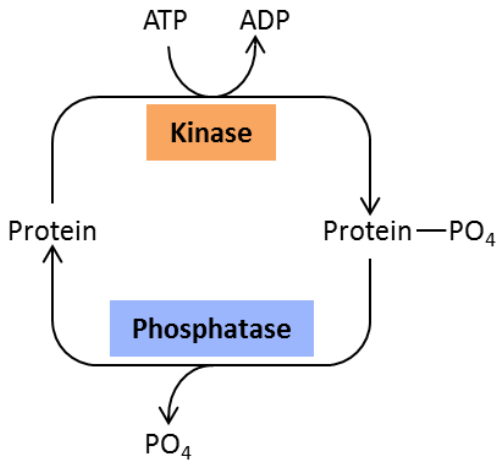

Figure 1.5: Schematic diagram of protein phosphoregulation.

The human genome encodes more than 500 protein kinases (Manning et al., 2002; Park et al., 2005), and certain kinase families are especially important in mitosis. These kinase families belong to serine/threonine kinases, which phosphorylate S or T residues in target proteins. The master regulators of the cell cycle are CDKs (Cyclin-dependent kinases). Mitotic CDKs are essential for initiation and progression through mitosis. CDK activity is controlled by specific proteins, cyclins, whose level of expression oscillates throughout the cell cycle.

There are other kinase families essential for the regulation of mitosis. Primarily, those are PLKs (Polo-Like kinases) and Aurora family of kinases. These kinases control the generation of the division apparatus and chromosome

segregation. They are also critical for preventing errors in mitosis (Carmena and Earnshaw, 2003; Fu et al. 2007, Barr et al. 2004).

1.3 **Family of Aurora kinases and their function in cell division**

The Aurora family of kinases contain only one member in yeast, Ipl1 (Increase in ploidy 1) in *S.cerevisiae* and Ark1 (Aurora related kinase) in *S.pombe* (Chan and Botstein, 1993; Petersen et al., 2001). There are two members of the Aurora family in *C.elegans*, *D.melanogaster* and *X.leavis*, while mammals have three: Aurora A, B and C (Glover et al., 1995; Nigg, 2001). The Aurora kinase family has a conserved function in cell division, from most simple eukaryotes to humans.

The three mammalian Aurora kinases share about 70% sequence identity in their catalytic domain at the C terminus (Scrittori et al., 2005). The high degree of sequence similarity suggests that they phosphorylate the same substrates. Their sub-cellular localization determines the substrate specificity of Aurora kinases and their distinct activators that bind the N terminus of Aurora kinases (Carmena and Earnshaw, 2003). Targeting Aurora A to the subcellular localization of Aurora B leads to phosphorylation of the Aurora B substrates, and same occurs when Aurora B is targeted to Aurora A localization (Li et al., 2015). One amino acid substitution in Aurora A catalytic domain converts it to Aurora B, reproducing Aurora B kinase localization, binding partners and phosphorylation substrates (Fu et al., 2009; Hans et al., 2009). In addition, several studies showed that Aurora kinases phosphorylate the same substrates in cells (Table 1.1 and Table 1.2, shared substrates are marked with asterisks; also see below). Aurora kinases also share a consensus motif in target proteins. However, the three mammalian kinases have mainly distinct functions in cells. Aurora C has role in meiosis (Bernard et al., 1998; Kimura et al., 1999), and a recent study showed function distinct from that of Aurora B at the chromosomes (Quartuccio et al., 2017). Aurora C has not been subject of this study; therefore, it will not be discussed further.

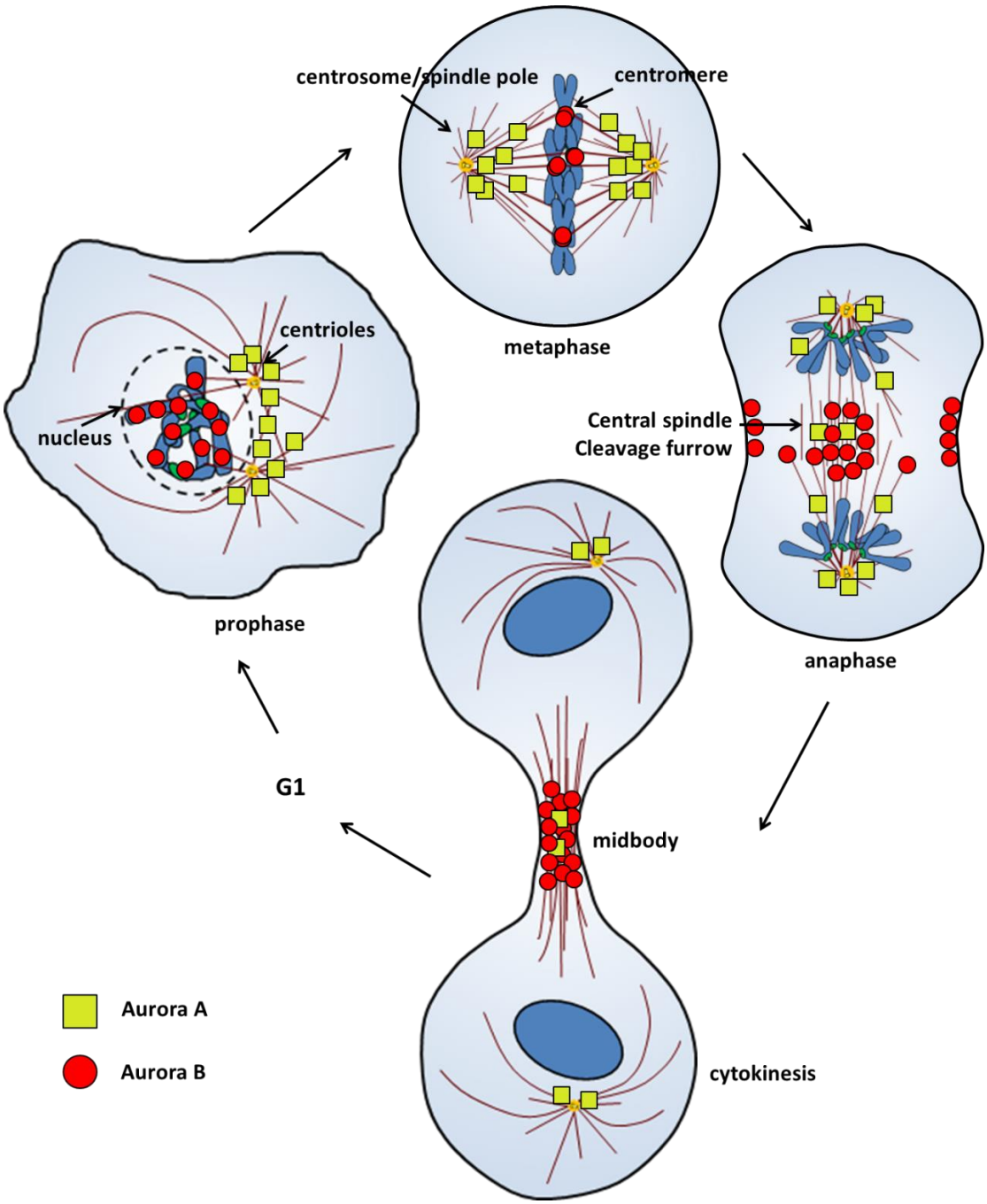

Figure 1.6: Localization of Aurora kinases during mitosis. Schematic diagram is presenting reported localization of Aurora kinases in cell undergoing division. Aurora A kinase is depicted with green squares and Aurora B kinase with red circles. Indicated are sub-cellular structures where Aurora kinases localize. Chromosomes and chromatin are depicted in blue, centrosomes in yellow, kinetochores in green and MTs are red (adapted from Carmena and Earnshaw, 2003).

Aurora A

Aurora A is essential for centrosome separation and maturation, bipolar spindle assembly and maintenance, and the timing of the mitotic entry. Aurora A kinase is activated by several proteins at specific places within the mitotic apparatus. Proteins Bora, CEP192 (centrosome protein 192 kDa), Ajuba and nucleophosmin (NPM) activate Aurora A at the centrosomes (Hutterer et al., 2006; Joukov et al., 2010; Hirota et al., 2003; Reboutier et al., 2012). TPX2 (targeting protein for Xklp2) activates Aurora A at the spindle MTs (Kufer et al., 2002). Activation of Aurora A is primarily achieved through autophosphorylation of T288, and this mechanism is best understood from the crystal structure of the Aurora A – TPX2 complex (Bayliss et al., 2003; Zorba et al., 2014). Nucleophosmin activates Aurora A by inducing autophosphorylation on S98 (Reboutier et al., 2012). Active Aurora A is associated with centrosomes following centrosome duplication in S phase. Aurora A maintains centrosomal/spindle pole localization throughout mitosis. It also associates with MTs close to the centrosomes. Low levels of this kinase can be found on the central spindle in anaphase and midbody in cytokinesis (Figure 1.6; Carmena and Earnshaw, 2003). Aurora A activity is directly regulated by protein phosphatases. It was reported that protein phosphatase 1 (PP1) regulates dephosphorylation of T288 (Katayama et al., 2001). This regulation is only observed in human and Xenopus. Moreover, PP6 was described to negatively regulate Aurora A activation (Zeng et al., 2010).

Aurora A controls centrosome separation and maturation. Centrosomal Aurora A controls the removal of components of the protein linker that connects two duplicated centrosomes, which then permits centrosome separation. This is achieved through phosphorylation of kinase PLK1 at T210, which then activates a complex cascade of phosphorylation by activating Nek2A kinase (Macůrek et al., 2008; Seki et al., 2008; Mardin et al., 2011). Aurora A also promotes centrosome maturation through recruitment of PCM components and enables MT nucleation at the centrosome (Joukov et al., 2010). This is achieved through Aurora A

phosphorylation and activation of kinase LATS2, which in turn recruits γ-tubulin to the PCM (Abe et al., 2006; Toji et al., 2004).

Aurora A then promotes the stabilization of MTs nucleated at the centrosomes. First, Aurora A recruits and activates MTs stabilization factors. Aurora A phosphorylates NDEL1 (Nuclear distribution element like 1) at S251, which is required for NDEL1 localization at the centrosomes and interaction with TACC3 (Transforming acidic coiled-coil-containing protein 3, also known as Maskin; Mori et al., 2007). Aurora A also directly phosphorylates TACC3 to recruit it to the centrosomes (Fu et al., 2010). The stabilization of centrosomal MTs is then achieved through TACC3 interaction with chTOG/XMAP215 which positively regulates MT dynamics (Barros et al., 2005; Kinoshita et al., 2005). Moreover, Aurora A directly phosphorylates and inhibits MT depolymerase Kif2c/MCAK, positively regulating dynamics of astral MTs (Zhang et al., 2008)

Aurora A phosphorylation is important for separation of stabilized centrosomal MT asters and formation of the bipolar spindle. Aurora A regulates MT aster separation through phosphorylation of evolutionary conserved kinesin-5 family member, Eg5/Kif11 (Giet et al., 1999). Eg5/Kif11 (also known as XlEg5) is a homotetramer that binds two antiparallel MTs of centrosomal MT asters and by moving toward the plus ends of each it slides those MTs apart, separating the MT asters and forming the bipolar spindle (Sawin et al., 1992; Sharp et al., 1999; van den Wildenberg et al., 2008). In addition, Aurora A controls pole focusing and spindle positioning through phosphorylation of $p150^{glued}$ dynactin subunit of dynein/dynactin comlex, a major minus-end-directed motor (Romé et al., 2010).

Once the bipolar spindle is formed, Aurora A still contributes to spindle maintenance and MT amplifications. Aurora A, activated by TPX2, regulates MT nucleation and polymerization (Tsai et al., 2003). TPX2 is activated by RanGTP near chromosomes (Gruss et al., 2001; Kufer et al., 2002; Tsai et al., 2003), and then directly interacts and activates Aurora A, specifically on the spindle MTs and not at the centrosomes (Kufer et al., 2002). It was proposed that TPX2-Aurora A forms a gradient of activity similarly to RanGTP gradient around chromosomes (Tsai et al.,

2003). However, the existence of TPX2-Aurora A gradient of activity has not been demonstrated experimentally. MT polymerization and stabilization around the chromosomes is additionally supported by Aurora A phosphorylation of HURP (Hepatoma upregulated protein) and NEDD1 (Neural precursor cell expressed developmentally down-regulated protein 1) that stabilize K-fibers and allow proper bipolar spindle formation (Yu et al., 2005; Wong et al., 2008; Pinyol et al., 2013). In addition to the centrosomal MT nucleation pathway, Aurora A may contribute to MT nucleation from pre-existing MT, through phosphorylation of Hice1/HAUS8, a part of Augmin complex (Tsai et al., 2011). This, in turn, contributes to the establishment of a proper bipolar spindle after centrosome separation, but the exact mechanism is still not clear.

Aurora A regulates chromosome segregation, independently of its role in bipolar spindle formation, since defects in spindle alignment at the metaphase plate were observed even when bipolar spindles formed (Marumoto et al., 2003; Hoar et al., 2007; Sasai et al., 2008). Aurora A regulation of kinetochore-MT attachment was a subject of this study and will be discussed further in Chapter 2. There are few kinetochore substrates, whose phosphorylation by Aurora A is reported to contribute to chromosome congression, and they can be seen in Table 1.1.

It was shown that Aurora A contributes to central spindle stabilization in anaphase through the regulation of TACC3 and dynein complex subunit $p150^{glued}$ (Reboutier et al., 2013; Lioutas and Vernos, 2013). It is unknown how Aurora A amplifies phosphorylation of Aurora B at the spindle midzone (Afonso et al., 2017; Ye et al., 2016). Additionally, the main Aurora A substrates in later phases of mitosis are still missing.

Table 1.1: List of Aurora A substrates with specific phosphorylation known to affect mitosis. Shared substrates with Aurora B are marked with *, Human refers to human cultured cells.

Aurora A kinase			
Substrate	Phosphosite	Organism	Reference
Aurora A/STK6	S89, T288 (T295 in frog)	Human, Frog	Eyers et al., 2003; Bayliss et al., 2003; Reboutier et al., 2012
Plk1	T210	Human	Macůrek et al., 2008; Seki et al., 2008; Bruinsma et al., 2014
LATS2/KPM	S83	Human	Toji et al., 2004
NDEL1/Nudel	S251	Human	Mori et al., 2007
CDC25B/MPIP2	S353	Human	Dutertre et al., 2004; Cazales et al., 2005
CPEB1	T174	Frog	Mendez et al., 2000; Groisman et al., 2002
NEDD1	S405	Human, Frog	Pinyol et al., 2013
CPAP/Sas-4	S467	Human	Chou et al., 2016
Centrin	S170 (S122 *in vitro*)	Human	Lukasiewicz et al., 2011
GEF-H1/ARHGEF2	S855	Human	Birkenfeld et al., 2007
Hist1H3A*	S10, T118	Human	Crosio et al., 2002; Wike et al., 2016
HP1γ/CBX3	S83 (unprocessed HP1γ S93)	Human	Grzenda et al., 2013
CENP-A*	S7	Human	Kunitoku et al., 2003
RalA	S194	Mammals (Human, Mouse, Canin cells)	Wu et al., 2005; Lim et al., 2010
p53*	S215	Human	Liu et al., 2004
c-FOS	not mapped	Human	Yu et al., 2008
TACC3/D-TACC/Maskin	S34, S552, S558 (S33, S620, S626 in Frog, S863 in Fly)	Human, Frog, Fly	Giet et al., 2002; LeRoy et al., 2007; Peset et al., 2005; Barros et al., 2005
HURP/DLG7	S627, S725, S757, S830	Human	Yu et al., 2005; Wong et al., 2008
TPX2	S121, S125 (S90, S94 in Frog)	Human, Frog	Kufer et al., 2002; Fu et al., 2015
CENP-E/Kinesin-7*	T422	Human	Kim et al., 2010
MAP9/ASAP	S625	Human	Venoux et al., 2008
Kif15/Kinesin-12/Hklp2	S1169	Human, Mouse	van Heesbeen et al., 2017
Kif2a*	not mapped	Human	Jang et al., 2009
Kif2c/MCAK*	S196, S719	Frog	Zhang et al., 2008
NuMA	S1969	Human	Gallini et al., 2016
Hice1/HAUS8	S/T-17-21 cluster	Human	Tsai et al., 2011
RASSF1A	T202, S203	Human	Rong et al., 2007; Song et al., 2009
MAPRE3/EB3*	S176	Human	Ban et al., 2009
IκBα/NFκBIα	S32, S36	Human	Briassouli et al., 2007; Chefetz et al., 2011
WDR62/C19orf14	S49, T50	Human	Lim et al., 2016
p150^{Glued}/Dynactin subunit 1	S19 (S85, S109, S117, S135, S137, S138, S144, S183)	Fly, Human	Romé et al., 2010; Reboutier et al., 2013
FAF1/UBXD12	S289/S291	Human	Jang et al., 2008
Kif11/Eg5/BimC	not mapped - S543 not important in vivo	Frog	Giet et al., 1999; Cahu et al., 2008
BRCA1	S308	Human	Ouchi et al., 2004-Retracted; Brodie and Henderson, 2012;
MBD3	S24	*in vitro*	Sakai et al., 2002

Aurora B

Aurora B regulates chromosome condensation, chromosome bi-orientation and SAC, local MT nucleation, central spindle organization and cytokinesis. Aurora B kinase forms a complex with the inner centromere protein (INCENP; Sli15 in yeast), Survivin (Bir1) and Borealin (also known as DASRA), the proteins responsible for Aurora B activation and localization (Earnshaw and Bernat, 1991; Gassmann et al., 2004; Klein et al. 2006). This complex is called the chromosome passenger complex (CPC). The mechanism of Aurora B activation has been fully understood from the crystal structure of Aurora B-INCENP complex (Sessa et al., 2005). The activation of Aurora B is initiated with binding to the IN-box domain of INCENP. This activates an initially low level of Aurora B, responsible for phosphorylation of TSS sequence in the C terminus of INCENP and T232 in the kinase domain of Aurora B (Bishop and Schumacher, 2002; Honda et al., 2003, Xu et al., 2010). Auto-phosphorylation increases the activity of Aurora B. The kinase activity is also regulated by MTs, mainly at the central spindle (Fuller et al., 2008; Rosasco-Nitcher et al., 2008; Tseng et al., 2010). The activated CPC changes localization during mitosis. First, the CPC localizes to the region of the inner centromere of chromosomes during early mitosis, it then transfers to the central spindle in anaphase, followed by transfer to the midbody and the cell cortex, where the contractile ring forms in cytokinesis (Carmena and Earnshaw, 2003; Figure 1.6).

In early mitosis, Aurora B controls chromosome compaction. Aurora B phosphorylates histone H3 on S10, and regulates chromosome condensation in budding yeast anaphase (Hsu et al., 2000; Sugiyama et al., 2002; Neurohr et al., 2011). Phosphorylation of S10 in histone H3 is conserved from yeast to human, but the role of this phosphorylation is not completely clear in higher eukaryotes (Hsu et al., 2000; Hauf et al., 2003; Adams et al., 2001). Histone H3 S10 might regulate the change of CPC localization from interphase to mitosis (Fischle et al., 2005; Hirota et al., 2005). Most likely, Aurora B affects chromosome condensation through phosphorylation of kleisin, part of the condensin complexes that are responsible for chromosome compaction (Tada et al., 2011; Nakazawa et al., 2011). The exact

mechanism of Aurora B regulation of chromatin compaction needs to be clarified further.

An important function of Aurora B is in regulation of kinetochore-MT attachments and chromosome bi-orientation. Interference with Aurora B function causes defects in chromosome congression (Kallio et al., 2002; Ditchfield et al., 2003; Hauf et al., 2003). Aurora B was shown to phosphorylate several proteins of the outer kinetochore and fibrous corona, and this regulates chromosome attachment to MTs and congression. This Aurora B function and proposed gradient of activity and regulation of SAC will be further discussed in Chapter 2, while the known kinetochore substrates and corresponding references can be found in Table 1.2. The involvement of Aurora B in SAC control is still not completely clear, and reduced requirement for Aurora B in SAC response observed in human cells, could indicate an Aurora B-independent mechanism (Matson et al., 2012).

Aurora B also contributes to chromosome-induced spindle assembly. In Xenopus egg extracts, chromosome-bound CPC is activated and targeted to the MTs via INCENP, where it promotes local spindle assembly (Sampath et al., 2004; Kelly et al., 2007; Tseng et al., 2010). Aurora B, in the vicinity of chromosomes, phosphorylates and inhibits the depolymerase kinesin-13, Kif2c/MCAK (Andrews et al., 2004; Ohi et al., 2004). This favours MTs polymerisation and stabilization. It is not clear whether Aurora B can promote MT nucleation from the kinetochore region, by phosphorylating proteins with direct MTs nucleation activity.

Aurora B is essential for cytokinesis. Aurora B regulates the later stages of mitosis, by translocation from chromosomes to the structure of the central spindle. Later, Aurora B/CPC transfers to the equatorial cell cortex, the region of the plasma membrane where the accession machinery is assembled (Carmena et al., 2012). Re-localization of the CPC is mediated by several factors. The ubiquitylation of Aurora B by E3 ubiquitin ligase cullin 3 (CUL3) regulates removal of CPC from chromosomes and promotes re-localization in anaphase (Sumara et al., 2007). At the same time, dephosphorylation of the CDK1 site in INCENP (Cdc14 site in SLi15) targets CPC to MTs (Hümmer and Mayer, 2009; Pereira and Schiebel, 2003). CPC is transported to

the central spindle by the kinesin-6 member, Kif20A/Mklp2 (Mitotic kinesin-like protein 2; also known as Subito in Drosophila; Gruneberg et al., 2004; Cesario et al., 2006). In budding yeast, which lack Kif20A/Mklp2, targeting of Ipl1 (Aurora B) to the spindle midzone is mediated through MT plus end binding protein Bim1 (a homolog of EB1) (Zimniak et al., 2012).

Once at the central spindle, Aurora B promotes stabilization of the spindle midzone, through phosphorylation of centralspindlin components kinesin-6 Kif23/Mklp1 (also known as Pavarotti in Drosophila) and MgcRacGAP (Guse et al., 2005; Neef et al., 2006; Douglas et al., 2010; Minoshima et al., 2003; Ban et al., 2004). This phosphorylation also contributes to the recruitment of factors important for telophase and cytokinesis. Aurora B also restricts the central spindle size through phosphorylation of Kif4A on T799, which promotes interaction with MT bundling protein PRC1 (Protein regulator of cytokinesis 1; Nunes Bastos et al., 2013; Mollinari et al., 2002). Stabilization of the central spindle is additionally promoted by the inhibitory effect of Aurora B on kinesin-13 Kif2a, which blocks kinesin depolymerising activity (Uehara et al., 2013).

In telophase, Aurora B is important for contractile ring maturation, and phosphorylates MgcRacGAP, GEF-H1/ARGHEF2 at S855, myosin regulatory light chain II, vimentin, desmin and GFAP (Glial fibrillar acidic protein), key substrates in this process (Minoshima et al., 2003; Birkenfeld et al., 2008; Murata-Hori et al., 2000; Goto et al., 2003; Kawajiri et al., 2003). It is not clear what role Aurora B/CPC has in the ring formation. In cytokinesis, CPC regulate timely abscission in higher eukaryotes through phosphorylation of CHMP4C/Snf7, a subunit of ESCRT-III, which is responsible for membrane fission at the end of cytokinesis (Elia et al., 2011; Guizetti et al., 2011; Carlton et al., 2012; Capalbo et al., 2012). Aurora B is capable of delaying abscission in response to lagging chromosomes, preventing chromosome breakage or tetraploidization (Norden et al., 2006; Steigemann et al., 2009). However, the role of Aurora B in the cytokinesis checkpoint is not completely clear.

Both Aurora A and Aurora B kinase have been associated with cancer. Many solid cancers including colorectal, rectal, breast, ovarian, prostate, neuroblastoma and cervical, as well as primary tumour tissue and cell lines, exhibited increased copy number of the Aurora A gene or Aurora A protein level was elevated (Bischoff et al., 1998; Tatsuka et al., 1998; Zhou et al., 1998; Takahashi et al., 2000; Tchatchou et al., 2007; Tanner et al., 2000; McKlveen Buschhorn et al., 2005; Twu et al., 2009). Overexpression of Aurora B has also been connected with cancer, such as oral, breast and lung cancer (Qi et al., 2007; Tchatchou et al., 2007; Takeshita et al., 2013). Based on their role in cancer development and progression, Aurora kinases have been drug targets for cancer treatment. Various inhibitors of Aurora kinases have undergone preclinical testing, first *in vitro*, then in animal models (Nikonova et al., 2013). Development of such drugs has significantly benefited studies of Aurora kinases function in mitosis. Some of those small molecule inhibitors have been used in this study too.

Table 1.2: List of Aurora B substrates with specific phosphorylation known to affect mitosis. Shared substrates with Aurora A are marked with *, Human refers to human cultured cells.

Aurora B kinase			
Substrate	Phosphosite	Organism	Reference
Aurora B	T232	Human	Yasui et al., 2004
INCENP	T893, S894, S895	Human, Chicken	Bishop et al., 2002; Honda et al., 2003, Xu et al., 2010
Survivin/BIRC5	T117	Human	Wheatley et al., 2004
CENP-A*	S7	Human	Zeitlin et al., 2001
Haspin/GSG2	S93, S108, S143 (possible more)	Human	Wang F. et al., 2011
Hist1H3A*	S10	Yeast, Human	Hsu et al., 2000; Sugiyama et al., 2002; Hauf et al., 2003
H2AX	S121	Human	Shimada et al., 2016
hCAP-H/cnd2*	S70 (S5,S41,S52 in Fission yeast)	Human, Fission yeast	Tada et al., 2011; Nakazawa et al., 2011; Ono et al., 2004
Repo-Man/CDCA2	S893	Human	Qian et al., 2013
p53*	S183, T211, S215	Human	Gully et al., 2012
HEC1/Ndc80	S5, S15, S44, S49, S55, S62, S69 (T21, S37, T54, T71, T74, S95, S100 in Budding Yeast)	Mammals, Budding yeast	Cheeseman et al., 2002 ; DeLuca et al., 2006; Ciferri et al., 2008; Akiyoshi et al., 2009
Dsn1/KNL-3	S100, S109 (S240, S250 in Budding yeast)	Human, Budding yeast	Welburn et al., 2010; Akiyoshi et al., 2013; Kim and Yu, 2015
KNL-1/CASC5/Blinkin	S24, S60	Human	Welburn et al., 2010; Nijenhuis et al., 2014
Dam1	S20,S527, S265, S292, S327	Budding yeast	Cheeseman et al., 2002; Kalantzaki et al., 2015
Spc34	T199	Budding yeast	Cheeseman et al., 2002
CENP-E/Kinesin-7*	T422	Human	Kim et al., 2010
Zwint-1	S250, T251, S262	Rat, Human	Kasuboski et al., 2011
Sgo2/Shugoshin 2	T537 (more detected in vitro)	Human	Tanno et al., 2010
Kif2c/MCAK*	T95, S110,S177,S196	Frog	Andrews et al., 2004; Ohi et al., 2004
Kif2a*	T97, S157	Human	Ueahara et al., 2013; Knowlton et al., 2009
Kif23/Mklp1/CHO1	S812, S911 (S708 in worm)	Worm, Human	Guse et al., 2005; Neef et al., 2006; Douglas et al., 2010
Kif4a	T799	Human	Nunes Bastos et al., 2013
SHCBP1	S634	Human	Asano et al., 2013
RacGAP1/MgcRacGAP	S144, T186, S387	Human	Minoshima et al., 2003; Ban et al., 2004
GEF-H1/ARHGEF2	S885	Human	Birkenfeld et al., 2007
CHMP4C/Snf7	S210	Human	Carlton et al., 2012; Capalbo et al., 2012
Desmin	S59	Human	Kawajiri et al., 2003
Vimentin	S72	Mouse, Human	Goto et al., 2003
MRLC2	S19	Human	Murata-Hori et al., 2000
MAPRE3/EB3*	S176	Human	Ferreira et al., 2013
MAPRE2/EB2	S222,S223	Human	Iimori et al., 2016
GFAP	T7, S13, S38	*in vitro*/Human cells?	Kawajiri et al., 2003
Borealin/CDCA8	S165	*in vitro*	Gassmann et al., 2004
HMGN2	S25, S29	*in vitro*	Hengeveld et al., 2012
HP1α/CBX5	S92	*in vitro*	Hengeveld et al., 2012
TopIIα	Not mapped	*in vitro*	Morrison et al., 2002

1.4 **Project aims**

Aurora kinases are a significant focus of cell biology research, owing to their essential function in controlling error-free cell division and their link with proliferative diseases, such as cancer. Despite many known mechanisms depending on Aurora kinase regulation of cell division apparatus, there are still processes likely to involve Auroras with unclear mechanisms. Some of these Aurora-regulated processes involve early or late mitotic events, such as local, non-centrosomal spindle assembly, regulation of chromosome congression and cytokinesis. It is thought that the substrates involved in these mechanisms might be shared between Aurora kinases, both Aurora A and Aurora B may phosphorylate these substrates at a specific time and localization within the division process.

The objective of this project was to better understand the role of Aurora kinases in the regulation of mitosis. I first aimed to reveal the molecular mechanism of Aurora A regulation of kinetochore-MT attachments that contributes to chromosome congression. Previously, this was thought to be exclusively Aurora B function. I examined the contribution of each Aurora kinase to the phosphorylation of the outer kinetochore component that binds MTs, HEC1/Ndc80, using imaging tools and molecular inhibitors.

The second aim of my project was to develop a tool to determine novel Aurora kinase substrates, which could contribute to further dissection of Aurora regulation of mitosis. I undertook a bioinformatic approach that predicts Aurora substrates based on shared consensus sequence of Aurora kinases in combination with several parameters that govern the substrate specificity of Auroras. First, I tested the candidate phosphorylation *in vitro*, and then confirmed and further characterized the phosphorylation of one selected protein substrate in cells.

2 Chapter 2: Aurora A kinase phosphorylates HEC1/Ndc80 contributing to the correction of mal-oriented chromosomes near the spindle poles

This chapter includes work published in Current Biology (2015) under joined authorship of Ye AA, **Deretic J**, Hoel CM, Hinman AW, Cimini D, Welburn JP and Maresca TJ. The title of the published work is 'Aurora A kinase contributes to a pole-based error correction pathway'.

2.1 **Introduction**

Errors in chromosome-MT attachments can occur frequently in early cell division but are corrected before anaphase can proceed (Cimini et al, 2003; Kitajima et al, 2011). These errors can be classified as syntelic attachment, which is characterised by the attachment of both sister kinetochores to the same pole, or merotelic attachment, which is characterised by the attachment of one of the sister kinetochore to both poles. Importantly, cells do possess the machinery to efficiently correct improper chromosome attachments or lack of attachments in the case of transient monotelic attachment, when single kinetochore is attached to one spindle pole (Figure 2.1).

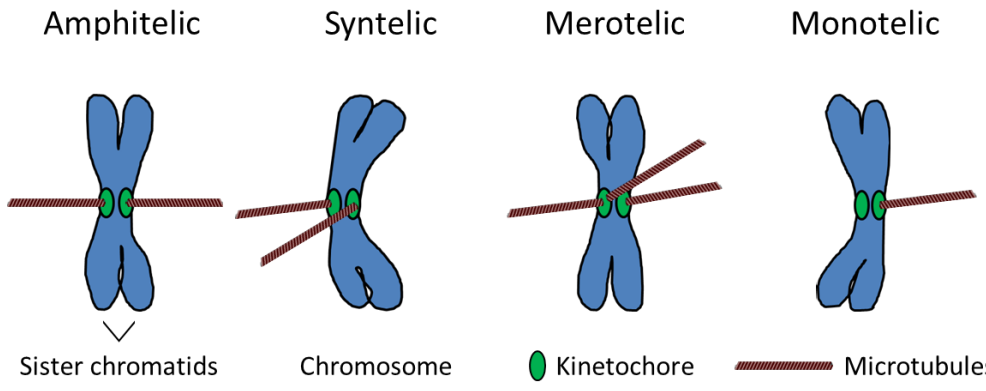

Figure 2.1: Different types of kinetochore-MT attachments in prometaphase. Four types of kinetochore-MT attachments are presented here with correct amphitelic attachments or bi-orientation depicted first. Chromosomes are drawn in blue, MTs in red, and kinetochores are presented as green ovals (adapted from Yamagishi et al., 2014).

2.1.1 The role of Aurora B in correction of erroneous kinetochore-microtubule attachments: centromere-based model

The model of resolving erroneous syntelic and merotelic attachments is focused on centromere-localized Aurora B and its activity (Biggins et al., 1999; Tanaka et al., 2002; Cheeseman et al., 2002; Hauf et al., 2003). This model proposes that the correction of improper attachments is regulated by the physical distance between Aurora B kinase and its substrates at the outer kinetochore. This in turn is proposed to be regulated by the tensions established at the kinetochores. When chromosomes are bi-oriented with established proper amphitelic attachments, the tension exerted on sister chromatids stretches the centromere and the kinetochore. Under tension the outer kinetochore substrates are positioned further away from Aurora B, and phosphorylation is low while SAC is silenced (Liu et al., 2009; Uchida et al., 2009). It was shown that the tension caused direct mechanical stabilization of proper kinetochore-MT attachments (Akiyoshi et al., 2010). These proper kinetochore-MT attachments are stabilized and maintained through the additional activity of PP1 (Protein phosphatase 1) that dephosphorylate kinetochore substrates (Sassoon et al., 1999; Liu et al., 2010; Kim et al., 2010; London et al., 2012).

In the presence of an incorrect kinetochore-MT attachment, the tension between sister kinetochores is low, and consequently the inter-kinetochore distance decreases, as well as the distance between individual kinetochore components (Maresca and Salmon, 2009). This prompts centromere-tethered Aurora B kinase to phosphorylate the kinetochore substrates, specifically the KMN network (Liu et al., 2009, Welburn et al., 2010). The HEC1/Ndc80 complex, as part of the KMN network, is one of the key Aurora B substrates in the outer kinetochore, and it is particularly the N terminus tail of HEC1/Ndc80 that directly connects kinetochores and MTs (DeLuca et al., 2006, Cheeseman et al., 2006; Wei et al., 2007; Ciferri et al., 2008; Guimaraes et al., 2008; Miller et al., 2008). Without tension at the kinetochores, the HEC1/Ndc80 N terminus is phosphorylated on multiple sites, which decreases its affinity for MTs and destabilizes incorrect

attachments (DeLuca et al., 2011; DeLuca et al., 2006; Cheeseman et al., 2006; Ciferri et al., 2008; Alushin et al., 2010). Additionally, the activity of Aurora B on the outer kinetochore recruits components of SAC, which then inhibits APC/C causing a delay in cell division until the proper kinetochore-MT attachments are established (Biggins and Murray, 2001; Ditchfield et al., 2003). SAC can be activated at the kinetochores without Aurora B by tethering the kinase Mps1, which is the upstream activator of SAC (Saurin et al., 2011; Maldonado and Kapoor, 2011). This may indicate that Aurora B is required for Mps1 recruitment to the kinetochore (Saurin et al., 2011; Maldonado and Kapoor, 2011).

The reported size of the CPC complex and the distances between sister kinetochores fit well with this model of phosphorylation of kinetochore substrates being merely controlled by physical separation from Aurora B due to tension (Bolton et al., 2002). The experiments employing Förster resonance energy transfer (FRET) sensor confirmed the Aurora B activity gradient. The substrate phosphorylation is the highest at the centromeric chromatin and decreases towards kinetochore, so that phosphorylation at the kinetochore depends on its distance from the Aurora B at the inner centromere, which increases with tension (Liu et al., 2009; Wang E. et al., 2011; Figure 2.2). The Aurora B gradient of activity around centromeres still remains unclear, as the gradient was also observed on the MTs (Tan and Kapoor, 2011).

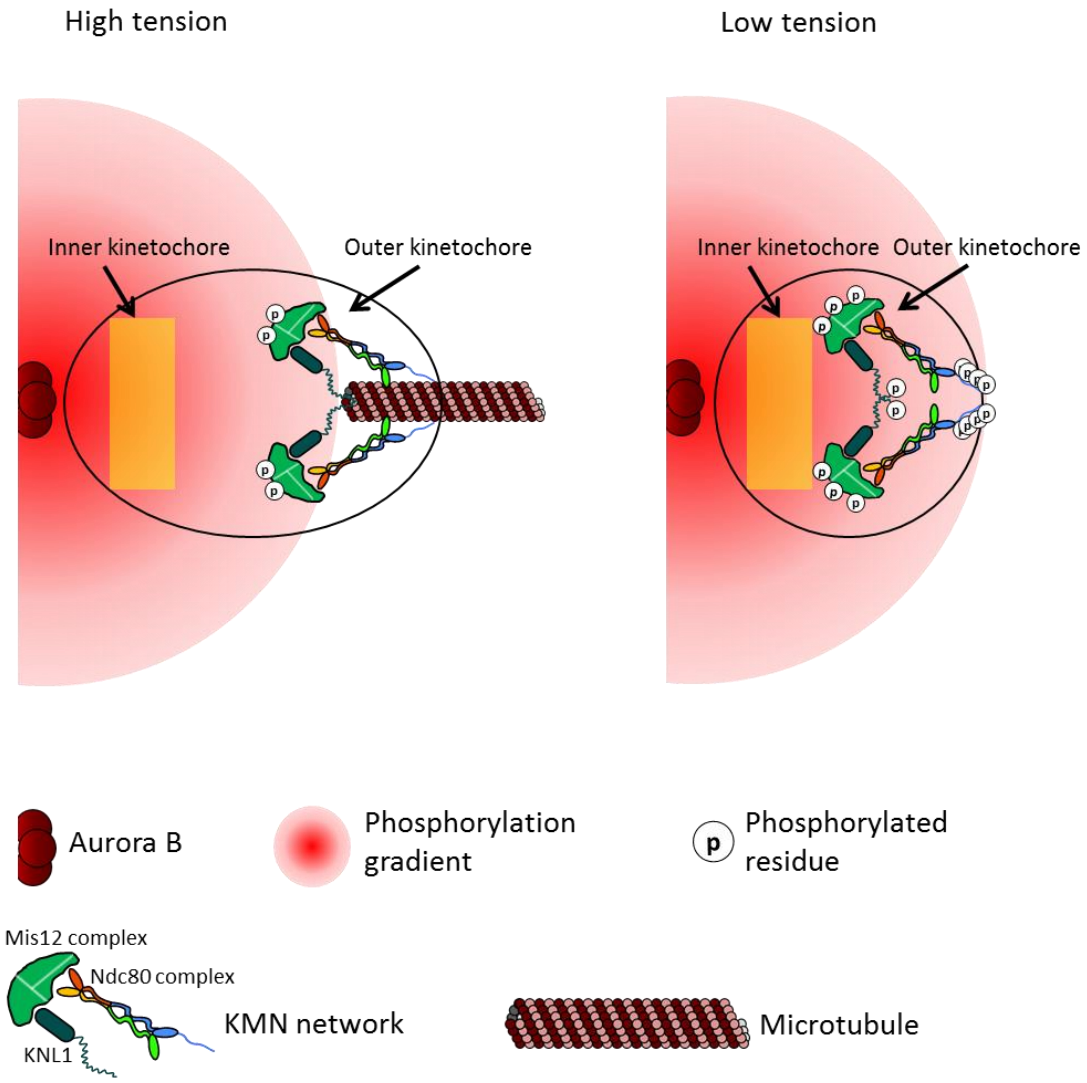

Figure 2.2: Centromere-based model of error correction, a schematic view. The phosphorylation gradient around centromere-localized Aurora B is presented in pink. For simplicity, the inner kinetochore is presented as yellow rectangular, while its structure and connections with outer kinetochore is omitted. The outer kinetochore is depicted in more details, showing KMN network and its component: KNL1, Mis12 complex and Ndc80 complex that directly binds MT drawn in red (adapted from Welburn et al., 2010).

This model cannot explain how the erroneous syntelic kinetochore-MT attachments are corrected when they come under tension due to polar ejection forces (PEF), which are highest near the spindle poles (Cassimeris et al., 1994; Ke et al., 2009). PEFs are produced by the polar MT arrays that push the chromosome arms away from the poles. PEFs can be mediated by the chromokinesins, which are specialized chromosome-associated kinesins that connect these interpolar MTs with chromosome arms (Antonio et al., 2000; Funabiki and Murray, 2000; Mazumdar and

Misteli, 2005; Wandke et al., 2012). PEFs oppose the kinetochore-mediated pulling forces, and this may create tension at the kinetochores. As chromokinesins are over-expressed, elevated PEFs cause a stabilization of syntelic attachments, likely due to overcoming the Aurora B destabilization activity (Cane et al., 2013). FRET data indicates that the Aurora B activity gradient is the weakest near the spindle poles where PEFs are the strongest (Tan and Kapoor 2011; Carmena et al., 2012).

Likewise, there is the evidence that targeting Aurora B to the centromere is not essential for early stages in mitosis and chromosome alignment at the metaphase plate in vertebrate cells (Yue et al., 2008). In budding yeast, the mutant of Aurora B/Ipl1 corrects attachment errors, though it does not localize to the centromere, but it is enriched at the MTs (Campbell and Desai, 2013). This again suggests that the centromeric pull of Aurora B is dispensable for chromosome bi-orientation, or that another kinase contributes to error correction.

2.1.2 **Correction of erroneous kinetochore-microtubule attachments near the spindle pole**

It was observed that after nuclear envelope breakdown, chromosomes with syntelic attachments move to the spindle pole. This is where erroneous attachments are corrected before chromosomes move to the metaphase plate (Skibbens et al., 1993; Lampson et al., 2004). The syntelic, mono-oriented chromosomes attached to the plus ends of MTs move to the closer pole through the process of K-fibre disassembly (Lampson et al., 2004). This is slower than Dynein-mediated poleward movement of chromosomes attached on lateral surface of MTs (Sharp et al., 2000; Li et al., 2007; Barisic et al, 2014). However, in both cases of poleward transport, incorrectly attached chromosomes temporarily stay near the pole, before they congress following bi-orientation, or through CENP-E-dependent transport to the spindle equator (Roos, 1976; Rieder and Alexander, 1990; Lampson et al., 2004; Kapoor et al., 2006).

At the spindle poles, the centrosome-based Aurora A kinase has been implicated in chromosome alignment in several studies using various human cell types and mouse embryos (Marumoto et al., 2003; Hoar et al., 2007; Sasai et al.,

2008). Down-regulation of human Aurora A using small interfering RNA (siRNA), or inhibition with antibody injection after initial centrosome separation, led to misaligned chromosomes during metaphase. This showed that Aurora A was directly involved in chromosome alignment at the metaphase plate independent of its function in centrosome separation and maturation (Marumoto et al., 2003). Inhibition of Aurora A with small molecule inhibitor, MLN8054 (Hoar et al., 2007; Manfredi et al., 2007), and a mouse Aurora A-null embryo (Sasai et al., 2008), confirmed the alignment defects during metaphase. Together these studies suggested that the lack of Aurora A delayed mitosis through impaired maintenance of SAC. It has also been suggested that Aurora A has a role in the regulation of kinetochore-MT interaction (Marumoto et al., 2003; Sasai et al., 2008). Aurora A has been implicated in the stabilization of kinetochore-MT attachment in human cells, specifically as a response to DNA damage (Katayama et al, 2008; Bakhoum et al, 2014).

However, the contribution of Aurora A to error correction is not well understood. Aurora A could promote higher kinetochore-MT destabilization close to the spindle poles. The evidence of centrosomal-based gradient of Aurora A activity would support this hypothesis. A centrosomal TPX2/Aurora A kinase activity gradient was first suggested in worms (Greenan et al, 2010).

The Maresca lab investigated whether there is a gradient of Aurora A activity, and whether Aurora A potently destabilizes incorrect kinetochore-MT attachments near poles in Drosophila cells. Importantly, the exact molecular mechanism of Aurora A action in error correction is not clear. I have contributed to this work by investigating the molecular mechanism of Aurora A correction of erroneous kinetochore-MT attachments close to the centrosomes in HeLa cells. I tested whether HEC1/Ndc80 at the kinetochore-MT interface is a major downstream target of Aurora A to correct kinetochore-MT attachments.

2.2 Results

2.2.1 Aurora A kinase inhibition reduces phosphorylation of the HEC1/Ndc80 N terminus

Since Aurora A is implicated in the regulation of chromosome congression, I tested whether Aurora A phosphorylation can regulate the outermost kinetochore protein HEC1/Ndc80 interaction with MTs. In this study I have used the antibody against phosphorylated S55 on HEC1/Ndc80 N terminus (described in DeLuca et al., 2011) to examine the Aurora A phosphorylation of the HEC1/Ndc80 N terminus in HeLa cells treated with Aurora kinases inhibitors.

First, I observed the S55 phosphorylation at unattached kinetochores in HeLa cells. When kinetochores are unattached to MTs, Aurora B and SAC are highly activated leading to more prominent phosphorylation of HEC1/Ndc80 S55. To create unattached kinetochores, I used high a concentration of nocodazole to depolymerize MTs. A strong signal of phosphorylated S55 on HEC1/Ndc80 was observed on unattached kinetochores, and it was adjacent to the CENP-A signal marking the centromere.

To examine the Aurora B contribution in phosphorylation of HEC1/Ndc80 S55, I used an Aurora B specific inhibitor ZM447439 (Ditchfield et al., 2003). Inhibition of Aurora B showed an expected and significant decrease of approximately 40% in phosphorylation levels of S55 in HEC1/Ndc80 N terminus compared to CENPA levels at centromeres. An even greater reduction in S55 phosphorylation, more than 60%, was observed when nocodazole treated cells were subjected to an Aurora A specific inhibitor Alisertib (MLN8237; Manfredi et al., 2011). Phosphorylation of S55 was most reduced upon simultaneous inhibition of both Aurora A and Aurora B (Figure 2.3). This indicates that S55 in the HEC1/Ndc80 N terminus is both a substrate of Aurora A and Aurora B.

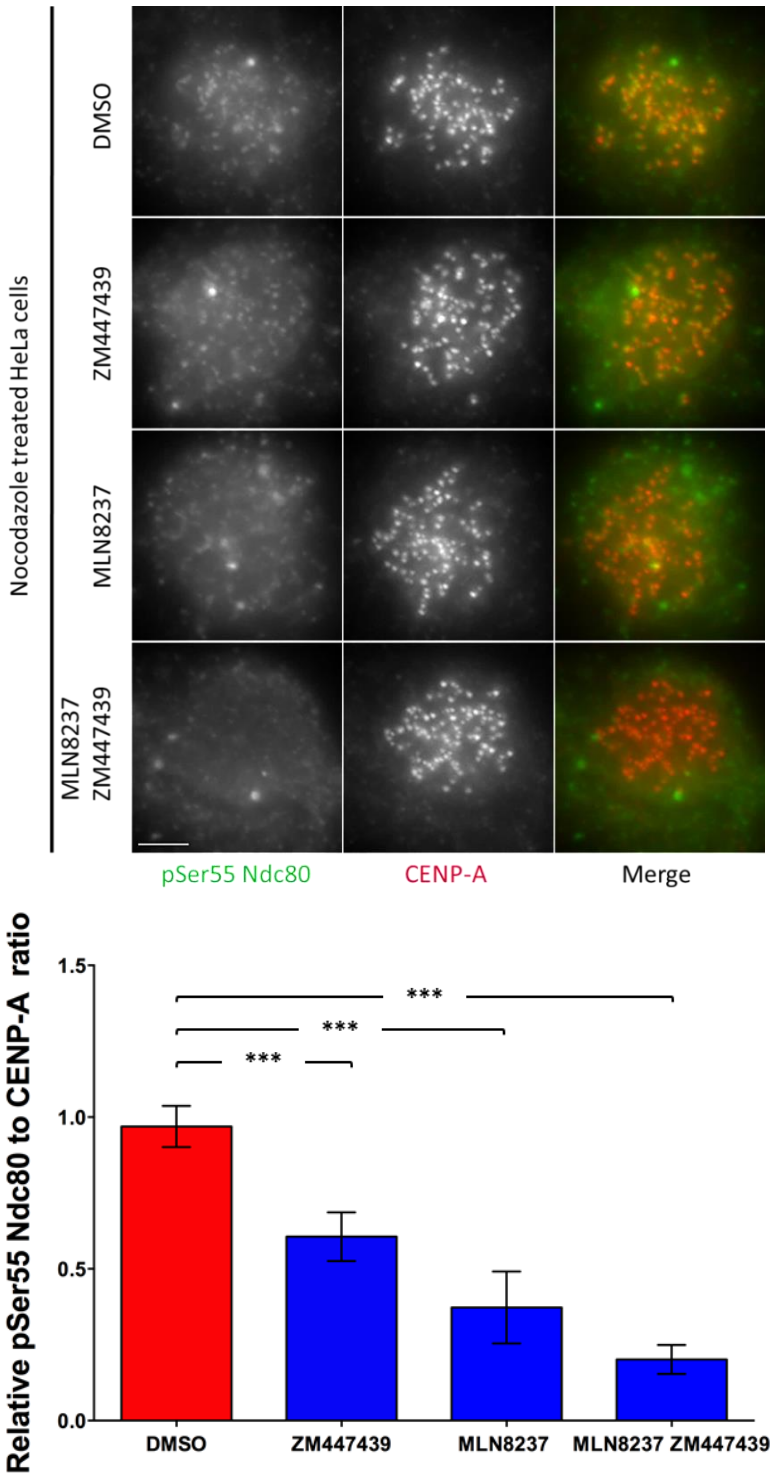

Figure 2.3: Aurora A phosphorylates outer kinetochore structure in HeLa cells. Representative images of HeLa cells treated with drug nocodazole for 2h together with either DMSO (control), 2 µM Aurora B inhibitor ZM447439, 300 nM Aurora A inhibitor MLN8237 or both inhibitors together. The cells were stained with antibodies against phosphorylated S55 on HEC1/Ndc80 and CENP-A. The bar graph presents the mean values of phosphorylated S55 HEC1/Ndc80 to CENP-A ratio. DMSO, n=1159 kinetochores from 23 cells; ZM447439, n=872 kinetochores from 14 cells; MLN8237, n=812 kinetochores from 17 cells MLN8237+ZM447439, n=874 kinetochores from 16 cells. The error bars represent the standard error of the mean. Two-tailed p values of a Student's t-test reported: ***p<0.0001. Scale bar is 5 µm.

Phosphorylation of HEC1/Ndc80 S55 was reported to vary with the concentration of nocodazole (DeLuca et al., 2011). Moreover, the Aurora B inhibitor ZM447439 was reported to decrease the level of HEC1/Ndc80 at the kinetochores to the extent ranging from 20% to 50% (Kim and Yu, 2015; Welburn et al., 2010). To test whether the observed decrease in phosphorylation of HEC1/Ndc80 S55 was not due to the decreased level of HEC1/Ndc80 at the outer kinetochore, I normalized levels of HEC1/Ndc80 S55 phosphorylation to HEC1/Ndc80, not CENP-A. I have also tested two different concentrations of MLN8237. To show that the phosphorylation of S55 decreases independently of kinetochores attachment states in the presence of Aurora A inhibitor, phosphorylation levels were measured in the cells without previous treatment with nocodazole. MLN8237 significantly reduced the phosphorylation of S55 on HEC1/Ndc80 in comparison with the total levels of HEC1/Ndc80 at the attached kinetochores, regardless of the applied concentration (Figure 2.4).

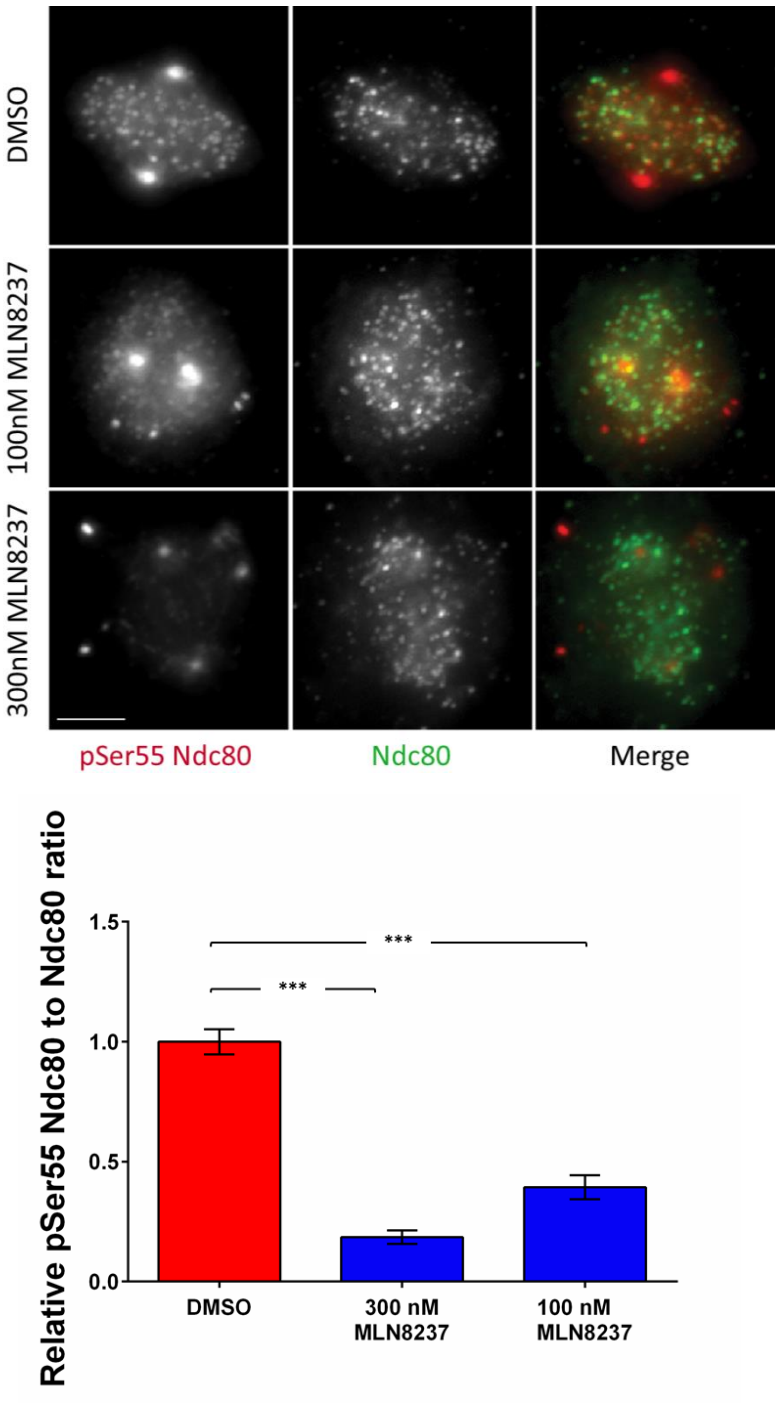

Figure 2.4: The total phosphorylation of HEC1/Ndc80 at attached kinetochores is reduced with Aurora A inhibition. The phosphorylation of HEC1/Ndc80 was analysed in HeLa cells treated with above indicated amounts of the Aurora A inhibitor MLN8237, without previous treatment with nocodazole. The cells were stained with antibody against phosphorylated S55 on HEC1/Ndc80 and antibody against HEC1/Ndc80. DMSO, n=280 kinetochores from 14 cells; 300 nM MLN8237, n=275 kinetochores from 12 cells; 100 nM MLN8237, n=299 kinetochores from 14 cells. The error bars represent the standard error of the mean. P values of one-way ANOVA multiple comparisons test are reported: ***p<0.0001 Scale bar is 5 µm.

2.2.2 **Kinetochores phosphorylation is higher at the spindle poles**

Due to the Aurora A localization around the centrosomes, and at regions of MTs proximal to the centrosomes (Roghi et al., 1998; Sugimoto et al., 2002; Carmena and Earnshaw, 2003), we hypothesised that Aurora A is involved in error correction near spindle poles/centrosomes. Using a kinetochore targeted FRET assay Ye showed that the FRET probe at the kinetochores was more phosphorylated when the kinetochores were closer to the spindle poles in Drosophila S2 cells. This phosphorylation was reduced in an Aurora A knock-down using siRNA (Ye et al., 2015). Likewise, I assessed the effect of pole proximity to changes in HEC1/Ndc80 phosphorylation with active or inhibited Aurora A. My previous experiments revealed that Aurora A phosphorylates HEC1/Ndc80, but the positional effect on kinetochore phosphorylation in HeLa cells was not clear.

To examine the spatial contribution of Aurora A to phosphorylation of S55 at the HEC1/Ndc80 N terminus I used centromere-associated protein E (CENP-E) inhibitor GSK923295 (Wood et al., 2010) as a tool to create misaligned kinetochores closer to one of the poles (polar kinetochores) and aligned kinetochores at the metaphase plate in HeLa cells (Gudimchuk et al., 2013). Increased phosphorylation of the polar kinetochores was observed after CENP-E inhibition. Aurora A and CENP-E inhibition significantly reduced the phosphorylation of S55 in both polar kinetochores and kinetochores further away from poles, although to a less extent than polar kinetochores (Figure 2.5). These data indicate that Aurora A contributes to the phosphorylation of S55 at the N terminus of HEC1/Ndc80.

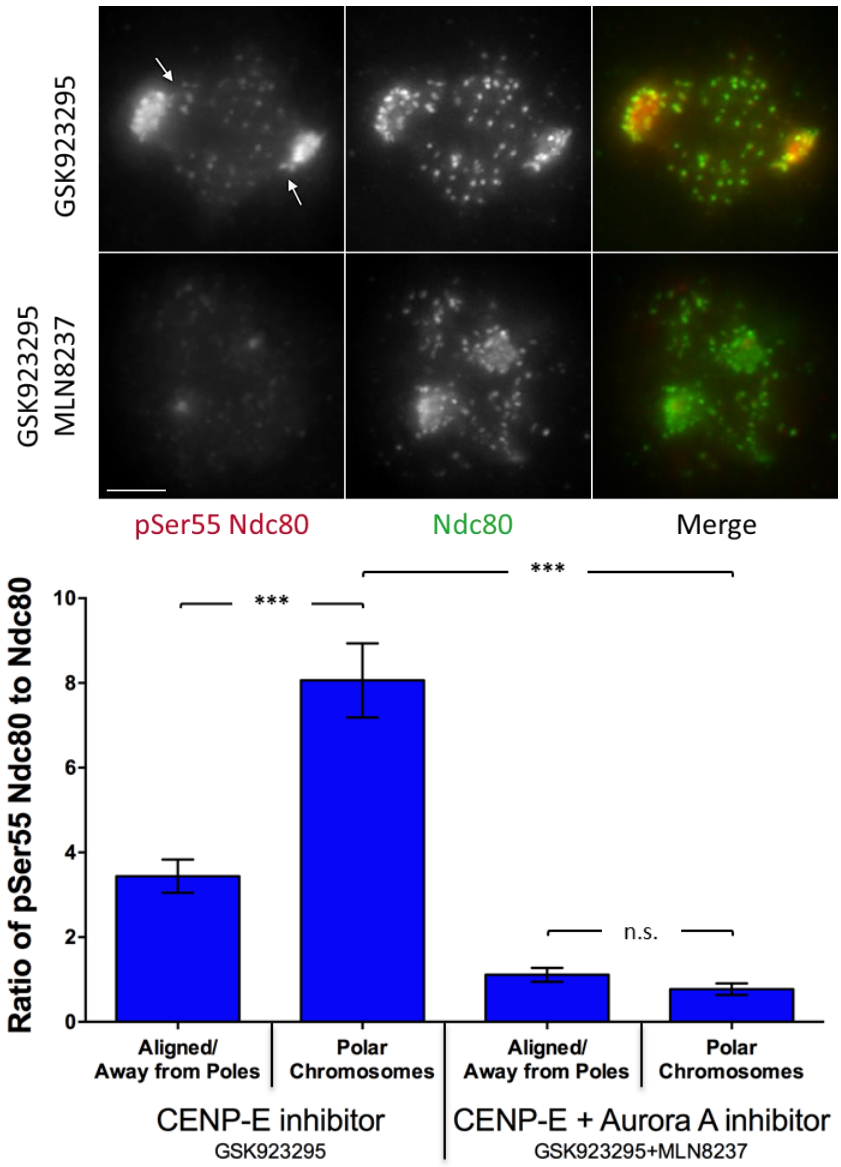

Figure 2.5: The phosphorylation of S55 in HEC1/Ndc80 by Aurora A is spatially regulated. The difference in spatial phosphorylation of kinetochore was assessed using the CENP-E inhibitor GSK923295 to generate polar and aligned chromosomes in the HeLa cells in the presence and absence of 300 nM Aurora A inhibitor. Arrows point to the polar kinetochores. Polar kinetochores in both CENP-E and CENP-E/Aurora A inhibition were defined as the kinetochores proximal to the unspecific staining at the spindle poles created by the pS55 HEC1/Ndc80 antibody (described in DeLuca et al., 2011). GSK923295, aligned/away from poles n = 408 kinetochores from 68 cells; polar n = 239 kinetochores from 68 cells; GSK923295 + MLN 8237, aligned/away from poles n = 465 kinetochores from 55 cells; polar n = 207 kinetochores from 55 cells. The error bars represent the standard error of the mean. P values of one-way ANOVA multiple comparisons test are reported: not significant (n.s.), ***p<0.0001. Scale bar is 5 µm.

2.2.3 **Aurora A directly phosphorylates the N terminus of HEC1/Ndc80 *in vitro***

The experiments in cell culture using small molecule inhibitors indicate Aurora A contribution in the phosphorylation of S55 at the HEC1/Ndc80 N terminus. To test if Aurora A directly phosphorylates S55, I performed an *in vitro* assay with a purified recombinant $Ndc80_{bonsai}$ complex (Ciferri et al., 2008; purified by Agata Głuszek-Kustusz) and recombinant Aurora A. Using a phosphospecific S55 HEC1/Ndc80 antibody, I observed that S55 in HEC1/Ndc80 was efficiently phosphorylated (Figure 2.6).

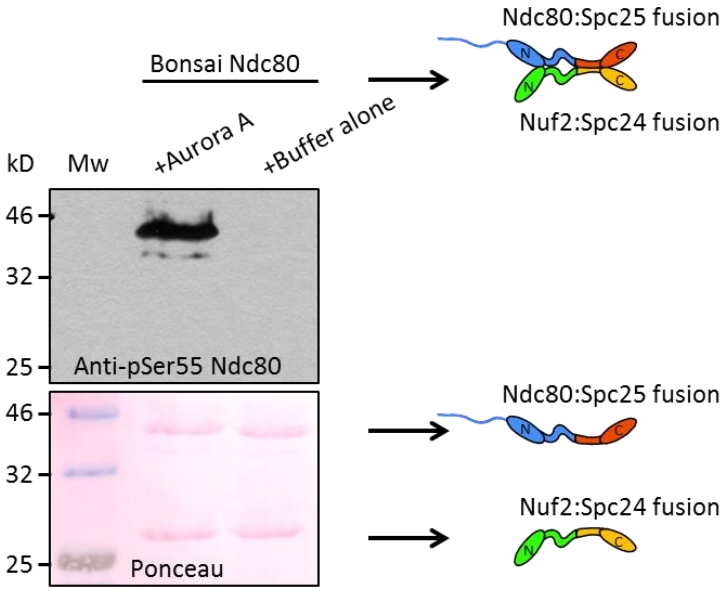

Figure 2.6: Recombinant $Ndc80_{bonsai}$ is phosphorylated by Aurora A kinase *in vitro*. Phosphorylation and the mock reactions were performed in the presence of 10 mM ATP in kinase buffer and 4µg of substrate for 30 min at 37°C. The reactions were terminated by addition of SDS sample loading buffer and the products were separated on SDS polyacrylamide gel. Ponceau staining of the nitrocellulose membrane after western blotting transfer showed the position of $Ndc80_{bonsai}$ complex relative to the molecular weight marker. Diagram of $Ndc80_{bonsai}$ complex was adopted from Ciferri et al., 2008. Phosphorylation was detected with antibody against phosphorylated S55 on HEC1/Ndc80.

2.2.4 **Characterizing the specificity of Aurora A inhibitor MLN8237 in HeLa cells**

MLN8237 is a potent inhibitor of Aurora A, and it is reported to be two hundred times more selective for Aurora A over Aurora B in cells (Manfredi et al., 2011). To test the selectivity of the inhibitor and to show that the reduction in phosphorylation levels of HEC1/Ndc80 was due to Aurora A and not Aurora B inhibition, I examined whether MLN8237 treatment affected the Aurora B kinase substrate H3 pS10 (Hsu et al., 2000; Murnion et al., 2001) and total levels of HEC1/Ndc80 at the kinetochores. Several studies have previously shown that Aurora A also phosphorylates S10 in the tail of H3 (Crosio et al., 2002; Ferrari et al., 2005). The phosphorylation levels of Histone H3 S10 were not significantly reduced in 300 nM or 100 nM MLN8237 with respect to the control metaphase cells (Figure 2.7A). However, 300 nM of Aurora A inhibitor MLN8237, the concentration used to assess the phosphorylation levels of S55 HEC1/Ndc80, reduced the total levels of HEC1/Ndc80 at the kinetochores with respect to the levels of CENP-A (Figure 2.7B). This indicates partial inhibition of Aurora B kinase with this concentration of inhibitor (Kim and Yu, 2015; Welburn et al., 2010), while 100 nM did not affect Aurora B or levels of HEC1/Ndc80 at the kinetochores (Figure 2.7B).

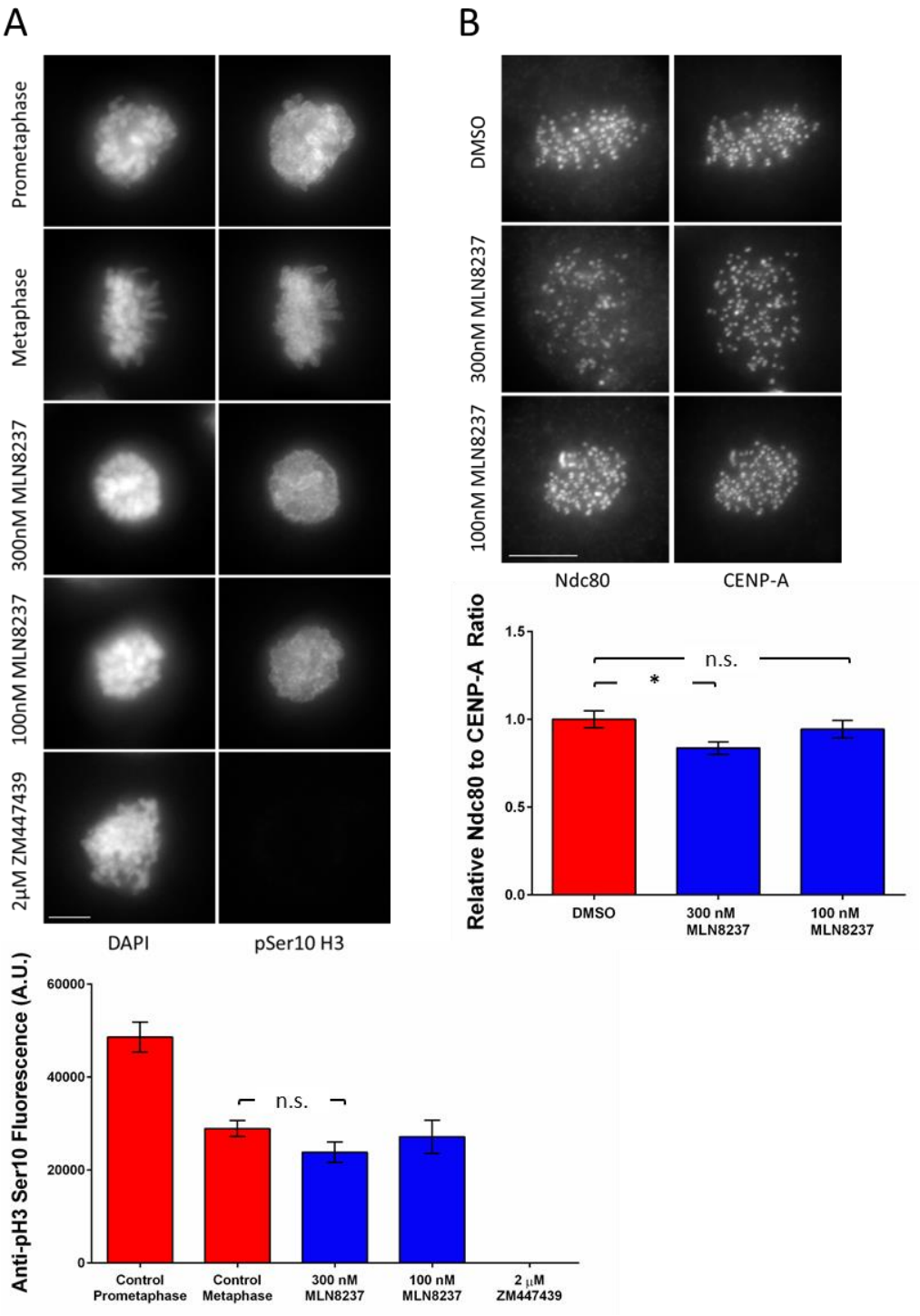

Figure 2.7: MLN8237 is Aurora A specific inhibitor. (A) Phosphorylation of Histone H3 analysis. The HeLa cells were stained with antibody against phosphorylated S10 H3, as primarily Aurora B substrate, after treatment with either DMSO (control), 2 µM ZM447439, 300 nM or 100 nM MLN8237. control prometaphase; n=12 cells, control metaphase; n=18 cells, 300 nM MLN8237; n=31 cells, and 2 µM ZM447439; n=10 cells. (B) Analysis of the HEC1/Ndc80 levels at the kinetochores. The HeLa cells were treated with either DMSO, 300 nM MLN8237 or 100 nM MLN8237, then fixed and stained with antibodies against Ndc80 and CENP-A. DMSO, n=578 kinetochores from 20 cells; 300 nM MLN8237, n=832 kinetochores from 21 cells; 100 nM MLN8237, n=731 kinetochores from 20 cells. P values of one-way ANOVA multiple comparisons test are reported: not significant (n.s.), *p<0.05 (0.035).The error bars represent the standard error of the mean. Scale bar is 5 µm.

2.3 **Discussion**

Aurora A was suggested to regulate chromosome congression and kinetochore-MT attachments (Marumoto et al., 2003; Hoar et al., 2007; Sasai et al., 2008; Katayama et al, 2008; Bakhoum et al, 2014). The molecular mechanism of Aurora regulation of the kinetochore-MT attachments was not known. In this study, I showed that centrosome-localized Aurora A contributes to the error correction of kinetochore-MT attachments in the vicinity of centrosomes. Aurora A kinase phosphorylates the outer kinetochore protein HEC1/Ndc80 (and possibly other components of the KMN network) to control the kinetochore-MT attachment state.

The concentration of 300nM MLN8237 I used to assess Aurora A contribution to the HEC1/Ndc80 phosphorylation did moderately affect Aurora B, so it may have interfered with the HEC1/Ndc80 recruitment at kinetochores. However, the reduction of 16% in the total level of HEC1/Ndc80 cannot account for the entire 65% decrease in phosphorylation of S55 in HEC1/Ndc80 after the treatment with 300 nM MLN8237 (Figure 2.7B and Figure 2.3). A significant reduction in S55 phosphorylation was still observed when compared to HEC1/Ndc80 (Figure 2.4). From the *in vitro* data, I showed that HEC1/Ndc80 is a direct substrate of Aurora A. Taken together, my results indicate that HEC1/Ndc80 is a shared Aurora A and Aurora B substrate. This is further supported by the phospho-proteomic analysis of the cell lysate, which suggests that HEC1/Ndc80 is predominately targeted by Aurora A (Kettenbach et al., 2011).

My data complement the results achieved by the Maresca lab, who showed that Aurora A destabilises erroneous syntelic kinetochore-MT attachments using an assay that counteracts the attachment stabilization effect of chromokinesin-generated PEFs near poles (Cane at al., 2013; Ye at al., 2015). Importantly, Ye and colleagues demonstrated that there is an Aurora A gradient of activity emanating from centrosomes using MT targeted FRET sensor via the Tau protein. This is analogous to the centromere-based gradient proposed for the Aurora B activity (Liu et al., 2009). Equally important, with a similar FRET sensor targeted to the Mis12 protein, they confirmed a higher phosphorylation of probe at the kinetochores in

the vicinity of spindle poles in Drosophila S2 cells, and that phosphorylation is decreased in Aurora A depletion (Ye et al., 2015). Interestingly, in Drosophila cells the phosphorylation level of FRET probe at the aligned kinetochores was comparable in the depletion of CENP-meta and co-depletion of Aurora A and CENP-meta, the Drosophila counterpart of CENP-E. The phosphorylation of FRET probe at the polar kinetochores decreased after Aurora A and CENP-meta co-depletion, confirming the spatial dependence of Aurora A phosphorylation at kinetochores (Ye et al., 2015). The experiment in HeLa cells, however, does not perfectly mimic the data acquired from Drosophila S2 cells. I have observed significant reduction in phosphorylation both at the kinetochores near the pole and the kinetochores further away with Aurora A and CENP-E co-inhibition. However, the phosphorylation of polar kinetochores decreased more than the phosphorylation of kinetochores further away from centrosomes. The human Aurora A kinase binds MTs in a TPX2-dependent manner and perhaps more actively affects kinetochore MTs and their attachments (Kufer et al., 2002; Özlü et al., 2005).

Altogether, this study presents the mechanism by which Aurora A contributes to the correction of improper kinetochore-MT attachments near spindle poles. The role of Aurora A kinase in error correction appears conserved across metazoans, as similar observations have been reported in Drosophila S2 cells, rat kangaroo cells, PtK1, and in mouse meiosis (Ye et al., 2015; Chmátal et al., 2015).

The findings emerged from this study establish a more comprehensive model of regulation of chromosome congression than previous models involving only the activity of centromere-based Aurora B. In this model, incorrectly attached chromosomes are being pulled towards the proximal spindle pole, either by dynein, or by selective MTs disassembly (disassembly of only K-fibres attached to mal-orientated, and not bi-orientated chromosomes; Kapoor et al., 2006; Barisic et al., 2014). At the spindle poles, Aurora A in co-operation with Aurora B phosphorylates the outer kinetochore components and counteracts premature, end-on stabilization of incorrect attachments promoted by PEFs (Ye at al., 2015; Chmátal et al., 2015). Additionally, Aurora A and Aurora B phosphorylate the kinetochore localized CENP-

E in the vicinity of poles, which is believed to be required, together with MT detyrosination, for guiding CENP-E-mediated transport of initially polar chromosomes towards the cell centre (Kim et al., 2010; Barisic et al., 2015; Figure 2.8).

In summary, the work described in this chapter provides a molecular mechanism for the error-correction of kinetochore-MT attachments close to centrosomes.

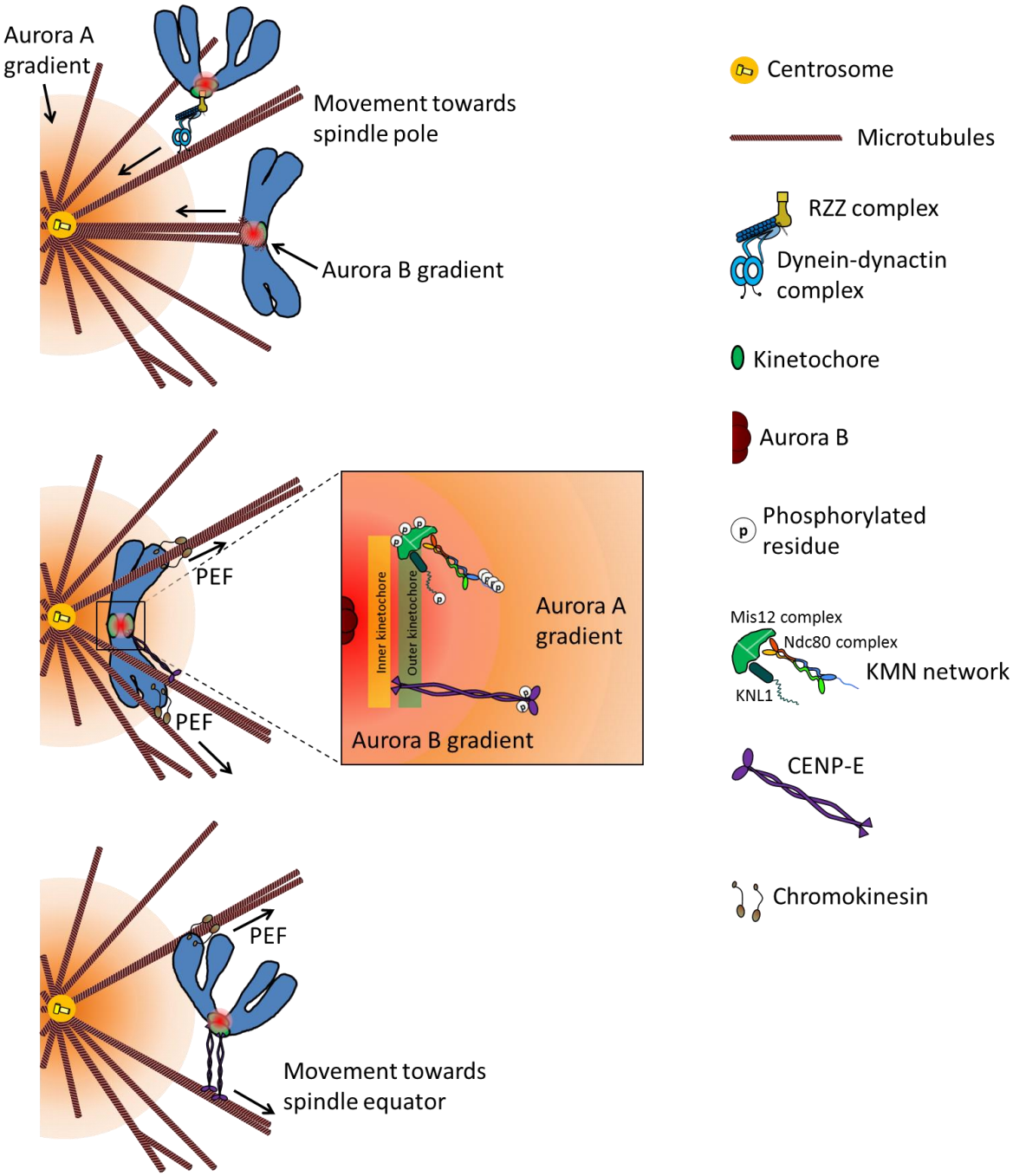

Figure 2.8: Mechanism of error correction with Aurora A contribution. Schematic diagram summarizes the mechanism of error correction near the spindle pole. Two different poleward chromosome movements were drawn, but for simplicity, subsequent fate of only a single polar chromosome is followed. The phosphorylation gradient around Aurora A and Aurora B is presented in orange and pink, respectively. The central inset depicts the phosphorylation of structures at the outer kinetochore and fibrous corona by Aurora kinases (adapted from Ye et al., 2015).

3 Chapter 3: Discovering new phosphorylation substrates of Aurora A and Aurora B kinases

3.1 **Introduction**

There are about 30 known substrates of Aurora A, and around 30 substrates of Aurora B. Phosphorylation of these substrates at specific sites by Aurora kinases regulates their mitotic functions *in vivo* or in cell culture (Table 1.1 and Table 1.2 in Chapter 1.3, references therein). Additionally, mass spectrometry studies using cell lysates and Aurora kinase inhibitors enabled identification of hundreds of proteins phosphorylated by Auroras (Kettenbach et al., 2011; Koch et al., 2011; Hegemann et al., 2011; Polat et al., 2015). However, there are still mitotic processes involving regulation by Auroras, whose molecular mechanisms are not completely clear.

Mass spectrometry is a widely used tool for the identification of protein phosphorylation. Mass spectrometry is also used to identify phosphorylation events specific to mitosis and even specific to mitotic structures, such as the mitotic spindle, mitotic chromosomes and centrosomes (Dephoure et al., 2008; Daub et al., 2008; Olsen et al., 2010; Nousiainen et al., 2006; Ohta et al., 2016; Andersen et al., 2003; Syred et al., 2013; Özlü et al., 2010). Phosphorylated sites reported in various studies, are deposited in public databases, such as PHOSIDA (Gnad et al., 2011), PhosphoELM (Diella et al., 2008), Human Proteinpedia (HPRD1; Mathivanan et al., 2008) and PhosphoSitePlus (Hornbeck et al., 2015). Important limitations of typical mass spectrometry analysis in identifying phosphorylation in proteins are: whether there is a sufficient amount of certain phosphorylated peptides and whether a particular phosphorylation is stable enough during mass spectrometry to be identified (Cantin and Yates, 2004). Phosphopeptides are detected less in standard mass spectrometry than their unmodified counterparts. The phosphopeptides are less abundant, have lower ionisation efficiency and often breakdown, losing phosphoric acids during mass spectrometry analysis (Dongré et al., 1996; Mann et al., 2002). Mass spectrometry alone does not provide any information about the

role or mechanism of phosphorylation *in vivo* and does not include information about the phosphorylating kinase if specific inhibitors are not used.

Given the limitations of mass spectrometry in the identification of new Aurora kinase substrates, I have developed a novel bioinformatic approach, in collaboration with Dr Alastair Kerr.

Only a few studies use bioinformatics to predict new phosphorylation sites. Some of these studies use already known protein-protein interaction data (Tien et al., 2004) or motif conservation over evolution (Lai et al., 2012) to predict substrates of various kinases. A computational tool, Scansite, enables proteome-wide prediction of cell signalling interactions using short sequence motifs, including substrate prediction for a broad range of kinases (Obenauer et al., 2003). A bioinformatic approach was used to identify Aurora A substrates, based on the Aurora kinase substrate consensus motif, substrate cellular localization and the conservation of consensus motifs through evolution (Sardon et al., 2010). However, these studies have not used current advances in computational tools and improvement in the protein sequence availability and coverage**.** Therefore, we incorporated new information from Ensembl, Gene Ontology database, and others in our bioinformatics search, providing a more comprehensive list of possible Aurora phosphorylation candidates.

3.2 **Results**

3.2.1 **Designing bioinformatics to identify unknown substrates of Aurora kinases and analysis of bioinformatic prediction**

In order to identify and characterise novel substrates of Aurora kinases, I developed a bioinformatic approach in collaboration with the Wellcome Trust Centre bioinformatician Dr Alastair Kerr. The bioinformatic search for Aurora kinase substrates is based on amino acids consensus preference of Aurora kinases. It also enables the use of parameters such as substrate localization and function – Gene Ontology (GO) terms from Gene Ontology database (Ashburner et al., 2000), conservation of phosphorylation motifs between vertebrate species, the number of

motifs per protein, the position of motifs in disordered regions of a protein and tissues in which the proteins are expressed via the Reactome database (Milacic et al., 2012; Fabregat et al., 2016).

The consensus sequence for the Aurora kinases was first discovered by analysing sequences flanking phosphorylated residues *in vitro* and *in vivo* for several budding yeast kinetochore proteins (Cheeseman et al., 2002). The consensus motif is defined for Ipl1/Aurora B as [RK]x[ST][ILV], where S or T are the phosphorylatable residues (marking position P0), x is any amino acid, R or K are required at P-2, while V, L and I represent preference for hydrophobic residues at P+1 (Cheeseman et al., 2002). Aurora B has a preference for R or K at the P-3 (Ohashi et al., 2006). Wide tolerance for the P+1 residue was also reported (Ohashi et al. 2006; Koch et al., 2011). For example, T follows phosphorylated S10 in Histone H3 (Hsu et al., 2000). However, it is considered that hydrophobic residues at P+1 are likely to be required for optimal activity of Auroras (Cheeseman et al., 2002).

A further study using synthetic peptide substrates defined the consensus motif for human Aurora A kinase as [RKN]Rx[ST][AFILMV] (Ferrari et al., 2005) or Rx[ST][ILV] (Ohashi et al., 2006), denoting that Aurora A kinase has strong preference for R at P-2, and any hydrophobic residue at P+1 except P (proline). It was reported that P at P+1 fully abrogates phosphorylation of the peptide substrates (Ferrari et al., 2005; Ohashi et al., 2006). Additionally, Aurora A displays tolerance for residues other than R or L at P-3. Since Aurora A and B phosphorylate the same sites on some target proteins (Andrews et al., 2004; Ohi et al., 2004; Zhang et al., 2007; see Tables 1.1 and 1.2 in Chapter 1.3 for the references), it is accepted that the target specificity of Aurora kinases is determined by their distinctive sub-cellular localization (see Chapter 1.3).

I have used this broad consensus motif of Auroras kinases based on 4 patterns (Figure 3.1A). This approach resulted in a list of 19516 human genes encoding for proteins with at least one motif site. Out of 22699 human genes in total, this makes 86% of human genome. 71302 proteins contain at least one of these motifs, representing 70% of total proteome.

With analysis of previously reported Aurora kinases phosphorylation sites (Table 1.1 and Table 1.2), I found that R or K make up more than 50% of the occupancy of the positions -3 and -1 (Figure 3.1B). Therefore, I also tried another more stringent bioinformatic approach with first the 3 patterns (Figure 3.1A), excluding pattern 4, which contribute most of the reported sequences. This reduced the list of candidates by almost two-thirds, leaving 6804 human genes encoding for proteins with at least one motif site. A large proportion of these candidates could represent false positives, so I decided to implement several criteria to refine my search.

A

	amino acid position				
	-3	-2	-1	0	+1
pattern 1	[RK]	[RK]	x	[S/T]	[ILVMFAST]
pattern 2	x	[RK]	[RK]	[S/T]	[ILVMFAST]
pattern 3	[RK]	[RK]	[RK]	[S/T]	[ILVMFAST]
pattern 4	{RK}	[RK]	{RK}	[S/T]	[ILVMFAST]

[] = required amino acids

{} = any of the amino acids except those in {}

B

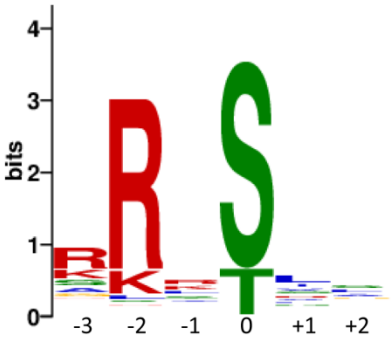

Figure 3.1: Consensus motif patterns of Aurora kinases. (A) Motif patterns used in this study. Patterns are based on published consensus sequences for Aurora kinases. (B) Sequence bias in validated putative phosphorylation sites of Aurora kinases. Aurora kinases consensus sequence logo was derived from alignment of all validated putative sites of Aurora kinases (see Table 1.1 and 1.2). The total height of each stack indicates the "information content" at that position (measured in bits). The height of symbols within the stack reflects the relative frequency of the corresponding amino acid at that position. The subsequent positions within the sequences are labelled -3 to +2. The figure was generated using http://meme-suite.org server (Bailey et al., 2009) by submitting 13 amino acid long sequences in fasta format.

Based on the literature, potential candidates seem to localize in proximity of Auroras to be phosphorylated by these kinases. To further narrow down the search for potential candidates, I introduced GO terms from the Gene Ontology database. In that way the search can be limited spatially or temporally (Ashburner et al., 2000). The selected GO terms implemented in our bioinformatics included cellular localizations where Aurora kinases reside, such as the spindle and MTs,

kinetochores, centrioles, centrosomes and spindle poles, the spindle midzone and midbody. Additionally, we used GO terms annotating a biological process: mitotic cell cycle or cell division, and more specifically, M phase of the mitotic cell cycle or cytokinesis as well as mitotic spindle assembly and organization. To avoid overlooking proteins that are not completely or correctly annotated in the GO database, we added an option not to choose specific GO terms into our bioinformatics design. However, the use of GO terms significantly reduces the search to the cell cycle stage and the cellular localizations where Aurora kinases are active. As an example, the GO term 'cell division' isolates 176 human genes encoding for proteins with at least one motif site of Aurora kinases, while the GO term 'mitotic cell cycle' isolates 227 genes. I have specifically limited my search for Aurora kinase substrates to those bound to MT structures and/or kinetochores. In the list there are 266 human genes encoding centrosomal proteins (including centrioles and spindle poles), 194 human genes encoding MT-associated proteins, 53 human genes encoding kinetochore or kinetochore-binding proteins (Figure 3.2).

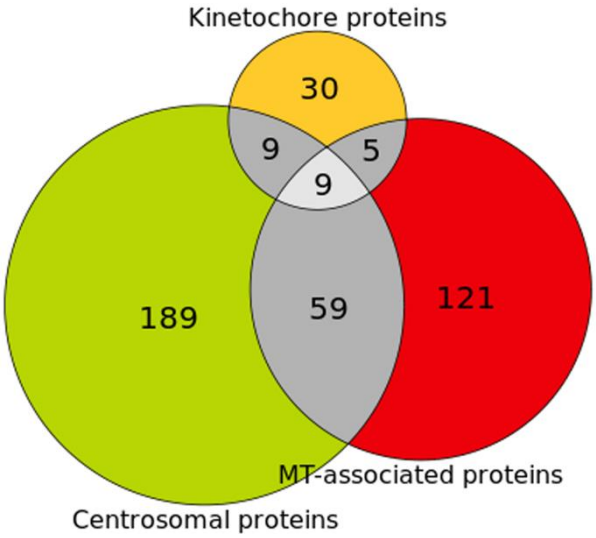

Figure 3.2: Selection of candidates based on GO terms. Venn diagram depicting the number and overlap between centrosomal, MT-associated and kinetochore localized proteins that contain at least one motif site of Aurora kinases.

Regulation of protein function by phosphorylation could be through unique phosphosites. Phosphorylation of histone H3 at S10 is an example of how phosphorylation of a single site in a protein by Aurora kinases can greatly influence the progression through mitosis. This phosphorylation is reported to drive condensation of chromatin compaction in yeast and it was shown that absence of phosphorylation caused defects in chromosome segregation (Hendzel et al., 1997; Hsu et al., 2000; Neurohr et al., 2011).

In contrast, there are well known examples of protein regulation through multiple phosphorylation sites by Auroras. HEC1/Ndc80, an outer kinetochore protein, is phosphorylated on multiple sites within N terminus, and this modulates HEC1/Ndc80 binding to MTs (Cheeseman et al., 2006; DeLuca et al., 2006; Ciferri et al., 2008). Multisite phosphorylation of kif2c/MCAK (Mitotic centromere-associated kinesin) by Aurora kinases negatively regulates MT depolymerisation activity and centromere targeting (Andrews et al., 2004; Ohi et al., 2004; Lan et al., 2004; Zhang et al., 2007). Multisite phosphorylation in p53 by Aurora kinases abrogates DNA binding and accelerates p53 degradation (Liu et al., 2004; Gully et al., 2012). Multisite phosphorylation can be associated with switch-like response of proteins (Ferrell and Bhatt, 1997; Ferrell and Machleder, 1998; Nash et al., 2001). Mathematical modelling showed that multisite phosphorylation is preferably associated with graded protein responses (Salazar and Höfer, 2007). The experimental evidence of graded control is Aurora kinases regulation of outer kinetochore attachment to MTs (Welburn et al., 2010). If multiple phosphorylation sites are closely spaced in the protein primary amino acid sequence they are often referred to as the cluster (Figure 3.3).

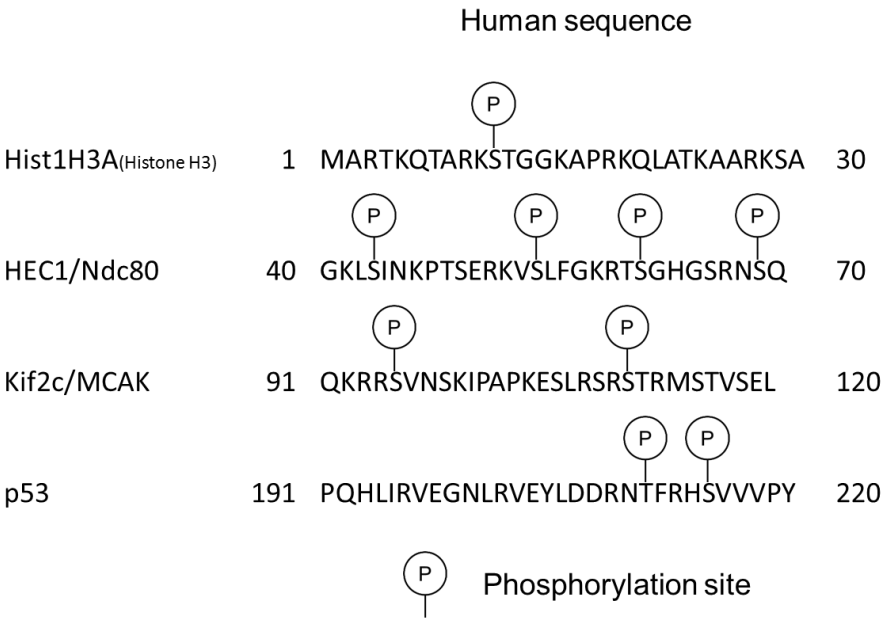

Figure 3.3: Examples of Auroras unique and multisite phosphorylation in substrates. Reported are human sequences of Histone H3 (UniProt ID P68431), HEC1/Ndc80 (O14777), Kif2c/MCAK (Q99661) and p53 (P04637). P marks validated phosphorylation sites in presented substrates (see Table 1.1 and 1.2 for references). Only zone 1 phosphorylation cluster in HEC1/Ndc80 is shown here, and also one reported phosphorylation site in Kif2c/ MCAK and p53 is omitted due to limited space.

Our bioinformatic tool contains a filter that enables us to select substrates based on the minimum number of phosphorylation motifs. In this way both substrates with unique sites or substrates containing multiple phosphorylations could be predicted. Further, the selection of different numbers of phosphorylation patterns is possible in protein regions of 0, 20, 50, 100 or 300 amino acids. By applying this filter, I found that a total 2538 human genes encode for proteins with a minimum of four consensus motifs. Additionally, using any of the GO terms implemented in bioinformatics, that number was decreased. For example, there are 43 human genes encoding centrosomal proteins with at least four motifs in at least 100 amino acids long protein region.

Next, we implemented a selecting filter based on the disorder in a protein. Functionally important phosphorylation sites are mostly found in regions of intrinsic sequence disorder, flexible regions like hinges and loops (Iakoucheva et al., 2004; Gnad et al., 2007; Collins et al., 2008). Those regions are found on the surface of a

protein, and this allows kinases to access the site and phosphorylate proteins to regulate their activity or protein-protein interactions.

To implement the sequence disorder percentage the IUPred system was used as a filter in our search for possible Aurora kinase substrates (Dosztányi et al., 2005a; Dosztányi et al., 2005b). This system is a developed to discriminate between disordered and folded regions in proteins from the amino acids sequence (Dosztányi et al., 2005a; Dosztányi et al., 2005b). By using this filter, I found that the number of proteins with at least one motif drastically decreased. For example, there are 980 genes encoding proteins with 50% intrinsic sequence disorder and at least one motif site of Aurora kinases. If this is combined with different number of consensus motifs and any of the available GO terms, number is again reduced. For example, only 16 human genes encode centrosomal proteins with 50% intrinsic sequence disorder and at least four consensus sites in a 100 amino acid protein region.

In addition to the previously described filters, a filter based on motif sequence conservation was implemented. It was shown that phosphorylation sites with relevant biological function are better conserved throughout evolution (Gnad et al., 2007; Malik et al., 2008; Landry et al., 2009). It was argued that phosphosites are more conserved than the same residues that are not phosphorylated when their enrichment in disorder regions of proteins was included (Landry et al., 2009). Furthermore, the evolutionary data of phosphorylation showed that it would be easier to predict functional phosphorylation in low abundance proteins than in very abundant proteins (Levy et al., 2012). In those low abundance proteins, it was also noticed that the sites that are frequently phosphorylated in cells are more conserved than rarely phosphorylated sites (Levy et al., 2012). Taken together, the use of evolutionary conservation in conjunction with structural information (order-disorder region) can significantly improve prediction of phosphorylation sites, specifically in the context of functional phosphorylation.

In my bioinformatic analysis I implemented a filter based upon sequence conservation among vertebrates. It has been shown that disordered regions, where

the most functional sites are found, evolve faster than order regions (Brown et al., 2002). More importantly, there is evidence that short motifs are fast-evolving and there is very limited conservation outside of closely related species (Neduva et al., 2005). Since I am interested in human proteins, I chose to look for conservation of sequences in phosphorylation candidates between human, chicken and zebrafish (Figure 3.4A). The chosen species are relatively closely related species by Neduva et al., 2005. The Figure 3.4B shows sequence conservation of known phosphorylation sites in HEC1/Ndc80 between human, chicken and zebrafish.

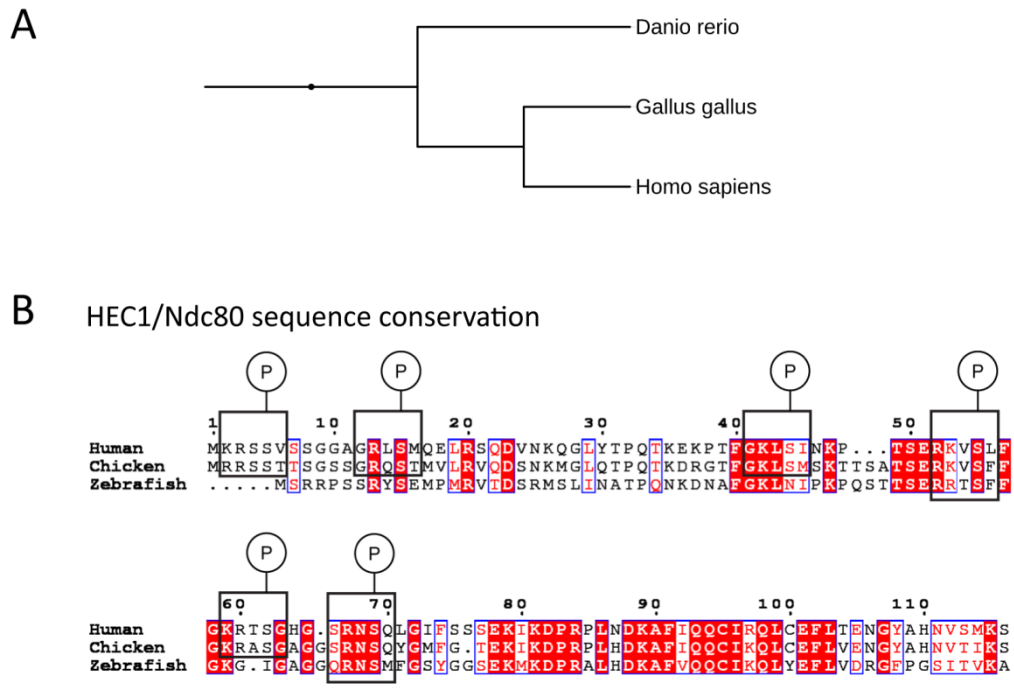

Figure 3.4: Motif sequence conservation. (A) Pruned phylogenetic tree depicting chosen vertebrate species, human (*H.sapiens*), chicken (*G.gallus*) and zebrafish (*D.rerio*). Phylogenetic tree was made in phyloT (http://phylot.biobyte.de/index.html) and visualized using iTol (Letunic and Bork, 2016). (B) Sequence alignment of HEC1/Ndc80 in human, chicken and zebrafish. Sequence UniProt IDs are O14777, Q76I89 and Q6DRJ7, respectively. Sequences were aligned using ClustalOmega (Sievers et al., 2011) and formatted with ESPRIPT (Gouet et al., 1999). The conserved residues are highlighted in red. Amino acid numbering is relative to the human HEC1/Ndc80 sequence. Reported pS are marked with P and the whole phosphomotif with a black rectangle.

In order to implement a conservation filter in our bioinformatics we looked for genes that have 1-1 orthologs in Chicken and Zebrafish. The number of human genes with 1-1 orthologs in Chicken and Zebrafish is 16524 out of which 6604

encode proteins with at least one motif site in all three species. This pre-requisite for 1-1 orthologs in human, chicken and zebrafish significantly decreased the number of possible candidates for Aurora kinases, without any filter applied. Importantly, all the mentioned numbers are derived based on 1-1 orthologs. Use of this filter in conjuction with all others revealed only 11 human genes encoding centrosomal proteins with 50% sequence disorder, at least four consensus sites in 100 amino acids region and 50% conservation in sequence between human, chicken and zebrafish.

The limitation of this filter is that stringent conservation analysis conflicts with the analysis of multisite phosphorylation. For instance, the function of phosphorylation might be the regulation of bulk electrostatic charges in some regions of a protein, which then influence interactions of different domains inside a protein or more often protein-protein interactions. In this case where the function of phosphorylation is more dependent on the number of phosphorylated residues than their position, the number of phosphosites is more conserved than position (Landry et al., 2009).

The last filter implemented was based on extracting genes involved in mitotic pathways. This filter serves to choose tissue of interest where new substrates could be identified. For that we incorporated the Rectome database into our bioinformatic search (Fabregat et al., 2016; Milacic et al., 2012). This filter enables specifying the search for possible phosphorylation candidates to genes involved in cell cycle pathways.

Reported substrates of both Aurora kinases, such as HEC1/Ndc80, Kif2c/MCAK, TPX2, Kif23/MKLP1, PLK1, TACC3, topoisomerase II alpha, LATS2, CENPE, NuMa and others, appeared in the bioinformatic list of candidates (Cheeseman et al., 2002 ; DeLuca et al., 2006; Ciferri et al., 2008; Akiyoshi et al., 2009; Andrews et al., 2004; Ohi et al., 2004; Kufer et al., 2002; Fu et al., 2015; Guse et al., 2005; Neef et al., 2006; Douglas et al., 2010; Macůrek et al., 2008; Seki et al., 2008; Bruinsma et al., 2014; Giet et al., 2002; LeRoy et al., 2007; Toji et al., 2004; Kim et al., 2010; Gallini et al., 2016).

3.2.2 **Validation of predicted candidates phosphorylation by Aurora kinases *in vitro***

Accuracy of prediction of Aurora kinase substrates by our bioinformatic tool was tested by direct phosphorylation of selected new candidates by Aurora kinases. I performed *in vitro* phosphorylation assays using recombinant Aurora kinases, purified recombinant candidate proteins and γ ^{32}P-ATP. Incorporation of radioactive γ ^{32}P by a candidate in the process of phosphorylation is detected by autoradiography. A simplified diagram of experimental design is presented in Figure 3.5.

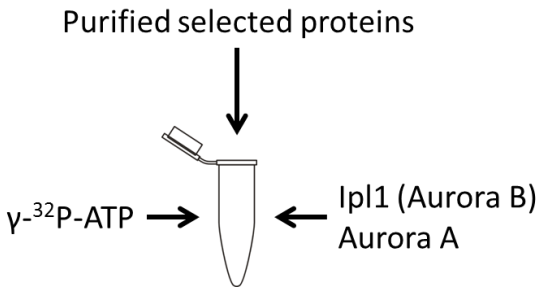

Figure 3.5: Schematic representation of experimental design for testing protein candidate phosphorylation by Aurora kinases.

3.2.2.1 **Selection of candidates for *in vitro* validation**

Selection of the candidates to test their phosphorylation by Aurora kinases was performed using a defined combination of filters. I first selected a combination of filters with less stringency, but with potential to narrow down and specify the search. I chose to search for the candidates with at least two phosphorylation motifs in a smaller region of 100 amino acids, and with minimum of 15% sequence disorder in a region, but with 60 % conservation between human, chicken and zebrafish. I filtered the search based on several GO terms connected with kinetochore, MTs and centrosomes. This set of filters decreased the number of potential candidates (Table 3.1). Then I narrow down the search more, with higher stringency in selected filters. I selected candidates with more phosphorylation motifs and higher disorder in the region of phosphorylation but with high

conservation, which can contribute to functionally more relevant phosphorylation (Table 3.2). Finally, I selected the following candidates based on the bioinformatics search results and their protein function in mitosis and/or reported cellular localization in proximity of either Aurora kinases: CLASP2, MEL-28/ELYS (AHCTF1), Nup107, TTLL4, SPICE1 and KIAA1468 as potential Auroras substrates.

Table 3.1: List of candidates derived from bioinformatics with less stringent filtering.

60% conservation + 15% disorder and min 2 motifs in region of 100 amino acids					
Kinetochore proteins	MT-associated proteins	Centrosomal proteins	Kinetochore proteins	MT-associated proteins	Centrosomal proteins
NUP107	KIF13A	AURKA		HSPB1	DTL
APC	KIF23	CEP41		SPICE1	KATNA1
NDC80	FEZ1	NUP107		MYH10	CEP350
KAT2B	SHROOM3	IFT81		CEP350	USP33
KIF2C	MAP1B	DZIP1		TTK	TRAF3IP1
TP53BP1	EML1	APC		PARD3	CEP78
PPP1R12A	DCX	KIF13A		NEDD9	RGCC
CENPT	MAPT	KIF23		NUMA1	KATNB1
CLASP2	PCNT	TOPBP1		CEP162	CEP162
CFDP1	MAP2	RAB11FIP3		CDC27	PPP1R12A
PHF6	KIF21A	IFT57		CLASP2	POC5
ERCC6L	KIF14	PLK4			TFAP2A
AHCTF1	TTLL4	FEZ1			FBXL7
	KATNA1	SASS6			CEP192
	SPRY2	SPICE1			CDC27
	KATNB1	NPM1			CEP290
	KIF19	CAPRIN2			NEDD1
	TEKT3	POLR3E			AATF
	KIF26B	RAB8A			CCDC92
	KIF3A	LRRC45			CDC6
	JAKMIP1	USP20			LRMP
	KIF5C	IFT88			MTCL1
	KLC2	TACC3			FAM110A
	RACGAP1	PCM1			SMC3
	KIF21B	ERCC6L			DNAAF1
	GAS2L3	TCEA2			NEDD9
	PKP4	PDE4D			LATS2
	MAK	KIAA0586			PKP4
	ECT2	MAK			NUMA1
	AURKA	ZFYVE19			LATS1
	RIF1	PCNT			

Table 3.1: List of candidates derived from bioinformatics with more stringent filtering.

60% conservation + 50% disorder and min 3 motifs in region of 100 amino acids		
Kinetochore proteins	MT-associated proteins	Centrosomal proteins
APC	SHROOM3	NUMA1
PPP1R12A	MAP1B	CCDC92
AHCTF1	MAP2	DZIP1
CLASP2	KIF14	SPICE1
	KLC2	CEP192
	CLASP2	APC
	RIF1	NPM1
	SPICE1	PCM1
	MYH10	KIAA0586
	CEP350	CEP350
	PARD3	TRAF3IP1
	NUMA1	PPP1R12A
	CDC27	CDC27
	PKP4	TOPBP1
		FAM110A
		LATS1
		LATS2
		PKP4

CLASP2

CLASP2 (CLIP-associating protein also known as Cytoplasmic linker associated protein) is a well known MAP, which localizes to MTs plus ends in interphase and in mitosis (Akhmanova, et al., 2001; Maiato et al., 2002; Mimori-Kiyosue et al., 2005). CLASP2 also localizes to other cellular structures, such as the outer corona of kinetochores (Maiato et al., 2003; Pereira et al., 2006; Mimori-Kiyosue et al., 2006), centrosomes (Pereira et al., 2006), spindle MTs and central spindle (Maiato et al., 2003; Inoue et al., 2004; Maiato et al., 2005; Dumont et al., 2010). CLASP2 can bind MTs directly through HEAT domains or TOG-like domains in its N terminus and through its central region, which is rich in S, P and R (Akhmanova, et al., 2001; Mimori-Kiyosue et al., 2005; Al-Bassam et al., 2010; Patel,

et al., 2012). CLASPs are targeted to the MT plus ends through interactions of their central region with EB1-related proteins and also through interaction of their C terminus with CLIP proteins (Akhmanova, et al., 2001; Mimori-Kiyosue et al., 2005; Galjart, 2005).

The CLASPs family of proteins are highly conserved and required for chromosome congression, spindle bipolarity and the attachment of MTs to kinetochores, through regulation of MT dynamics (Maiato et al., 2002; Maiato et al., 2003; Máthé et al., 2003; Pereira et al., 2006; Maffini et al., 2009; Maia et al., 2012). Additionally, CLASPs regulate steady-state spindle geometry (Young et al., 2014). Localizing at the MTs of the central spindle in anaphase, CLASPs also function in chromosome separation (Maiato et al., 2003; Inoue et al., 2004; Dumont et al., 2010). CLASPs mitotic function at the kinetochores is regulated through the activity of several kinases. Phosphorylation of CLASP2 by Cdk1 and Plk1 in mitosis is required for stable kinetochore-MT attachments (Maia et al., 2012). Phosphorylation sites for these kinases are mapped near the kinetochore-binding region in CLASP2 in the C terminus. It was reported that Aurora B indirectly controls recruitment of CLASP to the kinetochore via Astrin-SKAP complex (Schmidt et al., 2010). However, it is not known whether Aurora kinases directly phosphorylate CLASP2, while localization at the kinetochores and MT plus ends makes it a potential substrate of Aurora kinases.

Our bioinformatic approach predicts two clusters of five phosphorylation sites in central region of human CLASP2, just after MT- binding TOG-like domains as well as before and between EB-1 binding motifs. Interestingly, predicted phosphorylation sites from the second cluster are close or they overlap with glycogen synthase kinase-3 (GSK3) phosphorylation sites (Maki et al, 2015; Figure 3.6). There are two more phosphorylation sites at the C terminus, which is reported to be the kinetochore targeting domain (Mimori-Kiyosue et al., 2006; Pereira et al., 2006).

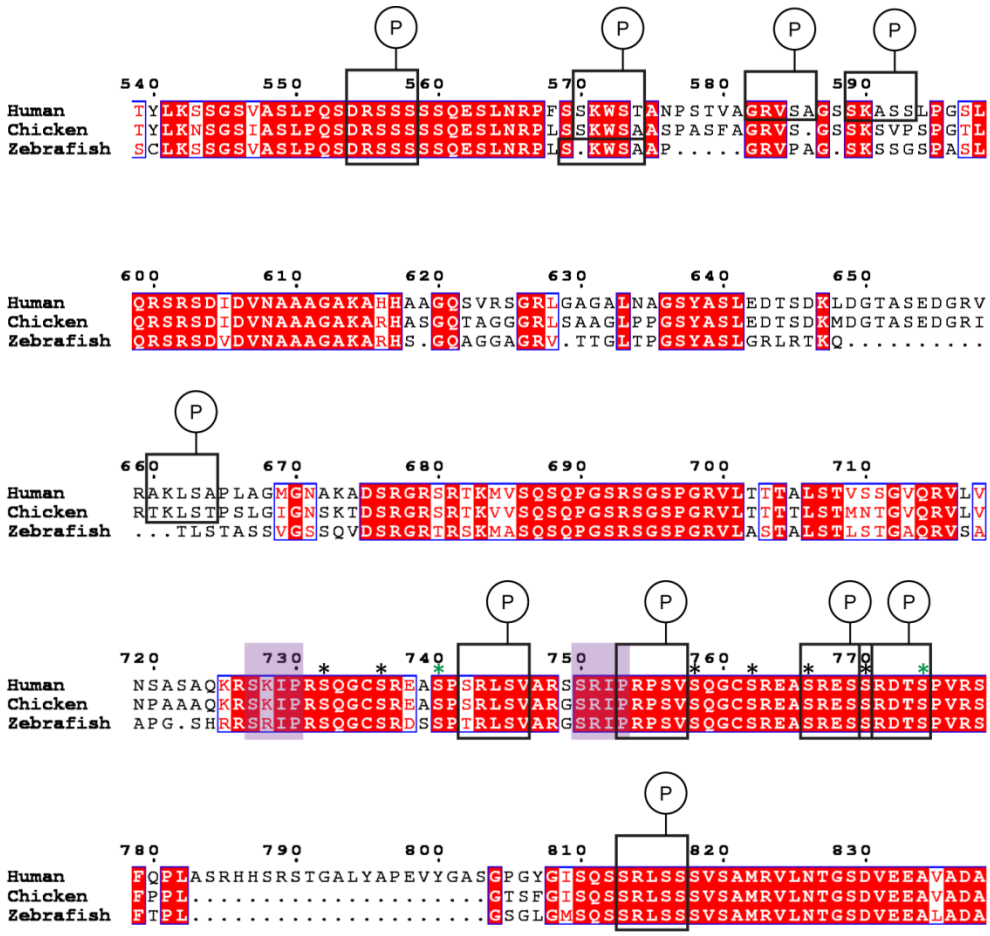

Figure 3.6: Predicted phosphorylation sites in CLASP2. Phosphorylation consensus motifs that our bioinformatics found are marked with black rectangles, while P marks position of predicted phosphorylation. Two SxIP, EB1-binding motifs, are shaded in purple. Black asterisks mark reported phosphorylation by GSK3 and green asterisk Cdk1 phosphorylation (Kumar et al., 2009). Human CLASP2 isoform X15 (NCBI: XP_006713112.1) that was used in this study was aligned with chicken (UniProt ID A0A1D5P1B0) and zebrafish CLASP2 (A3KPT4) using ClustalOmega (Sievers et al., 2011) and formatted with ESPRIPT (Gouet et al., 1999). The conserved residues are highlighted in red. Amino acid numbering is relative to the human CLASP2 sequence.

ELYS

ELYS (Embryonic large molecule derived from yolk sac, also known as AHCTF1 and MEL-28 in C.*elegans*) localizes to the nuclear rim and nucleoplasm in interphase and to the kinetochores, spindle poles and proximal MTs in mitosis (Galy et al., 2006; Fernandez and Piano, 2006; Rasala et al., 2006; Franz et al., 2007; Yokoyama et al., 2014; Gómez-Saldivar et al., 2016). Direct binding of MEL-28/ELYS to MTs is through the AT-hook and nuclear localization sequence (NLS) found within the C terminus (Yokoyama et al., 2014). MEL28/ELYS is recruited to chromatin in

late anaphase (Rasala et al., 2006). Recruitment of MEL28/ELYS to chromatin before telophase is essential for nuclear pore re-assembly at the nuclear envelope due to the recruitment of Nup107-160 complex and other nucleoporins (Rasala et al., 2006; Franz et al., 2007; Hattersley et al., 2016). The nuclear envelope forms in MEL-28/ELYS depletion, but without pores (Franz et al., 2007).

The function of MEL-28/ELYS in mitosis is likely to be species-specific. It is required for timely regulation of cytokinesis and *in vitro* spindle assembly (in Xenopus egg extracts) through a non-centrosomal pathway mediated by Ran-dependent recruitment of γ-tubulin to MTs (Rasala et al., 2006; Yokoyama et al., 2014). Moreover, MEL-28/ELYS interaction with the catalytic subunit of protein-phosphatase 1 (PP1c) is important to direct meiotic chromosome segregation and nuclear reassembly in *C.elegans* (Gómez-Saldivar et al., 2016; Hattersley et al., 2016). The mitotic function of human ELYS remains poorly understood. There are three Aurora kinase phosphorylation sites mapped by mass spectrometry in MEL-28/ELYS (Kettenbach et al., 2011), but the mechanism of MEL-28/ELYS regulation by phosphorylation remains unknown. Described localization at the kinetochores, spindle poles and proximal MT makes MEL-28/ELYS potential substrates of both Aurora kinases.

Bioinformatic analysis predicts multiple phosphorylation sites in the disordered C terminus of human ELYS; three sites closer to the central helical domain (CHD) (Bilokapic and Schwartz, 2013), four predicted sites closer to the far C terminus and six sites at the very end of the C terminus (some of these are presented in Figure 3.7A and B).

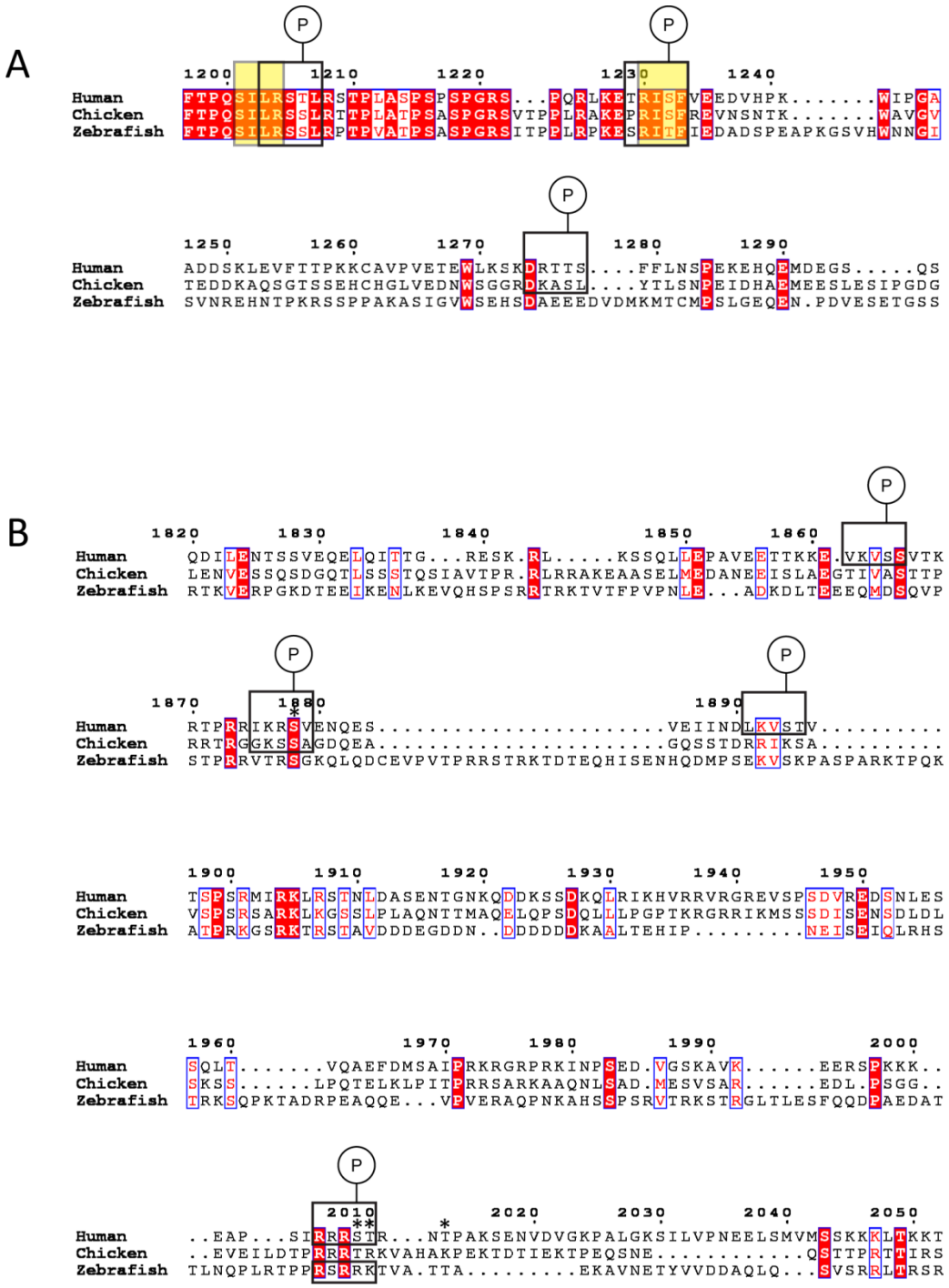

Figure 3.7: Predicted phosphorylation sites in ELYS. A and B presenting two segments of ELYS. Predicted phosphorylation consensus motifs are marked with black rectangles and predicted phosphorylation with letter P. Reported PP1c docking sites are shaded in yellow (Hattersley et al., 2016). Asterisks mark Aurora B reported phosphorylation from mass spectrometry study (Kettenbach et al., 2011). Human, chicken and zebrafish ELYS sequences (UniProt IDs Q8WYP5, E1C6A6, X1WE68, respectively) are aligned using ClustalOmega (Sievers et al., 2011) and formatted with ESPRIPT (Gouet et al., 1999). The conserved residues are highlighted in red, while amino acid numbering is relative to the human ELYS sequence.

Nup107

Nup107 (Nucleoporin 107 kDa) is the component of Nup107-Nup160 complex, which in vertebrates contains nine proteins: Nup160, Nup133, Nup107, Nup96, Nup85, Nup43, Nup37, Sec13 and Seh1 (Belgareh et al., 2001; Vasu et al., 2001; Cronshaw et al., 2002; Harel et al., 2003; Loïodice et al., 2004). Nup107 as part of this complex localizes to the nuclear rim and nucleoplasm in interphase (Boehmer et al., 2003; Walther et al., 2003). During mitosis, the Nup107-160 complex targets to kinetochores through CENP-F and Ndc80 and to the spindle poles and proximal MT in prometaphase in human cells (Belgareh et al., 2001; Harel et al., 2003; Loïodice et al., 2004; Orjalo et al., 2006; Zuccolo et al., 2007). In X.*leavis* egg extracts, Nup107-160 complex is found at the spindle MTs and kinetochores until late anaphase (Enninga et al., 2003; Orjalo et al., 2006).

Nup107, as part of Nup107-160 complex, is essential for nuclear pore re-assembly at the mitotic exit and maintenance of NPCs (Doye et al., 1994; Aitchison et al., 1995; Siniossoglou et al., 1996; Harel et al., 2003; Walther et al., 2003). The Nup107-160 complex regulates *in vitro* bipolar spindle assembly (Orjalo et al., 2006). The Nup107-160 complex contributes to kinetochore-MT assembly through recruitment of the γ-TuRC to the kinetochores in a Ran-GTP dependent manner (Mishra et al., 2010). Seh1 as part of Nup107-160 complex (Platani et al., 2009), as well as *C.elegans* Nup107/NPP-5, were implicated in regulation of the centromeric localization of Aurora B and other CPC proteins (Ródenas et al, 2012). Several components of the complex, proteins Nup160, Nup133, Nup96 and Nup107 are phosphorylated in mitosis by an unidentified kinase in their disordered N termini (Glavy et al., 2007). Phosphorylation regulates the interaction of Nup107-Nup160 complex with other proteins and not the interaction within the subcomplex (Glavy et al., 2007). The exact function of this phosphorylation remaines unknown. Kinetochore localization of the Nup107-160 complex makes it an ideal substrate of Aurora kinases.

Our bioinformatics predicts several phosphorylation sites in three components of this complex: Nup160, Nup133 and Nup107. The human Nup107

contains three predicted phosphorylation sites, one at the beginning of the disordered N terminus and two others at the part of N terminus containing α-helices, responsible for assembly of Nup107 and Nup130 into the Nup107-160 subcomplex and NPCs (Boehmer et al., 2008; Figure 3.8A). There is one phosphorylation site in Nup107 at the end of the C terminus. The Nup107 C terminus is responsible for interaction with the C terminus of Nup133 in the subcomplex (Belgareh at al., 2001; Berke et al., 2004; Figure 3.8B).

TTLL4

TTLL4 (Tubulin tyrosine ligase like) is a cytoplasmic polyglutamylase, responsible for adding glutamate amino acids to proteins (van Dijk et al., 2008; see 1.2), while its main function is the modification of the C terminus of tubulin in MTs (van Dijk et al., 2007; Rogowski et al., 2010). TTLL4 also localizes to the *C.elegans* sensory cilia (Kimura et al., 2010).

This enzyme is part of TTLL family of proteins that in humans count nine members, TTLL1/2/4/5/6/7/9/11/13, most of them with polyglutamylase activities (van Dijk et al., 2007). TTLL4 binds MTs through a highly conserved cationic catalytic domain found in all TTLLs (Garnham et al., 2015). TTLL4 is the main polyglutamylase enzyme in HeLa cells, which preferentially modifies the β-tubulin C terminus, but also other proteins, such as nucleosome assembly proteins NAP1 and NAP2, (van Dijk et al., 2007 and 2008; Garnham et al., 2015). Polyglutamylation of MTs regulates activity of many non-motor MAPs, kinesins and MT severing proteins (Boucher et al., 1994; Larcher et al., 1996; Bonnet et al., 2001; Lacroix et al., 2010; Sirajuddin et al., 2014; Valenstein and Roll-Mecak, 2016). Distribution of MT polyglutamylation is very specific in mitosis. Only spindle MTs and not astral MTs are polyglutamylated and centrosomes contain MTs with long polyglutamate chains (Lacroix et al., 2010). In cytokinesis, polyglutamylation is restricted to the midbody (Lacroix et al., 2010). It is not known whether MT polyglutamylation regulates mitosis. Additionally, the mechanism of polyglutamylation and its specific distribution in mitosis is not known. I was interested in examining whether Aurora

kinases are involved in the regulation of tubulin polyglutamylation, and through this process controlling the fidelity of mitosis.

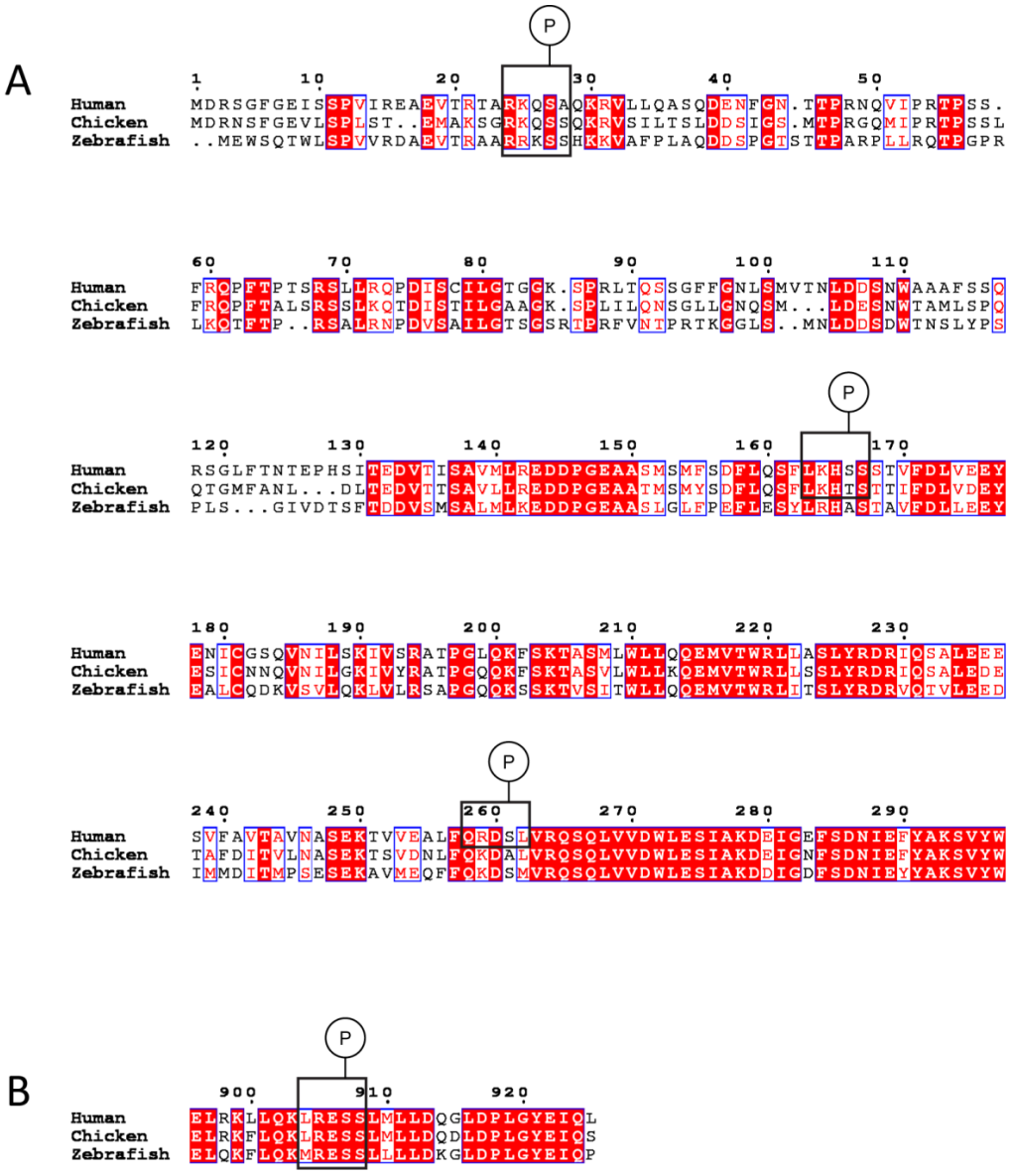

Figure 3.8: Predicted phosphorylation sites in Nup107. A and B depicting the N terminus and C terminus end of Nup107, respectively. Rectangles mark predicted consensus motifs, while P marks predicted phosphorylation. Aligned sequences of human, chicken and zebrafish Nup107 sequences (UniProt IDs P57740, F1NH49 and A0A0R4IJT3, respectively) using ClustalOmega (Sievers et al., 2011) are formatted with ESPRIPT (Gouet et al., 1999). The conserved residues are highlighted in red, while amino acid numbering is relative to the human Nup107 sequence.

Several phosphorylation sites are predicted by our bioinformatics in three members of TTLL family, TTLL11, TTLL9 and TTLL4. There is a cluster of five predicted sites in human TTLL4, adjacent to the catalytic domain (Garnham et al., 2015; Figure 3.9).

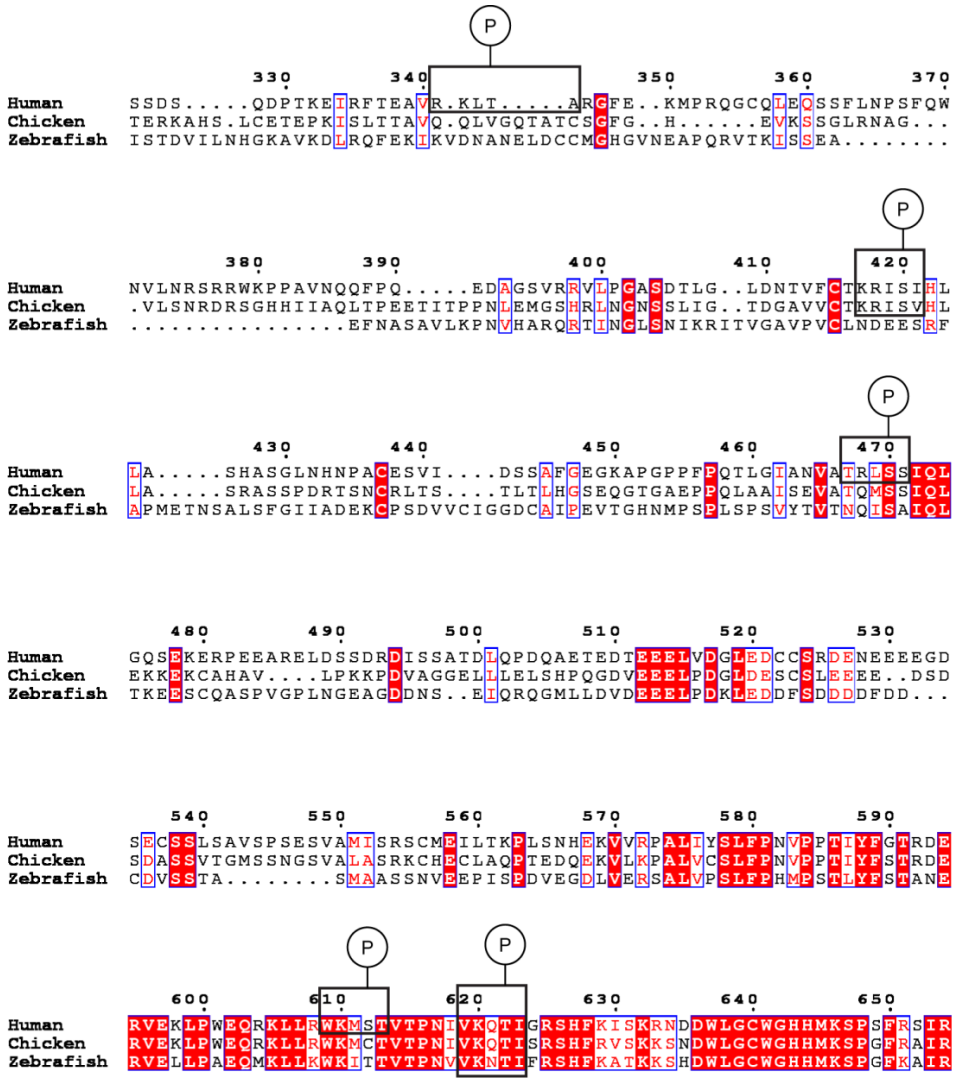

Figure 3.9: Predicted phosphorylation sites in TTLL4. Rectangles mark predicted consensus motifs, while P marks the position of predicted phosphorylation. Human TTLL4 sequence (UniProt ID Q14679) was aligned with chicken (F1P4H7) and zebrafish TTLL4 (F1Q6C4) using ClustalOmega (Sievers et al., 2011) and formatted with ESPRIPT (Gouet et al., 1999). The conserved residues are highlighted in red, and numbering of amino acids is relative to human TTLL4 sequence.

SPICE1

SPICE1 (spindle and centriole-associated protein 1, also known as ccdc25) localizes to the mitotic spindle and centrioles, as its name suggests (Andersen et al., 2003; Archinti et al., 2010). SPICE1 is required for centriole duplication, regulation of spindle architecture and chromosome congression in mitosis (Archinti et al., 2010). SPICE1 interacts with the centrosome proteins CEP120 and CPAP (Sas4 in Drosophila) and this interaction is required for centriole elongation (Comartin et al., 2013). SPICE1 over-expression does not lead to abnormal centriole elongation. SPICE1 depletion leads to shorter MTs in the centriole barrel observed by electron microscopy, as well as a decrease in acetylated and glutamylated tubulin in the centriole region (Comartin et al., 2013). Still, the function of SPICE1 is not very well characterized. Several large proteomics studies using HeLa cells identified phosphorylation sites in SPICE1, however, neither the function of this phosphorylation nor the kinases that contribute to the phosphorylation are known (Beausoleil et al., 2004; Olsen et al., 2006). SPICE1 localization at the centrosome and spindle makes it a potential substrate of Aurora kinases.

Our bioinformatics predicts five phosphorylation sites in the C terminus region of human SPICE1 (Archinti et al., 2010; Figure 3.10).

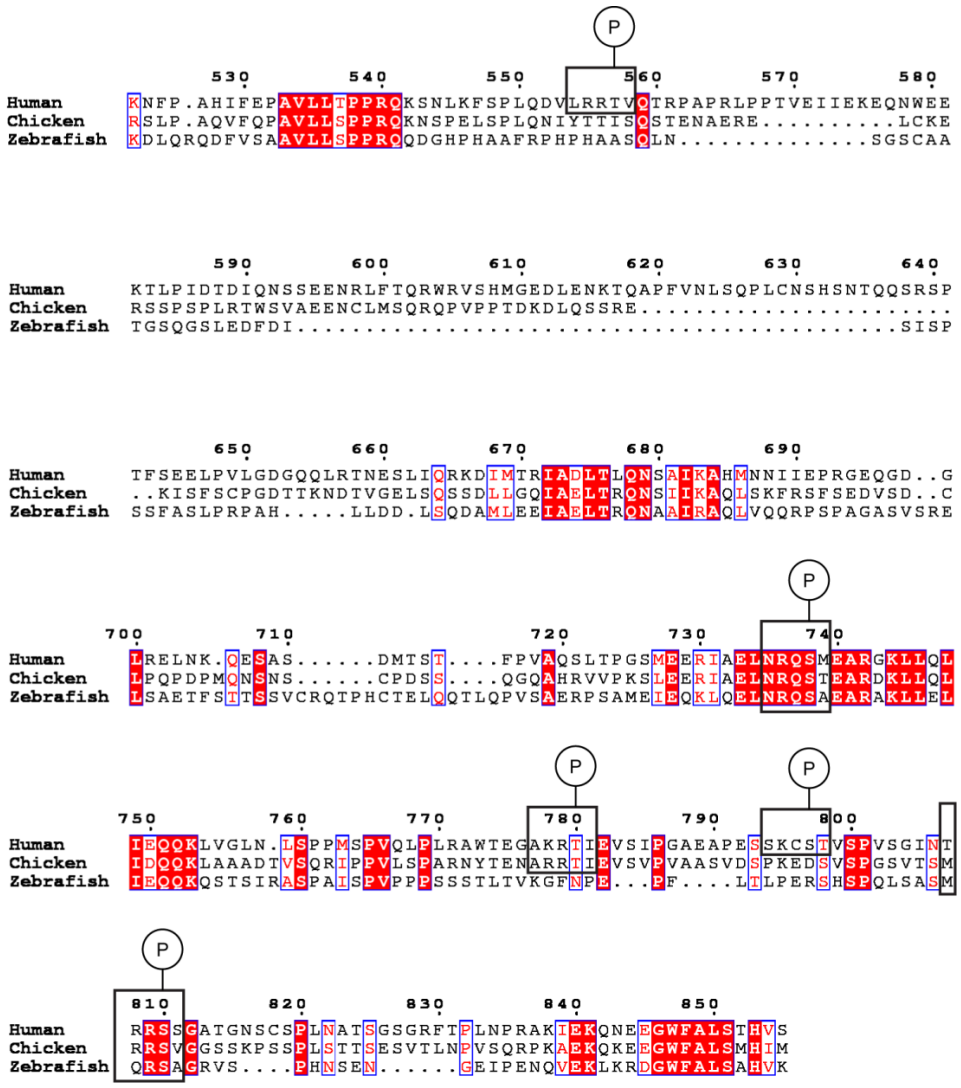

Figure 3.10: Predicted phosphorylation sites of SPICE1. Rectangles mark predicted consensus motifs, while P marks the position of predicted phosphorylation. Human, chicken and zebrafish sequences of SPICE1 (UniProt ID Q8N0Z3, A0A1L1RXK9, F1QIY8, respectively) are aligned using ClustalOmega (Sievers et al., 2011) and formatted with ESPRIPT (Gouet et al., 1999). The conserved residues are highlighted in red, and numbering of amino acids is relative to human SPICE1 sequence.

KIAA1468

KIAA1468 is selected based on our bioinformatic analysis as an uncharacterised protein. It is a lisH (lis homology) domain and HEAT-repeat-containing protein according to UniProt. HEAT domains are present in other MTs-binding proteins such as CLASP2 and XMAP215/Ch-TOG, where the HEAT domain interacts with the MTs (Akhmanova, et al., 2001). Thus I hypothesized that KIAA1468 interacts with MTs. RNAi-based KIAA1468 depletion in the Mitocheck database (Neumann et al., 2010; Hutchins et al., 2010) is associated with chromosome segregation defects, lagging chromosomes and multinucleated cells. Nonetheless, KIAA1468 is still a largely uncharacterised protein.

There is a cluster of five predicted phosphorylation sites in the middle of the longest isoform of human KIAA1468 and at the beginning of shorter CRA_a isoform, (Figure 3.11). Therefore, I hypothesized that KIAA1468 is a substrate of Aurora kinases, potentially on the MTs.

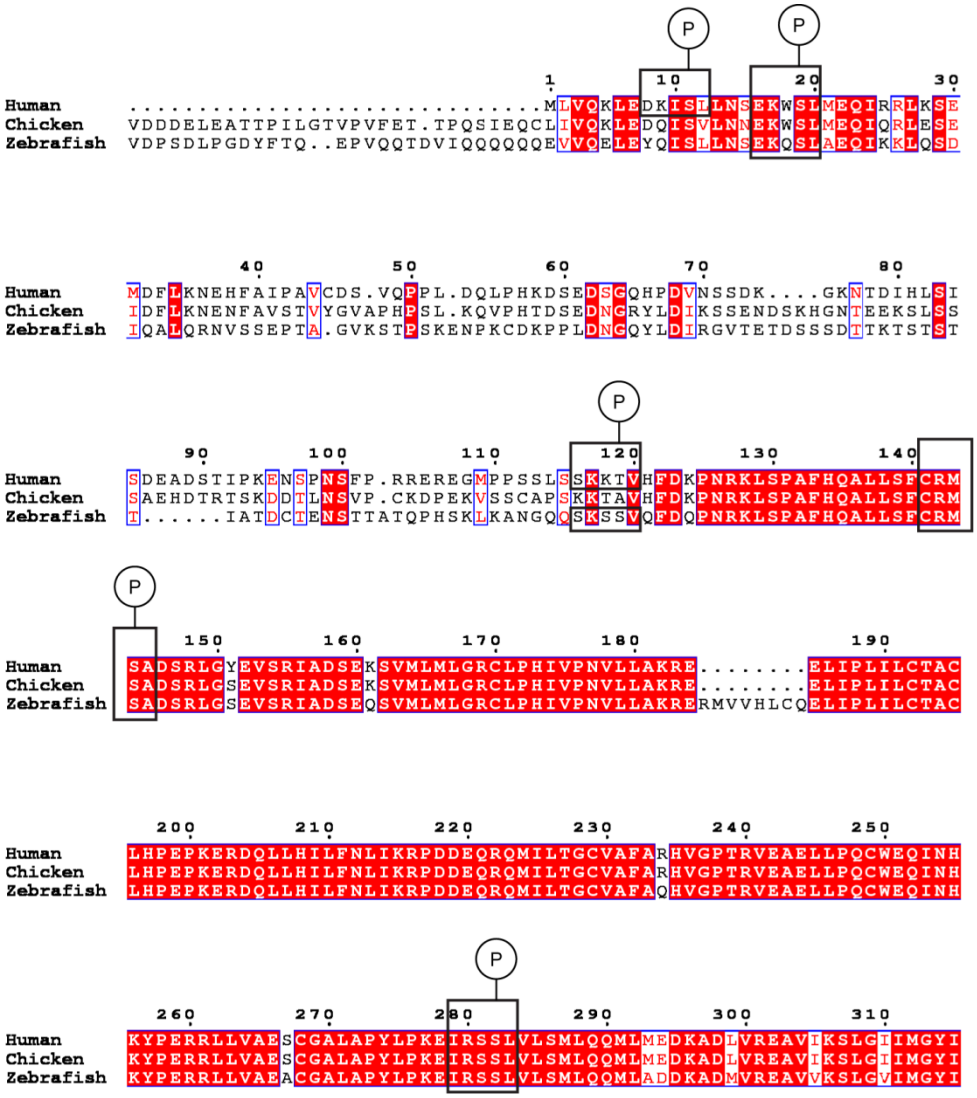

Figure 3.11: Predicted phosphorylation sites in KIAA1468. Sequence alignment of human KIAA1468 Cra_a isoform (Q96ES0), chicken KIAA1468 (F1NQF9) and zebrafish (A0A0R4IK69) was performed using ClustalOmega (Sievers et al., 2011) and formatted with ESPRIPT (Gouet et al., 1999). The conserved residues are highlighted in red. Amino acid numbering is relative to the human KIAA1468 sequence. Rectangles mark predicted consensus motifs, while P marks the position of predicted phosphorylation.

3.2.2.2 **Purification of recombinant proteins and protein fragments**

To test the phosphorylation of selected candidates by *in vitro* kinase assays, I used commercial His-tagged human recombinant Aurora A and recombinant GST-Ipl1 (yeast homologue of Aurora B). I expressed GST-Ipl1 in bacteria, and purified it by affinity chromatography, followed by size-exclusion chromatography (Figure 3.12A and B). After the second purification step, there were two pools of GST-Ipl1. A kinase pool with a contaminant was eluting first. Ipl1 degradation was most prominent in fractions with clean kinase without contaminant (Figure 3.12B). I performed a phosphorylation assay with outer kinetochore protein $Ndc80_{bonsai}$ (Ciferri et al., 2008) as a substrate to the test the activity of the purified pools of GST-Ipl1. I tested whether Ndc80 was phosphorylated using an antibody specific to phosphorylated S55, which is known to be phosphorylated by Aurora kinases (see 2.2.3). I found that both purified pools of GST-Ipl1 kinase phosphorylated $Ndc80_{bonsai}$ (Figure 3.13). This indicated that GST-Ipl1 is active.

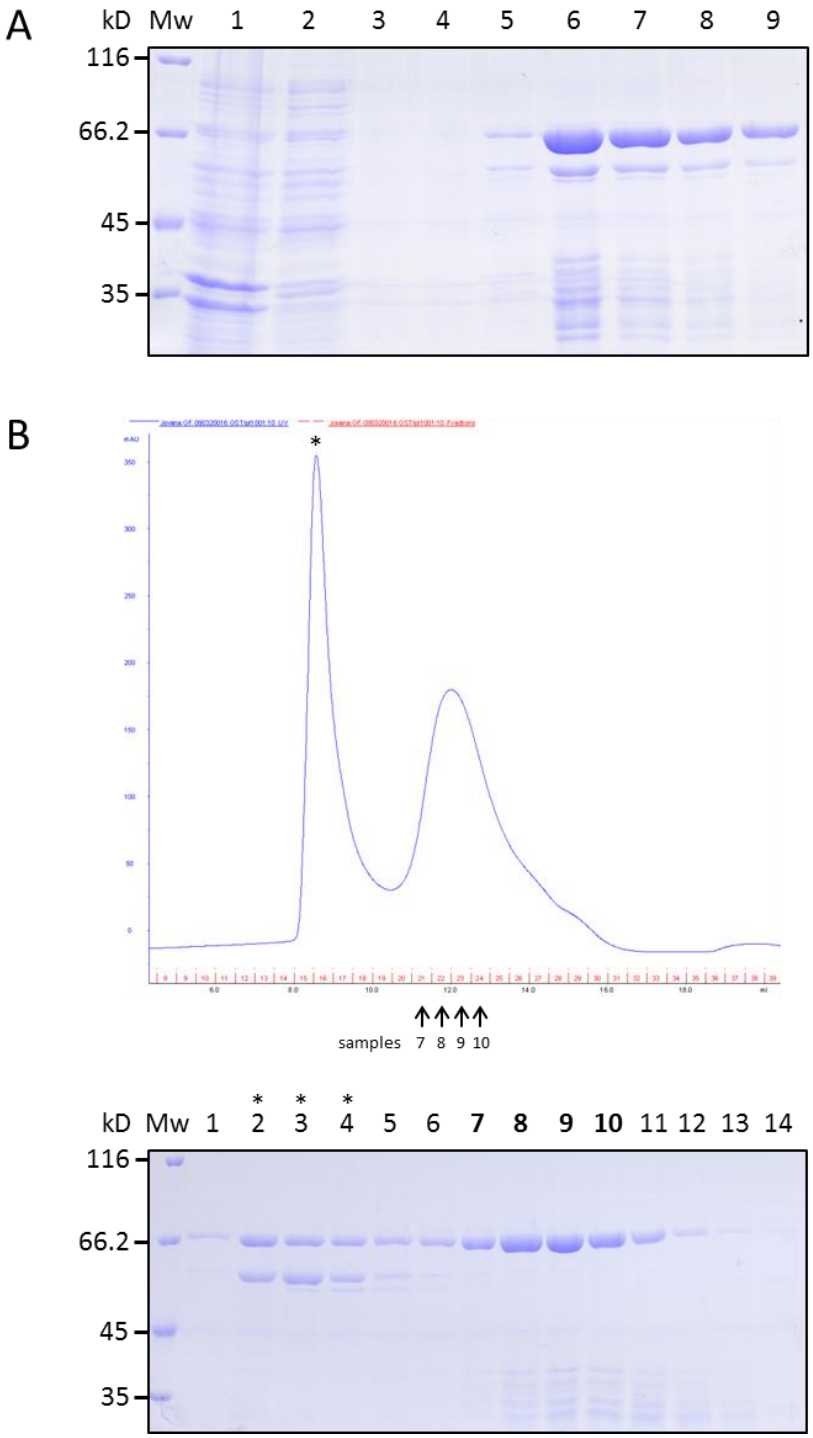

Figure 3.12: Two-step purification of recombinant yeast GST-Ipl1 kinase. (A) Sample analysis after affinity chromatography. Clarified bacterial lysate was loaded onto glutathione Sepharose beads after sonication (remaining pellet in Lane 1). Lanes 2, 3 and 4 shows the unbound fraction and the two wash fractions. Lanes 5-9 shows bound material eluted with 20 mM glutathione. (B) Size-exclusion chromatography and analysis. The eluted fractions from an S200increase column were analysed on SDS-PAGE (Lanes 1-14). Lanes 7-10, containing clean GST-Ipl1, were pooled and concentrated. Lanes 2-4 represent samples from gel filtration fractions corresponding to the first peak marked with an asterisk on the gel filtration profile. These fractions contain GST-Ipl1 with a contaminant and they were separately pooled and concentrated.

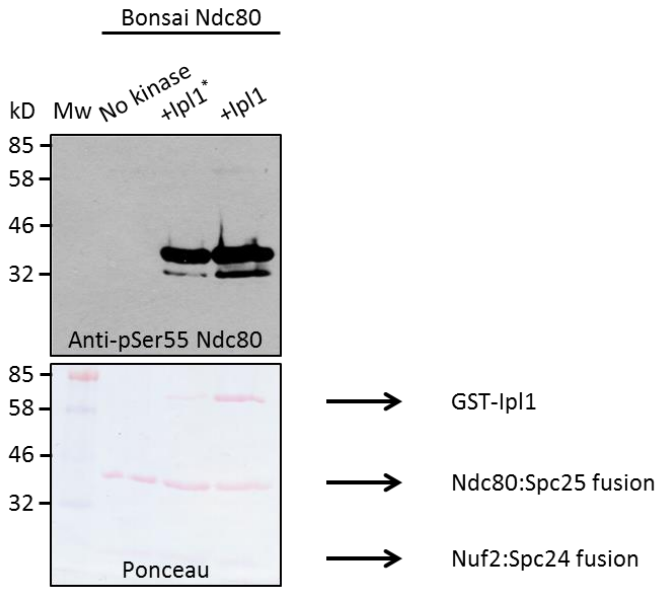

Figure 3.13: Purified GST-Ipl1 kinase is active. Phosphorylation reactions were performed in the presence of 10 mM ATP in kinase buffer and 4µg of substrate for 30 min at 37°C. Reactions were terminated by addition of SDS sample loading buffer and products were separated on SDS polyacrylamide gel. Ponceau staining of the nitrocellulose membrane after western blotting transfer showed the positions of $Ndc80_{bonsai}$ complex (Ciferri et al., 2008) and purified GST-Ipl1 relative to the molecular weight marker. GST-Ipl1 with a contaminant is labelled with an asterisk. Phosphorylation was detected with antibody against phosphorylated S55 on HEC1/Ndc80.

Next, I tested whether the predicted substrates were phosphorylated *in vitro* by Aurora kinases. Test expression was first conducted for three full-length human proteins Nup107, KIAA1468 and SPICE1, with 107 kDa, 97 kDa and 96 kDa molecular masses, respectively. Since the full-length proteins were insoluble, I purified fragments of those proteins containing the predicted phosphorylation sites. The same principle was applied for larger human proteins, ELYS (252 kDa), CLASP2 (169 kDa) and TTLL4 (133 kDa). All the fragments were expressed and purified with 6xHis tag at the C terminus, which is preceded by the 3C protease cleavage site so that, if needed, the tag can be cleaved with this protease.

CLASP2 has ten predicted phosphorylation sites clustered in the central disordered region of the protein (see 3.2.2.1 and Figure 3.6). I purified two short fragments, $CLASP2_{551-668}$ and $CLASP2_{741-818}$ each containing five predicted sites. Sequencing of the construct used for cloning revealed it was CLASP2 isoform X15, which differs from CLASP2 isoform α by an additional 63 bp in the second fragment.

The expected molecular masses of CLASP2$_{551-668}$ and CLASP2$_{741-818}$, based on their amino acids sequence, are 14 kDa and 10 kDa, respectively. Purified fragments were of expected size on the gel (Figure 3.14 and Figure 3.15). A third CLASP2 fragment tested *in vitro*, CLASP2$_{1232-1527}$ containing the C terminus, was previously purified in the lab by Sarah Young.

I purified two fragments from the ELYS C terminus. The first fragment, ELYS$_{1149-1329}$, contains three predicted sites and has a predicted molecular mass of 22 kDa. The second fragment, ELYS$_{1858-2014}$, contains four predicted sites and has a predicted mass of 20 kDa. ELYS$_{1149-1329}$ exhibited some minimal degradation indicated by smaller bands on the gel. ELYS$_{1858-2014}$ was purified with a low amount of contaminant indicated by the higher band on the gel (Figure 3.16 and Figure 3.17).

Next, I generated two fragments of nuleoporin Nup107, expressed as in Boehmer et al., 2008; Nup107$_{1-644}$ with 76 kDa mass and the 33 kDa C terminus, Nup107$_{658-925}$. Two-step-purification was performed for both fragments. The previously crystalized (Boehmer et al., 2007) Nup107 C terminus, was more stable and gave a higher yield. Despite that, there was some level of unfolding as noticed by the higher mass band containing chaperones, which were not separated after second step of purification (Figure 3.18 and Figure 3.19). Chaperones have been noticed previously in the purification of nucleoporins (Rasala et al., 2006).

I then expressed and purified TTLL4$_{330-624}$, with predicted mass of 35 kDa. This fragment contains multiple predicted phosphorylation sites in the central region, just before catalytic domain. The purified fragment run higher on the gel compared to the predicted size, and a contaminant with mass slightly higher than 25 kDa remained after second purification step. Similarly to purified Nup107 fragments, residual chaperons can be seen in the TTLL4 purification, running at 70 kDa and indicating a certain degree of unfolding (Figure 3.20).

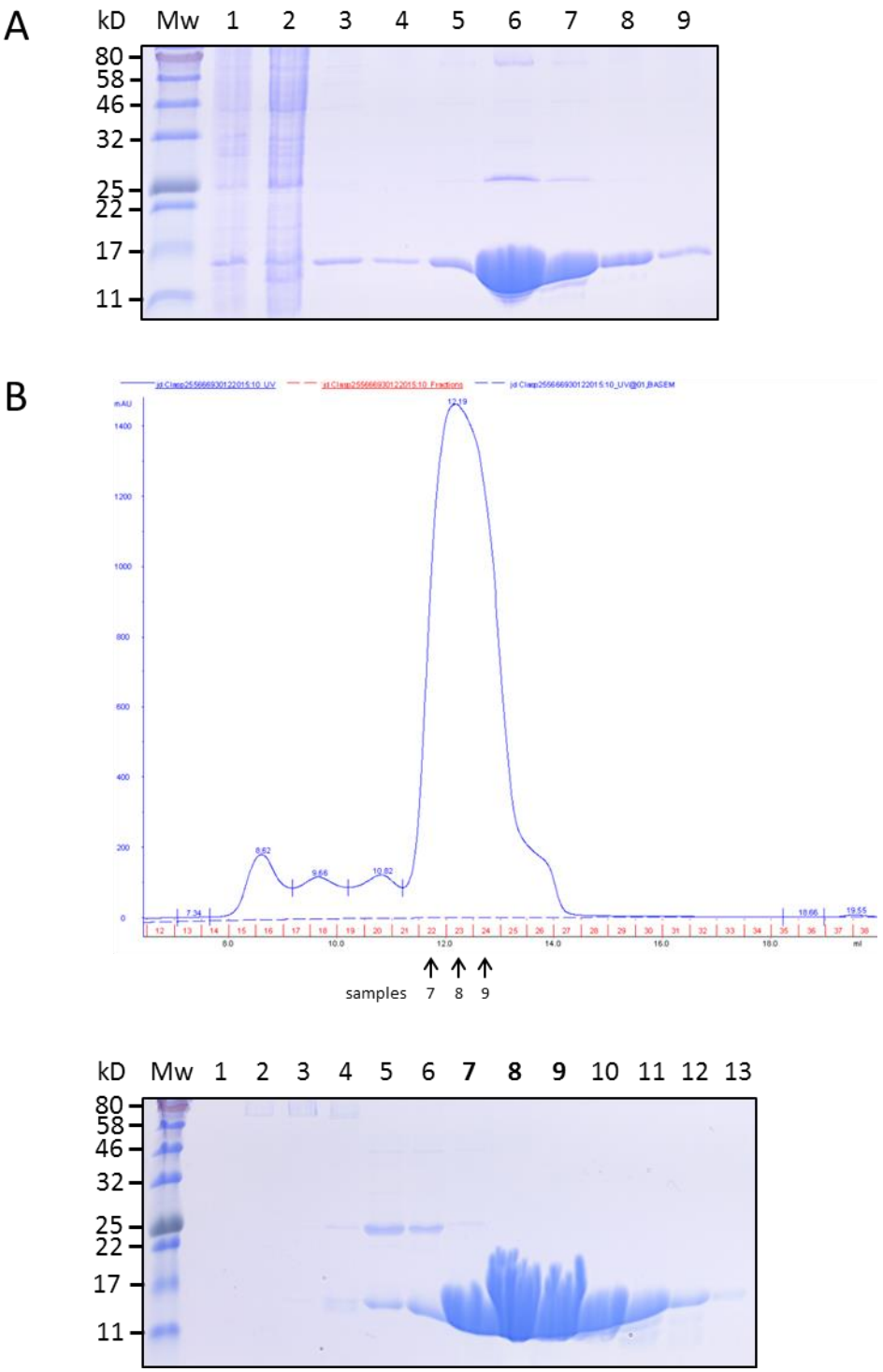

Figure 3.14: Two-step purification of recombinant human CLASP2$_{551-668}$. (A) Sample analysis after affinity chromatography. Clarified lysate was loaded onto Ni-NTA beads after sonication (remaining pellet in Lane 1). Lanes 2, 3 and 4 shows the unbound fraction and the two wash fractions. Lanes 5-9 shows bound material eluted with buffer containing 250 mM Imidazole. (B) Size-exclusion chromatography and analysis. The eluate absorbance from a Superdex75 column was monitored at 280 nm and 0.5 ml fractions were collected. The subsequent analysis was performed on SDS-PAGE (Lanes 1-13). Lanes 7-9, containing clean and highly concentrated CLASP2$_{551-668}$, were pooled.

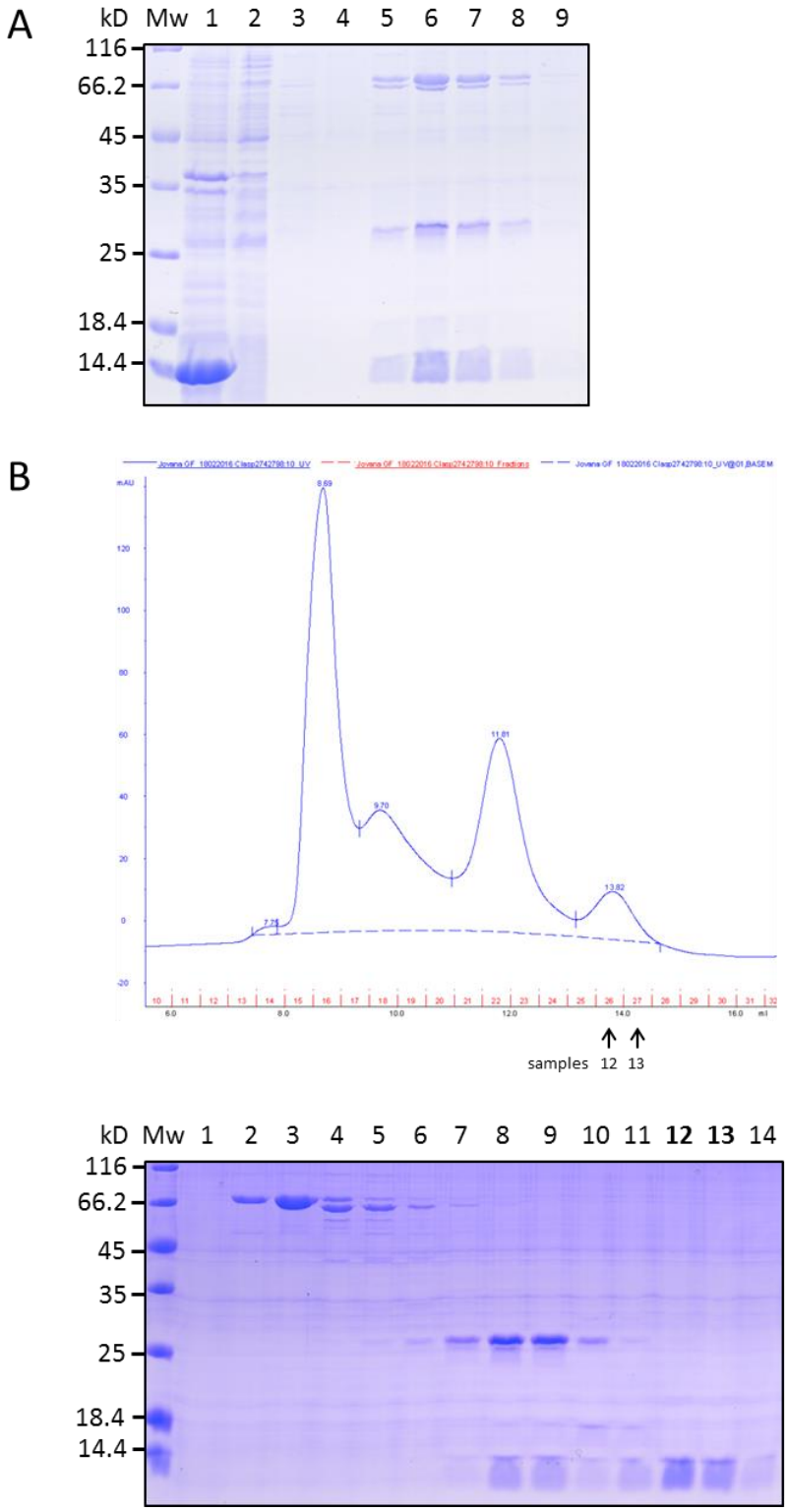

Figure 3.15: Two-step purification of recombinant human CLASP2$_{741-818}$. (A) Sample analysis after affinity chromatography. Clarified lysate was loaded onto Ni-NTA beads after sonication (remaining pellet in Lane 1). Lanes 2, 3 and 4 shows the unbound fraction and the two wash fractions. Lanes 5-9 shows bound material eluted with buffer containing 250 mM Imidazole. (B) Size-exclusion chromatography and analysis. The eluted fractions from a Superdex75 column were analysed on SDS-PAGE (Lanes 1-14). Lanes 12-13, containing 10 kDa CLASP2$_{741-818}$, were pooled and concentrated.

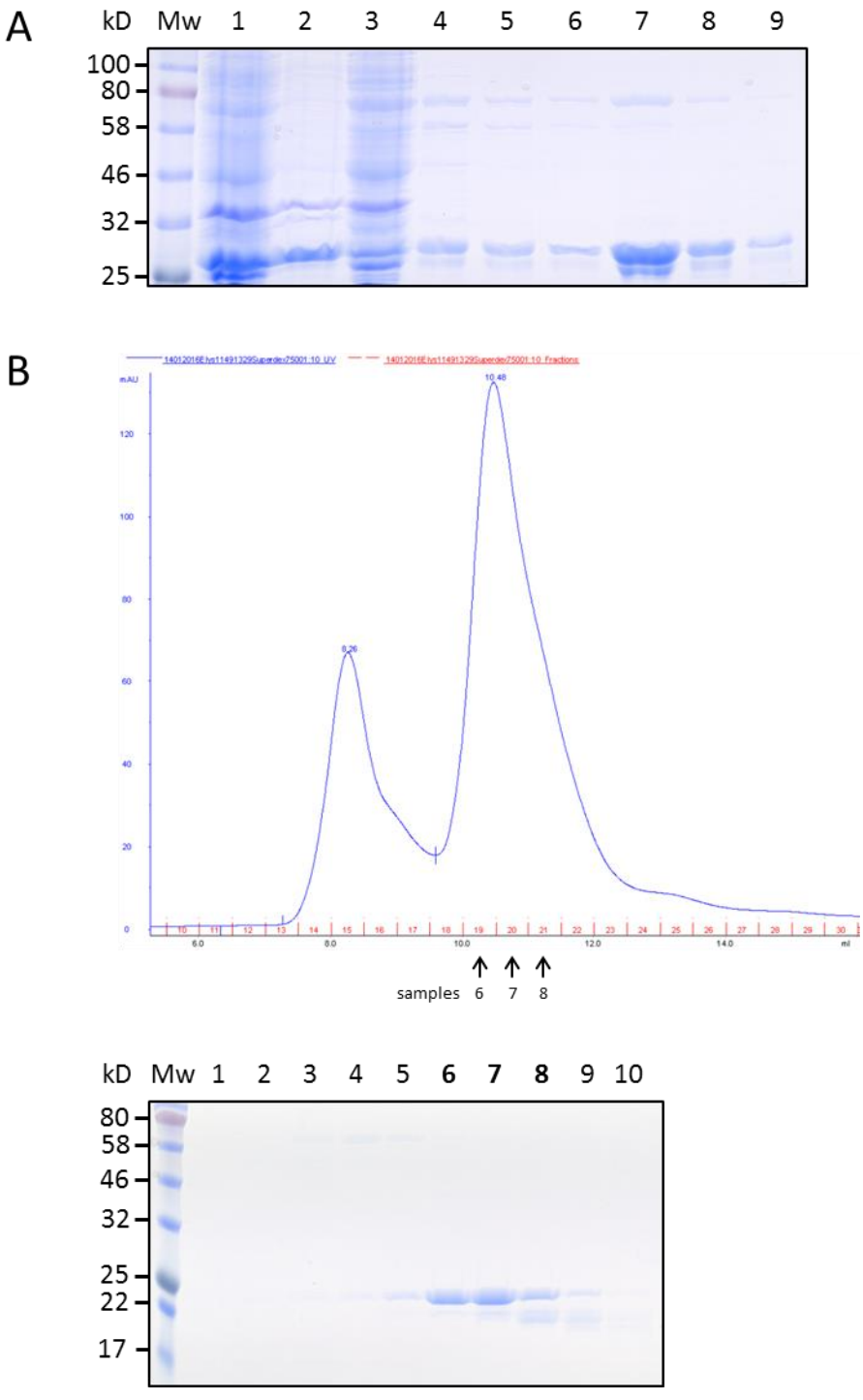

Figure 3.16: Two-step purification of recombinant human ELYS$_{1149\text{-}1329}$. (A) Sample analysis after affinity chromatography. Clarified lysate (Lane 1) was loaded onto Ni-NTA beads after sonication (remaining pellet in Lane 2). Lanes 3-6 shows the unbound fraction and the three wash fractions. Lanes 7-9 shows bound material eluted with Imidazole buffer. (B) Size-exclusion chromatography and analysis. The eluted fractions from a Superdex75 column were analysed on SDS-PAGE (Lanes 1-10). Lanes 6-8, containing ELYS$_{1149\text{-}1329}$, were pooled and concentrated.

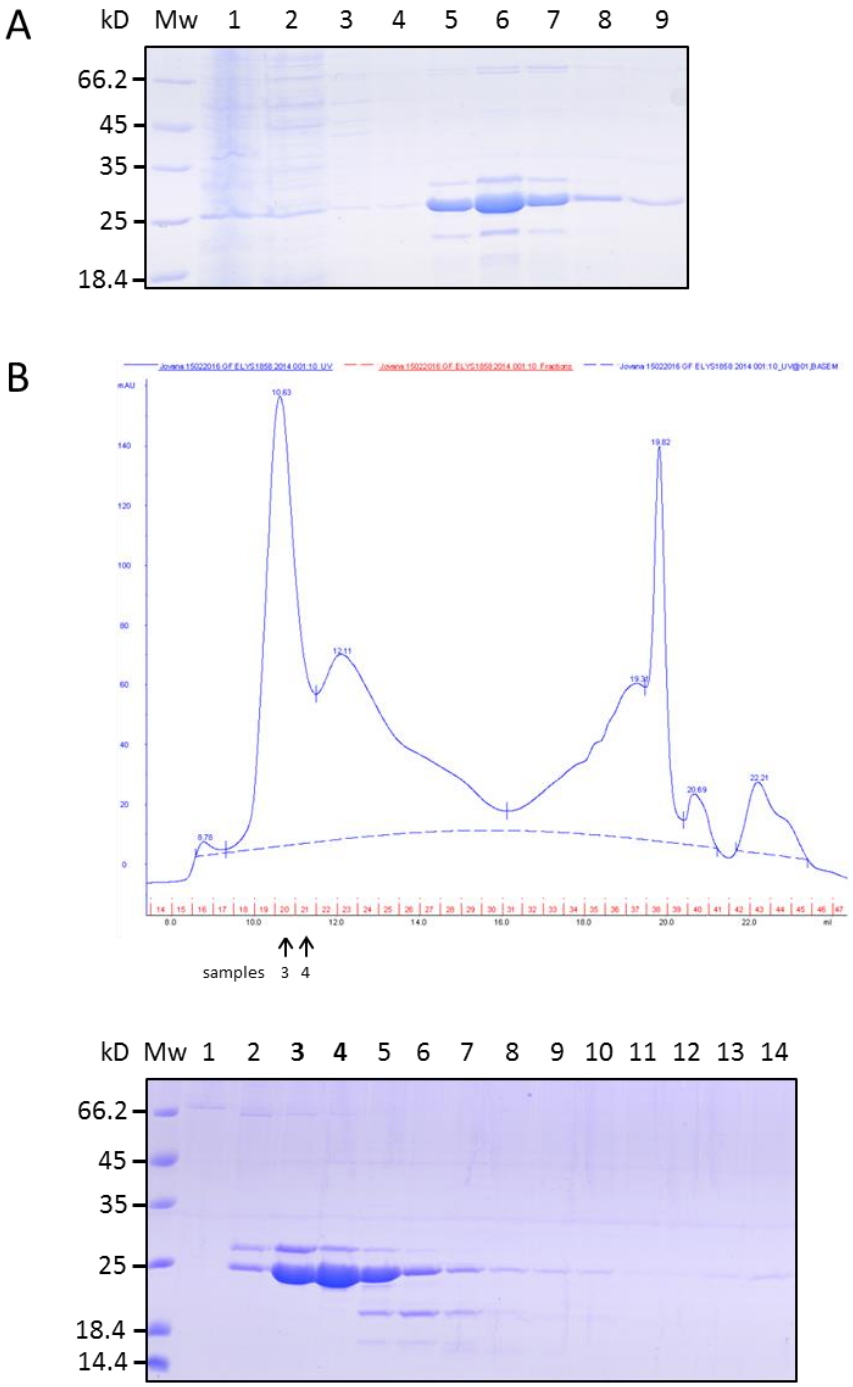

Figure 3.17: Two-step purification of recombinant human ELYS$_{1858-2014}$. (A) Sample analysis after affinity chromatography. Clarified lysate was loaded onto Ni-NTA beads after sonication (remaining pellet in Lane 1). Lanes 2-4 shows the unbound fraction and the two wash fractions. Lanes 5-9 shows bound material eluted with buffer containing 250 mM Imidazole. (B) Size-exclusion chromatography and analysis. The eluted fractions from a Superdex75 column were analysed on SDS-PAGE (Lanes 1-14). Lanes 3-4, containing ELYS$_{1858-2014}$, were pooled and concentrated.

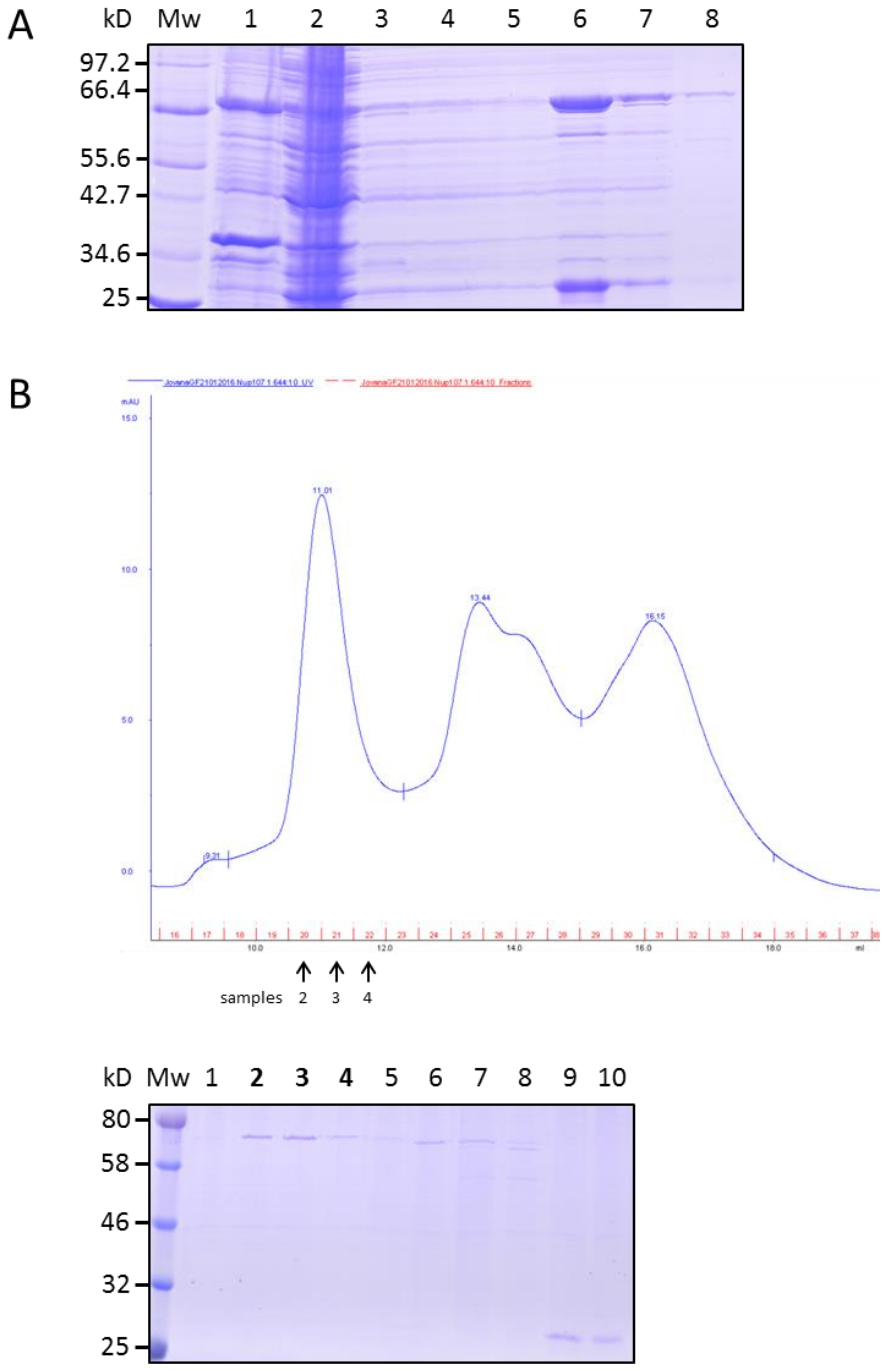

Figure 3.18: Two-step purification of recombinant human Nup107$_{1-644}$. (A) Sample analysis after affinity chromatography. Clarified lysate is loaded onto Ni-NTA beads after sonication and remaining pellet is in Lane 1. Lanes 2-5 shows the unbound fraction and the three wash fractions. The eluted material is in Lanes 6-8. (B) Size-exclusion chromatography and analysis. The eluted fractions from an S200increase column were analysed on SDS-PAGE (Lanes 1-10). Lanes 2-4, containing Nup107$_{1-644}$, were pooled and concentrated.

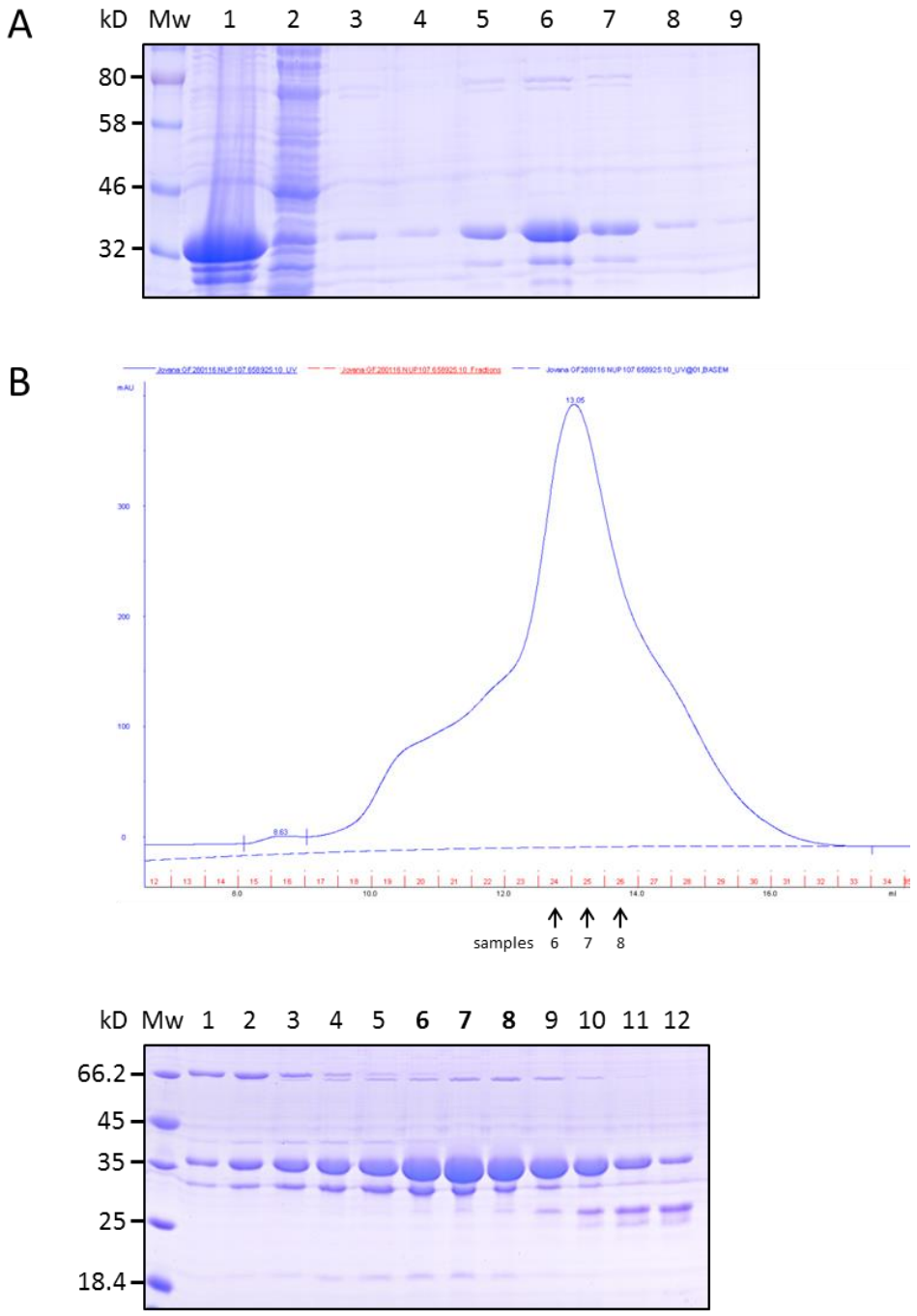

Figure 3.19: Two-step purification of recombinant human Nup107$_{658-925}$. (A) Sample analysis after affinity chromatography. Remaining pellet after loading clarified lysate onto Ni-NTA beads is in Lane 1. Lanes 2-4 shows the unbound fraction and the two wash fractions. The eluted material with 250 mM Imidazole is in Lanes 5-9. (B) Size-exclusion chromatography and analysis. The eluted fractions from an S200increase column were analysed on SDS-PAGE (Lanes 1-12). Lanes 6-8, containing the highest concentration of Nup107$_{658-925}$, were pooled and concentrated.

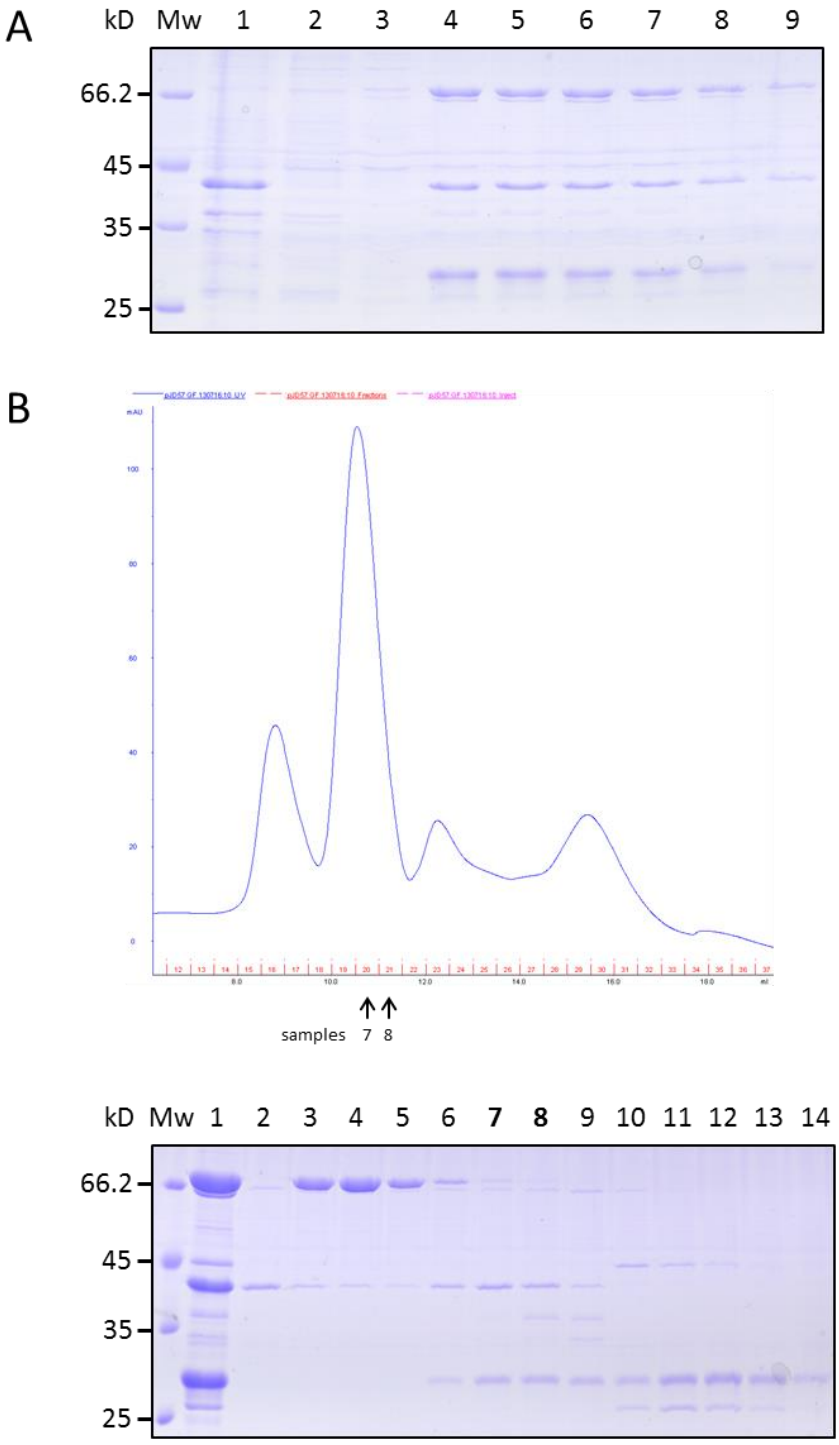

Figure 3.20: Two-step purification of recombinant TTLL4$_{330-624}$. (A) Sample analysis after affinity chromatography. Clarified lysate after sonication was loaded onto Ni-NTA beads; remaining pellet is in Lane 1. Lanes 2 and 3 shows the unbound fraction and the wash fraction. Lanes 4-9 shows bound material eluted with 250 mM Imidazole. (B) Size-exclusion chromatography and analysis. The eluted fractions from an S200increase column were analysed on SDS-PAGE (Lanes 2-12) and Lane 1 shows sample loaded onto S200 column. Lanes 7 and 8, containing 35 kDa TTLL4$_{330-624}$, were pooled and concentrated.

The SPICE1 C terminus, $SPICE1_{549-855}$, containing five predicted phosphorylation sites and with a predicted mass of 36 kDa, was purified by affinity chromatography, followed by buffer exchange (Figure 3.21A and B). The N terminus of KIAA1468, which contains six predicted phosphorylation sites, was insoluble and stayed in the pellet after affinity chromatography with only chaperons remaining in elution fractions as observed in Figure 3.21C. A process of isolation and solubilisation of inclusion bodies was applied, followed by refolding of solubilised protein (described in the Materials and Methods).

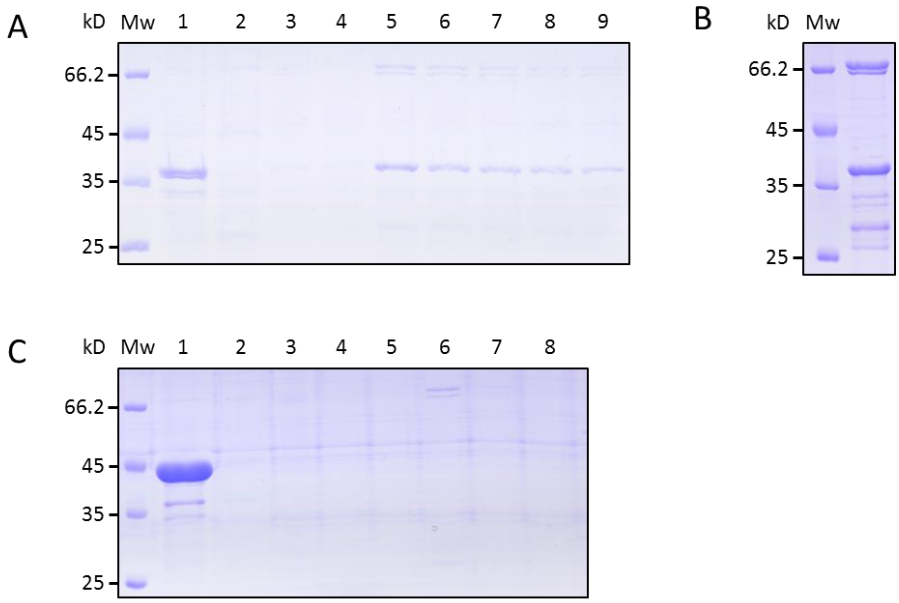

Figure 3.21: Purification of SPICE1 C terminus and N terminus of KIAA1468. (A) Sample analysis after affinity chromatography of $SPICE1_{549-855}$. Clarified lysate was loaded onto Ni-NTA beads and remaining pellet analysed in Lane 1. Lanes 2-4 shows the unbound fraction and the two wash fractions. Eluted material is in Lanes 5-9. (B) $SPICE1_{549-855}$ sample visualized on SDS-PAGE after buffer exchange. (C) Sample analysis after affinity chromatography of $KIAA1468_{1-292}$. Clarified lysate after sonication was loaded onto Ni-NTA beads and purification proceeded towards elution as usual. Lanes 2-5 shows the unbound fraction and the three wash fractions. Lanes 6-8 shows elution fractions. Lane 1 represents cell pellet.

3.2.2.3 AHCTF1, CLASP2, TTLL4, SPICE1 and KIAA1468 are *in vitro* phosphorylation substrates of Aurora A and Aurora B kinases

To test whether selected candidates are phosphorylated by Aurora kinases, purified protein fragments, containing predicted phosphorylation sites, were

subjected to *in vitro* radio-labelled phosphorylation assays. The first assay was performed with GST-Ipl1 (yeast Aurora B) against the purified candidate substrates. $Ndc80_{bonsai}$ (Ciferri et al., 2008) served as a positive control, while the recombinant C terminus of human Kif18b (Kinesin family member 18b) served as a negative control, since it does not contain phosphorylation sites of Aurora kinases as predicted by our bioinformatics. Approximately, 1 µg of each protein is used. $ELYS_{1149-1329}$ was heavily phosphorylated by Ipl1/Aurora B, while $CLASP2_{551-668}$ was phosphorylated only weakly as seen in Figure 3.22. No phosphorylation was observed in the CLASP2 C terminal kinetochore-targeting domain (Mimori-Kiyosue et al., 2006; Pereira et al., 2006), $CLASP2_{1232-1527}$. Neither $Nup107_{1-644}$ nor $Nup107_{658-925}$ showed phosphorylation by Ipl1/Aurora B. This indicates that Nup107 is not Aurora B substrate (Figure 3.22). Similar results were obtained in kinase assay with recombinant Aurora A (data not shown).

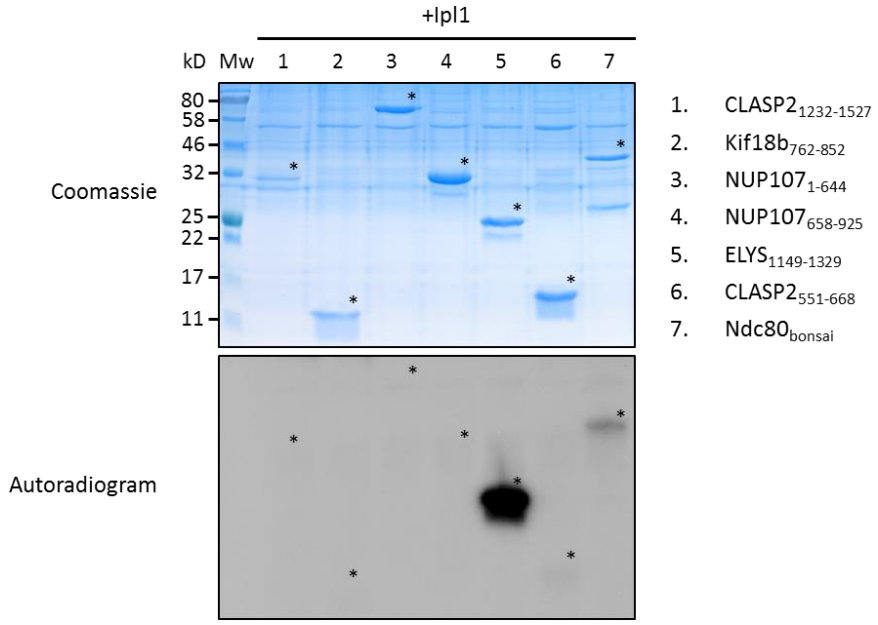

Figure 3.22: Radio-labelled kinase assay revealed ELYS and CLASP2 phosphorylation by Ipl1. Phosphorylation reactions were performed for 30 min at 37°C in the presence of 5 µCi γ ^{32}P-ATP, 10 mM cold ATP, 1 µg substrate and 1 µl GST-Ipl1. Simultaneously, the same reactions were performed without γ ^{32}P-ATP. Reactions were terminated by addition of SDS-sample loading buffer and proteins were separated by SDS-PAGE (15%). The gel with radioactive sample was dried and exposed to film overnight at -80°C, while the non-radioactive gel was stained with coomassie Blue. Asterisks mark the positions of protein fragments on the coomassie gel and autoradiogram.

I then tested remaining purified fragments of human CLASP2, ELYS, TTLL4, SPICE1 and KIAA1468 for phosphorylation with 1 µg of GST-Ipl1/Aurora B and much lower 0.2 µg of His-Aurora A. I observed phosphorylation in $CLASP2_{741-818}$, $ELYS_{1858-2014}$, $TTLL_{4330-624}$, $SPICE1_{549-855}$ and $KIAA1468_{1-292}$, while $Nup107_{658-925}$ was confirmed again not to be phosphorylated by both Aurora kinases (Figure 3.23). Strong auto-phosphorylation of Ipl1 was also visible, and some weak auto-phosphorylation of commercial Aurora A. This was expected as I used a higher amount of Ipl1 than Aurora A in the assay. GST-Ipl1 used in the assay showed degradation during purification (see 3.2.2.2). In the kinase assay, Ipl1 fragmentation products were also phosphorylated and observed on the autoradiograms. This phosphorylation of kinase degradation fragments was displayed as specific pattern below the auto-phosphorylation signal of full length GST-Ipl1.

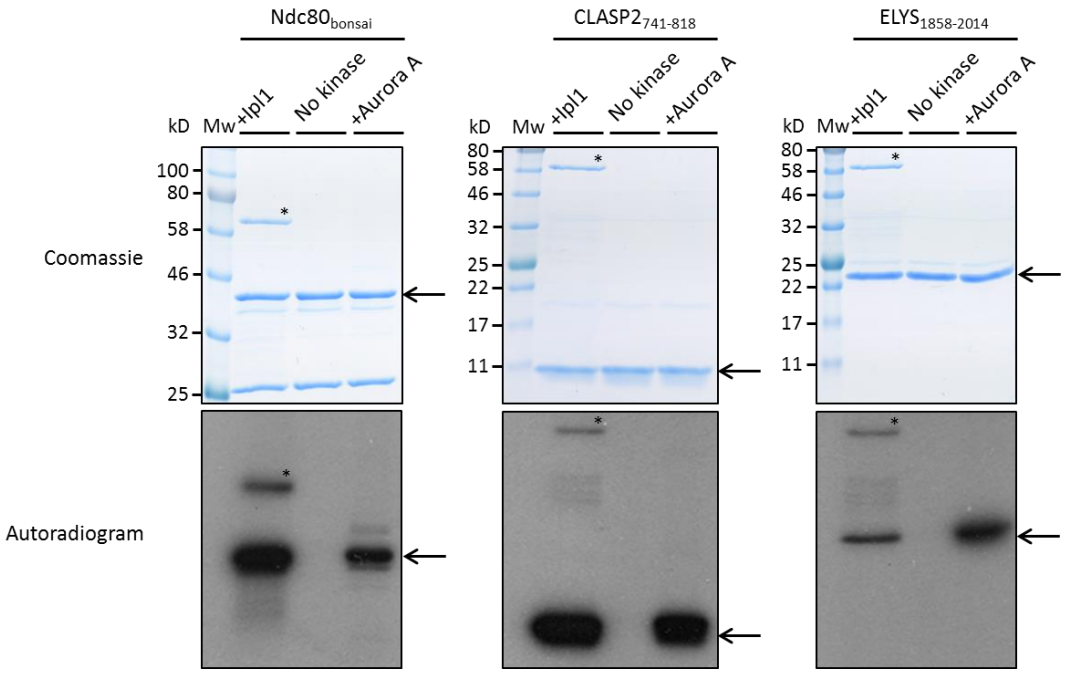

Figure 3.23: CLASP2, ELYS, TTLL4, SPICE1 and KIAA1468 are substrates of both Aurora kinases. Figure continues on the following page.

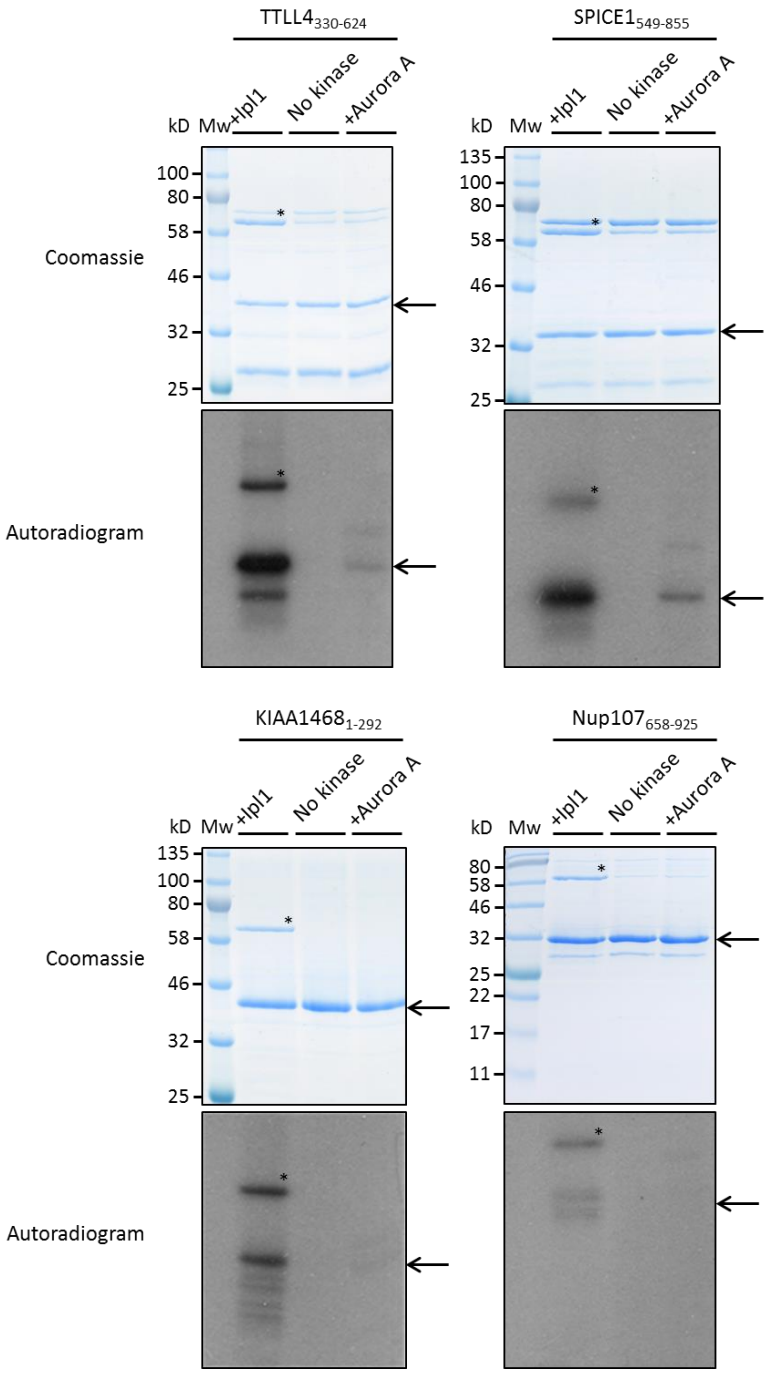

Figure 3.23: CLASP2, ELYS, TTLL4, SPICE1 and KIAA1468 are substrates of both Aurora kinases. Phosphorylation reactions were performed with either 1 µg GST-Ipl1 or 0.2 µg His-Aurora A and in the presence of 5 µCi γ ^{32}P-ATP, 10 mM cold ATP, 1 µg substrate for 30 min at 37°C. Additional reactions were prepared in the same manner but without γ ^{32}P-ATP and run simultaneously. Reactions were terminated by addition of SDS-sample loading buffer and proteins were separated by SDS-PAGE (15% and 10%). The gels with radioactive sample were dried and exposed to film at -80°C, while non-radioctive gels were stained with coomassie Blue. Asterisks mark the positions of GST-Ipl1 or its autophosphorylation on the coomassie gels and autoradiograms. Arrows indicate relative positions of protein fragments. Note that contaminants in the sample with TTLL4 and SPICE1 run at almost similar height as GST-Ipl1.

3.3 **Discussion**

There are still mitotic processes that are likely to involve regulation by Aurora kinases with unclear mechanisms. Identifying phosphorylation substrates of Aurora kinases will contribute to a better understanding of those mechanisms. I developed a bioinformatic tool in collaboration with bioinformatician Dr Alastair Kerr to predict new substrates of Aurora kinases. The novelty of our approach is to use existing tools not in a conventional linear manner but in a more flexible way, enabling us to narrow the search by using various combinations of the availiable filters at any time. This approach enables users to adjust bioinformatic filters and their search according to their needs (Figure 3.24).

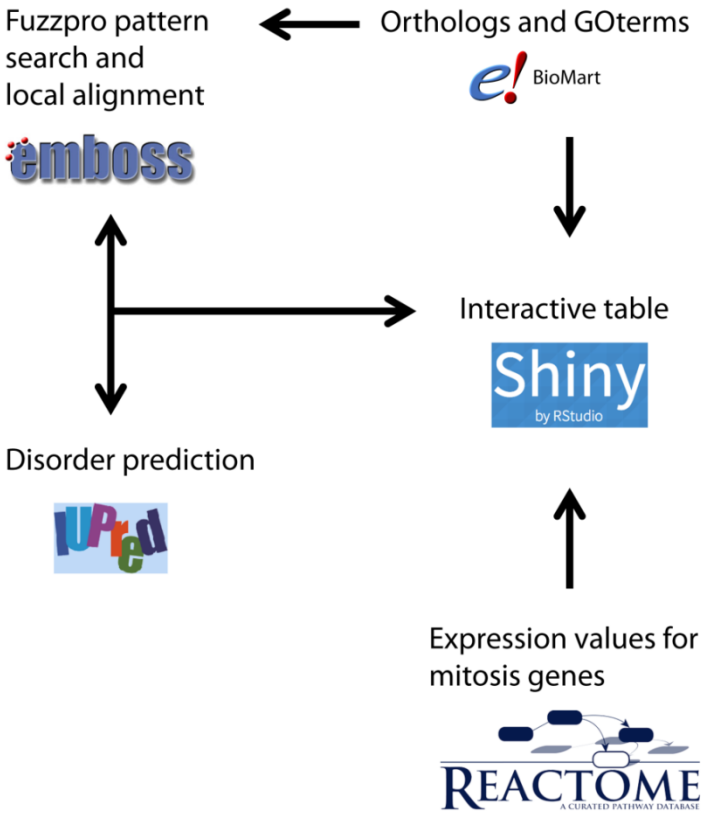

Figure 3.24: Schematic diagram of bioinformatic design with non-linear flow of available filters. An interactive table with filters was made by Dr Alastair Kerr, as well as all program scripts. Diagram of bioinformatics design is adapted using visual material from corresponding websites used to create bioinformatic tool; BioMart at: http://www.ensembl.org/biomart; EMBL tool for pairwise sequence alignment http://www.ebi.ac.uk/Tools/psa/emboss_stretcher/; Disorder region finder at http://iupred.enzim.hu/; Reactome database at http://reactome.org/. Web-available, user-friendly interactive interface is made using Shiny (available at https://shiny.rstudio.com/).

Using the bioinformatic approach developed, I found new putative phosphorylation sites in proteins that have not been previously demonstrated as Aurora kinase substrates. I then selected candidates derived from my bioformatics analysis to validate them as Aurora kinase substrates *in vitro*. With this approach, I found that five out of six selected candidates were directly phosphorylated by Aurora kinases. In this study, I revealed that Aurora kinases phosphorylate the MT plus end protein CLASP2, kinetochore-bound nucleoporin Mel28/ELYS, polyglutamlylase TTLL4, spindle and centrosome protein SPICE1 and uncharacterized protein KIAA1468. It was not clear how many sites were phosphorylated by Aurora kinases from the *in vitro* assay. Future mass spectroscopy analysis would help to identify this.

Although, the function of these phosphorylation sites needs to be determined in cells, it is interesting to discuss the data from *in vitro* assays in the context of the reported function and regulation of these selected proteins. For instance, two purified fragments of CLASP2 were found to be phosphorylated by both Aurora kinases in this study. Particularly strong phosphorylation was observed in the fragment $CLASP2_{741\text{-}818}$. Predicted sites in this fragment are near to the SxIP EB1-binding motifs, and also flanked by closely spaced phosphorylation sites of GSK3 (Kumar et al., 2009). These predicted sites of Aurora kinases are present in an intrinsically disordered region of CLASP2 that is conserved between species (see Figure 3.6). As suggested previously, GSK3 multisite phosphorylation of this central region in CLASP2 negatively regulates binding of CLASP2 to the EB1 and subsequent accumulation at the MT plus ends, both in interphase and in mitosis (Kumar et al., 2012). It was also reported that this GSK3 phosphorylation is dependent on previous Cdk1 phosphorylation of S740 and S774 in CLASP2. Protein interactions with EB1 are not just mediated via the SxIP motifs, but also through electrostatic interactions between basic residues surrounding these motifs and the acidic C terminus of EB1. Hence, it is expected that phosphorylation of S or T in the vicinity of an SxIP motif, introducing negative charge, also reduces the attractive electrostatic interaction of a protein with EB1 (Honnappa et al., 2009). It would be

interesting to see, both in cells and *in vitro*, whether Aurora kinase phosphorylation of the CLASP2 central region influences CLASP2 binding to MT plus ends in the same manner as GSK3 phosphorylation. Additionally, cooperativity between Cdk1, GSK3 and Auroras, in the regulation of this region in CLASP2 could be investigated. However, resolving this question in cells could be complicated, as many different kinases may be interconnected in the regulation of CLASP2 activity. Hence, the mutation of predicted phosphorylation could produce very subtle phenotypes, as was similarly noted for GSK3 phosphomutants (Pemble et al., 2017).

Two recombinant fragments of Mel28/ELYS, $hELYS_{1149-1329}$ and $hELYS_{1858-2014}$ were found to be particularly strongly phosphorylated by both Aurora kinases in this study. These fragments are positioned in the disordered C terminus of the protein. A recent study by Hattersley et al., 2016 found two docking sites for PP1c in the proximal part of the Mel28/ELYS C terminus. PP1c interaction with the C terminus of kinetochore-bound Mel28/ELYS was shown to be important for recruiting the phosphatase to the kinetochores in order to drive chromosome segregation in meiosis I in *C.elegans*. Later, during exit from M phase, as Mel28/ELYS shifts from kinetochores to chromatin, it pulls along the phosphatase, which is then important for correct nuclear reassembly through dephosphorylation of other nucleoporins (Hattersley et al., 2016). It was reported previously that PP1c docking onto proteins is often regulated through phosphorylation of partner proteins within or in the vicinity of the PP1c-docking site (Bollen et al., 2010). That is why Hattersley and colleagues speculated that PP1c docking on the Mel28/ELYS C terminus during meiosis is probably regulated through phosphorylation of this region. Lack of Mel28/ELYS has already been connected with defects in cytokinesis (Rasala et al., 2006; Yokoyama et al., 2014). Importantly, the sites predicted by our bioinformatics in $hELYS_{1149-1329}$ exactly coincide with both reported docking sites of PP1c (Figure 3.7A). This fragment was directly phosphorylated by both Aurora kinases *in vitro*. Further, both predicted phosphorylation sites are well conserved between vertebrate species (Figure 3.7A). This phosphorylation was not detected previously in the mass spectrometry study by Kettenbach et al. in 2011. Neither was

it predicted by bioinformatics developed by Sardon and colleagues in 2010. This could indicate that our bioinformatics predicted a completely new and conserved mechanism of Aurora kinase regulation of cell division exit through phosphorylation of the Mel28/ELYS C terminus. Of course, the functionality of this phosphorylation detected *in vitro* has to be confirmed *in vivo* or in cells. Testing the role of phosphorylation using phosphomutants in cells might be more challenging (but not impossible), due to the multiple roles ELYS has in cells.

Regulation of other candidates by phosphorylation, TTLL4, SPICE1 and KIAA1468, has not been previously described. In the case of KIAA1468, first its mitotic function and localization in cells would have to be determined. Only if the protein has important function in mitosis, it would be possible to test the effect of Aurora kinase phosphorylation on that function. In the case of polyglutamylase TTLL4, I can speculate that Aurora-driven multisite phosphorylation of the central region near the catalytic domain, which also binds MTs, could potentially destabilize MT binding of this enzyme through electrostatic repulsion. In this way, Aurora kinases could selectively regulate polyglutamylation of distinct subsets of MTs, in order to control the activity of numerous MAPs in cell division. This would be difficult to test in cells. There are no inhibitors developed so far targeting specifically TTLL4, due to the similarity in structure between numerous members in TTLL family of polyglutamylases. Additional redundancy of function in the TTLL family means it would be difficult to discover a mitotic phenotype of TTLL4 depletion, using siRNA or other methods. Without an established mitotic phenotype it would impossible to test the effect of TTLL4 phosphorylation in mitosis. On the contrary, SPICE1 has an established phenotype in mitosis, although the exact mechanism of how SPICE1 influences centriole elongation and bipolar spindle formation is not well understood (Archinti et al., 2010). I have found that the SPICE1 C terminus is phosphorylated *in vitro* by Aurora kinases. Since this fragment has not been reported to bind either centrioles or the mitotic spindle (Archinti et al., 2010), I can speculate that phosphorylation of this region could regulate SPICE1 centriolar and MT-binding activities indirectly.

In summary, the results presented in this chapter shows that I have developed a bioinformatic tool, which is successful at predicting substrates of Aurora kinases. Five out of six selected candidates from our bioinformatic list were phosphorylated by Aurora kinases *in vitro*. It is next important to determine whether our bioinformatic approach predicts functional phosphorylation. For this reason, I further selected one of the five candidates to test whether this predicted phosphorylation by Auroras affects candidate function in cells. In the following chapter, I analyse the regulation of SPICE1 by Aurora kinases.

4 Chapter 4: Characterization of SPICE1 phosphorylation by Aurora kinases in cells

4.1 Introduction

In Chapter 3, I showed that the bioinformatics approach I developed predicts five phosphorylation sites of Aurora kinases in the SPICE1 C terminus. I also showed that the SPICE1 C terminus is phosphorylated by Aurora kinases *in vitro*. Based on the fact that the regulation of SPICE1 was uncharacterised, I decided to examine the regulation of SPICE1 through phosphorylation by Aurora kinases at five predicted residues in the SPICE1 C terminus. SPICE1 is a spindle and centriole associated protein with a reported function in centriole elongation and duplication, as well as in bipolar spindle formation and chromosome congression in mitosis (Archinti et al., 2010).

SPICE1 is localized to the walls of the mother and daughter centriole. It is required for centriole elongation and duplication during S and G2 phases of the cell cycle (Comartin et al., 2013). The elongation of newly formed daughter centrioles is an essential part of the centriole duplication cycle and maturation to generate two fully functional centrosomes (Firat-Karalar and Stearns, 2014). Recruitment and activation of SPICE1 during centriole elongation has been precisely determined (Comartin et al., 2013). CPAP recruits CEP120, CEP135 and SPICE1 to initiate the elongation and stabilization of procentriole MTs (Lin et al., 2013; Comartin et al., 2013; Figure 4.1). In this pathway, the localization and function of SPICE1, CEP120 and CEP135 are mutually dependent on their interaction (Comartin et al., 2013). SPICE1 is also required for the recruitment of Centrin and other centriole components to complete centriole assembly (Comartin et al., 2013). The core centriole assembly pathway is conserved in metazoans (Nigg and Raff, 2009; Gönczy, 2012). However, SPICE1 is only present in vertebrates (Archinti et al., 2010). The exact mechanism of how SPICE1 co-operates with CEP120 and CPAP to enable centriole elongation, is not currently understood.

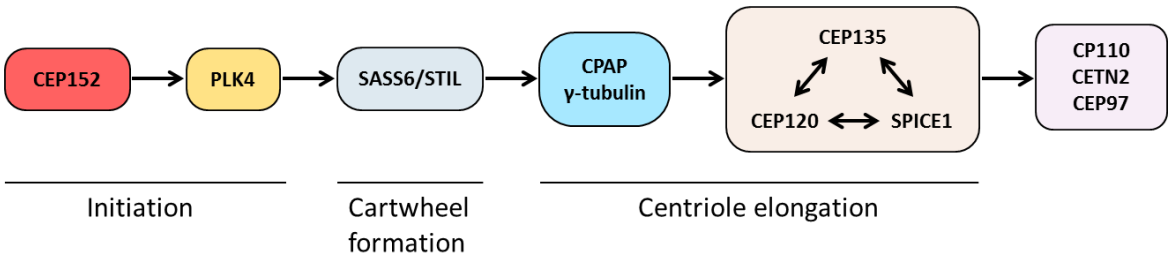

Figure 4.1: Schematic diagram of centriole assembly pathway in vertebrates. Adapted from Comartin et al., 2013.

In a study by Archinti and colleagues, SPICE1 depletion caused defects of mitotic spindle geometry, impaired chromosome congression, and decreased centriole number in cells. An increase in multipolar spindles, observed in SPICE1 depletion, is due to the acentriolar ectopic foci of PCM, which contained γ-tubulin (Archinti et al., 2010). The SPICE1-depleted cells containing two centrin foci at each pole had abnormally long spindles compared to the control cells. The authors suggest that SPICE1 regulates the spindle stability independently of centriole elongation/duplication (Archinti et al., 2010). The mislocalization of the K-fiber stabilization factor, HURP, was observed in SPICE1 depletion, which could indicate disruption in the K-fiber organization (Archinti et al., 2010). Nonetheless, it is still unknown how SPICE1 regulates the MT stability and spindle formation. Additionally, it is unknown how SPICE1 function is regulated in mitosis.

I hypothesized that Aurora kinases regulate SPICE1 function in cells, based on the evidence that these kinases phosphorylate the C terminus of SPICE1 *in vitro* and the fact that SPICE1 is proximal to Aurora A at the centrosomes. SPICE1 is also proximal to Aurora A and Aurora B at the mitotic spindle. The Aurora A kinase is involved in centrosome maturation and separation, and both Aurora kinases regulate spindle assembly, spindle stability, and proper chromosome segregation, as discussed in Chapter 1. Additionally, Aurora A phosphorylates CPAP, upstream of SPICE1, to maintain integrity of the PCM and spindle architecture (Chou et al., 2016). However, it was never demonstrated before that Aurora kinases directly phosphorylate SPICE1 to regulate its function.

The function of the C terminus of SPICE1 is unknown, and this region of SPICE1 does not target to a subcellular structure (Archinti et al., 2010). The N terminus of SPICE1 targets to the spindle, while centriole targeting is mediated by the first conserved coiled-coil (CC1), out of two existing coiled-coil regions in SPICE1 (Archinti et al., 2010). Therefore, we hypothesized that the phosphorylation of the SPICE1 C terminus may indirectly regulate SPICE1 function and targeting to the spindle and centrioles.

I examined whether the Aurora kinases phosphorylate SPICE1 in cells and regulate SPICE1 function and localization during mitosis. I tested the role of the predicted Aurora phosphorylation sites on the localization and function of SPICE1, using a SPICE1 non-phosphorylatable mutant (S to A mutation) and a phosphomimicking mutant (S to E) and small molecule inhibitors.

4.2 **Results**

4.2.1 **The SPICE1 C terminus is required for full-length SPICE1 binding to the spindle, but does not bind directly to microtubules**

To investigate the role of SPICE1 C terminal phosphorylation, I first verified the localization of GFP-tagged full-length SPICE1. Then, I tested the cellular localization of GFP-tagged SPICE1 truncated mutants: the SPICE1 C terminus, $SPICE1_{444-855}$, and SPICE1 in which the C terminus is depleted, $SPICE1_{1-550}$. GFP-tagged full-length SPICE1 and truncated mutants were first observed by live-cell imaging in HeLa cells. In live cells, transiently expressed GFP-full-length SPICE1 associates with spindle MTs and both mother and daughter centrioles, as previously reported (Archinti et al., 2010; Figure 4.2). GFP-full-length SPICE1 also associated with centrioles and MTs in interphase cells. The HeLa cells used in this experiment do not have a cellular marker, and the spindle localization was concluded based on a distinctive shape of the GFP signal, and the centriole localization was inferred from two GFP foci at both spindle poles. This localization to the mitotic spindle and the centrioles was then further confirmed using immunofluorescence to co-stain with β-tubulin and the centriole marker Centrin (Figure 4.3A). Centrin localizes to the distal lumen of centrioles (Paoletti et al., 1996), while SPICE1 localizes to the

proximal part of the centriole lumen (Archinti et al., 2010; Comartin et al., 2013). As expected, I detected a GFP-SPICE1 signal adjacent to the Centrin signal (Figure 4.3A).

I then examined GFP-SPICE1$_{444-855}$ and found it had a cytoplasmic localization in mitotic and interphase cells (Figure 4.2). Similar to the full-length SPICE1, GFP-SPICE1$_{1-550}$ localized to the centrioles and mitotic spindle in mitosis, and to the centriole and MTs in interphase (Figure 4.2 and Figure 4.3A). However, GFP-SPICE1$_{1-550}$ association with MTs was visibly reduced in the mitotic and interphase cells (Figure 4.2). I then quantified the levels of SPICE1$_{1-550}$ relative to the full-length protein on the mitotic spindle and confirmed a significant reduction of GFP-SPICE1$_{1-550}$ signal on MTs relative to the full-length SPICE1 (Figure 4.3B). This suggests that the C terminus of SPICE1 is required for enhanced SPICE1 localization at the spindle.

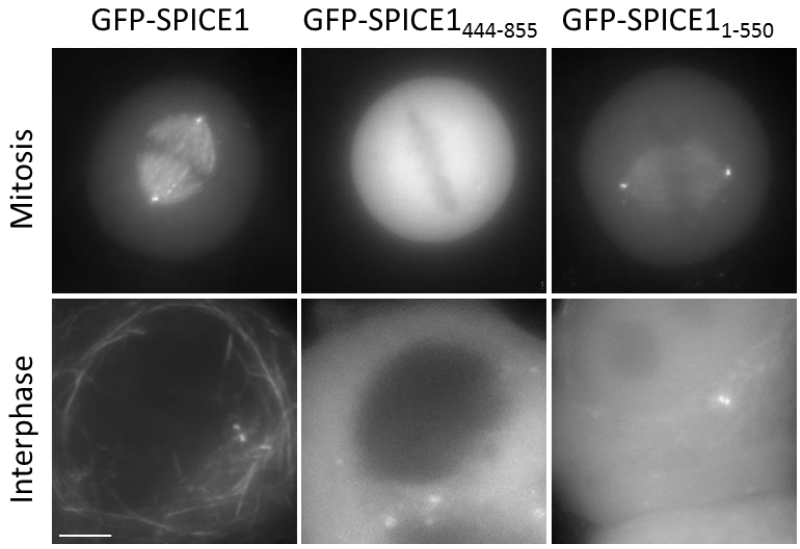

Figure 4.2: Live-cell imaging of GFP-tagged SPICE1 constructs. Representative images of live HeLa cells transiently expressing moderate amounts of GFP-SPICE1, GFP-SPICE1$_{444-855}$ or GFP-SPICE1$_{1-550}$ in mitosis and interphase. Scale bar is 5 µm.

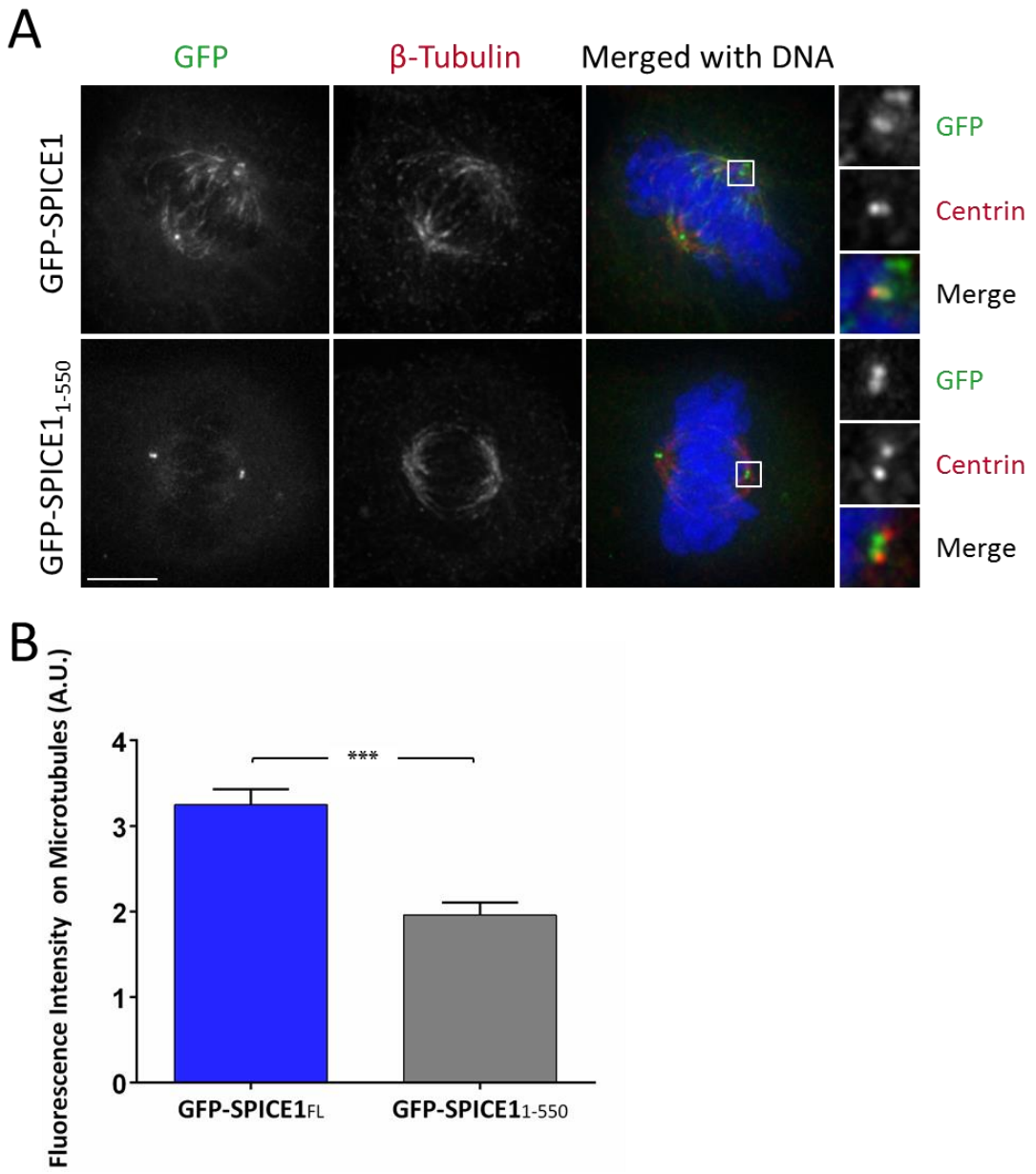

Figure 4.3: C terminus of SPICE1 is important for spindle localization. (A) Localization analysis of GFP-SPICE1 constructs. Images show the maximum projections of deconvolved z-stacks of the HeLa cells transiently expressing GFP-SPICE1 or GFP-SPICE1$_{1-550}$, stained with antibodies against β-tubulin and Centrin. Regions of one of the two spindle poles are 3x magnified in the insets. Scale bar is 5 µm. (B) The bar graph presents mean values of background-corrected integrated intensity of the GFP levels at the MTs (selected based on co-localization with β-tubulin) in metaphase cells (assessed by chromosome alignment). GFP-SPICE1, n=21 cells; GFP-SPICE1$_{1-550}$, n=32 cells. The error bars represent the standard error of the mean. Two-tailed p value of a Student's t-test is ***p<0.0001.

Additionally, I observed that the overexpression of SPICE1 causes an increase in centriole number, so I quantified the number of centrioles in SPICE1-overexpressed cells based on Centrin staining (Figure 4.4). On average the HeLa control cells had 4 centrioles, while the cells overexpressing SPICE1 had 6 centrioles. Interestingly, $SPICE1_{1-550}$ does not cause overamplification of centrioles, and the number of centrioles is comparable to the centriole number in the control non-transfected HeLa cells (Figure 4.4). This is the first report that SPICE1 overexpression causes centriole overamplification. The overexpression seems to require the C terminus of SPICE1, suggesting it has an important role in controlling centriole numbers. The inducible overexpression of STIL in human cells causes an increase in centriole number, and STIL is important to initiate centriole biogenesis (Arquint et al., 2012; Vulprecht et al., 2012; see Figure 4.1). I observed the same phenotype in SPICE1 overexpression, which indicates a SPICE1 function in centriole biogenesis, possibly in addition to the role in centriole elongation.

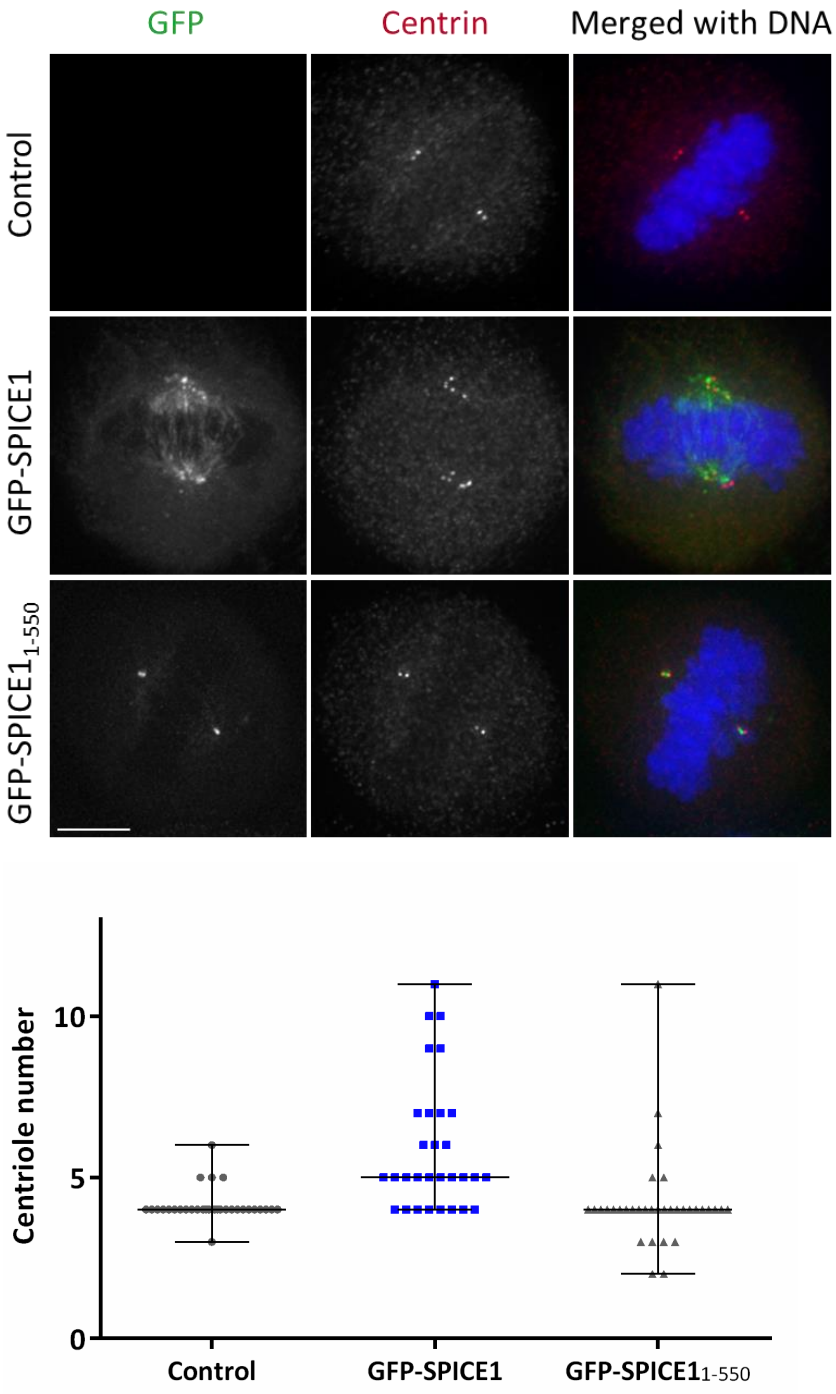

Figure 4.4: Overexpression of SPICE1 causes overamplification of centrioles. Images show the maximum projections of deconvolved z-stacks of the HeLa cells not transfected (control), transiently expressing GFP-SPICE1 or GFP-SPICE1$_{1-550}$, stained with the anti-Centrin antibody. Control, n=31 cells; GFP-SPICE1, n=30 cells; GFP-SPICE1$_{1-550}$, n=34 cells. The values of centriole number in each condition are presented with the scatter plot, and the range is represented with whiskers and the median as the middle line. Reported p value of Kruskal-Wallis test is $p<0.0001$. Scale bar is 5 µm.

4.2.2 **SPICE1 knock-down and conditional knock-out cause defects in mitosis**

To further define the role of SPICE1 in mitosis and develop assays to test the role of C terminus phosphorylation on SPICE1 function, I depleted endogenous SPICE1 from cells and analysed the loss-of-function phenotypes. Previous work which reported mitotic defects in spindle morphology, chromosome congression, and centriole number in the SPICE1-depleted cells, did not employ a rescue experiment with ectopically expressed SPICE1 construct (Archinti et al., 2010). Therefore, I first examined whether I could reproduce the SPICE1 depletion phenotype and whether the full-length wild type GFP-SPICE1 can rescue phenotypes observed in the reported SPICE1 depletion. Then I examined whether a non-phosphorylatable mutant or phosphomimicking mutants of SPICE1 could rescue the loss-of-function phenotypes.

The cells depleted of SPICE1 using siRNA were lacking the normal chromosome congression in metaphase. Chromosome congression defects were observed in 50% of the cells depleted of SPICE1 (Figure 4.5). The cells with less than five misaligned chromosomes were scored as cells with mild congression defects. The observed cells with more than five misaligned chromosomes around poles were scored as cells with severe defects. Importantly, co-transfection with siRNA-resistant GFP-SPICE1 rescued the severe chromosome defects (Figure 4.5).

Twenty-five percent of the SPICE1-depleted cells had multipolar spindles. This was rescued in cells co-transfected with siRNA-resistant GFP-SPICE1 (Figure 4.5). Interestingly, the increase in multipolar spindles was not the consequence of overamplified centrioles, since the SPICE1-depleted cells had a reduced centriole number, based on Centrin staining (Figure 4.5). Fifty-four percent of the SPICE1-depleted cells contained two pairs of centrioles compared to 91% of the control cells. The centriole quantification showed that a significant decrease in centriole number upon SPICE1-depletion was successfully rescued with ectopic expression of GFP-SPICE1 (Figure 4.5).

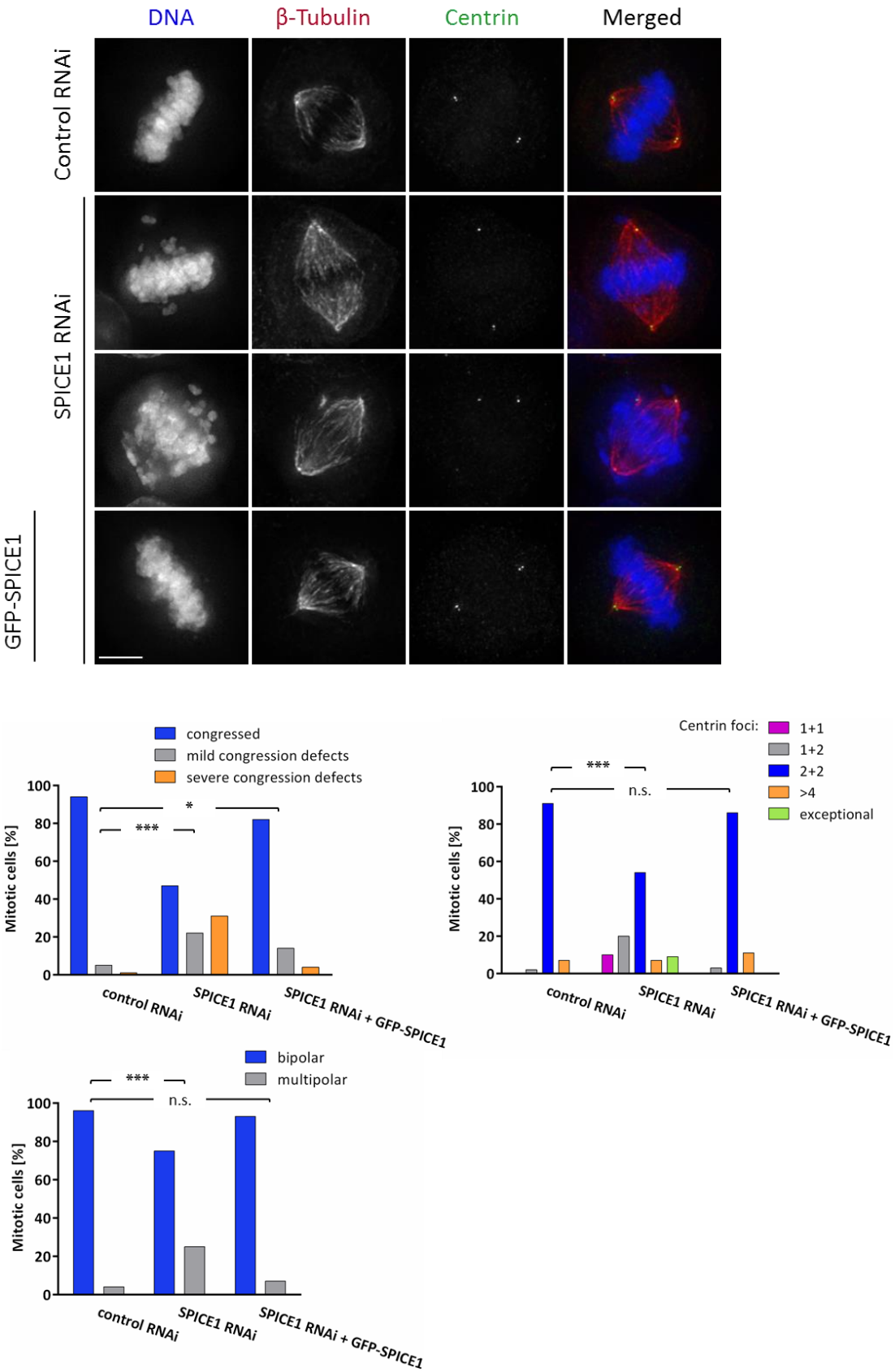

Figure 4.5: Mitotic defects in the SPICE1-depleted cells are rescued with expression of GFP-SPICE1.
Figure description on the following page.

Figure 4.5: Mitotic defects in the SPICE1-depleted cells are rescued with expression of GFP-SPICE1. Representative images show the maximum projections of deconvolved z-stacks of the HeLa cells. The cells were transfected with either control or SPICE1 siRNA, or co-transfected with SPICE1 siRNA and GFP-SPICE1 for 48h and then fixed and stained with antibodies against β-tubulin and Centrin. n=100 cells for each treatment. P values of Chi-square tests and Fisher's exact tests are reported: not significant (n.s.), *p<0.05 (p=0.032), ***p<0.0001. Scale bar is 5 µm.

To confirm that the depletion with siRNA was working efficiently, I tested the cell lysates from siRNA treatments by western blotting with a commercial antibody against SPICE1 (Figure 4.6A). The SPICE1 depletion was additionally confirmed by immunofluorescence (Figure 4.6B). This also confirmed the spindle and centriole localization of endogenous protein and justified the use of GFP-tagged SPICE1 constructs (Figure 4.6B).

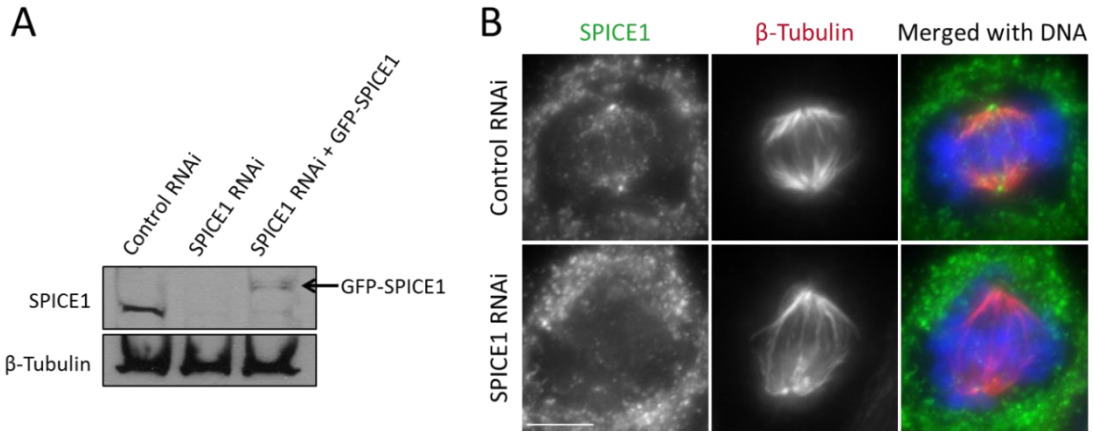

Figure 4.6: SPICE1 siRNA specifically targets SPICE1 in cells. (A) Western blot analysis of the control and SPICE1-depleted cells. The HeLa cells were lysed and cell extracts were analysed by western blotting using antibodies against SPICE1 and β-tubulin, as loading control, 48h after transfection with control or SPICE1 siRNA, or co-transfection with SPICE1 siRNA and GFP-SPICE1. Arrow points the position of GFP-SPICE1 on the nitrocellulose membrane. (B) Immunofluorescence analysis of the control and SPICE1-depleted cells. The HeLa cells transfected with either control or SPICE1 siRNA were fixed 48h after transfection and stained with antibodies against SPICE1 and β-tubulin. Scale bar is 5 µm.

As SPICE1 is essential, I generated a conditional knock-out (KO) of the *SPICE*1 gene to further verify the mitotic function of SPICE1. I generated an inducible *SPICE1* KO cell line using the CRISPR/Cas9 system. I stably integrated a guideRNA

targeting exon 3 of *SPICE1* in a HeLa cell line already containing the Cas9 gene expressed under a doxycycline inducible promoter (McKinley et al., 2015). Exon 3 was chosen as the early constitutive exon found in all splice variants of SPICE1. Then I observed the phenotype in HeLa cells knocked-out for *SPICE1* after a 96h treatment with doxycycline. The majority of them do not possess the *SPICE1* gene and consequently the SPICE1 protein. The observed mitotic defects in the *SPICE1* KO cells were similar with those observed after siRNA-SPICE1 knockdown. The cells lacking the *SPICE1* gene displayed an increase in multipolar spindles, chromosome congression defects ranging from mild to severe, and reduced centriole number (Figure 4.7). Only 47% of KO cells contained two pairs of centrioles. More than 20% of KO cells had more than 4 centrioles, and this was the only difference in comparison with the siRNA treatment (Figure 4.7A). The efficiency of gene KO was assessed using western blotting to look at the SPICE1 protein levels (Figure 4.7B). The inducible *SPICE1* KO cell line further confirmed that SPICE1 is required for accurate mitosis.

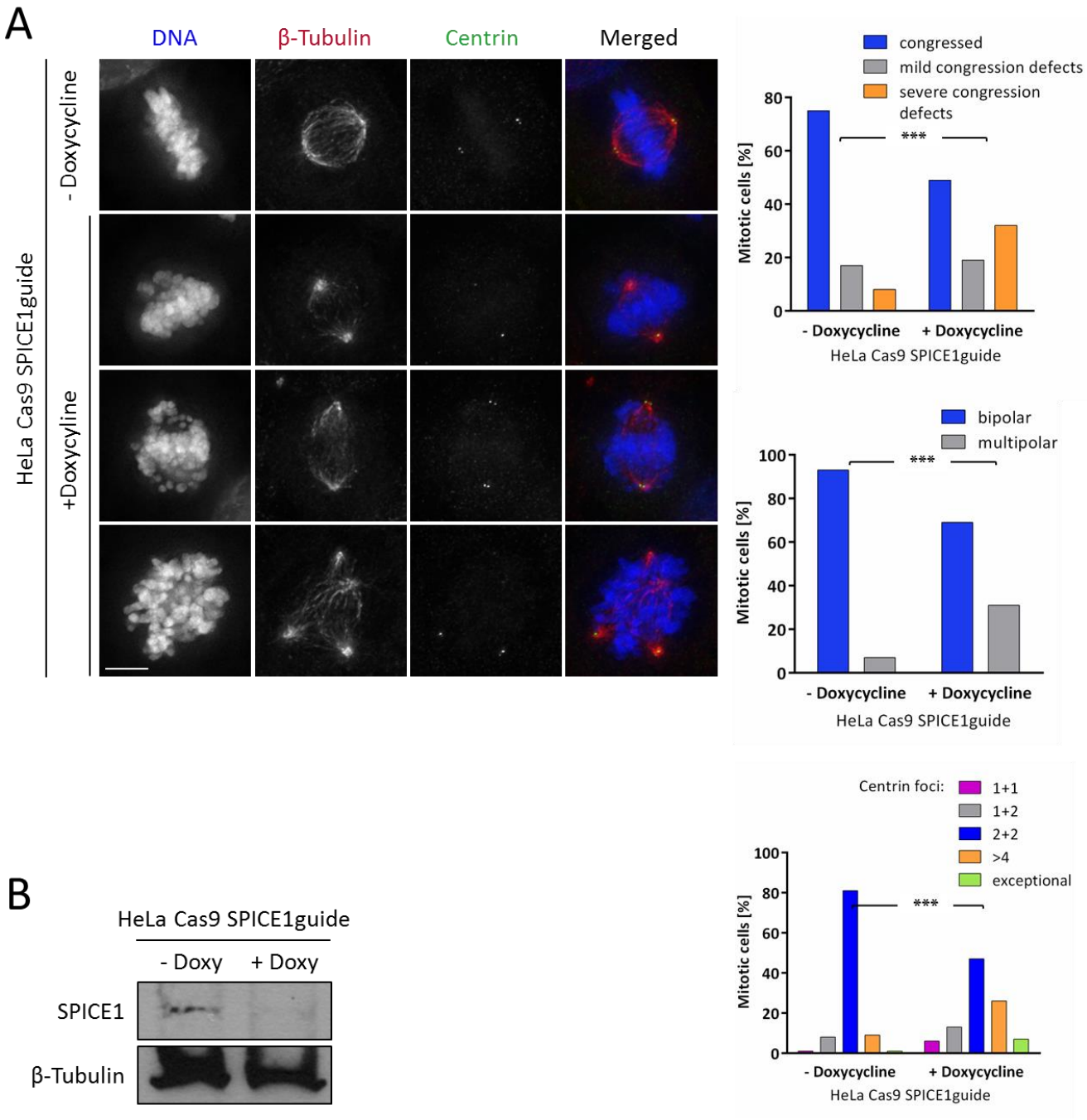

Figure 4.7: Inducible KO of the *SPICE1* gene confirmed defects in the mitotic spindle, chromosome congresion and centriole number. (A) Immunofluorescence analysis of the control and doxyciline treated HeLa Cas9 SPICE1guide cell line. Representative images show the maximum projections of deconvolved z-stacks of the HeLa Cas9 SPICE1guide cells. The cells were treated with DMSO or doxyciline for 96h, then fixed and stained with antibodies against β-tubulin and Centrin. n>100 cells for each treatment. P values of Chi-square tests and Fisher's exact test are ***p<0.0001. Scale bar is 5 µm. (B) Western blot analysis of the doxycycline and no doxycycline treated HeLa Cas9 SPICE1guide cells. Ninety-six hours after the indicated treatment, cells were lysed and cell extracts were analysed by western blotting using antibodies against SPICE1 and β-tubulin, as loading control.

4.2.3 **Analysis of SPICE1 phosphorylation mutants in SPICE1 knock-down cells**

Since the ectopic expression of siRNA resistant GFP-SPICE1 rescued mitotic defects in SPICE1-depleted cells, the siRNA assay proved to be a suitable test to examine the effect of SPICE1 C terminus phosphorylation on the loss-of-function phenotype. I have generated a non-phosphorylatable mutant which has all Aurora-specific phosphosites predicted by bioinformatics mutated to alanine (T557A, S738A, T780A, S797A and S810A). I also generated a 7A mutant with two additional mutated sites (T798A and S811A). These adjacent T and S are shown to be phosphorylated in cells by mass spectrometry studies (Beausoleil et al., 2004; Olsen et al., 2006; PhosphoSitePlus database). I generated the corresponding phosphomimicking mutant 7E, with glutamic acid substituting S or T. The 5E mutant was not made to date.

I tested whether the phosphomutants could rescue mitotic phenotypes observed in the absence of endogenous SPICE1. I found that both of the non-phosphorylatable mutants, $SPICE1_{5A}$ and $SPICE1_{7A}$, rescued the mitotic defects in SPICE1-depleted cells. The percentage of cells with multipolar spindles was similar to the control cells. The centriole number in cells transfected with GFP-$SPICE1_{5A}$ or GFP-$SPICE1_{7A}$ mutants where comparable to the control cells or cells rescued with wild type SPICE1, and very few severe chromosome congression defects were recorded (Figure 4.8 and Figure 4.9). Interestingly, $SPICE1_{7E}$ failed to rescue defects in spindle morphology, chromosome congression, and reduction in centriole number in the absence of endogenous SPICE1 (Figure 4.8 and Figure 4.9). The SPICE1-depleted cells transfected with GFP-$SPICE1_{7E}$ displayed variable centriole numbers. Twenty-three percent of these cells had less than two pairs of centrioles, and 19% had more than 4 centrioles. Additionally, 15% of the SPICE1-depleted cells transfected with GFP-$SPICE1_{7E}$ had multipolar spindles, and around 50% of the cells had defects in chromosome congression (Figure 4.9).

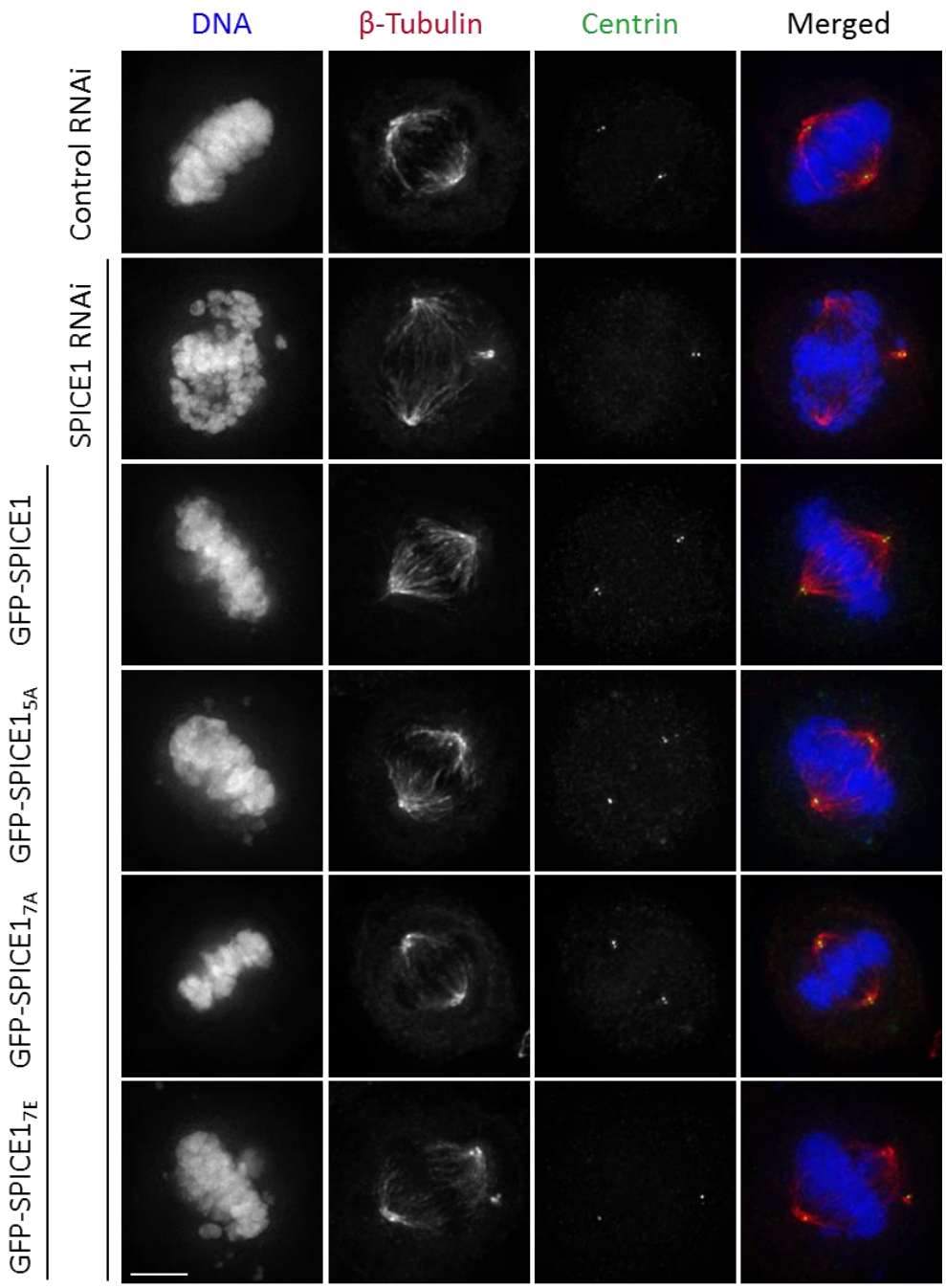

Figure 4.8: Non-phosphorylatable mutant rescued mitotic defects caused by SPICE1 depletion, while phosphomicking mutant did not. Representative images show the maximum projections of deconvolved z-stacks of the HeLa cells. The cells were transfected with either control or SPICE1 siRNA, or co-transfected with SPICE1 siRNA and indicated GFP-SPICE1 constructs for 48h. The cells were stained with antibodies against β-tubulin and Centrin. Scale bar is 5 µm.

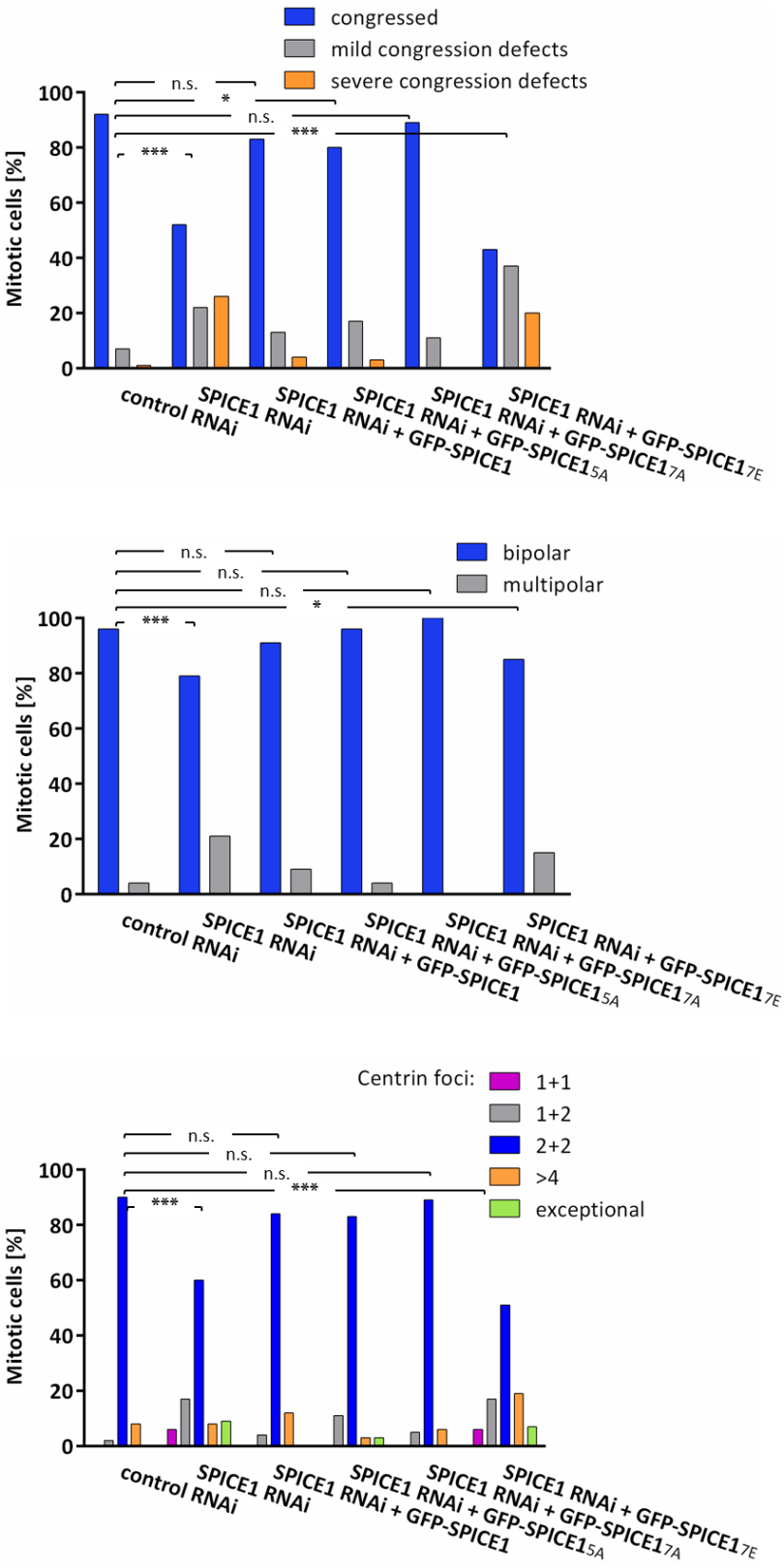

Figure 4.9: Quantification of rescue experiment with phosphorylation mutants. n>60 cells for each treatment. P values of Chi-square tests for three quantified defects are p<0.0001. Chi-square and Fisher's exact tests were used to separately compare treatments. P values of Chi-square tests and Fisher's exact tests are reported: not significant (n.s.), *p<0.05 (p=0.049 or p=0.014), ***p<0.0001.

Additionally, I observed that the GFP signal of the non-phosphorylatable mutants, SPICE1$_{5A}$ and SPICE1$_{7A}$, was visibly reduced at the spindle MTs, while the GFP signal was still present at the centrioles (Figure 4.10). This is similar to the observation I made for the SPICE1$_{1-550}$ mutant (Figure 4.3). GFP-SPICE1$_{7E}$ localized to both MTs and centrioles as the wild type GFP-SPICE1 (Figure 4.10). This suggests that phosphorylation of the SPICE1 C terminus is required for the targeting of SPICE1 to the spindle.

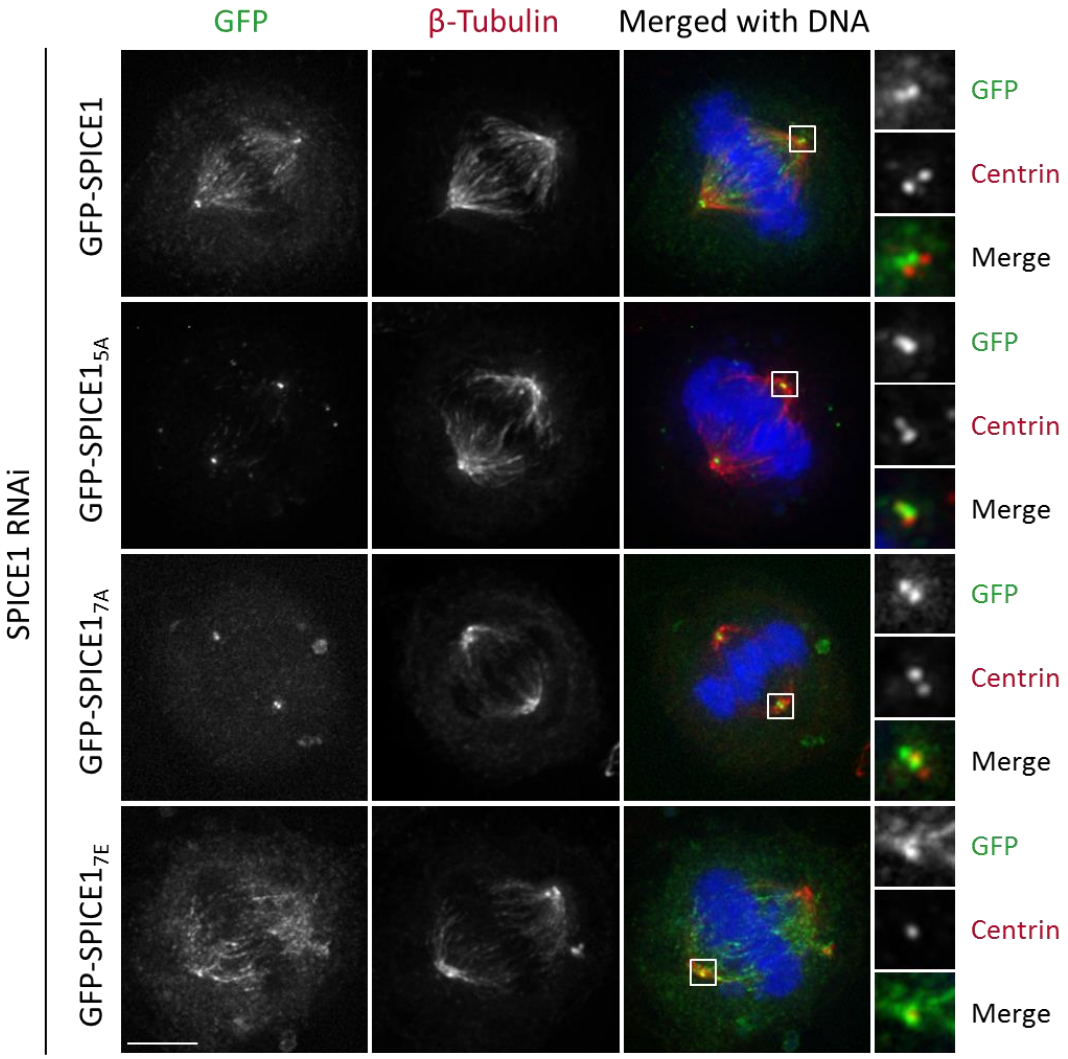

Figure 4.10 Phosphorylation of predicted sites in the C terminus of SPICE1 is required for SPICE1 localization at the mitotic spindle. Images show the maximum projections of deconvolved z-stacks of the HeLa cells co-transfected with SPICE1 siRNA and indicated GFP-tagged SPICE1 constructs. The cells are stained with antibodies against β-tubulin and Centrin. Insets show 3x magnified regions of one of the spindle pole for each condition. Scale bar is 5 µm.

To further test whether SPICE1 localization is controlled by Aurora kinases, I treated HeLa cells co-transfected with SPICE1 siRNA and wild type GFP-SPICE1, with the Aurora A inhibitor, MLN8237, and the Aurora B inhibitor, ZM447439. Inhibition of Aurora kinases lead to a reduction of GFP-SPICE1 on the mitotic spindle, but not on the centrioles (Figure 4.11). This is again similar to the observation for the $SPICE1_{5A}$, $SPICE1_{7A}$ and $SPICE1_{1-550}$ mutants (Figure 4.3 and Figure 4.10). Taken together, these results described here strongly indicate that Aurora kinases phosphorylate the C terminus of SPICE1 to control SPICE1 targeting to the spindle. Aurora-specific phosphosites in the SPICE1 C terminus were identified using the bioinformatic approach, and I identified a role for these phosphorylation sites in cells. My results confirm that our approach can identify novel substrates of Aurora kinases.

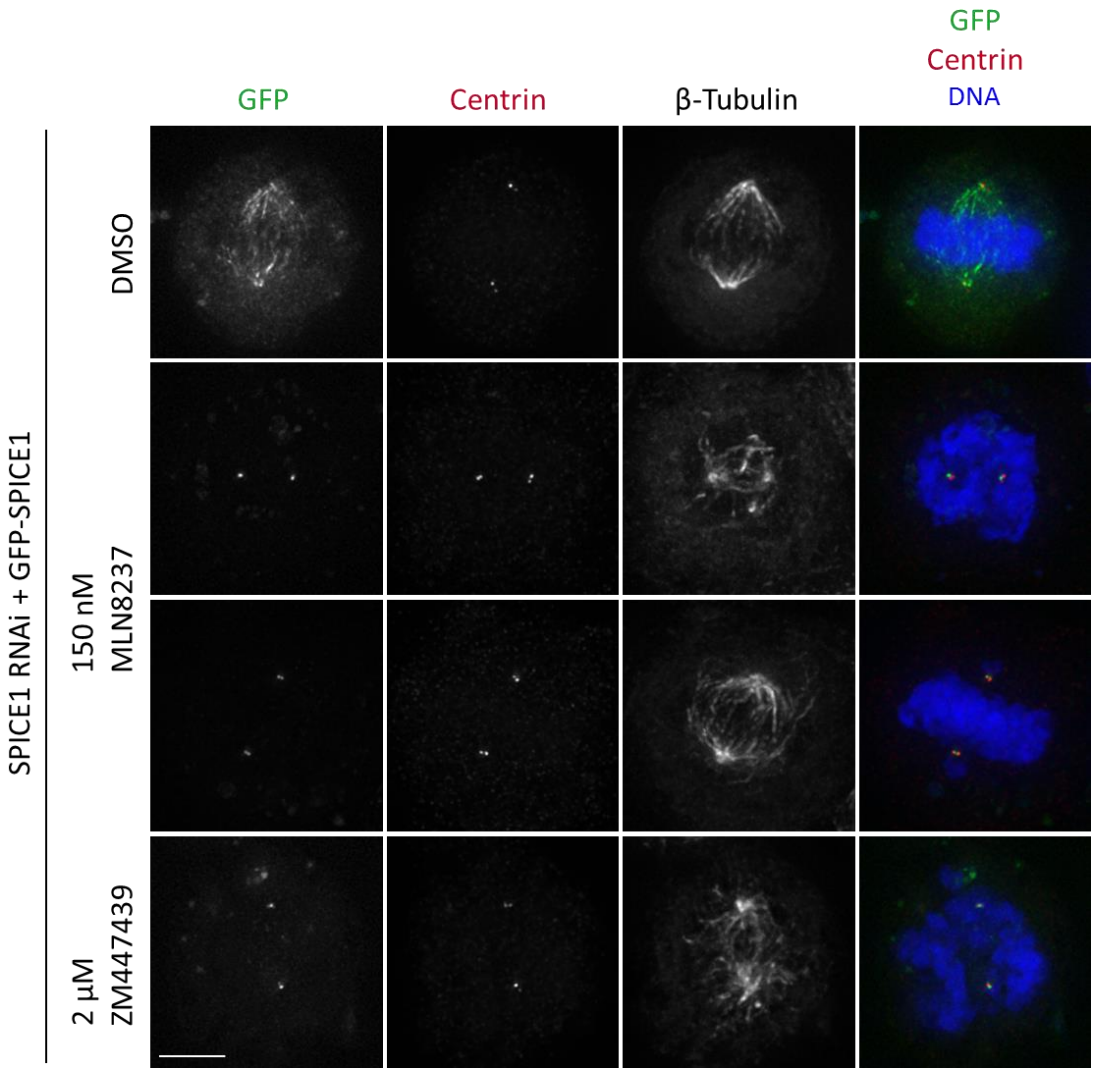

Figure 4.11: Inhibition of Aurora kinases using inhibitors reduces wild type GFP-SPICE1 binding to the spindle. Deconvolved representative images show HeLa cells co-transfected with SPICE1 siRNA and GFP-SPICE1 treated for 1.5h with either DMSO (control), 150 nM Aurora A inhibitor MLN8237 or 2 µM Aurora B inhibitor ZM447439 48h after transfection. The cells were stained with antibodies against Centrin and β-tubulin. Scale bar is 5 µm.

4.3 **Discussion**

My aim was to validate SPICE1 as a novel substrate of Aurora kinases in cells. I predicted multiple phosphorylation sites for Aurora kinases in the C terminus of SPICE1, and showed that the SPICE1 C terminus was phosphorylated by both Aurora kinases *in vitro* (Chapter 3).

I examined the function of Aurora phosphorylation of SPICE1. First, I generated a $SPICE1_{1-550}$ lacking the C terminus, which contains the predicted Aurora phosphorylation sites. I found that the absence of the C terminus reduced the association of the full-length SPICE1 with the mitotic spindle. The overexpression of $SPICE1_{1-550}$ did not cause overamplification of centrioles, unlike the full-length SPICE1. This suggests that the C terminus regulates the function of SPICE1 in addition to the regulation of SPICE1 localization. The observed overamplification of centrioles in SPICE1 overexpression has not been previously reported. In a previous study, SPICE1 was tagged at the C terminus (Comartin et al., 2013), so it is possible that overamplification of centrioles was not observed due to the inhibition of the C terminus. My results suggest that the C terminus of SPICE1 has a role in centriole duplication, since the SPICE1 overexpression phenotype was similar to STIL overexpression (Vulprecht et al., 2012). However, I have not investigated this further.

To test whether the predicted Aurora phosphorylation sites in SPICE1 regulate its function and localization, I used siRNA depletion and CRISPR/Cas9 knockdown to disrupt the gene and the expression of SPICE1. I showed that Aurora kinases control SPICE1 spindle targeting in cells. Phosphorylation does not affect SPICE1 centriole localization. Interestingly, phosphorylation usually prevents protein binding to MTs due to electrostatic repulsion (Kumar et al., 2012; Cormier et al., 2013; Zaytsev et al., 2015). However, here phosphorylation promotes SPICE1 association with MTs. The C terminus of SPICE1 does not bind MTs. Hence, this phosphorylation does not regulate SPICE1 binding to the MTs directly. For example, phosphorylation of the SPICE1 C terminus might promote interactions with other MT-binding proteins.

Since phosphorylation of the C terminus did not affect SPICE1 centriole localization, it is possible that only the MT-associated function of SPICE1 is affected, if the function of SPICE1 in centriole elongation and function in bipolar spindle formation are independent. Similarly, Aurora A phosphorylation of CPAP is not involved in CPAP-mediated centriole elongation, but it is required for the coalescence of PCM and the spindle pole integrity during mitosis (Chou et al., 2016). CPAP is known to interact with SPICE1 at the centrosomes/centrioles (Comartin et al., 2013). However, it is unlikely that Aurora kinases regulate SPICE1 in the same manner. First, SPICE1 depletion causes an increase in multipolar spindles and not various spindle abnormalities including monopolar spindles, which were observed in CPAP depletion (Chou et al., 2016). More importantly, the $CPAP_{S467A}$ mutant was more strongly associated with MTs during mitosis than wild type CPAP or the phosphomimicking mutant (Chou et al., 2016), and this is opposite to my observation for the $SPICE1_{5A}$ and $SPICE1_{7A}$ mutants.

In this study, I showed that the non-phosphorylatable SPICE1 mutants rescued severe mitotic phenotypes observed in depletion of endogenous SPICE1. There are at least two possible explanations. Phosphorylation of SPICE1 on predicted sites by Aurora kinases may have only a subtle biological function. Secondly, it is possible that there are additional, important phosphorylation sites which do not fit the Aurora consensus sites, which I have not mutated in this study. This could be examined by mutating all of the predicted sites in the recombinant protein and then testing phosphorylation *in vitro*. If any residual phosphorylation is observed, those phosphorylation sites could be identified by mass spectroscopy, followed by the examination of phosphorylation function in cells, with additional sites mutated in GFP-constructs. I have not examined this, because my focus was to test the sites predicted by bioinformatics.

My result also shows that the $SPICE1_{7E}$ mutant was not able to rescue the mitotic defects in SPICE1 depletion. This could indicate that phosphorylation of SPICE1 has to be dynamically regulated to allow accurate bipolar spindle formation and centriole biogenesis, or S to E mutation disrupted some important intra- or

inter-molecular interaction, for example. More experiments should be done to further understand the role of SPICE1 phosphorylation by Aurora kinases in cells. Due to the time constrains and difficulties in the generation of the multisite mutants, I have not tested the localization/function of $SPICE1_{5E}$ mutant, but that will be performed in the near future. Similarly, I plan to test the dominant negative effect of all the phosphorylation mutants in an overexpression experiment and examine whether these mutants cause overamplifications of centrioles as the wild type protein. The $SPICE1_{1-550}$, lacking the C terminus, did not cause excessive amplification of centrioles, so it would be interesting to see if the $SPICE1_{5A}$ or $SPICE1_{5E}$ mutants are giving the same result when overexpressed.

In summary, this study showed for the first time that SPICE1 is substrate of Aurora kinases in cells, and that this phosphorylation affects SPICE1 localization to the mitotic spindle.

5 Chapter 5: Conclusions

Mitosis is a highly regulated process, and the phosphorylation of many components of the mitotic division apparatus is the most effective mean of regulation. The Aurora family of kinases are one of the key factors that provide error-free mitosis, controlling each step of mitosis through the phosphorylation of various proteins of the mitotic apparatus. Despite the extensive research on Aurora kinases and many molecular targets identified, understanding the exact molecular mechanisms underlying the regulation of all the important mitotic processes by Auroras is still incomplete. To better understand how Aurora kinases control the chromosome condensation, MT nucleation and bipolar spindle assembly, chromosome segregation, as well as the mitotic exit, identifying the substrates of Aurora kinases that mediate those processes is of great importance.

Several studies showed that Aurora A is important for chromosome alignment at the metaphase plate, and proposed the role for Aurora A in regulation of kinetochore-MT attachments (Marumoto et al., 2003; Hoar et al., 2007; Sasai et al., 2008). Before this study, it had been accepted that Aurora B at the centromere is the key factor correcting aberrant MT attachments to chromosomes, and the precise molecular mechanism of Aurora A's role in this process was not known. I investigated and uncovered the kinetochore substrate of Aurora A, which is important for establishment of attachments to MTs. My results revealed that Aurora A phosphorylates HEC1/Ndc80 at the outer kinetochore and contributes to the activity of Aurora B. In this study, I defined a known Aurora B substrate, S55 of Ndc80, as an Aurora A phosphorylation target at kinetochores, providing deeper insights into the molecular mechanism of Aurora A-based error correction in the vicinity of centrosomes.

To further contribute to the identification of new Aurora kinase substrates, I developed bioinformatic approach in collaboration with centre bionformatician, Dr. Alastair Kerr. I based my approach on the shared consensus sequence in Aurora protein substrates, and directed the search applying additional parameters known

to determine the substrate specificity of Aurora kinases. I confirmed that our bioinformatic tool is successful in predicting new substrates of Aurora kinases, as I found that previously unknown substrates, CLASP2, MEL-28/ELYS (AHCTF1), TTLL4, SPICE1 and KIAA1468, are directly phosphorylated by both Aurora A and Aurora B kinases *in vitro*. This result suggests a new mechanism of Aurora regulation of mitosis. Future work could contribute in characterizing the precise function of the phosphorylation of these proteins by Auroras in cells.

I aimed to discover and characterize a new phosphorylation substrate of Aurora kinases in cells. I showed for the first time that SPICE1 is phosphorylated by Aurora kinases in cells and that the Aurora-based phosphorylation of the SPICE1 C terminus control SPICE1 targeting to the mitotic spindle. Future work will be focused on determining the precise role of SPICE1 phosphorylation by Aurora kinases in regulation of bipolar spindle formation, using different phosphorylation mutants and overexpression in cells. I have found these phosphorylation sites in SPICE1 using bioinformatics, and since I identified the role for these phosphorylation sites in cells, our approach proved to enable identification of novel substrates of Aurora kinases.

In conclusion, my results gave the first insight into the molecular mechanism of Aurora A contribution in correction of erroneous kinetochore-MT attachments near centrosomes. My work also provided the evidence that the genome-wide bioinformatic approach I developed in collaboration with Dr Alastair Kerr is successful in identifying novel substrates of Aurora kinases. This bioinformatic tool is a successful method to find new substrates with high confidence for future studies seeking to understand how Aurora kinases regulate the complex mitotic apparatus.

6 Chapter 6: Materials and Methods

6.1 Molecular Biology techniques

6.1.1 Standard solutions and buffers

Most chemical reagents were provided by Sigma-Aldrich (Merck), VWR International, Thermo Fisher Scientific/Invitrogen and BioRad, and were of analytical grade. Suppliers of other kits, enzymes and reagents are stated below.

6.1.2 PCR amplification

Human adult male testis cDNA and fetus brain cDNA libraries (Invitrogen) were used for PCR amplification. KIAA1468 was amplified from Image clone 4339646 (Open Biosystems). Vector pET3aTr, used for bacterial protein expression, was obtained from Song Tan. All oligonucleotides were purchased from Sigma-Aldrich or Integrated DNA Technologies (IDT). The primers for Gibson assembly contain 5'-end sequence that is identical to the adjacent segment in cloning vector, in this case pET3aTr sequence (lower case letters in Table 6.1). The primers used for cDNA PCR amplification and standard PCR, Gibson cloning and site-directed mutagenesis are listed in Tables 6.1, 6.2, 6.3 and 6.4. The primers used for site-directed mutagenesis PCR were designed using QuikChange Primer Design Tool (Agilent Technologies). The standard PCR amplification was performed with Phusion DNA polymerase (New England Biolabs - NEB) with the following proportions of reagents: 5x Phusion Buffer 10 µl, 10 mM dNTPs 1 µl, DMSO 2 µl, Forward primer (10 µM) 2.5 µl, Reverse primer (10 µM) 2.5µl, template DNA 5µl, Phusion polymerase 0.5 µl and ddH_2O to 50 µl. The reaction programme was as follows: (Heat lead at 110°C for 2 min, 98°C for 3 min) x1, (98°C for 30 sec, annealing °C for 45 sec, 72°C for time corresponding to 1kb/min) x30, (72°C for 8 min) x1 and store at 8°C. Site-directed mutagenesis were performed with PfuUltra II fusion HS DNA polymerase (Agilent Technologies) using the following proportions of reagents: 10x PfuUltra II Buffer 5 µl, 100 mM dNTPs 1 µl, Forward primer (125 ng/µl) 0.5 µl, Reverse primer (125 ng/µl) 0.5 µl, template DNA (25 ng/µl) 4µl, polymerase 1 µl,

ddH_2O 38 µl and followed by programme: (Heat lead at 110°C for 2 min, 95°C for 30 sec) x1, (95°C for 30 sec, 55°C for 1 min, 68°C for 4 min 30 sec) x18 and store at 8°C.

6.1.3 **Restriction digestion**

Prior to the restriction digestion, the PCR products were cleaned using PCR purification kit (Qiagen) as per manufacturer's protocol and eluted in 40 µl provided EB buffer. Restriction enzyme digestion of the PCR products was performed using Cut Smart enzymes from NEB, with provided Cut Smart buffer. The digestion reactions were carried out using the following protocol: 40 µl of product, 1.5 µl of two enzymes, 5 µl Cut Smart buffer and 2 µl ddH_2O. Total reaction volume was subjected to electrophoresis on 1% or 0.8% agarose gel containing SYBR Safe DNA gel stain (Invitrogen). The band corresponding to the desired DNA fragment was excised from the gel using a clean razor blade. DNA was extracted from the gel using the QIAquick Gel Extraction Kit (Qiagen) as per manufacturer's protocol. The sample was eluted in 30 µl of provided EB buffer. The DNA concentration was measured using NanoDrop (Thermo Fisher), and the sample was kept at -20°C.

6.1.4 **DNA ligation and Gibson assembly**

Sticky-end ligation of digested PCR product into plasmids was carried out using the T4 Ligase and provided enzyme (NEB). Ligation reactions were performed in total volume of 10 µl containing: 1 µl T4 DNA ligase, 1 µl 10x T4 DNA ligase buffer, 7 µl digested PCR product (or water for control reaction) and 1 µl vector plasmid. Ligation reactions were incubated at RT for 2 h, and then transformed into *E. coli.* Gibson cloning is assembly of vector and PCR product without ligation (Gibson et al., 2009). PCR amplified products were mixed with PCR amplified plasmid (pET3aTr) in 2:1 or 3:1 molar ratio and 15 µl Gibson mix (8.59 µl ddH_2O, 4 µl 5x Isotermal buffer, 2 µl Taq ligase (NEB), 0.25 µl Phusion polymerase (NEB), 0.16 T5 exonuclease (NEB)), adding the ddH_2O to 20 µl. Isothermal buffer (5x) was made with: 3 ml of 1M Tris-HCl (pH 7.5), 150 µl of 2M $MgCl_2$, 60 µl of 100 mM dGTP, 100 mM dATP, 100 mM dTTP, 100 mM dCTP (Qiagen), 300 µl of 1M DTT, 1.5 g PEG-8000 and 300 µl of 100 mM NAD. Gibson reactions were incubated 15 min at 50°C, then transformed in *E.coli.*

Table 6.1: Primers used for PCR amplification and subsequent Gibson assembly.

	Cloning primers (5'→3')
pET3aTr Forward	CATATGTATATCTCCTTCTTAAAGTTAAAC
pET3aTr Reverse	GGATCCAGATCTAAGCTTGG
ELYS from cDNA Forward	GTGGAACTCGGTTTTGTCGG
ELYS from cDNA Reverse	CCTGGACTGAAACAATCACTCC
ELYS$_{1149-1329}$ Forward	gaaggagatatacatatgCGTTCACTGCCCTCAAGTTC
ELYS$_{1149-1329}$-3Ccleavage site-6His Reverse	ccaagcttagatctggatccTCAGTGGTGATGATGATGATGGCTGCTGCCGGGCCCCT GGAACAGAACTTCCAGGTCTTCCGGTGACGGTGCATCC
ELYS$_{1858-2014}$ Forward	gaaggagatatacatatgACTAAAAAAGAAGTTAAGGTTTCATC
ELYS$_{1858-2014}$-3Ccleavage site-6His Reverse	ccaagcttagatctggatccTCAGTGGTGATGATGATGATGGCTGCTGCCGGGCCCCT GGAACAGAACTTCCAGTGGGGTATTTCTTGTAGATCTCC
CLASP2 from cDNA Forward	GGTTTCAGAGAGCTCCCTGGACCA
CLASP2 from cDNA Reverse	GACCTGGTTCGCTGTGATGAGCTTCA
CLASP2$_{551-668}$ Forward	gaaggagatatacatatgCCACAATCAGACAGGTCCTC
CLASP2$_{551-668}$-3Ccleavage site-6His Reverse	ccaagcttagatctggatccTCAGTGGTGATGATGATGATGGCTGCTGCCGGGCCCCT GGAACAGAACTTCCAGGCCAGCAAGTGGTGCTGAAAGTTTTG
CLASP2$_{741-818}$ Forward	gaaggagatatacatatgCCATCTAGGCTTTCAGTGGC
CLASP2$_{741-818}$-3Ccleavage site-6His Reverse	ccaagcttagatctggatccTCAGTGGTGATGATGATGATGGCTGCTGCCGGGCCCCT GGAACAGAACTTCCAGAGAAGACGACAGTCGACTTGATTG
TTLL4 from cDNA Forward	CAGACTGACAGACTTCAAGGATGC
TTLL4 from cDNA Reverse	AGGCTTTTGGAGAGAGGCCAG
TTLL4$_{330-624}$ Forward	tttaagaaggagatatacatatgCCAACTAAGGAGATTCGGTTC
TTLL4$_{330-624}$-3Ccleavage site-6His Reverse	ccaagcttagatctggatccTCAGTGGTGATGATGATGATGGCTGCTGCCGGGCCCCT GGAACAGAACTTCCAGTCCAATGGTCTGCTTGACAATG
SPICE1 from cDNA Forward	CTGTGTTTTGAGAGTGCAAGTACG
SPICE1 from cDNA Reverse	GAACAAACTCAGTGAGACTTGACTTC
SPICE1$_{549-855}$ Forward	tttaagaaggagatatacatatgCCTCTTCAGGACGTATTGAG
SPICE1$_{549-855}$-3Ccleavage site-6His Reverse	ccaagcttagatctggatccTCAGTGGTGATGATGATGATGGCTGCTGCCGGGCCCCT GGAACAGAACTTCCAGTGATACATGGGTAGAAAGAGCA
KIAA1468$_{1-292}$ Forward	tttaagaaggagatatacatatgTTAGTACAGAAATTAGAAGATAAAATTAGTTTG
KIAA1468$_{1-292}$-3Ccleavage site-6His Reverse	ccaagcttagatctggatccTCAGTGGTGATGATGATGATGGCTGCTGCCGGGCCCCT GGAACAGAACTTCCAGTAACATTTGTTGCAACATTGAAAG
Nup107 from cDNA Forward	GTTGTGTGTGGAAAAGGCTTTAGCC
Nup107 from cDNA Reverse	AAACTTCATTTATCATGAAAATTAGTGAGATTACAAAG
Nup107$_{1-644}$ Forward	gaaggagatatacatatgGACAGGAGTGGCTTTGGAGAG
Nup107$_{1-644}$-3Ccleavage site-6His Reverse	ccaagcttagatctggatccTCAGTGGTGATGATGATGATGGCTGCTGCCGGGCCCCT GGAACAGAACTTCCAGTCCTCGAATATTCTCAACTACAGTTTTTGTTATTG
Nup107$_{658-925}$ Forward	gaaggagatatacatatgGCCCTAGATACTGGCACTAC
Nup107$_{658-925}$-3Ccleavage site-6His Reverse	caagcttagatctggatccTCAGTGGTGATGATGATGATGGCTGCTGCCGGGCCCCTG GAACAGAACTTCCAGTCCTAACTGAATTTCATACCCTAATGGGTC

Table 6.2: Primers used for PCR amplifications.

	Cloning primers (5'→3')
SPICE1 Forward	CCCGCTCGAGATGTCATTTGTCAGAGTGAACCG
SPICE1 Reverse	CCCCCGCGGTTATGATACATGGGTAGAAAGAGCAAAC
SPICE1$_{444-855}$ Forward	CCCCTCGAGATATCACTCACACATGCTATTAAGAACT
SPICE1$_{1-550}$ Reverse	TCCCCCGCGGTTAAAGAGGAGAGAATTTTAAGT

Table 6.3: Primers used for SPICE1 site-directed mutagenesis to resist SPICE1 siRNA.

	Site-directed mutagenesis primers (5'→3')
SPICE1 hardened 1st 5 bases Forward	CTCCCAGTACTGGGAGATGGGCAGCAATTAAGGACTAATGAGTCATT AATACAAAGAAAGGAC
SPICE1 hardened 1st 5 bases Reverse	GTCCTTTCTTTGTATTAATGACTCATTAGTCCTTAATTGCTGCCCATCTC CCAGTACTGGGAG
SPICE1 hardened 2nd 5 bases Forward	CTGGGAGATGGGCAGCAATTAAGGACTAACGAAAGTTTAATACAAAG AAAGGACATAATGACACG
SPICE1 hardened 2nd 5 bases Forward	CGTGTCATTATGTCCTTTCTTTGTATTAAACTTTCGTTAGTCCTTAATTG CTGCCCATCTCCCAG

6.1.5 **Preparation and transformation of *E.coli* competent cells**

E.coli cells, XL-10 Gold, BL21 and Codon+ (Agilent Technologies), were streaked on agar plates without antibiotics and grown overnight at 37°C. The following day, one colony was selected and grown in liquid LB medium (10 g tryptone, 5 g yeast extract, 10 g NaCl in ddH_2O to 1 L) overnight at 37°C, with shaking at 180 rpm. The following day, 2-3 ml of overnight culture was used to make new 1 L of culture, which was grown in LB plus 10 ml 1M $MgCl_2$ at 18°C with 225 rpm shaking until the OD reached approximately 0.12. The cells were transferred in cooled centrifuge bottles and incubated for 10 minutes on ice. After centrifugation at 5000 rpm for 10 min at 0°C, the cells were resuspended in 150 ml cold transformation buffer (final concentration 15 ml 1M $CaCl_2$, 55 ml 1M $MnCl_2$, 250 mM KCl, 10 mM PIPES pH 6.7). The cells were centrifuged again at 5000 rpm for 10 min at 0°C and then resuspended in 40 ml cold transformation buffer. DMSO (3 ml) was added to the cells and mixed. The 500 µl aliquots of cells were immediately frozen in liquid nitrogen. The competent cells were stored at –80°C.

Transformation of *E.coli* cells was performed by adding 10 µl of ligation reaction or 5 µl of Gibson assembly reaction to 100 µl of XL-10 Gold competent cells, fallowed by incubation on ice for 10 min. Chemically competent cells were then exposed to 42°C for 45 sec and restored on ice for additional 2 min. The cells were platted on agar plates containing the appropriate antibiotic (100 µg/ml ampicillin).

Table 6.4: Primers used for SPICE1 site-directed mutagenesis to make phosphorylation mutants.

	Site-directed mutagenesis primers (5'→3')
SPICE1 T557A Forward	AGGACGTATTGAGAAGGGCTGTTCAAACTCGTCCT
SPICE1 T557A Reverse	AGGACGAGTTTGAACAGCCCTTCTCAATACGTCCT
SPICE1 S738A Forward	TTGCAGAATTGAATCGACAAGCTATGGAGGCTCGTGGAAAAC
SPICE1 S738A Reverse	GTTTTCCACGAGCCTCCATAGCTTGTCGATTCAATTCTGCAA
SPICE1 T780A Forward	GACTGAAGGAGCAAAGAGGGCAATTGAGGTATCTATTCC
SPICE1 T780A Reverse	GGAATAGATACCTCAATTGCCCTCTTTGCTCCTTCAGTC
SPICE1 S797A Forward	CCCAGAAAGCTCAAAATGTGCTACTGTCTCTCCCGTCAGC
SPICE1 S797A Reverse	GCTGACGGGAGAGACAGTAGCACATTTTGAGCTTTCTGGG
SPICE1 S810A Forward	GCGGGATAAATACAAGAAGAGCTTCCGGGGCTACT
SPICE1 S810A Reverse	AGTAGCCCCGGAAGCTCTTCTTGTATTTATCCCGC
SPICE1 S797A/T798A Forward	GCCCCAGAAAGCTCAAAATGTGCTGCTGTCTCTCCCGTCAG
SPICE1 S797A/T798A Reverse	CTGACGGGAGAGACAGCAGCACATTTTGAGCTTTCTGGGGC
SPICE1 S810A/S811A Forward	TCAGCGGGATAAATACAAGAAGAGCTGCCGGGGCTACTG
SPICE1 S810A/S811A Reverse	CAGTAGCCCCGGCAGCTCTTCTTGTATTTATCCCGCTGA
SPICE1 T557E Forward	CTTCAGGACGTATTGAGAAGGGAAGTTCAAACTCGTCCTGCTCCA
SPICE1 T557E Reverse	TGGAGCAGGACGAGTTTGAACTTCCCTTCTCAATACGTCCTGAAG
SPICE1 S738E Forward	GGAACGGATTGCAGAATTGAATCGACAAGAAATGGAGGCTCGTGGA
SPICE1 S738E Reverse	TCCACGAGCCTCCATTTCTTGTCGATTCAATTCTGCAATCCGTTCC
SPICE1 T780E Forward	GGACTGAAGGAGCAAAGAGGGAAATTGAGGTATCTATTCCAG
SPICE1 T780E Reverse	CTGGAATAGATACCTCAATTTCCCTCTTTGCTCCTTCAGTCC
SPICE1 S797E/T798E Forward	GGAGCAGAAGCCCCAGAAAGCTCAAAATGTGAAGAAGTCTCTCCCGTCAGC GGGA
SPICE1 S797E/T798E Reverse	TCCCGCTGACGGGAGAGACTTCTTCACATTTTGAGCTTTCTGGGGCTTCTGCT CC
SPICE1 S810E/S811E Forward	AGAAGTCTCTCCCGTCAGCGGGATAAATACAAGAAGAGAAGAGGGGGCTAC TGGTAATTCTT
SPICE1 S810E/S811E Reverse	AAGAATTACCAGTAGCCCCCTCTTCTCTTCTTGTATTTATCCCGCTGACGGGAG AGACTTCT

6.1.6 **Isolation of plasmid DNA from *E.coli***

A single bacterial colony was used to inoculate 5 ml of LB medium with the appropriate antibiotic (100 µg/ml ampicillin) and grown overnight. DNA was isolated using QIAquick Mini-Prep Kit (Qiagen) according to the manufacturer's protocol. The identity of an insert within a cloning vector was confirmed by 1 h digestion of 5 µl DNA with 0.3 µl corresponding enzymes in provided buffer (NEB) at 37°C followed by identification of bands position on 1% agarose gel. If tested plasmid contained the correct insert, 1 µl of that plasmid was transformed in 100 µl competent cells. The cells were grown and DNA isolated as described above. The confirmed plasmid (50 µl) was stored at –20°C but previously confirmed by DNA sequencing reaction (see below).

6.1.7 **Sequencing reaction**

To check the sequence of the generated plasmids BigDye Sequencing Kit was used (Thermo Fisher). In 10 µl reaction volume 2 µl BigDye solution was added together with 1 µl DNA (approximately 400 ng), 1 µl 3.6 µM sequencing primer and ddH_2O to adjust the volume. The thermal cycler programme used for sequencing was as follows: (Heat lead at 110°C for 2 min, 96°C for 2 min) x1, (96°C for 30 sec, 50°C for 15 sec, 60°C for 4 min) x25 and store at 8°C. The samples were analysed by the GenePool Sequencing Facility (The University of Edinburgh) and the chromatograms were examined with the free software ApE (A Plasmid Editor). Primer used for sequencing of vectors pET3aTr and pIC242 (a gift from I.Cheeseman) are as follows: 5'-GCCGGCTCCGGAGAGCTCCAATTGGAATTCGC-3' forward primer and 5'-CGGTGATGTCGGCGATATAG-3' reverse primer for pET3aTr and 5'- GGCATGGACGAGCTGTACAAG-3' forward primer and 5'-GCATTCATTTTATGTTTCAGG-3' for pIC242. The primer used to confirm guideRNA sequence in pLenti-sgRNA (Feng Zhang) is 5'-ACTATCATATGCTTACCGTAAC-3'.

6.2 Biochemistry techniques

6.2.1 Standard biochemistry techniques

For Western blotting, collected samples were first separated on denaturing protein gel (SDS-PAGE) using the Tris-glycine buffer system and 30% (v/v) acrylamide/bisacrylamide mixture (Severn Biotech), which were assembled in a vertical electrophoresis apparatus (BioRad). The proportions of reagents are listed in Table 6.5. The samples were loaded on the gels and run for 15 min at 100 V, then for additional 45 min at 220 V in Running buffer (1.5M Tris-HCL pH 8.8, 0.4% SDS).

Protein samples were transferred from the gel to a nitrocellulose membrane (Amersham GE) at 80 mA constant current for 1 h using BioRad Semi-dry blotting apparatus and 20 ml of transfer buffer (5.82 g Tris Base, 2.93 g Glycine, 200 ml methanol and ddH_2O up to 1 L). Both the membrane and gel were left in transfer buffer for 5 min before transfer. The membranes were blotted with rabbit anti-pS55 HEC1/Ndc80 (Pierce/Thermo) or rabbit anti-SPICE1 (HPA064843, Atlas Antibodies), and mouse anti-β-tubulin (Sigma) as loading control.

Table 6.5: Reagents proportions in SDS-PAGE gels.

Reagents	4% Stacking (6 ml)	Reagents	10% Stacking (10 ml)	15% Stacking (10 ml)
ddH_2O	4.3 ml	**ddH_2O**	4 ml	2.3 ml
1.5 M Tris (pH 6.8)	0.76 ml	**1.5 M Tris (pH 8.8)**	2.5 ml	2.5 ml
30% Acrylamide	0.8 ml	**30% Acrylamide**	3.3 ml	5 ml
10% SDS	60 µl	**10% SDS**	100 µl	100 µl
10% APS	60 µl	**10% APS**	100 µl	100 µl
TEMED	6 µl	**TEMED**	10 µl	10 µl

6.2.2 Protein expression

E.coli codon optimized cells (Codon+) were transformed with cDNA constructs of selected CLASP2, ELYS, Nup107, TTLL4, SPICE1 and KIAA1468 fragments (all of them containing 3C cleavage site and 6His tag at the C terminus) in pET3aTR vector for bacterial expression. Test expression of protein constructs was performed first. One or two colonies of transformed Codon+ cells were grown in 5 ml of LB medium at 37°C with shaking, until the cells reached log phase, then the

protein expression was induced with 0.5 mM IPTG and the cells were promoted to express proteins by shaking at 220 rpm either for 4 h at 37°C, 4 h at 25°C or overnight at 18°C. After incubation, the cells were pelleted and protein expression assessed by SDS-PAGE. The condition for large scale expression was chosen based on the most abundant level of protein on the gel. Large scale expression of protein fragments was performed as follows: the colonies were grown in 25 ml LB medium at 37°C with shaking at 220 rpm overnight, then 2-3 ml of overnight culture was used to make 1 L or 3 L cultures that were subsequently grown at 37°C with shaking at 220 rpm until OD reached 0.5 or 0.6. At this OD protein expression was induced with 0.5 mM IPTG for the appropriate time and temperature, and in most cases that corresponded to the overnight incubation at 18°C. GST-Ipl1 was expressed for 4 h at 37°C.

6.2.3 **Protein purification**

6.2.3.1 **GST-fusion protein purification**

Yeast Ipl1 was expressed as GST-Ipl1 (plasmid was a gift from I.Cheeseman) and purified in two steps. The cells expressing GST-Ipl1 were centrifuged and cell pellet was resuspended in lysis buffer (50 mM Tris-HCl pH 7.5, 1 mM EGTA, 1 mM EDTA, 250 mM NaCl, 1% Tween-20, 1 mM freshly added DTT, 1 mM PMSF). Lysed cells were sonicated and centrifuged at 22000 rpm for 1 h at 4°C. A supernatant was collected and added to the 1.5 ml of glutathione-sepharose beads (GE Healthcare) equilibrated in wash buffer (50 mM Tris-HCl pH 7.5, 1 mM EDTA, 250 mM NaCl, 1 mM freshly added DTT) beforehand. Protein-coupled beads were washed three times with wash buffer, by centrifugation of 5 min at 500 xg at 4°C, followed by removal of supernatant and addition of more wash buffer. The periods of 10 min incubation with beads rotating at 4°C were performed between each centrifugation. The protein was eluted by using chromatography column with 20 mM glutathione in wash buffer adjusted to pH 8.0. Elution fractions of 1 ml were collected, and protein levels were examined with SDS-PAGE. Fractions in which protein was observed were pooled, concentrated and run on Superdex 200 increase column (GE Healthcare) to separate the proteins based on size in filtered and degassed buffer (50 mM Tris-HCl

pH 7.5, 1 mM EDTA, 150 mM NaCl, 50% glycerol). The eluate absorbance was monitored at 280 nm and 0.5 ml fractions were collected. After SDS-PAGE analysis of eluted fractions, those containing the cleanest protein fragments of interest were pooled, concentrated and stored at -80°C.

6.2.3.2 **His-tagged protein purification**

His-tagged protein fragments were also purified in two steps. The cells expressing His-tagged proteins were centrifuged and cell pellet was resuspended in corresponding lysis buffer with 10 mM Imidazole. Lysed cells were sonicated and centrifuged at 22000 rpm for 1 h at 4°C. The supernatant was collected and added to the 1.5 ml of Ni-NTA beads (GE Healthcare) equilibrated beforehand in the corresponding wash buffer containing 30 mM Imidazole. Protein-coupled beads were washed three times with wash buffer, by 5 min centrifugation at 500 xg and 4°C, followed by removal of supernatant and addition of more wash buffer. The proteins were eluted using chromatography column and elution buffer with high concentration of Imidazole, 250 mM. Elution fractions of 1 ml were collected and protein levels were examined with SDS-PAGE. Fractions containing protein were pooled, concentrated and run on Superdex 200 increase column or Superdex 75 (for better resolution of smaller protein fragments) (GE Healthcare) to separate proteins based on size in filtered and degassed buffer with low salt concentration and glycerol. The eluate absorbance was monitored at 280 nm and 0.5 ml fractions were collected. After SDS-PAGE analysis of eluted fractions, those containing the cleanest protein fragments of interest were pooled, concentrated and stored at -80°C. For $CLASP2_{551-668}$, $CLASP2_{741-818}$, $ELYS_{1858-2014}$, $TTLL4_{330-624}$ and $SPICE1_{549-855}$ buffers used were as follows: lysis buffer (20 mM HEPES pH 7.0 (pH 7.5 for TTLL4 and SPICE1), 10 mM Imidazole, 150 mM NaCl, 0.1% Tween-20, 5 mM freshly added BME, 1 mM PMSF); wash buffer (20 mM HEPES pH 7.0 (pH 7.5 for TTLL4 and SPICE1), 30 mM Imidazole, 300 mM NaCl, 0.1% Tween-20, 5 mM freshly added BME); elution buffer (20 mM HEPES pH 7.0 (pH 7.5 for TTLL4 and SPICE1), 250 mM Imidazole, 300 mM NaCl, 5 mM freshly added BME), GF buffer (20 mM HEPES pH 7.0 (pH 7.5 for TTLL4 and SPICE1), 150 mM NaCl, 1 mM EDTA, 5% glycerol). For $ELYS_{1149-1329}$, $Nup107_{1-644}$

and Nup107$_{658-925}$ buffers used were as follows: lysis buffer (20 mM KPO_4 pH 8.0, 10 mM Imidazole, 150 mM NaCl, 0.1% Tween-20, 5 mM freshly added BME, 1 mM PMSF); wash buffer (20 mM KPO_4 pH 8.0, 30 mM Imidazole, 300 mM NaCl, 0.1% Tween-20, 5 mM freshly added BME); elution buffer (20 mM KPO_4 pH 8.0, 250 mM Imidazole, 250 mM NaCl, 5 mM freshly added BME); GF buffer (20 mM KPO_4 pH 8.0, 150 mM NaCl, 1 mM EDTA, 5% glycerol).

6.2.3.3 **Isolation of bacterially expressed proteins from inclusion bodies**

Test purification of KIAA1468$_{1-292}$ showed that protein fragment was insoluble. To isolate the protein fragment from the inclusion bodies and refold it, 100 ml of the cells expressing KIAA1468$_{1-292}$ was centrifuged and cell pellets were resuspended in lysis buffer (50 mM Tris-HCl pH 8.0, 100 mM NaCl, 1 mM EDTA, 0.5% Triton-X100, and 10 mM DTT) and frozen. After repeated freeze-thaw cycles, the cell lysate was sonicated and insoluble fraction was collected by centrifugation for 20 min at 15000 rpm and 4°C. Inclusion bodies in pellet were washed three times with wash buffer (50 mM Tris-HCl pH 8.0, 100 mM NaCl, 1 mM EDTA, 1% Triton-X100, and 1 mM DTT), sonicated shortly and pelleted at 15000 rpm for 20 min at 4°C. Inclusion bodies were solubilized into 6 M Gdn-HCl pH 4.5 and 5 mM BME, and stirred at room temperature until completely colourless solution was retrieved. After solubilisation, the buffer was exchanged using desalting column (BioRad) with wash buffer (50 mM Tris-HCl pH 8.0, 100 mM NaCl, 6 M Urea, 10 mM Imidazole, and 5 mM BME). The sample was then dialysed against refolding buffer (50 mM Tris-HCl pH 8.0, 100 mM NaCl, 4 M Urea, 1 mM EDTA, 10% glycerol, 0.5 mM L-arginine) for 4 h at 4°C. Subsequently, the buffer was exchanged several times with decreasing concentration of Urea and finished with buffer without Urea. The protein refolded properly without aggregation.

6.2.3.4 ***In vitro* kinase assays**

Purified recombinant protein fragments (1 to 2 µg) were incubated with either 1.1 µg purified recombinant yeast GST-Ipl1, 0.2 µg recombinant His-Aurora A (AMS Biotechnology Ltd) or water in kinase buffer (150 mM NaCl, 40 mM HEPES pH 7, 5 mM $MgCl_2$, 2 mM DTT, 20% glycerol) for 30 min at 37°C in the presence of 10

mM ATP and 5 µCi γ-^{32}P ATP. The kinase reaction mixtures were resuspended in SDS sample buffer and separated using 10% or 15% SDS-polyacrylamide gels. The gels were dried using vacuum gel dryer (AlphaMetrix) and phosphorylation of protein fragments was detected using autoradiography. The autoradiographs were obtained by exposing the gel to an X-ray film (Fuji-Film). Simultaneously, the same samples were prepared without γ-^{32}P ATP, resuspended in SDS sample buffer, separated using SDS-polyacrylamide gels and the gels were stained with Coomassie Brilliant Blue (0.05% w/v coomassie brilliant blue (R250), 50% methanol, 10% acetic acid and 40% H_2O). Non-radioactive kinase assay with $Ndc80_{bonsai}$ and His-Aurora A and GST-Ipl1 was performed as follows: 4 µg of recombinant $Ndc80_{bonsai}$ was incubated with 0.2 µg Aurora A or 1,1 µg of GST-Ipl1 in kinase buffer for 30 min at 37°C in the presence of 10 mM ATP. More of the protein is used in this reaction since phosphorylation was determined by western blotting using the rabbit anti-phospho-HEC1/Ndc80 pS55 antibody (Pierce/Thermo Fisher) and HRP-Anti Rabbit IgG (Sigma).

6.3 Cytological techniques and microscopy

6.3.1 Cell culture and cell line generation

HeLa, HEK-293T and HeLa Cas9 cells (McKinley et al., 2015; a kind gift from I. Cheeseman) were maintained in DMEM (Lonza) supplemented with 10% FBS and penicillin/streptomycin (Gibco) at 37°C in a humidified atmosphere with 5% CO_2. DNA transfection in HeLa cells was performed using effectene transfection reagent (QIAGEN) as per manufacturer's instructions. DNA and siRNA co-transfection of HeLa cells was performed with jetPRIME (Polyplus) transfection reagent following manufacturer's instructions. For RNAi-mediated depletion of SPICE1, siRNA (Dharmacon) targeting the sequence within C terminus of SPICE1 is used: 5'-GCUGAGAACAAAUGAGUCA-3'. The inducible *SPICE1* KO cell line was generated as previously described (McKinley et al., 2015; Wang et al., 2016). Transfection mixture, containing 5 µg guideRNA, 4.5 µg pCMV-dR8.2, 500 ng pCMV-VSV-G, 25 µL X-tremeGENE 9 DNA Transfection Reagent (Sigma-Aldrich) and 250 µl Opti-MEM (Gibco), was incubated for 15 min at room temperature and added in a drop-wise

manner to HEK-293T cells. The cells were incubated at 37°C for 24 h, after which the medium was replenished and the cells incubated for additional 24 h. The virus was harvested after 48 h of transfection, filtered using 0.22-µm syringe filter (Millipore) and 1000000 HeLa Cas9 cells were infected in 6-well dish. Spin infection was performed to enhance the efficiency; cells with the virus were centrifuged at 1200 x g for 45 min in a pre-warmed centrifuge at 37°C. The cells were incubated at 37˚C for 24 h, followed by selection of the cells containing guideRNA targeting SPICE1 with 0.5 µg/ml puromycin (Abcam). CRISPR design tool by Zhang lab was used in order to select the best guideRNA targeting SPICE1 gene, and guideRNA 5'-TTCGGGAGTTGCCCGATGAA-3', targeting exon 3 of SPICE1, scored 94 by inverse likelihood of off-target binding. *SPICE1* KO was introduced with 1 µg/ml doxycycline (Sigma) treatment of stable HeLa Cas9 guideRNASPICE1 cells for 96 h.

6.3.2 **Immunostaining**

In order to perform fluorescence microscopy experiments, HeLa cells were plated on 18-mm glass coverslips coated with poly-L-lysine, and allowed to grow for one day prior to the treatments. The culture medium was discarded and coverslips were washed with 1X PBS. The cells were fixed with 3.7% FA (37% Formaldehyde, Sigma) diluted in 1X PHEM pH 7.0 (120 mM PIPES pH 7.0, 50 mM HEPES, 20 mM EGTA, 8 mM $MgSO_4$) for 10 min. The coverslips were washed 3 times in 1X TBS-TX (100ml 10X TBS (0.15 M NaCl, 0.01 M Tris-Cl pH 7.4), 5 ml 20% Triton X-100, 895 ml ddH_20) to remove any trace of formaldehyde. For anti-pS55-HEC1/Ndc80 and anti-pS10-H3 antibodies permeabilization of cells was carried out by applying 1% Triton X-100 (BioRad) diluted in 1X PHEM for 5 min before fixation. The cells were blocked with AbDil solution (TBS-TX, 2% BSA, 0.1% Azide) for 30 min at room temperature. Subsequently, the cells were stained with primary antibody for 1 h at room temperature, followed by extensive washing with TBS-TX. Secondary antibody was applied for 1 h followed by extensive washing with TBS-TX. After this step, 1 µg/ml Hoechst33342 (Thermo Fisher) was applied on cells for 5 min and the cells were mounted in 10 µl ProlongGold (Invitrogen). For methanol fixation, the culture medium was discarded and coverslips were washed with 1X PBS. The cells were

fixed with ice-cold glacial methanol for 10 min at -20°C, followed by permeabilization with ice-cold aceton for 1 min at -20°C. The coverslips were abundantly washed in 1X PBS and the proceeding steps were as described above. Primary antibodies used were as follows: rabbit anti-pS55 HEC1/Ndc80 (Pierce/Thermo), mouse anti HEC1/Ndc80 (Abcam), mouse anti-CENP-A (Abcam), rabbit anti-pS10 H3 (a gift from T.Maresca), mouse anti-β-tubulin (Sigma), rabbit anti-Centrin (Covance, custom-made), rabbit anti-SPICE1 (HPA064843, Atlas Antibodies). Secondary antibody used are anti-mouse Cy2 488, Cy3 594 and Cy5 644, as well as anti-rabbit Cy2 488 and Cy3 594, all from Jackson Immuno Laboratories.

6.3.3 **Microscopy and data analysis**

Live and fixed HeLa cells were observed on a DeltaVision Core deconvolution microscope with Olympus U-PlanApo 100x NA 1.3 objective. Images were taken with a CoolSnap HQ2 CCD camera, controlled by the softWoRx software (formerly Applied Precision, now GE Healthcare).

HEC1/Ndc80 fluorescent imaging and analysis

Thirty Z-sections were acquired at 0.2 µm steps. Equivalent exposure conditions were used between control and drug-treated cells. The cells were treated with 300 ng/ml nocodazole (Acros Organics) for 1.5 h together with 2 µM ZM447439 (Selleckchem), or 300 nM MLN8237 (Selleckchem), followed by fixation. For the experiment with polar chromosomes, the cells were first treated with 10 µM MG132 (Cambridge Biosciences), washed and then treated with 200 nM GSK923295 (Selleckchem) for 30 min. The co-treatment with Aurora A inhibitor was performed first with 300 nM MLN8237 for 1 h followed by addition of 200 nM GSK923295. To quantify fluorescent intensities, individual kinetochores were selected from projections based on co-localization with CENP-A or HEC1/Ndc80, and the integrated intensities were determined after subtracting the background fluorescence measured from an area adjacent to the kinetochore for the individual kinetochores (to take into account background fluorescence). The analysis was performed using MetaMorph software (Molecular Devices). For measuring

fluorescent intensities of polar or aligned kinetochores, individual kinetochores were selected from 2-3 planes based on HEC1/Ndc80 signal, either close to the pole or at the metaphase plate, or distant to the poles. Spindle pole markers were not used, but rabbit anti-pS55-HEC1/Ndc80 creates unspecific staining that marks the spindle poles (DeLuca et al., 2011). Integrated intensities of pS10-H3 signals were measured from chromatin surface using Image-Pro-Premier software (Media Cybernetics). All the quantifications were performed with GraphPad Prims software using Student t-test or one-way ANOVA.

SPICE1 fluorescent imaging and analysis

Between 20 to 40 Z-sections were acquired at 0.2 µm steps as to capture both centrosomes in cells. Equivalent exposure conditions were used between all the transfected cells in a single experiment. HeLa Cas9 SPICE1guide cells were treated with 1µg/ml doxycycline for 96h to knock-out SPICE1 gene and observe the phenotype. Drug treatment of HeLa cells with Aurora kinases inhibitors was performed with 150 nM MLN8237 and 2µM ZM447439 for 1.5 h before fixation. The GFP-SPICE1 and GFP-SPICE1$_{1-550}$ signal intensities at spindle MTs were measured using MetaMorph software. Integrated intensities of GFP signal on MTs from projections were determined based on co-localizations with β-tubulin signal and after subtracting the background fluorescence measured from an area adjacent to the MTs for the individual MTs. Images were deconvolved for easier assessment of centriole number. To quantify chromosome congression defects in SPICE1 knockdown and KO, the cells were scored as having congressed chromosome, mild congression defects and severe congression defects based on Hoechst 33342 staining. The cells with at least 5 mis-aligned chromosomes were scored as mild congression defects; the cells with more than 5 misaligned chromosomes as cells with severe defects. To quantify spindle morphology defects, the cells were scored as having bipolar or multipolar spindle based on β-tubulin staining and spindle morphology. To quantify defects in centriole numbers, the cells were scored as having 1+1, 2+1, 2+2, >4 centrioles or exceptional, which included isolated cases such as 1+1+1, 1+2+1, 3+1, 1+1+1+1 and similar, which resulted in the total number

of centrioles being 4 or less but did not correspond to previously determined categories. Statistical analysis of data was performed with GraphPad Prims software using Student t-test (in the case of GFP signal intensities) and non-parametric tests. Kruskal-Wallis test was used for centriole number in over-expression experiment, while Chi-square tests and Fisher's exact tests were used for analysis of chromosome alignment, spindle morphology and centriole number defects in SPICE1 knockdown and KO.

7 References

Abe, Y., Ohsugi, M., Haraguchi, K., Fujimoto, J., and Yamamoto, T. 2006. LATS2–Ajuba complex regulates γ-tubulin recruitment to centrosomes and spindle organization during mitosis. *FEBS Letters* 580 (3):782-8.

Adams, R. R., Maiato, H., Earnshaw, W. C., and Carmena, M. 2001. Essential Roles of *Drosophila* Inner Centromere Protein (Incenp) and Aurora B in Histone H3 Phosphorylation, Metaphase Chromosome Alignment, Kinetochore Disjunction, and Chromosome Segregation. *The Journal of Cell Biology* 153 (4):865-80.

Afonso, O., Figueiredo, A. C., and Maiato, H. 2017. Late mitotic functions of Aurora kinases. *Chromosoma* 126 (1):93-103.

Aitchison, J. D., Blobel, G., and Rout, M. P. 1995. Nup120p: a yeast nucleoporin required for NPC distribution and mRNA transport. *The Journal of Cell Biology* 131 (6):1659-75.

Akhmanova, A., Hoogenraad, C. C., Drabek, K., Stepanova, T., Dortland, B., Verkerk, T., Vermeulen, W., Burgering, B. M., De Zeeuw, C. I., Grosveld, F., and Galjart, N. 2001. CLASPs Are CLIP-115 and -170 Associating Proteins Involved in the Regional Regulation of Microtubule Dynamics in Motile Fibroblasts. *Cell* 104 (6):923-35.

Akiyoshi, B., Nelson, C. R., and Biggins, S. 2013. The Aurora B Kinase Promotes Inner and Outer Kinetochore Interactions in Budding Yeast. *Genetics* 194 (3):785-9.

Akiyoshi, B., Nelson, C. R., Ranish, J. A., and Biggins, S. 2009. Analysis of Ipl1-mediated phosphorylation of the Ndc80 kinetochore protein in Saccharomyces cerevisiae. *Genetics* 183 (4):1591-5.

Akiyoshi, B., Sarangapani, K. K., Powers, A. F., Nelson, C. R., Reichow, S. L., Arellano-Santoyo, H., Gonen, T., Ranish, J. A., Asbury, C. L., and Biggins, S. 2010. Tension directly stabilizes reconstituted kinetochore-microtubule attachments. *Nature* 468 (7323):576-9.

Al-Bassam, J., Kim, H., Brouhard, G., van Oijen, A., Harrison, S. C., and Chang, F. 2010. CLASP promotes microtubule rescue by recruiting tubulin dimers to the microtubule. *Developmental Cell* 19 (2):245-58.

Allshire, R. C. and Karpen, G. H. 2008. Epigenetic regulation of centromeric chromatin: old dogs, new tricks? *Nature Reviews Genetics* 9 (12):923-37.

Alushin, G. M., Lander, G. C., Kellogg, E. H., Zhang, R., Baker, D., and Nogales, E. 2014. High-resolution microtubule structures reveal the structural transitions in αβ-tubulin upon GTP hydrolysis. *Cell* 157 (5):1117-29.

Alushin, G. M., Ramey, V. H., Pasqualato, S., Ball, D. A., Grigorieff, N., Musacchio, A., and Nogales, E. 2010. The Ndc80 kinetochore complex forms oligomeric arrays along microtubules. *Nature* 467 (7317):805-10.

Andersen, J. S., Wilkinson, C. J., Mayor, T., Mortensen, P., Nigg, E. A., and Mann, M. 2003. Proteomic characterization of the human centrosome by protein correlation profiling. *Nature* 426:570-4.

Andrews, P. D., Ovechkina, Y., Morrice, N., Wagenbach, M., Duncan, K., Wordeman, L., and Swedlow, J. R. 2004. Aurora B Regulates MCAK at the Mitotic Centromere. *Developmental Cell* 6 (2):253-68.

Antonio, C., Ferby, I., Wilhelm, H., Jones, M., Karsenti, E., Nebreda, A. R., and Vernos, I. 2000. Xkid, a Chromokinesin Required for Chromosome Alignment on the Metaphase Plate. *Cell* 102 (4):425-35.

Archinti, M., Lacasa, C., Teixido-Travesa, N., and Luders, J. 2010. SPICE--a previously uncharacterized protein required for centriole duplication and mitotic chromosome congression. *Journal of Cell Science* 123 (Pt 18):3039-46.

Arquint, C., Sonnen, K. F., Stierhof, Y. D., and Nigg, E. A. 2012. Cell-cycle-regulated expression of STIL controls centriole number in human cells. *Journal of Cell Science* 125 (Pt 5):1342-52.

Asano, E., Hasegawa, H., Hyodo, T., Ito, S., Maeda, M., Takahashi, M., Hamaguchi, M., and Senga, T. 2013. The Aurora-B-mediated phosphorylation of SHCBP1 regulates cytokinetic furrow ingression. *Journal of Cell Science* 126 (Pt 15):3263-70.

Ashburner, M., Ball, C. A., Blake, J. A., Botstein, D., Butler, H., Cherry, J. M., Davis, A. P., Dolinski, K., Dwight, S. S., Eppig, J. T., Harris, M. A., Hill, D. P., Issel-Tarver, L., Kasarskis, A., Lewis, S., Matese, J. C., Richardson, J. E., Ringwald, M., Rubin, G. M., and Sherlock, G. 2000. Gene Ontology: tool for the unification of biology. *Nature Genetics* 25:25-9.

Bailey, T. L., Boden, M., Buske, F. A., Frith, M., Grant, C. E., Clementi, L., Ren, J., Li, W. W., and Noble, W. S. 2009. MEME Suite: tools for motif discovery and searching. *Nucleic Acids Research* 37 (suppl_2):W202-W208.

Bakhoum, S. F., Kabeche, L., Murnane, J. P., Zaki, B. I., and Compton, D. A. 2014. DNA-Damage Response during Mitosis Induces Whole-Chromosome Missegregation. *Cancer Discovery* 4 (11):1281-9.

Ban, R., Irino, Y., Fukami, K., and Tanaka, H. 2004. Human mitotic spindle-associated protein PRC1 inhibits MgcRacGAP activity toward Cdc42 during the metaphase. *Journal of Biological Chemistry* 279 (16):16394-402.

Ban, R., Matsuzaki, H., Akashi, T., Sakashita, G., Taniguchi, H., Park, S. Y., Tanaka, H., Furukawa, K., and Urano, T. 2009. Mitotic regulation of the stability of microtubule plus-end tracking protein EB3 by ubiquitin ligase SIAH-1 and Aurora mitotic kinases. *Journal of Biological Chemistry* 284 (41):28367-81.

Barisic, M., Aguiar, P., Geley, S., and Maiato, H. 2014. Kinetochore motors drive congression of peripheral polar chromosomes by overcoming random arm-ejection forces. *Nature Cell Biology* 16 (12):1249-56.

Barisic, M., Silva e Sousa, R., Tripathy, S. K., Magiera, M. M., Zaytsev, A. V., Pereira, A. L., Janke, C., Grishchuk, E. L., and Maiato, H. 2015. Microtubule detyrosination guides chromosomes during mitosis. *Science* 348 (6236):799-803.

Barr, F. A., Sillje, H. H., and Nigg, E. A. 2004. Polo-like kinases and the orchestration of cell division. *Nature Reviews: Molecular Cell Biology* 5 (6):429-40.

Barros, T. P., Kinoshita, K., Hyman, A. A., and Raff, J. W. 2005. Aurora A activates D-TACC-Msps complexes exclusively at centrosomes to stabilize centrosomal microtubules. *Journal of Cell Biology* 170 (7):1039-46.

Basto, R., Lau, J., Vinogradova, T., Gardiol, A., Woods, C. G., Khodjakov, A., and Raff, J. W. 2006. Flies without Centrioles. *Cell* 125 (7):1375-86.

Bastos, R. N., Cundell, M. J., and Barr, F. A. 2014. KIF4A and PP2A-B56 form a spatially restricted feedback loop opposing Aurora B at the anaphase central spindle. *Journal of Cell Biology* 207 (6):683-93.

Bayliss, R., Sardon, T., Vernos, I., and Conti, E. 2003. Structural Basis of Aurora-A Activation by TPX2 at the Mitotic Spindle. *Molecular Cell* 12 (4):851-62.

Beausoleil, S. A., Jedrychowski, M., Schwartz, D., Elias, J. E., Villén, J., Li, J., Cohn, M. A., Cantley, L. C., and Gygi, S. P. 2004. Large-scale characterization of HeLa cell nuclear phosphoproteins. *Proc Natl Acad Sci U S A* 101 (33):12130-5.

Belgareh, N., Rabut, G., Bai, S. W., van Overbeek, M., Beaudouin, J., Daigle, N., Zatsepina, O. V., Pasteau, F., Labas, V., Fromont-Racine, M., Ellenberg, J., and Doye, V. 2001. An evolutionarily conserved NPC subcomplex, which redistributes in part to kinetochores in mammalian cells. *Journal of Cell Biology* 154 (6):1147-60.

Berke, I. C., Boehmer, T., Blobel, G., and Schwartz, T. U. 2004. Structural and functional analysis of Nup133 domains reveals modular building blocks of the nuclear pore complex. *Journal of Cell Biology* 167 (4):591-7.

Bernard, M., Sanseau, P., Henry, C., Couturier, A., and Prigent, C. 1998. Cloning of STK13, a Third Human Protein Kinase Related to *Drosophila* Aurora and Budding Yeast Ipl1 That Maps on Chromosome 19q13.3–ter. *Genomics* 53 (3):406-9.

Beroukhim, R., Mermel, C. H., Porter, D., Wei, G., Raychaudhuri, S., Donovan, J., Barretina, J., Boehm, J. S., Dobson, J., Urashima, M., Mc Henry, K. T., Pinchback, R. M., Ligon, A. H., Cho, Y.-J., Haery, L., Greulich, H., Reich, M., Winckler, W., Lawrence, M. S., Weir, B. A., Tanaka, K. E., Chiang, D. Y., Bass, A. J., Loo, A., Hoffman, C., Prensner, J., Liefeld, T., Gao, Q., Yecies, D., Signoretti, S., Maher, E., Kaye, F. J., Sasaki, H., Tepper, J. E., Fletcher, J. A., Tabernero, J., Baselga, J., Tsao, M.-S., Demichelis, F., Rubin, M. A., Janne, P. A., Daly, M. J., Nucera, C., Levine, R. L., Ebert, B. L., Gabriel, S., Rustgi, A. K., Antonescu, C. R., Ladanyi, M., Letai, A., Garraway, L. A., Loda, M., Beer, D. G., True, L. D., Okamoto, A., Pomeroy, S. L., Singer, S., Golub, T. R., Lander, E. S., Getz, G., Sellers, W. R., and Meyerson, M. 2010. The landscape of somatic copy-number alteration across human cancers. *Nature* 463 (7283):899-905.

Bettencourt-Dias, M. and Glover, D. M. 2007. Centrosome biogenesis and function: centrosomics brings new understanding. *Nature Reviews: Molecular Cell Biology* 8 (6):451-63.

Biggins, S. and Murray, A. W. 2001. The budding yeast protein kinase Ipl1/Aurora allows the absence of tension to activate the spindle checkpoint. *Genes & Development* 15 (23):3118-29.

Biggins, S., Severin, F. F., Bhalla, N., Sassoon, I., Hyman, A. A., and Murray, A. W. 1999. The conserved protein kinase Ipl1 regulates microtubule binding to kinetochores in budding yeast. *Genes & Development* 13 (5):532-44.

Bilokapic, S. and Schwartz, T. U. 2013. Structural and functional studies of the 252 kDa nucleoporin ELYS reveal distinct roles for its three tethered domains. *Structure* 21 (4):572-80.

Birkenfeld, J., Nalbant, P., Bohl, B. P., Pertz, O., Hahn, K. M., and Bokoch, G. M. 2007. GEF-H1 modulates localized RhoA activation during cytokinesis under the control of mitotic kinases. *Developmental Cell* 12 (5):699-712.

Bischoff, J. R., Anderson, L., Zhu, Y., Mossie, K., Ng, L., Souza, B., Schryver, B., Flanagan, P., Clairvoyant, F., Ginther, C., Chan, C. S. M., Novotny, M., Slamon, D. J., and Plowman, G. D. 1998. A homologue of *Drosophila aurora* kinase is oncogenic and amplified in human colorectal cancers. *The EMBO Journal* 17 (11):3052-65.

Bishop, J. D. and Schumacher, J. M. 2002. Phosphorylation of the carboxyl terminus of inner centromere protein (INCENP) by the Aurora B Kinase stimulates Aurora B kinase activity. *Journal of Biological Chemistry* 277 (31):27577-80.

Boehmer, T., Enninga, J., Dales, S., Blobel, G., and Zhong, H. 2003. Depletion of a single nucleoporin, Nup107, prevents the assembly of a subset of nucleoporins into the nuclear pore complex. *Proc Natl Acad Sci U S A* 100 (3):981-5.

Boehmer, T., Jeudy, S., Berke, I. C., and Schwartz, T. U. 2008. Structural and functional studies of Nup107/Nup133 interaction and its implications for the architecture of the nuclear pore complex. *Molecular Cell* 30 (6):721-31.

Boehmer, T. and Schwartz, T. U. 2007. Purification, crystallization and preliminary X-ray analysis of a Nup107-Nup133 heterodimeric nucleoporin complex. *Acta crystallographica. Section F, Structural biology and crystallization communications.* 63 (Pt 9):816-8.

Bollen, M., Peti, W., Ragusa, M. J., and Beullens, M. 2010. The extended PP1 toolkit: designed to create specificity. *Trends in Biochemical Sciences* 35 (8):450-8.

Bolton, M. A., Lan, W., Powers, S. E., McCleland, M. L., Kuang, J., and Stukenberg, P. T. 2002. Aurora B kinase exists in a complex with survivin and INCENP and its kinase activity is stimulated by survivin binding and phosphorylation. *Mol Biol Cell* 13 (9):3064-77.

Bonnet, C., Boucher, D., Lazereg, S., Pedrotti, B., Islam, K., Denoulet, P., and Larcher, J. C. 2001. Differential Binding Regulation of Microtubule-associated Proteins MAP1A, MAP1B, and MAP2 by Tubulin Polyglutamylation. *Journal of Biological Chemistry* 276 (16):12839-48.

Boucher, D., Larcher, J.-C., Gros, F., and Denoulet, P. 1994. Polyglutamylation of Tubulin as a Progressive Regulator of in Vitro Interactions between the Microtubule-Associated Protein Tau and Tubulin. *Biochemistry* 33 (41):12471-7.

Briassouli, P., Chan, F., Savage, K., Reis-Filho, J. S., and Linardopoulos, S. 2007. Aurora-A Regulation of Nuclear Factor-κB Signaling by Phosphorylation of IκBα. *Cancer Research* 67 (4):1689-95.

Brodie, K. M. and Henderson, B. R. 2012. Characterization of BRCA1 protein targeting, dynamics, and function at the centrosome: a role for the nuclear export signal, CRM1, and Aurora A kinase. *Journal of Biological Chemistry* 287 (10):7701-16.

Brouhard, G. J., Stear, J. H., Noetzel, T. L., Al-Bassam, J., Kinoshita, K., Harrison, S. C., Howard, J., and Hyman, A. A. 2008. XMAP215 is a processive microtubule polymerase. *Cell* 132 (1):79-88.

Brown, C. J., Takayama, S., Campen, A. M., Vise, P., Marshall, T. W., Oldfield, C. J., Williams, C. J., and Dunker, A. K. 2002. Evolutionary rate heterogeneity in proteins with long disordered regions. *Journal of Molecular Evolution* 55 (1):104-10.

Bruinsma, W., Macurek, L., Freire, R., Lindqvist, A., and Medema, R. H. 2014. Bora and Aurora-A continue to activate Plk1 in mitosis. *Journal of Cell Science* 127 (Pt 4):801-11.

Cahu, J., Olichon, A., Hentrich, C., Schek, H., Drinjakovic, J., Zhang, C., Doherty-Kirby, A., Lajoie, G., and Surrey, T. 2008. Phosphorylation by Cdk1 increases the binding of Eg5 to microtubules in vitro and in Xenopus egg extract spindles. *PLoS One* 3 (12):e3936.

Cai, S., O'Connell, C. B., Khodjakov, A., and Walczak, C. E. 2009. Chromosome congression in the absence of kinetochore fibres. *Nature Cell Biology* 11 (7):832-8.

Campbell, C. S. and Desai, A. 2013. Tension sensing by Aurora B kinase is independent of survivin-based centromere localization. *Nature* 497 (7447):118-21.

Cane, S., Ye, A. A., Luks-Morgan, S. J., and Maresca, T. J. 2013. Elevated polar ejection forces stabilize kinetochore-microtubule attachments. *Journal of Cell Biology* 200 (2):203-18.

Cantin, G. T. and Yates, J. R. 2004. Strategies for shotgun identification of post-translational modifications by mass spectrometry. *Journal of Chromatography A* 1053 (1-2):7-14.

Capalbo, L., Montembault, E., Takeda, T., Bassi, Z. I., Glover, D. M., and D'Avino, P. P. 2012. The chromosomal passenger complex controls the function of endosomal sorting complex required for transport-III Snf7 proteins during cytokinesis. *Open Biology* 2 (5):120070.

Carazo-Salas, R. E., Gruss, O. J., Mattaj, I. W., and Karsenti, E. 2001. Ran–GTP coordinates regulation of microtubule nucleation and dynamics during mitotic-spindle assembly. *Nature Cell Biology* 3 (3):228-34.

Carazo-Salas, R. E., Guarguaglini, G., Gruss, O. J., Segref, A., Karsenti, E., and Mattaj, I. W. 1999. Generation of GTP-bound Ran by RCC1 is required for chromatin-induced mitotic spindle formation. *Nature* 400 (6740):178-81.

Carlton, J. G., Caballe, A., Agromayor, M., Kloc, M., and Martin-Serrano, J. 2012. ESCRT-III Governs the Aurora B–Mediated Abscission Checkpoint Through CHMP4C. *Science* 336 (6078):220-5.

Carmena, M. and Earnshaw, W. C. 2003. The cellular geography of aurora kinases. *Nature Reviews: Molecular Cell Biology* 4 (11):842-54.

Carmena, M., Wheelock, M., Funabiki, H., and Earnshaw, W. C. 2012. The chromosomal passenger complex (CPC): from easy rider to the godfather of mitosis. *Nature Reviews: Molecular Cell Biology* 13 (12):789-803.

Cassimeris, L., Rieder, C. L., and Salmon, E. D. 1994. Microtubule assembly and kinetochore directional instability in vertebrate monopolar spindles: implications for the mechanism of chromosome congression. *Journal of Cell Science* 107 (1):285-97.

Cazales, M., Schmitt, E., Montembault, E., Dozier, C., Prigent, C., and Ducommun, B. 2005. CDC25B phosphorylation by Aurora-A occurs at the G2/M transition and is inhibited by DNA damage. *Cell Cycle* 4 (9):1233-8.

Cesario, J. M., Jang, J. K., Redding, B., Shah, N., Rahman, T., and McKim, K. S. 2006. Kinesin 6 family member Subito participates in mitotic spindle assembly and interacts with mitotic regulators. *Journal of Cell Science* 119 (Pt 22):4770-80.

Chan, C. S. and Botstein, D. 1993. Isolation and characterization of chromosome-gain and increase-in-ploidy mutants in yeast. *Genetics* 135 (3):677-91.

Cheerambathur, D. K., Prevo, B., Hattersley, N., Lewellyn, L., Corbett, K. D., Oegema, K., and Desai, A. 2017. Dephosphorylation of the Ndc80 Tail Stabilizes Kinetochore-Microtubule Attachments via the Ska Complex. *Developmental Cell* 41 (4):424-437.e4.

Cheeseman, I. M., Anderson, S., Jwa, M., Green, E. M., Kang, J.-s., Yates, J. R., Chan, C. S. M., Drubin, D. G., and Barnes, G. 2002. Phospho-Regulation of Kinetochore-Microtubule Attachments by the Aurora Kinase Ipl1p. *Cell* 111 (2):163-72.

Cheeseman, I. M., Chappie, J. S., Wilson-Kubalek, E. M., and Desai, A. 2006. The Conserved KMN Network Constitutes the Core Microtubule-Binding Site of the Kinetochore. *Cell* 127 (5):983-97.

Cheeseman, I. M. and Desai, A. 2008. Molecular architecture of the kinetochore-microtubule interface. *Nature Reviews: Molecular Cell Biology* 9 (1):33-46.

Cheeseman, I. M., Hori, T., Fukagawa, T., and Desai, A. 2008. KNL1 and the CENP-H/I/K Complex Coordinately Direct Kinetochore Assembly in Vertebrates. *Molecular Biology of the Cell* 19 (2):587-94.

Chefetz, I., Holmberg, J. C., Alvero, A. B., Visintin, I., and Mor, G. 2011. Inhibition of Aurora-A kinase induces cell cycle arrest in epithelial ovarian cancer stem cells by affecting NFκB pathway. *Cell Cycle* 10 (13):2206-14.

Chmátal, L., Yang, K., Schultz, Richard M., and Lampson, Michael A. 2015. Spatial Regulation of Kinetochore Microtubule Attachments by Destabilization at Spindle Poles in Meiosis I. *Current Biology* 25 (14):1835-41.

Chou, E.-J., Hung, L.-Y., Tang, C.-Ju C., Hsu, W.-B., Wu, H.-Y., Liao, P.-C., and Tang, Tang K. 2016. Phosphorylation of CPAP by Aurora-A Maintains Spindle Pole Integrity during Mitosis. *Cell Reports* 14 (12):2975-87.

Ciferri, C., De Luca, J., Monzani, S., Ferrari, K. J., Ristic, D., Wyman, C., Stark, H., Kilmartin, J., Salmon, E. D., and Musacchio, A. 2005. Architecture of the human ndc80-hec1 complex, a critical constituent of the outer kinetochore. *Journal of Biological Chemistry* 280 (32):29088-95.

Ciferri, C., Pasqualato, S., Screpanti, E., Varetti, G., Santaguida, S., Dos Reis, G., Maiolica, A., Polka, J., De Luca, J. G., De Wulf, P., Salek, M., Rappsilber, J., Moores, C. A., Salmon, E. D., and Musacchio, A. 2008. Implications for kinetochore-microtubule attachment from the structure of an engineered Ndc80 complex. *Cell* 133 (3):427-39.

Cimini, D., Moree, B., Canman, J. C., and Salmon, E. D. 2003. Merotelic kinetochore orientation occurs frequently during early mitosis in mammalian tissue cells and error correction is achieved by two different mechanisms. *Journal of Cell Science* 116 (Pt 20):4213-25.

Collins, M. O., Yu, L., Campuzano, I., Grant, S. G. N., and Choudhary, J. S. 2008. Phosphoproteomic Analysis of the Mouse Brain Cytosol Reveals a Predominance of Protein Phosphorylation in Regions of Intrinsic Sequence Disorder. *Molecular & Cellular Proteomics* 7 (7):1331-48.

Comartin, D., Gupta, G. D., Fussner, E., Coyaud, E., Hasegan, M., Archinti, M., Cheung, S. W., Pinchev, D., Lawo, S., Raught, B., Bazett-Jones, D. P., Luders, J., and Pelletier, L. 2013. CEP120 and SPICE1 cooperate with CPAP in centriole elongation. *Current Biology* 23 (14):1360-6.

Cormier, A., Drubin, D. G., and Barnes, G. 2013. Phosphorylation regulates kinase and microtubule binding activities of the budding yeast chromosomal passenger complex in vitro. *Journal of Biological Chemistry* 288 (32):23203-11.

Cronshaw, J. M., Krutchinsky, A. N., Zhang, W., Chait, B. T., and Matunis, M. J. 2002. Proteomic analysis of the mammalian nuclear pore complex. *Journal of Cell Biology* 158 (5):915-27.

Crosio, C., Fimia, G. M., Loury, R., Kimura, M., Okano, Y., Zhou, H., Sen, S., Allis, C. D., and Sassone-Corsi, P. 2002. Mitotic Phosphorylation of Histone H3: Spatio-Temporal Regulation by Mammalian Aurora Kinases. *Molecular and Cellular Biology* 22 (3):874-85.

Daub, H., Olsen, J. V., Bairlein, M., Gnad, F., Oppermann, F. S., Korner, R., Greff, Z., Keri, G., Stemmann, O., and Mann, M. 2008. Kinase-selective enrichment enables

quantitative phosphoproteomics of the kinome across the cell cycle. *Molecular Cell* 31 (3):438-48.

De Brabander, M., Geuens, G., Nuydens, R., Willebrords, R., and De Mey, J. 1981. Taxol induces the assembly of free microtubules in living cells and blocks the organizing capacity of the centrosomes and kinetochores. *Proc Natl Acad Sci U S A* 78 (9):5608-12.

DeLuca, J. G., Gall, W. E., Ciferri, C., Cimini, D., Musacchio, A., and Salmon, E. D. 2006. Kinetochore microtubule dynamics and attachment stability are regulated by Hec1. *Cell* 127 (5):969-82.

DeLuca, K. F., Lens, S. M., and DeLuca, J. G. 2011. Temporal changes in Hec1 phosphorylation control kinetochore-microtubule attachment stability during mitosis. *Journal of Cell Science* 124 (Pt 4):622-34.

Dephoure, N., Zhou, C., Villén, J., Beausoleil, S. A., Bakalarski, C. E., Elledge, S. J., and Gygi, S. P. 2008. A quantitative atlas of mitotic phosphorylation. *Proceedings of the National Academy of Sciences* 105 (31):10762-7.

Desai, A. and Mitchison, T. J. 1997. MICROTUBULE POLYMERIZATION DYNAMICS. *Annual Review of Cell and Developmental Biology* 13 (1):83-117.

Desai, A., Verma, S., Mitchison, T. J., and Walczak, C. E. 1999. Kin I Kinesins Are Microtubule-Destabilizing Enzymes. *Cell* 96 (1):69-78.

Diella, F., Gould, C. M., Chica, C., Via, A., and Gibson, T. J. 2008. Phospho.ELM: A database of phosphorylation sites - Update 2008. *Nucleic Acids Research* 36:240-4.

Ditchfield, C., Johnson, V. L., Tighe, A., Ellston, R., Haworth, C., Johnson, T., Mortlock, A., Keen, N., and Taylor, S. S. 2003. Aurora B couples chromosome alignment with anaphase by targeting BubR1, Mad2, and Cenp-E to kinetochores. *Journal of Cell Biology* 161 (2):267-80.

Dongré, A. R., Jones, J. L., Somogyi, Á., and Wysocki, V. H. 1996. Influence of Peptide Composition, Gas-Phase Basicity, and Chemical Modification on Fragmentation Efficiency: Evidence for the Mobile Proton Model. *Journal of the American Chemical Society* 118 (35):8365-74.

Dosztányi, Z., Csizmok, V., Tompa, P., and Simon, I. 2005a. IUPred: web server for the prediction of intrinsically unstructured regions of proteins based on estimated energy content. *Bioinformatics* 21 (16):3433-34.

Dosztányi, Z., Csizmók, V., Tompa, P., and Simon, I. 2005b. The pairwise energy content estimated from amino acid composition discriminates between folded and intrinsically unstructured proteins. *Journal of Molecular Biology* 347:827-39.

Douglas, M. E., Davies, T., Joseph, N., and Mishima, M. 2010. Aurora B and 14-3-3 Coordinately Regulate Clustering of Centralspindlin during Cytokinesis. *Current Biology* 20:927-33.

Doye, V., Wepf, R., and Hurt, E. C. 1994. A novel nuclear pore protein Nup133p with distinct roles in poly(A)+ RNA transport and nuclear pore distribution. *The EMBO Journal* 13 (24):6062-75.

Drechsel, D. N. and Kirschner, M. W. 1994. The minimum GTP cap required to stabilize microtubules. *Current Biology* 4 (12):1053-61.

Du, Y., English, C. A., and Ohi, R. 2010. The Kinesin-8 Kif18A Dampens Microtubule Plus-End Dynamics. *Current Biology* 20 (4):374-80.

Dumont, J., Oegema, K., and Desai, A. 2010. A kinetochore-independent mechanism drives anaphase chromosome separation during acentrosomal meiosis. *Nature Cell Biology* 12 (9):894-901.

Dutertre, S., Cazales, M., Quaranta, M., Froment, C., Trabut, V., Dozier, C., Mirey, G., Bouché, J.-P., Theis-Febvre, N., Schmitt, E., Monsarrat, B., Prigent, C., and Ducommun, B. 2004. Phosphorylation of CDC25B by Aurora-A at the centrosome contributes to the G2–M transition. *Journal of Cell Science* 117 (12):2523-31.

Earnshaw, W. C. and Bernat, R. L. 1991. Chromosomal passengers: Toward an integrated view of mitosis. *Chromosoma* 100 (3):139-46.

Earnshaw, W. C. and Rothfield, N. 1985. Identification of a family of human centromere proteins using autoimmune sera from patients with scleroderma. *Chromosoma* 91 (3):313-21.

Elia, N., Sougrat, R., Spurlin, T. A., Hurley, J. H., and Lippincott-schwartz, J. 2011. Dynamics of endosomal sorting complex required for transport (ESCRT) machinery during cytokinesis and its role in abscission. *Proc Natl Acad Sci U S A* 108 (12):4846-51.

Enninga, J., Levay, A., and Fontoura, B. M. A. 2003. Sec13 Shuttles between the Nucleus and the Cytoplasm and Stably Interacts with Nup96 at the Nuclear Pore Complex. *Molecular and Cellular Biology* 23 (20):7271-84.

Evans, L., Mitchison, T., and Kirschner, M. 1985. Influence of the centrosome on the structure of nucleated microtubules. *The Journal of Cell Biology* 100 (4):1185-91.

Eyers, P. A., Erikson, E., Chen, L. G., and Maller, J. L. 2003. A Novel Mechanism for Activation of the Protein Kinase Aurora A. *Current Biology* 13 (8):691-7.

Fabregat, A., Sidiropoulos, K., Garapati, P., Gillespie, M., Hausmann, K., Haw, R., Jassal, B., Jupe, S., Korninger, F., McKay, S., Matthews, L., May, B., Milacic, M., Rothfels, K., Shamovsky, V., Webber, M., Weiser, J., Williams, M., Wu, G., Stein, L., Hermjakob, H., and D'Eustachio, P. 2016. The Reactome pathway Knowledgebase. *Nucleic Acids Research* 44 (D1):D481-D487.

Fernandez, A. G. and Piano, F. 2006. MEL-28 Is Downstream of the Ran Cycle and Is Required for Nuclear-Envelope Function and Chromatin Maintenance. *Current Biology* 16 (17):1757-63.

Ferrari, S., Marin, O., Pagano, Mario A., Meggio, F., Hess, D., El-Shemerly, M., Krystyniak, A., and Pinna, Lorenzo A. 2005. Aurora-A site specificity: a study with synthetic peptide substrates. *Biochemical Journal* 390 (1):293-302.

Ferreira, J. G., Pereira, A. J., Akhmanova, A., and Maiato, H. 2013. Aurora B spatially regulates EB3 phosphorylation to coordinate daughter cell adhesion with cytokinesis. *Journal of Cell Biology* 201 (5):709-24.

Ferrell, J. E. and Bhatt, R. R. 1997. Mechanistic Studies of the Dual Phosphorylation of Mitogen-activated Protein Kinase. *Journal of Biological Chemistry* 272 (30):19008-16.

Ferrell, J. E. and Machleder, E. M. 1998. The Biochemical Basis of an All-or-None Cell Fate Switch in *Xenopus* Oocytes. *Science* 280 (5365):895-8.

Fırat-Karalar, E. N. and Stearns, T. 2014. The centriole duplication cycle. *Philosophical Transactions of the Royal Society B: Biological Sciences* 369 (1650).

Fischle, W., Tseng, B. S., Dormann, H. L., Ueberheide, B. M., Garcia, B. A., Shabanowitz, J., Hunt, D. F., Funabiki, H., and Allis, C. D. 2005. Regulation of HP1–chromatin binding by histone H3 methylation and phosphorylation. *Nature* 438 (22):1116-22.

Fournane, S., Krupina, K., Kleiss, C., and Sumara, I. 2012. Decoding Ubiquitin for Mitosis. *Genes & Cancer* 3 (11-12):697-711.

Franz, C., Walczak, R., Yavuz, S., Santarella, R., Gentzel, M., Askjaer, P., Galy, V., Hetzer, M., Mattaj, I. W., and Antonin, W. 2007. MEL-28/ELYS is required for the recruitment of nucleoporins to chromatin and postmitotic nuclear pore complex assembly. *EMBO reports* 8 (2):165-72.

Fu, J., Bian, M., Jiang, Q., and Zhang, C. 2007. Roles of Aurora Kinases in Mitosis and Tumorigenesis. *Molecular Cancer Research* 5 (1):1-10.

Fu, J., Bian, M., Liu, J., Jiang, Q., and Zhang, C. 2009. A single amino acid change converts Aurora-A into Aurora-B-like kinase in terms of partner specificity and cellular function. *Proc Natl Acad Sci U S A* 106 (17):6939-44.

Fu, J., Bian, M., Xin, G., Deng, Z., Luo, J., Guo, X., Chen, H., Wang, Y., Jiang, Q., and Zhang, C. 2015. TPX2 phosphorylation maintains metaphase spindle length by regulating microtubule flux. *Journal of Cell Biology* 210 (3):373-83.

Fu, W., Tao, W., Zheng, P., Fu, J., Bian, M., Jiang, Q., Clarke, P. R., and Zhang, C. 2010. Clathrin recruits phosphorylated TACC3 to spindle poles for bipolar spindle assembly and chromosome alignment. *Journal of Cell Science* 123 (21):3645-51.

Fuller, B. G., Lampson, M. A., Foley, E. A., Rosasco-Nitcher, S., Le, K. V., Tobelmann, P., Brautigan, D. L., Stukenberg, P. T., and Kapoor, T. M. 2008. Midzone activation of aurora B in anaphase produces an intracellular phosphorylation gradient. *Nature* 453:1132-6.

Funabiki, H. and Murray, A. W. 2000. The Xenopus Chromokinesin Xkid Is Essential for Metaphase Chromosome Alignment and Must Be Degraded to Allow Anaphase Chromosome Movement. *Cell* 102 (4):411-24.

Galjart, N. 2005. CLIPs and CLASPs and cellular dynamics. *Nature Reviews: Molecular Cell Biology* 6:487-98.

Gallini, S., Carminati, M., De Mattia, F., Pirovano, L., Martini, E., Oldani, A., Asteriti, I. A., Guarguaglini, G., and Mapelli, M. 2016. NuMA phosphorylation by aurora-a orchestrates spindle orientation. *Current Biology* 26:458-69.

Galy, V., Askjaer, P., Franz, C., López-Iglesias, C., and Mattaj, I. W. 2006. MEL-28, a Novel Nuclear-Envelope and Kinetochore Protein Essential for Zygotic Nuclear-Envelope Assembly in C. elegans. *Current Biology* 16:1748-56.

Ganem, N. J., Godinho, S. A., and Pellman, D. 2009. A mechanism linking extra centrosomes to chromosomal instability. *Nature* 460:278-82.

Garnham, C. P. and Roll-Mecak, A. 2012. The chemical complexity of cellular microtubules: Tubulin post-translational modification enzymes and their roles in tuning microtubule functions. *Cytoskeleton* 69:442-63.

Garnham, C. P., Vemu, A., Wilson-Kubalek, E. M., Yu, I., Szyk, A., Lander, G. C., Milligan, R. A., and Roll-Mecak, A. 2015. Multivalent microtubule recognition by tubulin tyrosine ligase-like family glutamylases. *Cell* 161:1112-23.

Gascoigne, K. E., Takeuchi, K., Suzuki, A., Hori, T., Fukagawa, T., and Cheeseman, I. M. 2011. Induced ectopic kinetochore assembly bypasses the requirement for CENP-A nucleosomes. *Cell* 145:410-22.

Gassmann, R., Carvalho, A., Henzing, A. J., Ruchaud, S., Hudson, D. F., Honda, R., Nigg, E. A., Gerloff, D. L., and Earnshaw, W. C. 2004. Borealin: A novel chromosomal passenger

required for stability of the bipolar mitotic spindle. *Journal of Cell Biology* 166:179-91.

Gibson, D. G., Young, L., Chuang, R.-Y., Venter, J. C., Hutchison Iii, C. A., and Smith, H. O. 2009. Enzymatic assembly of DNA molecules up to several hundred kilobases. *Nature Methods* 6(5):343-5.

Giet, R., McLean, D., Descamps, S., Lee, M. J., Raff, J. W., Prigent, C., and Glover, D. M. 2002. Drosophila Aurora A kinase is required to localize D-TACC to centrosomes and to regulate astral microtubules. *Journal of Cell Biology* 156:437-51.

Giet, R., Uzbekov, R., Cubizolles, F., Le Guellec, K., and Prigent, C. 1999. The Xenopus laevis aurora-related protein kinase pEg2 associates with and phosphorylates the kinesin-related protein XlEg5. *Journal of Biological Chemistry* 274:15005-13.

Glavy, J. S., Krutchinsky, A. N., Cristea, I. M., Berke, I. C., Boehmer, T., Blobel, G., and Chait, B. T. 2007. Cell-cycle-dependent phosphorylation of the nuclear pore Nup107-160 subcomplex. *Proc. Nati. Acad. Sci. USA* 104:3811-6.

Glover, D. M., Leibowitz, M. H., McLean, D. A., and Parry, H. 1995. Mutations in aurora prevent centrosome separation leading to the formation of monopolar spindles. *Cell* 81:95-105.

Gnad, F., Gunawardena, J., and Mann, M. 2011. PHOSIDA 2011: The posttranslational modification database. *Nucleic Acids Research* 39:253-60.

Gnad, F., Ren, S., Cox, J., Olsen, J. V., Macek, B., Oroshi, M., and Mann, M. 2007. PHOSIDA (phosphorylation site database): management, structural and evolutionary investigation, and prediction of phosphosites. *Genome Biology* 8:R250.

Gómez-Saldivar, G., Fernandez, A., Hirano, Y., Mauro, M., Lai, A., Ayuso, C., Haraguchi, T., Hiraoka, Y., Piano, F., and Askjaer, P. 2016. Identification of Conserved MEL-28/ELYS Domains with Essential Roles in Nuclear Assembly and Chromosome Segregation. *PLoS Genetics* 12:1-27.

Gönczy, P. 2012. Towards a molecular architecture of centriole assembly. *Nature Reviews Molecular Cell Biology* 13:425-35.

Gordon, D. J., Resio, B., and Pellman, D. 2012. Causes and consequences of aneuploidy in cancer. *Nature Reviews Genetics* 13 (3):189-203.

Goshima, G., Mayer, M., Zhang, N., Stuurman, N., and Vale, R. D. 2008. Augmin: A protein complex required for centrosome-independent microtubule generation within the spindle. *Journal of Cell Biology* 181:421-9.

Goto, H., Yasui, Y., Kawajiri, A., Nigg, E. A., Terada, Y., Tatsuka, M., Nagata, K. i., and Inagaki, M. 2003. Aurora-B regulates the cleavage furrow-specific vimentin phosphorylation in the cytokinetic process. *Journal of Biological Chemistry* 278:8526-30.

Gouet, P., Courcelle, E., Stuart, D., and Métoz, F. 1999. ESPript: analysis of multiple sequence alignments in PostScript. *Bioinformatics* 15 (4):305-8.

Greenan, G., Brangwynne, C. P., Jaensch, S., Gharakhani, J., Jülicher, F., and Hyman, A. A. 2010. Centrosome Size Sets Mitotic Spindle Length in Caenorhabditis elegans Embryos. *Current Biology* 20:353-8.

Groisman, I., Jung, M.-Y., Sarkissian, M., Cao, Q., and Richter, J. D. 2002. Translational control of the embryonic cell cycle. *Cell* 109:473-83.

Gruneberg, U., Neef, R., Honda, R., Nigg, E. A., and Barr, F. A. 2004. Relocation of Aurora B from centromeres to the central spindle at the metaphase to anaphase transition requires MKlp2. *Journal of Cell Biology* 166:167-72.

Gruss, O. J., Carazo-Salas, R. E., Schatz, C. A., Guarguaglini, G., Kast, J., Wilm, M., Le Bot, N., Vernos, I., Karsenti, E., and Mattaj, I. W. 2001. Ran induces spindle assembly by reversing the inhibitory effect of importin α on TPX2 activity. *Cell* 104:83-93.

Grzenda, A., Leonard, P., Seo, S., Mathison, A. J., Urrutia, G., Calvo, E., Iovanna, J., Urrutia, R., and Lomberk, G. 2013. Functional impact of Aurora A-mediated phosphorylation of HP1γ at serine 83 during cell cycle progression. *Epigenetics & chromatin* 6 (1):21.

Gudimchuk, N., Vitre, B., Kim, Y., Kiyatkin, A., Cleveland, D. W., Ataullakhanov, F. I., and Grishchuk, E. L. 2013. Kinetochore kinesin CENP-E is a processive bi-directional tracker of dynamic microtubule tips. *Nature Cell Biology* 15:1079-88.

Guimaraes, G. J., Dong, Y., McEwen, B. F., and DeLuca, J. G. 2008. Kinetochore-Microtubule Attachment Relies on the Disordered N-Terminal Tail Domain of Hec1. *Current Biology* 18:1778-84.

Guizetti, J., Schermelleh, L., Mäntler, J., Maar, S., Poser, I., Leonhardt, H., Müller-Reichert, T., and Gerlich, D. W. 2011. Cortical Constriction During Abscission Involves Helices of ESCRT-III–Dependent Filaments. *Science* 331 (6024):1616-20.

Gully, C. P., Velazquez-Torres, G., Shin, J.-H., Fuentes-Mattei, E., Wang, E., Carlock, C., Chen, J., Rothenberg, D., Adams, H. P., Choi, H. H., Guma, S., Phan, L., Chou, P.-C., Su, C.-H., Zhang, F., Chen, J.-S., Yang, T.-Y., Yeung, S.-C. J., and Lee, M.-H. 2012. Aurora B kinase phosphorylates and instigates degradation of p53. *Proc Natl Acad Sci U S A* 109:E1513-22.

Gupta, G. D., Coyaud, É., Gonçalves, J., Mojarad, B. A., Liu, Y., Wu, Q., Gheiratmand, L., Comartin, D., Tkach, J. M., Cheung, S. W. T., Bashkurov, M., Hasegan, M., Knight, J. D., Lin, Z. Y., Schueler, M., Hildebrandt, F., Moffat, J., Gingras, A. C., Raught, B., and Pelletier, L. 2015. A Dynamic Protein Interaction Landscape of the Human Centrosome-Cilium Interface. *Cell* 163:1483-99.

Gupta, K. K., Joyce, M. V., Slabbekoorn, A. R., Zhu, Z. C., Paulson, B. A., Boggess, B., and Goodson, H. V. 2010. Probing Interactions between CLIP-170, EB1, and Microtubules. *Journal of Molecular Biology* 395:1049-62.

Guse, A., Mishima, M., and Glotzer, M. 2005. Phosphorylation of ZEN-4/MKLP1 by aurora B regulates completion of cytokinesis. *Current Biology* 15:778-86.

Hans, F., Skoufias, D. A., Dimitrov, S., and Margolis, R. L. 2009. Molecular Distinctions between Aurora A and B: A Single Residue Change Transforms Aurora A into Correctly Localized and Functional Aurora B. *Molecular Biology of the Cell* 20 (15):3491-502.

Harel, A., Orjalo, A. V., Vincent, T., Lachish-Zalait, A., Vasu, S., Shah, S., Zimmerman, E., Elbaum, M., and Forbes, D. J. 2003. Removal of a single pore subcomplex results in vertebrate nuclei devoid of nuclear pores. *Molecular Cell* 11:853-64.

Hattersley, N., Cheerambathur, D., Moyle, M., Stefanutti, M., Richardson, A., Lee, K. Y., Dumont, J., Oegema, K., and Desai, A. 2016. A Nucleoporin Docks Protein Phosphatase 1 to Direct Meiotic Chromosome Segregation and Nuclear Assembly. *Developmental Cell* 38:463-77.

Hauf, S., Cole, R. W., LaTerra, S., Zimmer, C., Schnapp, G., Walter, R., Heckel, A., Van Meel, J., Rieder, C. L., and Peters, J. M. 2003. The small molecule Hesperadin reveals a role for Aurora B in correcting kinetochore-microtubule attachment and in maintaining the spindle assembly checkpoint. *Journal of Cell Biology* 161:281-94.

Heald, R., Tournebize, R., Blank, T., Sandaltzopoulos, R., Becker, P., Hyman, A., and Karsenti, E. 1996. Self-organization of microtubules into bipolar spindles around artificial chromosomes in *Xenopus* egg extracts. *Nature* 382 (6590):420-25.

Hegemann, B., Hutchins, J. R. A., Hudecz, O., Novatchkova, M., Rameseder, J., Sykora, M. M., Liu, S., Mazanek, M., Lénárt, P., Hériché, J.-K., Poser, I., Kraut, N., Hyman, A. A., Yaffe, M. B., Mechtler, K., and Peters, J.-M. 2011. Systematic Phosphorylation Analysis of Human Mitotic Protein Complexes. *Science Signaling* 4 (198):rs12-rs12.

Hein, J. B. and Nilsson, J. 2014. Stable MCC binding to the APC/C is required for a functional spindle assembly checkpoint. *EMBO reports* 15 (3):264-72.

Hendzel, M. J., Wei, Y., Mancini, M. A., Van Hooser, A., Ranalli, T., Brinkley, B. R., Bazett-Jones, D. P., and Allis, C. D. 1997. Mitosis-specific phosphorylation of histone H3 initiates primarily within pericentromeric heterochromatin during G2 and spreads in an ordered fashion coincident with mitotic chromosome condensation. *Chromosoma* 106:348-60.

Hengeveld, R. C. C., Hertz, N. T., Vromans, M. J. M., Zhang, C., Burlingame, A. L., Shokat, K. M., and Lens, S. M. A. 2012. Development of a chemical genetic approach for human aurora B kinase identifies novel substrates of the chromosomal passenger complex. *Molecular & Cellular Proteomics* 11:47-59.

Hinchcliffe, E. H., Miller, F. J., Cham, M., Khodjakov, A., and Sluder, G. 2001. Requirement of a Centrosomal Activity for Cell Cycle Progression Through G_1 into S Phase. *Science* 291 (5508):1547-50.

Hirota, T., Kunitoku, N., Sasayama, T., Marumoto, T., Zhang, D., Nitta, M., Hatakeyama, K., and Saya, H. 2003. Aurora-A and an interacting activator, the LIM protein Ajuba, are required for mitotic commitment in human cells. *Cell* 114:585-98.

Hirota, T., Lipp, J. J., Toh, B.-H., and Peters, J.-M. 2005. Histone H3 serine 10 phosphorylation by Aurora B causes HP1 dissociation from heterochromatin. *Nature* 438:1176-80.

Hoar, K., Chakravarty, A., Rabino, C., Wysong, D., Bowman, D., Roy, N., and Ecsedy, J. A. 2007. MLN8054, a Small-Molecule Inhibitor of Aurora A, Causes Spindle Pole and Chromosome Congression Defects Leading to Aneuploidy. *Molecular and Cellular Biology* 27:4513-25.

Honda, R., Körner, R., and Nigg, E. A. 2003. Exploring the Functional Interactions between Aurora B, INCENP, and Survivin in Mitosis. *Molecular Biology of the Cell* 14 (8):3325-41.

Honnappa, S., Gouveia, S. M., Weisbrich, A., Damberger, F. F., Bhavesh, N. S., Jawhari, H., Grigoriev, I., van Rijssel, F. J. A., Buey, R. M., Lawera, A., Jelesarov, I., Winkler, F. K., Wüthrich, K., Akhmanova, A., and Steinmetz, M. O. 2009. An EB1-Binding Motif Acts as a Microtubule Tip Localization Signal. *Cell* 138:366-76.

Hori, T., Amano, M., Suzuki, A., Backer, C. B., Welburn, J. P., Dong, Y., McEwen, B. F., Shang, W. H., Suzuki, E., Okawa, K., Cheeseman, I. M., and Fukagawa, T. 2008. CCAN Makes Multiple Contacts with Centromeric DNA to Provide Distinct Pathways to the Outer Kinetochore. *Cell* 135:1039-52.

Hornbeck, P. V., Zhang, B., Murray, B., Kornhauser, J. M., Latham, V., and Skrzypek, E. 2015. PhosphoSitePlus, 2014: Mutations, PTMs and recalibrations. *Nucleic Acids Research* 43:D512-D520.

Hornung, P., Maier, M., Alushin, G. M., Lander, G. C., Nogales, E., and Westermann, S. 2011. Molecular architecture and connectivity of the budding yeast Mtw1 kinetochore complex. *Journal of Molecular Biology* 405:548-59.

Hsu, J.-Y., Sun, Z.-W., Li, X., Reuben, M., Tatchell, K., Bishop, D. K., Grushcow, J. M., Brame, C. J., Caldwell, J. A., Hunt, D. F., Lin, R., Smith, M. M., and Allis, C. D. 2000. Mitotic Phosphorylation of Histone H3 Is Governed by Ipl1/aurora Kinase and Glc7/PP1 Phosphatase in Budding Yeast and Nematodes. *Cell* 102:279-91.

Hümmer, S. and Mayer, T. U. 2009. Cdk1 Negatively Regulates Midzone Localization of the Mitotic Kinesin Mklp2 and the Chromosomal Passenger Complex. *Current Biology* 19:607-12.

Hutchins, J. R. A., Toyoda, Y., Hegemann, B., Poser, I., Hériché, J.-K., Sykora, M. M., Augsburg, M., Hudecz, O., Buschhorn, B. A., Bulkescher, J., Conrad, C., Comartin, D., Schleiffer, A., Sarov, M., Pozniakovsky, A., Slabicki, M. M., Schloissnig, S., Steinmacher, I., Leuschner, M., Ssykor, A., Lawo, S., Pelletier, L., Stark, H., Nasmyth, K., Ellenberg, J., Durbin, R., Buchholz, F., Mechtler, K., Hyman, A. A., and Peters, J.-M. 2010. Systematic Analysis of Human Protein Complexes Identifies Chromosome Segregation Proteins. *Science* 328 (5978):593-9.

Hutterer, A., Berdnik, D., Wirtz-Peitz, F., Žigman, M., Schleiffer, A., and Knoblich, J. A. 2006. Mitotic Activation of the Kinase Aurora-A Requires Its Binding Partner Bora. *Developmental Cell* 11 (2):147-57.

Iakoucheva, L. M., Radivojac, P., Brown, C. J., O'Connor, T. R., Sikes, J. G., Obradovic, Z., and Dunker, A. K. 2004. The importance of intrinsic disorder for protein phosphorylation. *Nucleic Acids Research* 32:1037-49.

Iimori, M., Watanabe, S., Kiyonari, S., Matsuoka, K., Sakasai, R., Saeki, H., Oki, E., Kitao, H., and Maehara, Y. 2016. Phosphorylation of EB2 by Aurora B and CDK1 ensures mitotic progression and genome stability. *Nature Communications* 7:11117.

Inoue, Y. H., Savoian, M. S., Suzuki, T., Máthé, E., Yamamoto, M. T., and Glover, D. M. 2004. Mutations in orbit/mast reveal that the central spindle is comprised of two microtubule populations, those that initiate cleavage and those that propagate furrow ingression. *Journal of Cell Biology* 166:49-60.

Izawa, D. and Pines, J. 2014. The mitotic checkpoint complex binds a second CDC20 to inhibit active APC/C. *Nature* 517(7536):631-4.

Janczyk, P., Skorupka, K. A., Tooley, J. G., Matson, D. R., Kestner, C. A., West, T., Pornillos, O., and Stukenberg, P. T. 2017. Mechanism of Ska Recruitment by Ndc80 Complexes to Kinetochores. *Developmental Cell* 41:438-449.e4.

Jang, C.-Y., Coppinger, J. a., Seki, A., Yates, J. R., and Fang, G. 2009. Plk1 and Aurora A regulate the depolymerase activity and the cellular localization of Kif2a. *Journal of Cell Science* 122:1334-41.

Jang, M. S., Sul, J. W., Choi, B. J., Lee, S. J., Suh, J. H., Kim, N. S., Woo, H. K., Lim, D. S., Lee, C. W., and Kim, E. 2008. Negative feedback regulation of Aurora-A via phosphorylation of Fas-associated factor-1. *Journal of Biological Chemistry* 283:32344-51.

Joukov, V., De Nicolo, A., Rodriguez, A., Walter, J. C., and Livingston, D. M. 2010. Centrosomal protein of 192 kDa (Cep192) promotes centrosome-driven spindle assembly by engaging in organelle-specific Aurora A activation. *Proc Natl Acad Sci U S A* 107:21022-7.

Kalab, P. 2002. Visualization of a Ran-GTP Gradient in Interphase and Mitotic Xenopus Egg Extracts. *Science* 295:2452-6.

Kalab, P., Pu, R. T., and Dasso, M. 1999. The Ran GTPase regulates mitotic spindle assembly. *Current Biology* 9:481-4.

Kalantzaki, M., Kitamura, E., Zhang, T., Mino, A., Novák, B., and Tanaka, T. U. 2015. Kinetochore–microtubule error correction is driven by differentially regulated interaction modes. *Nature Cell Biology* 17(4):421-33.

Kallio, M. J., McCleland, M. L., Todd Stukenberg, P., and Gorbsky, G. J. 2002. Inhibition of Aurora B kinase blocks chromosome segregation, overrides the spindle checkpoint, and perturbs microtubule dynamics in mitosis. *Current Biology* 12:900-5.

Kamasaki, T., O'Toole, E., Kita, S., Osumi, M., Usukura, J., McIntosh, R. R., and Goshima, G. 2013. Augmin-dependent microtubule nucleation at microtubule walls in the spindle. *Journal of Cell Biology* 202:25-32.

Kapoor, T. M., Lampson, M. A., Hergert, P., Cameron, L., Cimini, D., Salmon, E. D., McEwen, B. F., and Khodjakov, A. 2006. Chromosomes Can Congress to the Metaphase Plate Before Biorientation. *Science* 311 (5759):388-91.

Karess, R. 2005. Rod–Zw10–Zwilch: a key player in the spindle checkpoint. *Trends in Cell Biology* 15 (7):386-92.

Karsenti, E., Newport, J., and Kirschner, M. 1984. Respective roles of centrosomes and chromatin in the conversion of microtubule arrays from interphase to metaphase. *Journal of Cell Biology* 99(Pt 2):47s-54s.

Kasuboski, J. M., Bader, J. R., Vaughan, P. S., Tauhata, S. B. F., Winding, M., Morrissey, M. A., Joyce, M. V., Boggess, W., Vos, L., Chan, G. K., Hinchcliffe, E. H., and Vaughan, K. T. 2011. Zwint-1 is a novel Aurora B substrate required for the assembly of a dynein-binding platform on kinetochores. *Molecular Biology of the Cell* 22:3318-30.

Katayama, H., Sasai, K., Kloc, M., Brinkley, B. R., and Sen, S. 2008. Aurora kinase-A regulates kinetochore/chromatin associated microtubule assembly in human cells. *Cell Cycle* 7:2691-704.

Katayama, H., Zhou, H., Li, Q., Tatsuka, M., and Sen, S. 2001. Interaction and Feedback Regulation between STK15/BTAK/Aurora-A Kinase and Protein Phosphatase 1 through Mitotic Cell Division Cycle. *Journal of Biological Chemistry* 276 (49):46219-24.

Kawajiri, A., Yasui, Y., Goto, H., Tatsuka, M., Takahashi, M., Nagata, K.-i., and Inagaki, M. 2003. Functional Significance of the Specific Sites Phosphorylated in Desmin at Cleavage Furrow: Aurora-B May Phosphorylate and Regulate Type III Intermediate Filaments during Cytokinesis Coordinatedly with Rho-kinase. *Molecular Biology of the Cell* 14 (4):1489-500.

Ke, K., Cheng, J., and Hunt, A. J. 2009. The Distribution of Polar Ejection Forces Determines the Amplitude of Chromosome Directional Instability. *Current Biology* 19:807-815.

Kelly, A. E., Sampath, S. C., Maniar, T. A., Woo, E. M., Chait, B. T., and Funabiki, H. 2007. Chromosomal Enrichment and Activation of the Aurora B Pathway Are Coupled to Spatially Regulate Spindle Assembly. *Developmental Cell* 12:31-43.

Kettenbach, A. N., Schweppe, D. K., Faherty, B. K., Pechenick, D., Pletnev, A. A., and Gerber, S. A. 2011. Quantitative Phosphoproteomics Identifies Substrates and Functional Modules of Aurora and Polo-Like Kinase Activities in Mitotic Cells. *Science Signaling* 4:rs5-rs5.

Khodjakov, A., Copenagle, L., Gordon, M. B., Compton, D. A., and Kapoor, T. M. 2003. Minus-end capture of preformed kinetochore fibers contributes to spindle morphogenesis. *Journal of Cell Biology* 160 (5):671-83.

Khodjakov, A. and Rieder, C. L. 1999. The Sudden Recruitment of gamma-Tubulin to the Centrosome at the Onset of Mitosis and its Dynamic Exchange Throughout the Cell Cycle, Do Not Require Microtubules. *The Journal of Cell Biology* 146 (3):585-96.

Khodjakov, A., Rieder, C. L., Sluder, G., Cassels, G., Sibon, O., and Wang, C.-L. 2002. De novo formation of centrosomes in vertebrate cells arrested during S phase. *The Journal of Cell Biology* 158 (7):1171-81.

Kim, J. O., Zelter, A., Umbreit, N. T., Bollozos, A., Riffle, M., Johnson, R., MacCoss, M. J., Asbury, C. L., and Davis, T. N. 2017. The Ndc80 complex bridges two dam1 complex rings. *Elife* 6:1-22.

Kim, S. and Yu, H. 2015. Multiple assembly mechanisms anchor the KMN spindle checkpoint platform at human mitotic kinetochores. *Journal of Cell Biology* 208:181-196.

Kim, Y., Holland, A. J., Lan, W., and Cleveland, D. W. 2010. Aurora kinases and protein phosphatase 1 mediate chromosome congression through regulation of CENP-E. *Cell* 142:444-55.

Kimura, M., Kotani, S., Hattori, T., Sumi, N., Yoshioka, T., Todokoro, K., and Okano, Y. 1997. Cell cycle-dependent expression and spindle pole localization of a novel human protein kinase, aik, related to aurora of Drosophila and yeast Ipl1. *Journal of Biological Chemistry* 272:13766-71.

Kimura, M., Matsuda, Y., Yoshioka, T., and Okano, Y. 1999. Cell Cycle-dependent Expression and Centrosome Localization of a Third Human Aurora/Ipl1-related Protein Kinase, AIK3. *Journal of Biological Chemistry* 274:7334-40.

Kimura, Y., Kurabe, N., Ikegami, K., Tsutsumi, K., Konishi, Y., Kaplan, O. I., Kunitomo, H., Iino, Y., Blacque, O. E., and Setou, M. 2010. Identification of tubulin deglutamylase among Caenorhabditis elegans and mammalian cytosolic carboxypeptidases (CCPs). *Journal of Biological Chemistry* 285:22936-41.

Kinoshita, K., Noetzel, T. L., Pelletier, L., Mechtler, K., Drechsel, D. N., Schwager, A., Lee, M., Raff, J. W., and Hyman, A. A. 2005. Aurora A phosphorylation of TACC3/maskin is required for centrosome-dependent microtubule assembly in mitosis. *Journal of Cell Biology* 170:1047-55.

Kitajima, T. S., Ohsugi, M., and Ellenberg, J. 2011. Complete kinetochore tracking reveals error-prone homologous chromosome biorientation in mammalian oocytes. *Cell* 146:568-81.

Klein, U. R., Nigg, E. A., and Gruneberg, U. 2006. Centromere Targeting of the Chromosomal Passenger Complex Requires a Ternary Subcomplex of Borealin, Survivin, and the N-Terminal Domain of INCENP. *Molecular Biology of the Cell* 17 (6):2547-58.

Kline, S. L., Cheeseman, I. M., Hori, T., Fukagawa, T., and Desai, A. 2006. The human Mis12 complex is required for kinetochore assembly and proper chromosome segregation. *Journal of Cell Biology* 173:9-17.

Knowlton, A. L., Vorozhko, V. V., Lan, W., Gorbsky, G. J., and Stukenberg, P. T. 2009. ICIS and Aurora B Coregulate the Microtubule Depolymerase Kif2a. *Current Biology* 19 (9):758-63.

Kobayashi, T. 1975. Dephosphorylation of Tubulin-bound Guanosine Triphosphate during Microtubule Assembly. *The Journal of Biochemistry* 77 (6):1193-7.

Koch, A., Krug, K., Pengelley, S., Macek, B., and Hauf, S. 2011. Mitotic Substrates of the Kinase Aurora with Roles in Chromatin Regulation Identified Through Quantitative Phosphoproteomics of Fission Yeast. *Science Signaling* 4:rs6-rs6.

Kollman, J. M., Merdes, A., Mourey, L., and Agard, D. A. 2011. Microtubule nucleation by γtubulin complexes. *Nature Reviews: Molecular Cell Biology* 12 (11):709-21.

Komarova, Y. A., Akhmanova, A. S., Kojima, S. I., Galjart, N., and Borisy, G. G. 2002. Cytoplasmic linker proteins promote microtubule rescue in vivo. *Journal of Cell Biology* 159:589-99.

Kufer, T. A., Silljé, H. H. W., Körner, R., Gruss, O. J., Meraldi, P., and Nigg, E. A. 2002. Human TPX2 is required for targeting Aurora-A kinase to the spindle. *The Journal of Cell Biology* 158 (4):617-23.

Kumar, P., Chimenti, M. S., Pemble, H., Schönichen, A., Thompson, O., Jacobson, M. P., and Wittmann, T. 2012. Multisite phosphorylation disrupts arginine-glutamate salt bridge networks required for binding of cytoplasmic linker-associated protein 2 (CLASP2) to end-binding protein 1 (EB1). *Journal of Biological Chemistry* 287:17050-64.

Kumar, P., Lyle, K. S., Gierke, S., Matov, A., Danuser, G., and Wittmann, T. 2009. GSK33 phosphorylation modulates CLASP-microtubule association and lamella microtubule attachment. *Journal of Cell Biology* 184:895-908.

Kunitoku, N., Sasayama, T., Marumoto, T., Zhang, D., Honda, S., Kobayashi, O., Hatakeyama, K., Ushio, Y., Saya, H., and Hirota, T. 2003. CENP-A phosphorylation by Aurora-A in prophase is required for enrichment of Aurora-B at inner centromeres and for kinetochore function. *Developmental Cell* 5:853-64.

Lacroix, B., Van Dijk, J., Gold, N. D., Guizetti, J., Aldrian-Herrada, G., Rogowski, K., Gerlich, D. W., and Janke, C. 2010. Tubulin polyglutamylation stimulates spastin-mediated microtubule severing. *Journal of Cell Biology* 189:945-54.

Lai, A. C. W., Ba, A. N. N., and Moses, A. M. 2012. Predicting kinase substrates using conservation of local motif density. *Bioinformatics* 28:962-9.

Lampson, M. A., Renduchitala, K., Khodjakov, A., and Kapoor, T. M. 2004. Correcting improper chromosome–spindle attachments during cell division. *Nature Cell Biology* 6(3):232-7.

Lan, W., Zhang, X., Kline-Smith, S. L., Rosasco, S. E., Barrett-Wilt, G. A., Shabanowitz, J., Hunt, D. F., Walczak, C. E., and Stukenberg, P. T. 2004. Aurora B phosphorylates centromeric MCAK and regulates its localization and microtubule depolymerization activity. *Current Biology* 14:273-86.

Landry, C. R., Levy, E. D., and Michnick, S. W. 2009. Weak functional constraints on phosphoproteomes. *Trends in Genetics* 25:193-7.

Larcher, J.-C., Boucher, D., Lazereg, S., Gros, F., and Denoulet, P. 1996. Interaction of Kinesin Motor Domains with α- and β-Tubulin Subunits at a Tau-independent Binding Site: REGULATION BY POLYGLUTAMYLATION. *Journal of Biological Chemistry* 271 (36):22117-24.

Lengauer, C., Kinzler, K. W., and Vogelstein, B. 1997. Genetic instability in colorectal cancers. *Nature* 386 (6625):623-7.

LeRoy, P. J., Hunter, J. J., Hoar, K. M., Burke, K. E., Shinde, V., Ruan, J., Bowman, D., Galvin, K., and Ecsedy, J. A. 2007. Localization of human TACC3 to mitotic spindles is

mediated by phosphorylation on Ser558 by Aurora A: A novel pharmacodynamic method for measuring Aurora A activity. *Cancer Research* 67:5362-70.

Letunic, I. and Bork, P. 2016. Interactive tree of life (iTOL) v3: an online tool for the display and annotation of phylogenetic and other trees. *Nucleic Acids Research* 44:W242-W245.

Levy, E. D., Michnick, S. W., and Landry, C. R. 2012. Protein abundance is key to distinguish promiscuous from functional phosphorylation based on evolutionary information. *Philosophical Transactions of the Royal Society B: Biological Sciences* 367:2594-606.

Li, S., Deng, Z., Fu, J., Xu, C., Xin, G., Wu, Z., Luo, J., Wang, G., Zhang, S., Zhang, B., Zou, F., Jiang, Q., and Zhang, C. 2015. Spatial compartmentalization specializes the function of Aurora A and Aurora B. *Journal of Biological Chemistry* 290:17546-58.

Li, Y., Yu, W., Liang, Y., and Zhu, X. 2007. Kinetochore dynein generates a poleward pulling force to facilitate congression and full chromosome alignment. *Cell Research* 17:701-12.

Lim, K.-H., Brady, D. C., Kashatus, D. F., Ancrile, B. B., Der, C. J., Cox, A. D., and Counter, C. M. 2010. Aurora-A Phosphorylates, Activates, and Relocalizes the Small GTPase RalA. *Molecular and Cellular Biology* 30:508-23.

Lim, N. R., Yeap, Y. Y. C., Ang, C. S., Williamson, N. A., Bogoyevitch, M. A., Quinn, L. M., and Ng, D. C. H. 2016. Aurora A phosphorylation of WD40-repeat protein 62 in mitotic spindle regulation. *Cell Cycle* 15:413-24.

Lin, Y. N., Wu, C. T., Lin, Y. C., Hsu, W. B., Tang, C. J. C., Chang, C. W., and Tang, T. K. 2013. CEP120 interacts with CPAP and positively regulates centriole elongation. *Journal of Cell Biology* 202:211-9.

Lioutas, A. and Vernos, I. 2013. Aurora A kinase and its substrate TACC3 are required for central spindle assembly. *EMBO reports* 14:829-36.

Liu, D., Vader, G., Vromans, M. J. M., Lampson, M. A., and Lens, S. M. A. 2009. Sensing Chromosome Bi-Orientation by Spatial Separation of Aurora B Kinase from Kinetochore Substrates. *Science* 323 (5919):1350-3.

Liu, D., Vleugel, M., Backer, C. B., Hori, T., Fukagawa, T., Cheeseman, I. M., and Lampson, M. A. 2010. Regulated targeting of protein phosphatase 1 to the outer kinetochore by KNL1 opposes Aurora B kinase. *Journal of Cell Biology* 188:809-20.

Liu, Q., Kaneko, S., Yang, L., Feldman, R. I., Nicosia, S. V., Chen, J., and Cheng, J. Q. 2004. Aurora-A abrogation of p53 DNA binding and transactivation activity by phosphorylation of serine 215. *Journal of Biological Chemistry* 279:52175-82.

Loïodice, I., Alves, A., Rabut, G., van Overbeek, M., Ellenberg, J., Sibarita, J.-B., and Doye, V. 2004. The Entire Nup107-160 Complex, Including Three New Members, Is Targeted as One Entity to Kinetochores in Mitosis. *Molecular Biology of the Cell* 15 (7):3333-44.

London, N., Ceto, S., Ranish, J. A., and Biggins, S. 2012. Phosphoregulation of Spc105 by Mps1 and PP1 regulates Bub1 localization to kinetochores. *Current Biology* 22 (10):900-6.

Ludueña, R. F., Shooter, E. M., and Wilson, L. 1977. Structure of the tubulin dimer. *Journal of Biological Chemistry* 252 (20):7006-14.

Lukasiewicz, K. B., Greenwood, T. M., Negron, V. C., Bruzek, A. K., Salisbury, J. L., and Lingle, W. L. 2011. Control of centrin stability by Aurora A. *PLoS One* 6(6):e21291.

Macůrek, L., Lindqvist, A., Lim, D., Lampson, M. A., Klompmaker, R., Freire, R., Clouin, C., Taylor, S. S., Yaffe, M. B., and Medema, R. H. 2008. Polo-like kinase-1 is activated by aurora A to promote checkpoint recovery. *Nature* 455 (7209):119-23.

Maffini, S., Maia, A. R. R., Manning, A. L., Maliga, Z., Pereira, A. L., Junqueira, M., Shevchenko, A., Hyman, A., Yates, J. R., Galjart, N., Compton, D. A., and Maiato, H. 2009. Motor-Independent Targeting of CLASPs to Kinetochores by CENP-E Promotes Microtubule Turnover and Poleward Flux. *Current Biology* 19:1566-72.

Maia, A. R. R., Garcia, Z., Kabeche, L., Barisic, M., Maffini, S., Macedo-Ribeiro, S., Cheeseman, I. M., Compton, D. A., Kaverina, I., and Maiato, H. 2012. Cdk1 and Plk1 mediate a CLASP2 phospho-switch that stabilizes kinetochore-microtubule attachments. *Journal of Cell Biology* 199:285-301.

Maiato, H., Fairley, E. A. L., Rieder, C. L., Swedlow, J. R., Sunkel, C. E., and Earnshaw, W. C. 2003. Human CLASP1 is an outer kinetochore component that regulates spindle microtubule dynamics. *Cell* 113:891-904.

Maiato, H., Hergert, P. J., Moutinho-Pereira, S., Dong, Y., Vandenbeldt, K. J., Rieder, C. L., and McEwen, B. F. 2006. The ultrastructure of the kinetochore and kinetochore fiber in Drosophila somatic cells. *Chromosoma* 115:469-80.

Maiato, H., Khodjakov, A., and Rieder, C. L. 2005. Drosophila CLASP is required for the incorporation of microtubule subunits into fluxing kinetochore fibres. *Nature Cell Biology* 7:42-7.

Maiato, H., Rieder, C. L., and Khodjakov, A. 2004. Kinetochore-driven formation of kinetochore fibers contributes to spindle assembly during animal mitosis. *Journal of Cell Biology* 167:831-40.

Maiato, H., Sampaio, P., Lemos, C. L., Findlay, J., Carmena, M., Earnshaw, W. C., and Sunkel, C. E. 2002. MAST/Orbit has a role in microtubule-kinetochore attachment and is essential for chromosome alignment and maintenance of spindle bipolarity. *Journal of Cell Biology* 157:749-60.

Maki, T., Grimaldi, A. D., Fuchigami, S., Kaverina, I., and Hayashi, I. 2015. CLASP2 has two distinct TOG domains that contribute differently to microtubule dynamics. *Journal of Molecular Biology* 427:2379-95.

Maldonado, M. and Kapoor, T. M. 2011. Constitutive Mad1 targeting to kinetochores uncouples checkpoint signalling from chromosome biorientation. *Nature Cell Biology* 13 (4):475-82.

Malik, R., Lenobel, R., Santamaria, A., Ries, A., Nigg, E. A., and Körner, R. 2009. Quantitative Analysis of the Human Spindle Phosphoproteome at Distinct Mitotic Stages. *Journal of Proteome Research* 8 (10):4553-63.

Malik, R., Nigg, E. A., and Körner, R. 2008. Comparative conservation analysis of the human mitotic phosphoproteome. *Bioinformatics* 24:1426-32.

Manfredi, M. G., Ecsedy, J. A., Chakravarty, A., Silverman, L., Zhang, M., Hoar, K. M., Stroud, S. G., Chen, W., Shinde, V., Huck, J. J., Wysong, D. R., Janowick, D. A., Hyer, M. L., LeRoy, P. J., Gershman, R. E., Silva, M. D., Germanos, M. S., Bolen, J. B., Claiborne, C. F., and Sells, T. B. 2011. Characterization of alisertib (MLN8237), an investigational small-molecule inhibitor of Aurora A kinase using novel in vivo pharmacodynamic assays. *Clinical Cancer Research* 17:7614-24.

Manfredi, M. G., Ecsedy, J. A., Meetze, K. A., Balani, S. K., Burenkova, O., Chen, W., Galvin, K. M., Hoar, K. M., Huck, J. J., LeRoy, P. J., Ray, E. T., Sells, T. B., Stringer, B., Stroud, S. G., Vos, T. J., Weatherhead, G. S., Wysong, D. R., Zhang, M., Bolen, J. B., and

Claiborne, C. F. 2007. Antitumor activity of MLN8054, an orally active small-molecule inhibitor of Aurora A kinase. *Proc Natl Acad Sci U S A* 104:4106-11.

Mann, M., Ong, S.-e., Gr, M., Steen, H., Jensen, O. N., and Pandey, A. 2002. Analysis of protein phosphorylation using mass spectrometry: deciphering the phosphoproteome. *Trends in Biotechnology* 20:261-8.

Manning, G., Whyte, D. B., Martinez, R., Hunter, T., and Sudarsanam, S. 2002. The Protein Kinase Complement of the Human Genome. *Science* 298 (5600):1912-34.

Mardin, B. R., Agircan, F. G., Lange, C., and Schiebel, E. 2011. Plk1 controls the Nek2A-PP1γ Antagonism in centrosome disjunction. *Current Biology* 21:1145-51.

Maresca, T. J. and Salmon, E. D. 2009. Intrakinetochore stretch is associated with changes in kinetochore phosphorylation and spindle assembly checkpoint activity. *Journal of Cell Biology* 184:373-81.

Marumoto, T., Honda, S., Hara, T., Nitta, M., Hirota, T., Kohmura, E., and Saya, H. 2003. Aurora-A Kinase Maintains the Fidelity of Early and Late Mitotic Events in HeLa Cells. *Journal of Biological Chemistry* 278:51786-95.

Maskell, D. P., Hu, X. W., and Singleton, M. R. 2010. Molecular architecture and assembly of the yeast kinetochore MIND complex. *Journal of Cell Biology* 190:823-34.

Máthé, E., Inoue, Y. H., Palframan, W., Brown, G., and Glover, D. M. 2003. Orbit/Mast, the CLASP orthologue of *Drosophila*, is required for asymmetric stem cell and cystocyte divisions and development of the polarised microtubule network that interconnects oocyte and nurse cells during oogenesis. *Development* 130 (5):901-15.

Mathivanan, S.Ahmed, M.Ahn, N. G.Alexandre, H.Amanchy, R.Andrews, P. C.Bader, J. S.Balgley, B. M.Bantscheff, M.Bennett, K. L.Björling, E.Blagoev, B.Bose, R.Brahmachari, S. K.Burlingame, A. S.Bustelo, X. R.Cagney, G.Cantin, G. T.Cardasis, H. L.Celis, J. E.Chaerkady, R.Chu, F.Cole, P. A.Costello, C. E.Cotter, R. J.Crockett, D.DeLany, J. P.De Marzo, A. M.DeSouza, L. V.Deutsch, E. W.Dransfield, E.Drewes, G.Droit, A.Dunn, M. J.Elenitoba-Johnson, K.Ewing, R. M.Eyk, J. V.Faca, V.Falkner, J.Fang, X.Fenselau, C.Figeys, D.Gagné, P.Gelfi, C.Gevaert, K.Gimble, J. M.Gnad, F.Goel, R.Gromov, P.Hanash, S. M.Hancock, W. S.Harsha, H. C.Hart, G.Hays, F.He, F.Hebbar, P.Helsens, K.Hermeking, H.Hide, W.Hjernø, K.Hochstrasser, D. F.Hofmann, O.Horn, D. M.Hruban, R. H.Ibarrola, N.James, P.Jensen, O. N.Jensen, P. H.Jung, P.Kandasamy, K.Kheterpal, I.Kikuno, R. F.Korf, U.Körner, R.Kuster, B.Kwon, M.-S.Lee, H.-J.Lee, Y.-J.Lefevre, M.Lehvaslaiho, M.Lescuyer, P.Levander, F.Lim, M. S.Löbke, C.Loo, J. A.Mann, M.Martens, L.Martinez-Heredia, J.McComb, M.McRedmond, J.Mehrle, A.Menon, R.Miller, C. A.Mischak, H.Mohan, S. S.Mohmood, R.Molina, H.Moran, M. F.Morgan, J. D.Moritz, R.Morzel, M.Muddiman, D. C.Nalli, A.Navarro, J. D.Neubert, T. A.Ohara, O.Oliva, R.Omenn, G. S.Oyama, M.Paik, Y.-K.Pennington, K.Pepperkok, R.Periaswamy, B.Petricoin, E. F.Poirier, G. G.Prasad, T. S. K.Purvine, S. O.Rahiman, B. A.Ramachandran, P.Ramachandra, Y. L.Rice, R. H.Rick, J.Ronnholm, R. H.Salonen, J.Sanchez, J.-C.Sayd, T.Seshi, B.Shankari, K.Sheng, S. J.Shetty, V.Shivakumar, K.Simpson, R. J.Sirdeshmukh, R.Michael Siu, K. W.Smith, J. C.Smith, R. D.States, D. J.Sugano, S.Sullivan, M.Superti-Furga, G.Takatalo, M.Thongboonkerd, V.Trinidad, J. C.Uhlen, M.Vandekerckhove, J.Vasilescu, J.Veenstra, T. D.Vidal-Taboada, J.-M.Vihinen, M.Wait, R.Wang, X.Wiemann, S.Wu, B.Xu, T.Yates, J. R.Zhong, J.Zhou, M.Zhu, Y.Zurbig, P. and Pandey, A. 2008. Human Proteinpedia enables sharing of human protein data. *Nature Biotechnology* 26:164-7.

Matson, D. R., Demirel, P. B., Stukenberg, P. T., and Burke, D. J. 2012. A conserved role for COMA / CENP-H / I / N kinetochore proteins in the spindle checkpoint. *Genes & Development* 26 (6):542-7.

Maure, J. F., Komoto, S., Oku, Y., Mino, A., Pasqualato, S., Natsume, K., Clayton, L., Musacchio, A., and Tanaka, T. U. 2011. The Ndc80 loop region facilitates formation of kinetochore attachment to the dynamic microtubule plus end. *Current Biology* 21:207-13.

Mazumdar, M. and Misteli, T. 2005. Chromokinesins: Multitalented players in mitosis. *Trends in Cell Biology* 15:349-55.

McAinsh, A. D. and Meraldi, P. 2011. The CCAN complex: Linking centromere specification to control of kinetochore-microtubule dynamics. *Seminars in Cell and Developmental Biology* 22:946-52.

McKinley, K. L., Sekulic, N., Guo, L. Y., Tsinman, T., Black, B. E., and Cheeseman, I. M. 2015. The CENP-L-N Complex Forms a Critical Node in an Integrated Meshwork of Interactions at the Centromere-Kinetochore Interface. *Molecular Cell* 60:886-98.

McKlveen Buschhorn, H., Klein, R. R., Chambers, S. M., Hardy, M. C., Green, S., Bearss, D., and Nagle, R. B. 2005. Aurora-A over-expression in high-grade PIN lesions and prostate cancer. *The Prostate* 64 (4):341-6.

Mendez, R., Murthy, K. G. K., Ryan, K., Manley, J. L., and Richter, J. D. 2000. Phosphorylation of CPEB by Eg2 Mediates the Recruitment of CPSF into an Active Cytoplasmic Polyadenylation Complex. *Molecular Cell* 6:1253-9.

Merbl, Y. and Kirschner, M. W. 2009. Large-scale detection of ubiquitination substrates using cell extracts and protein microarrays. *Proc Natl Acad Sci U S A* 106:2543-8.

Milacic, M., Haw, R., Rothfels, K., Wu, G., Croft, D., Hermjakob, H., D'Eustachio, P., and Stein, L. 2012. Annotating cancer variants and anti-cancer therapeutics in Reactome. *Cancers* 4:1180-211.

Miller, S. A., Johnson, M. L., and Stukenberg, P. T. 2008. Kinetochore Attachments Require an Interaction between Unstructured Tails on Microtubules and Ndc80Hec1. *Current Biology* 18:1785-91.

Mimori-Kiyosue, Y., Grigoriev, I., Lansbergen, G., Sasaki, H., Matsui, C., Severin, F., Galjart, N., Grosveld, F., Vorobjev, I., Tsukita, S., and Akhmanova, A. 2005. CLASP1 and CLASP2 bind to EB1 and regulate microtubule plus-end dynamics at the cell cortex. *Journal of Cell Biology* 168:141-53.

Mimori-Kiyosue, Y., Grigoriev, I., Sasaki, H., Matsui, C., Akhmanova, A., Tsukita, S., and Vorobjev, I. 2006. Mammalian CLASPs are required for mitotic spindle organization and kinetochore alignment. *Genes to Cells* 11:845-57.

Minoshima, Y., Kawashima, T., Hirose, K., Tonozuka, Y., Kawajiri, A., Bao, Y. C., Deng, X., Tatsuka, M., Narumiya, S., May, W. S., Nosaka, T., Semba, K., Inoue, T., Satoh, T., Inagaki, M., and Kitamura, T. 2003. Phosphorylation by Aurora B converts MgcRacGAP to a RhoGAP during cytokinesis. *Developmental Cell* 4:549-60.

Mishra, R. K., Chakraborty, P., Arnaoutov, A., Fontoura, B. M. A., and Dasso, M. 2010. The Nup107-160 complex and γ-TuRC regulate microtubule polymerization at kinetochores. *Nature Cell Biology* 12:164-9.

Mitchison, T. 1993. Localization of an exchangeable GTP binding site at the plus end of microtubules. *Science* 261 (5124):1044-7.

Mitchison, T. and Kirschner, M. 1984. Dynamic instability of microtubule growth. *Nature* 312:237-42.

Mitchison, T. J. and Salmon, E. D. 2001. Mitosis: a history of division. *Nature Cell Biology* 3:E17-21.

Mollinari, C., Kleman, J. P., Jiang, W., Schoehn, G., Hunter, T., and Margolis, R. L. 2002. PRC1 is a microtubule binding and bundling protein essential to maintain the mitotic spindle midzone. *Journal of Cell Biology* 157:1175-86.

Mori, D., Yano, Y., Toyo-oka, K., Yoshida, N., Yamada, M., Muramatsu, M., Zhang, D., Saya, H., Toyoshima, Y. Y., Kinoshita, K., Wynshaw-Boris, A., and Hirotsune, S. 2007. NDEL1 Phosphorylation by Aurora-A Kinase Is Essential for Centrosomal Maturation, Separation, and TACC3 Recruitment. *Molecular and Cellular Biology* 27:352-67.

Morrison, C., Henzing, A. J., Jensen, O. N., Osheroff, N., Dodson, H., Kandels-Lewis, S. E., Adams, R. R., and Earnshaw, W. C. 2002. Proteomic analysis of human metaphase chromosomes reveals topoisomerase II alpha as an Aurora B substrate. *Nucleic Acids Research* 30:5318-27.

Murata-Hori, M., Fumoto, K., Fukuta, Y., Iwasaki, T., Kikuchi, A., Tatsuka, M., and Hosoya, H. 2000. Myosin II Regulatory Light Chain as a Novel Substrate for AIM-1, an Aurora/Ipllp-related Kinase from Rat. *The Journal of Biochemistry* 128 (6):903-7.

Murnion, M. E., Adams, R. R., Callister, D. M., Allis, C. D., Earnshaw, W. C., and Swedlow, J. R. 2001. Chromatin-associated Protein Phosphatase I Regulates Aurora-B and Histone H3 Phosphorylation. *Journal of Biological Chemistry* 276:26656-65.

Musacchio, A. and Salmon, E. D. 2007. The spindle-assembly checkpoint in space and time. *Nature Reviews: Molecular Cell Biology* 8 (5):379-93.

Nakazawa, N., Mehrotra, R., Ebe, M., and Yanagida, M. 2011. Condensin phosphorylated by the Aurora-B-like kinase Ark1 is continuously required until telophase in a mode distinct from Top2. *Journal of Cell Science* 124:1795-807.

Nakazawa, Y., Hiraki, M., Kamiya, R., and Hirono, M. 2007. SAS-6 is a Cartwheel Protein that Establishes the 9-Fold Symmetry of the Centriole. *Current Biology* 17 (24):2169-74.

Nash, P., Tang, X., Orlicky, S., Chen, Q., Gertler, F. B., Mendenhall, M. D., Sicheri, F., Pawson, T., and Tyers, M. 2001. Multisite phosphorylation of a CDK inhibitor sets a threshold for the onset of DNA replication. *Nature* 414 (6863):514-21.

Neduva, V., Linding, R., Su-Angrand, I., Stark, A., De Masi, F., Gibson, T. J., Lewis, J., Serrano, L., and Russell, R. B. 2005. Systematic discovery of new recognition peptides mediating protein interaction networks. *PLoS Biology* 3:1-10.

Neef, R., Klein, U. R., Kopajtich, R., and Barr, F. A. 2006. Cooperation between mitotic kinesins controls the late stages of cytokinesis. *Current Biology* 16:301-7.

Neumann, B., Walter, T., Hériché, J.-K., Bulkescher, J., Erfle, H., Conrad, C., Rogers, P., Poser, I., Held, M., Liebel, U., Cetin, C., Sieckmann, F., Pau, G., Kabbe, R., Wünsche, A., Satagopam, V., Schmitz, M. H. A., Chapuis, C., Gerlich, D. W., Schneider, R., Eils, R., Huber, W., Peters, J.-M., Hyman, A. A., Durbin, R., Pepperkok, R., and Ellenberg, J. 2010. Phenotypic profiling of the human genome by time-lapse microscopy reveals cell division genes. *Nature* 464:721-7.

Neurohr, G., Naegeli, A., Titos, I., Theler, D., Greber, B., Díez, J., Gabaldón, T., Mendoza, M., and Barral, Y. 2011. A Midzone-Based Ruler Adjusts Chromosome Compaction to Anaphase Spindle Length. *Science* 332 (6028):465-8.

Nigg, E. A. 2001. Mitotic kinases as regulators of cell division and its checkpoints. *Nature reviews. Molecular cell biology* 2:21-32.

Nigg, E. A. and Raff, J. W. 2009. Centrioles, Centrosomes, and Cilia in Health and Disease. *Cell* 139:663-78.

Nijenhuis, W., Vallardi, G., Teixeira, A., Kops, G. J. P. L., and Saurin, Adrian T. 2014. Negative feedback at kinetochores underlies a responsive spindle checkpoint signal. *Nature Cell Biology* 16:1257-64.

Nikonova, A. S., Astsaturov, I., Serebriiskii, I. G., Dunbrack, R. L., and Golemis, E. A. 2013. Aurora A kinase (AURKA) in normal and pathological cell division. *Cellular and Molecular Life Sciences* 70 (4):661-87.

Nishino, T., Takeuchi, K., Gascoigne, K. E., Suzuki, A., Hori, T., Oyama, T., Morikawa, K., Cheeseman, I. M., and Fukagawa, T. 2012. CENP-T-W-S-X forms a unique centromeric chromatin structure with a histone-like fold. *Cell* 148:487-501.

Nogales, E., Downing, K. H., Amos, L. A., and Löwe, J. 1998. Tubulin and FtsZ form a distinct family of GTPases. *Nature Structural Biology* 5 (6):451-8.

Nogales, E., Wolf, S. G., and Downing, K. H. 1998. Electron Crystallography. *Nature* 391:199-204.

Norden, C., Mendoza, M., Dobbelaere, J., Kotwaliwale, C. V., Biggins, S., and Barral, Y. 2006. The NoCut Pathway Links Completion of Cytokinesis to Spindle Midzone Function to Prevent Chromosome Breakage. *Cell* 125:85-98.

Nousiainen, M., Silljé, H. H. W., Sauer, G., Nigg, E. A., and Körner, R. 2006. Phosphoproteome analysis of the human mitotic spindle. *Proceedings of the National Academy of Sciences, USA* 103:5391-6.

Nunes Bastos, R., Gandhi, S. R., Baron, R. D., Gruneberg, U., Nigg, E. A., and Barr, F. A. 2013. Aurora B suppresses microtubule dynamics and limits central spindle size by locally activating KIF4A. *The Journal of Cell Biology* 202 (4):605-21.

Oakley, C. E. and Oakley, B. R. 1989. Identification of γ-tubulin, a new member of the tubulin superfamily encoded by mipA gene of *Aspergillus nidulans*. *Nature* 338 (6217):662-4.

Obenauer, J. C., Cantley, L. C., and Yaffe, M. B. 2003. Scansite 2.0: Proteome-wide prediction of cell signalling interactions using short sequence motifs. *Nucleic Acids Research* 31:3635-41.

Ohashi, S., Sakashita, G., Ban, R., Nagasawa, M., Matsuzaki, H., Murata, Y., Taniguchi, H., Shima, H., Furukawa, K., and Urano, T. 2006. Phospho-regulation of human protein kinase Aurora-A: analysis using anti-phospho-Thr288 monoclonal antibodies. *Oncogene* 25:7691-702.

Ohi, R., Sapra, T., Howard, J., and Mitchison, T. J. 2004. Differentiation of cytoplasmic and meiotic spindle assembly MCAK functions by Aurora B-dependent phosphorylation. *Molecular Biology of the Cell* 15:2895-906.

Ohta, S., Kimura, M., Takagi, S., Toramoto, I., and Ishihama, Y. 2016. Identification of Mitosis-Specific Phosphorylation in Mitotic Chromosome-Associated Proteins. *Journal of Proteome Research* 15:3331-41.

Okita, K., Kiyonari, H., Nobuhisa, I., Kimura, N., Aizawa, S., and Taga, T. 2004. Targeted disruption of the mouse ELYS gene results in embryonic death at peri-implantation development. *Genes to Cells* 9:1083-91.

Olsen, J. V., Blagoev, B., Gnad, F., Macek, B., Kumar, C., Mortensen, P., and Mann, M. 2006. Global, In Vivo, and Site-Specific Phosphorylation Dynamics in Signaling Networks. *Cell* 127:635-48.

Olsen, J. V., Vermeulen, M., Santamaria, A., Kumar, C., Miller, M. L., Jensen, L. J., Gnad, F., Cox, J., Jensen, T. S., Nigg, E. A., Brunak, S., and Mann, M. 2010. Quantitative Phosphoproteomics Reveals Widespread Full Phosphorylation Site Occupancy During Mitosis. *Science Signaling* 3:ra3-ra3.

Ono, T., Fang, Y., Spector, D. L., and Hirano, T. 2004. Spatial and Temporal Regulation of Condensins I and II in Mitotic Chromosome Assembly in Human Cells. *Molecular Biology of the Cell* 15 (7):3296-308.

Orjalo, A. V., Arnaoutov, A., Shen, Z., Boyarchuk, Y., Zeitlin, S. G., Fontoura, B., Briggs, S., Dasso, M., and Forbes, D. J. 2006. The Nup107-160 Nucleoporin Complex Is Required for Correct Bipolar Spindle Assembly. *Molecular Biology of the Cell* 17 (9):3806-18.

Ouchi, M., Fujiuchi, N., Sasai, K., Katayama, H., Minamishima, Y. A., Ongusaha, P. P., Deng, C., Sen, S., Lee, S. W., and Ouchi, T. 2004. BRCA1 Phosphorylation by Aurora-A in the Regulation of G2 to M Transition. *Journal of Biological Chemistry* 279 (19):19643-8.

Özlü, N., Monigatti, F., Renard, B. Y., Field, C. M., Steen, H., Mitchison, T. J., and Steen, J. J. 2010. Binding Partner Switching on Microtubules and Aurora-B in the Mitosis to Cytokinesis Transition. *Molecular & Cellular Proteomics* 9 (2):336-50.

Özlü, N., Srayko, M., Kinoshita, K., Habermann, B., O'Toole, E. T., Müller-Reichert, T., Schmalz, N., Desai, A., and Hyman, A. A. 2005. An Essential Function of the *C. elegans* Ortholog of TPX2 Is to Localize Activated Aurora A Kinase to Mitotic Spindles. *Developmental Cell* 9:237-48.

Palmer, D., O'Day, K., Wener, M., Andrews, B., and Margolis, R. 1987. A 17-kD centromere protein (CENP-A) copurifies with nucleosome core particles and with histones. *The Journal of Cell Biology* 104 (4):805-15.

Paoletti, A., Moudjou, M., Paintrand, M., Salisbury, J. L., and Bornens, M. 1996. Most of centrin in animal cells is not centrosome-associated and centrosomal centrin is confined to the distal lumen of centrioles. *Journal of Cell Science* 109 (Pt 13):3089-102.

Park, J., Hu, Y., Murthy, T. V. S., Vannberg, F., Shen, B., Rolfs, A., Hutti, J. E., Cantley, L. C., Labaer, J., Harlow, E., and Brizuela, L. 2005. Building a human kinase gene repository: bioinformatics, molecular cloning, and functional validation. *Proc Natl Acad Sci U S A* 102:8114-9.

Patel, K., Nogales, E., and Heald, R. 2012. Multiple domains of human CLASP contribute to microtubule dynamics and organization in vitro and in Xenopus egg extracts. *Cytoskeleton* 69:155-65.

Pemble, H., Kumar, P., van Haren, J., and Wittmann, T. 2017. GSK3-mediated CLASP2 phosphorylation modulates kinetochore dynamics. *Journal of Cell Science* 130 (8):1404-12.

Pereira, A. L., Pereira, A. J., Maia, A. R. R., Drabek, K., Sayas, C. L., Hergert, P. J., Lince-Faria, M., Matos, I., Duque, C., Stepanova, T., Rieder, C. L., Earnshaw, W. C., Galjart, N., and Maiato, H. 2006. Mammalian CLASP1 and CLASP2 Cooperate to Ensure Mitotic Fidelity by Regulating Spindle and Kinetochore Function. *Molecular Biology of the Cell* 17 (10):4526-42.

Pereira, G. and Schiebel, E. 2003. Separase Regulates INCENP-Aurora B Anaphase Spindle Function Through Cdc14. *Science* 302 (5653):2120-4.

Peris, L., Wagenbach, M., Lafanechère, L., Brocard, J., Moore, A. T., Kozielski, F., Job, D., Wordeman, L., and Andrieux, A. 2009. Motor-dependent microtubule disassembly driven by tubulin tyrosination. *Journal of Cell Biology* 185:1159-66.

Perpelescu, M. and Fukagawa, T. 2011. The ABCs of CENPs. *Chromosoma* 120:425-46.

Peset, I., Seiler, J., Sardon, T., Bejarano, L. A., Rybina, S., and Vernos, I. 2005. Function and regulation of Maskin, a TACC family protein, in microtubule growth during mitosis. *The Journal of Cell Biology* 170 (7):1057-66.

Petersen, J., Paris, J., Willer, M., Philippe, M., and Hagan, I. M. 2001. The *S. pombe* aurora-related kinase Ark1 associates with mitotic structures in a stage dependent manner and is required for chromosome segregation. *Journal of Cell Science* 114:4371-84.

Petrovic, A., Pasqualato, S., Dube, P., Krenn, V., Santaguida, S., Cittaro, D., Monzani, S., Massimiliano, L., Keller, J., Tarricone, A., Maiolica, A., Stark, H., and Musacchio, A. 2010. The MIS12 complex is a protein interaction hub for outer kinetochore assembly. *Journal of Cell Biology* 190:835-52.

Petry, S., Pugieux, C., Nedelec, F. J., and Vale, R. D. 2011. Augmin promotes meiotic spindle formation and bipolarity in Xenopus egg extracts. *Proc Natl Acad Sci U S A* 108:14473-8.

Piehl, M., Tulu, U. S., Wadsworth, P., and Cassimeris, L. 2004. Centrosome maturation: measurement of microtubule nucleation throughout the cell cycle by using GFP-tagged EB1. *Proc Natl Acad Sci U S A* 101:1584-8.

Pinyol, R., Scrofani, J., and Vernos, I. 2013. The role of NEDD1 phosphorylation by aurora a in chromosomal microtubule nucleation and spindle function. *Current Biology* 23:143-9.

Platani, M., Santarella-Mellwig, R., Posch, M., Walczak, R., Swedlow, J. R., and Mattaj, I. W. 2009. The Nup107-160 Nucleoporin Complex Promotes Mitotic Events via Control of the Localization State of the Chromosome Passenger Complex. *Molecular Biology of the Cell* 20 (24):5260-75.

Polat, A. N., Karayel, Ö., Giese, S. H., Harmanda, B., Sanal, E., Hu, C. K., Renard, B. Y., and Özlü, N. 2015. Phosphoproteomic analysis of aurora kinase inhibition in monopolar cytokinesis. *Journal of Proteome Research* 14:4087-98.

Qi, G., Ogawa, I., Kudo, Y., Miyauchi, M., Siriwardena, B. S. M. S., Shimamoto, F., Tatsuka, M., and Takata, T. 2007. Aurora-B expression and its correlation with cell proliferation and metastasis in oral cancer. *Virchows Archiv* 450 (3):297-302.

Qian, J., Beullens, M., Lesage, B., and Bollen, M. 2013. Aurora B defines its own chromosomal targeting by opposing the recruitment of the phosphatase scaffold Repo-Man. *Current Biology* 23:1136-43.

Quartuccio, S. M., Dipali, S. S., and Schindler, K. 2017. Haspin inhibition reveals functional differences of interchromatid axis–localized AURKB and AURKC. *Molecular Biology of the Cell* 28 (17):2233-40.

Rasala, B. A., Orjalo, A. V., Shen, Z., Briggs, S., and Forbes, D. J. 2006. ELYS is a dual nucleoporin/kinetochore protein required for nuclear pore assembly and proper cell division. *Proc Natl Acad Sci U S A* 103:17801-6.

Reboutier, D., Troadec, M. B., Cremet, J. Y., Chauvin, L., Guen, V., Salaun, P., and Prigent, C. 2013. Aurora A is involved in central spindle assembly through phosphorylation of ser 19 in P150Glued. *Journal of Cell Biology* 201:65-79.

Reboutier, D., Troadec, M. B., Cremet, J. Y., Fukasawa, K., and Prigent, C. 2012. Nucleophosmin/B23 activates aurora a at the centrosome through phosphorylation of serine 89. *Journal of Cell Biology* 197:19-26.

Richter, M. M., Poznanski, J., Zdziarska, A., Czarnocki-Cieciura, M., Lipinszki, Z., Dadlez, M., Glover, D. M., and Przewloka, M. R. 2016. Network of protein interactions within the *Drosophila* inner kinetochore. *Open Biology* 6 (2):150238.

Rieder, C. L. and Alexander, S. P. 1990. Kinetochores are transported poleward along a single astral microtubule during chromosome attachment to the spindle in newt lung cells. *Journal of Cell Biology* 110:81-95.

Ródenas, E., González-Aguilera, C., Ayuso, C., and Askjaer, P. 2012. Dissection of the NUP107 nuclear pore subcomplex reveals a novel interaction with spindle assembly checkpoint protein MAD1 in Caenorhabditis elegans. *Molecular Biology of the Cell* 23 (5):930-44.

Roghi, C., Giet, R., Uzbekov, R., Morin, N., Chartrain, I., Le Guellec, R., Couturier, a., Dorée, M., Philippe, M., and Prigent, C. 1998. The Xenopus protein kinase pEg2 associates with the centrosome in a cell cycle-dependent manner, binds to the spindle microtubules and is involved in bipolar mitotic spindle assembly. *Journal of Cell Science* 111 (Pt 5):557-72.

Rogowski, K., van Dijk, J., Magiera, M. M., Bosc, C., Deloulme, J. C., Bosson, A., Peris, L., Gold, N. D., Lacroix, B., Grau, M. B., Bec, N., Larroque, C., Desagher, S., Holzer, M., Andrieux, A., Moutin, M. J., and Janke, C. 2010. A family of protein-deglutamylating enzymes associated with neurodegeneration. *Cell* 143:564-78.

Romé, P., Montembault, E., Franck, N., Pascal, A., Glover, D. M., and Giet, R. 2010. Aurora A contributes to p150glued phosphorylation and function during mitosis. *Journal of Cell Biology* 189:651-9.

Rong, R., Jiang, L. Y., Sheikh, M. S., and Huang, Y. 2007. Mitotic kinase Aurora-A phosphorylates RASSF1A and modulates RASSF1A-mediated microtubule interaction and M-phase cell cycle regulation. *Oncogene* 26:7700-8.

Roos, U. P. 1976. Light and electron microscopy of rat kangaroo cells in mitosis - III. Patterns of chromosome behavior during prometaphase. *Chromosoma* 54:363-85.

Rosasco-Nitcher, S. E., Lan, W., Khorasanizadeh, S., and Stukenberg, P. T. 2008. Centromeric Aurora-B Activation Requires TD-60, Microtubules, and Substrate Priming Phosphorylation. *Science* 319:469-72.

Sakai, H., Urano, T., Ookata, K., Kim, M. H., Hirai, Y., Saito, M., Nojima, Y., and Ishikawa, F. 2002. MBD3 and HDAC1, two components of the NuRD complex, are localized at aurora-A-positive centrosomes in M phase. *Journal of Biological Chemistry* 277:48714-23.

Salazar, C. and Höfer, T. 2007. Versatile regulation of multisite protein phosphorylation by the order of phosphate processing and protein–protein interactions. *FEBS Journal* 274 (4):1046-61.

Salmon, E. D. and Wolniak, S. M. 1990. Role of Microtubules in Stimulating Cytokinesis in Animal Cellsa. *Annals of the New York Academy of Sciences* 582 (1):88-98.

Sampath, S. C., Ohi, R., Leismann, O., Salic, A., Pozniakovski, A., and Funabiki, H. 2004. The chromosomal passenger complex is required for chromatin-induced microtubule stabilization and spindle assembly. *Cell* 118:187-202.

Sardon, T., Pache, R. A., Stein, A., Molina, H., Vernos, I., and Aloy, P. 2010. Uncovering new substrates for Aurora A kinase. *EMBO reports* 11:977-84.

Sasai, K., Parant, J. M., Brandt, M. E., Carter, J., Adams, H. P., Stass, S. A., Killary, A. M., Katayama, H., and Sen, S. 2008. Targeted disruption of Aurora A causes abnormal mitotic spindle assembly, chromosome misalignment and embryonic lethality. *Oncogene* 27:4122-7.

Sassoon, I., Severin, F. F., Andrews, P. D., Taba, M. R., Kaplan, K. B., Ashford, A. J., Stark, M. J. R., Sorger, P. K., and Hyman, A. A. 1999. Regulation of Saccharomyces cerevisiae kinetochores by the type 1 phosphatase Glc7p. *Genes and Development* 13:545-55.

Saurin, A. T., van der Waal, M. S., Medema, R. H., Lens, S. M. A., and Kops, G. J. P. L. 2011. Aurora B potentiates Mps1 activation to ensure rapid checkpoint establishment at the onset of mitosis. *Nature Communications* 2:316.

Sawin, K. E., LeGuellec, K., Philippe, M., and Mitchison, T. J. 1992. Mitotic spindle organization by a plus-end-directed microtubule motor. *Nature* 359:540-3.

Schmidt, J. C., Kiyomitsu, T., Hori, T., Backer, C. B., Fukagawa, T., and Cheeseman, I. M. 2010. Aurora B kinase controls the targeting of the Astrin-SKAP complex to bioriented kinetochores. *Journal of Cell Biology* 191:269-80.

Screpanti, E., De Antoni, A., Alushin, G. M., Petrovic, A., Melis, T., Nogales, E., and Musacchio, A. 2011. Direct binding of Cenp-C to the Mis12 complex joins the inner and outer kinetochore. *Current Biology* 21:391-8.

Scrittori, L., Skoufias, D. A., Hans, F., Gerson, V., Sassone-Corsi, P., Dimitrov, S., and Margolis, R. L. 2005. A Small C-Terminal Sequence of Aurora B Is Responsible for Localization and Function. *Molecular Biology of the Cell* 16 (1):292-305.

Seki, A., Coppinger, J. A., Jang, C.-Y., Yates, J. R., and Fang, G. 2008. Bora and the Kinase Aurora A Cooperatively Activate the Kinase Plk1 and Control Mitotic Entry. *Science* 320:1655-8.

Sessa, F., Mapelli, M., Ciferri, C., Tarricone, C., Areces, L. B., Schneider, T. R., Stukenberg, P. T., and Musacchio, A. 2005. Mechanism of Aurora B Activation by INCENP and Inhibition by Hesperadin. *Molecular Cell* 18 (3):379-91.

Sharp, D. J., McDonald, K. L., Brown, H. M., Matthies, H. J., Walczak, C., Vale, R. D., Mitchison, T. J., and Scholey, J. M. 1999. The bipolar kinesin, KLP61F, cross-links microtubules within interpolar microtubule bundles of *Drosophila* embryonic mitotic spindles. *Journal of Cell Biology* 144:125-38.

Sharp, D. J., Rogers, G. C., and Scholey, J. M. 2000. Cytoplasmic dynein is required for poleward chromosome movement during mitosis in *Drosophila* embryos. *Nature Cell Biology* 2:922-30.

Sharp, D. J. and Ross, J. L. 2012. Microtubule-severing enzymes at the cutting edge. *Journal of Cell Science* 125:2561-9.

Shimada, M., Goshima, T., Matsuo, H., Johmura, Y., Haruta, M., Murata, K., Tanaka, H., Ikawa, M., Nakanishi, K., and Nakanishi, M. 2016. Essential role of autoactivation circuitry on Aurora B-mediated H2AX-pS121 in mitosis. *Nature Communications* 7:12059.

Sievers, F., Wilm, A., Dineen, D., Gibson, T. J., Karplus, K., Li, W., Lopez, R., McWilliam, H., Remmert, M., Söding, J., Thompson, J. D., and Higgins, D. G. 2011. Fast, scalable generation of high-quality protein multiple sequence alignments using Clustal Omega. *Molecular Systems Biology* 7 (1):1-6.

Siniossoglou, S., Wimmer, C., Rieger, M., Doye, V., Tekotte, H., Weise, C., Emig, S., Segref, A., and Hurt, E. C. 1996. A novel complex of nucleoporins, which includes Sec13p and a Sec13p homolog, is essential for normal nuclear pores. *Cell* 84:265-75.

Sirajuddin, M., Rice, L. M., and Vale, R. D. 2014. Regulation of microtubule motors by tubulin isotypes and post-translational modifications. *Nature Cell Biology* 16:335-44.

Skibbens, R. V., Skeen, V. P., and Salmon, E. D. 1993. Directional instability of kinetochore motility during chromosome congression and segregation in mitotic newt lung cells: A push-pull mechanism. *Journal of Cell Biology* 122:859-75.

Song, S. J., Song, M. S., Kim, S. J., Kim, S. Y., Kwon, S. H., Kim, J. G., Calvisi, D. F., Kang, D., and Lim, D. S. 2009. Aurora a regulates prometaphase progression by inhibiting the ability of RASSF1A to suppress APC-Cdc20 activity. *Cancer Research* 69:2314-23.

Stearns, T., Evans, L., and Kirschner, M. 1991. γ-Tubulin is a highly conserved component of the centrosome. *Cell* 65 (5):825-36.

Steigemann, P., Wurzenberger, C., Schmitz, M. H. A., Held, M., Guizetti, J., Maar, S., and Gerlich, D. W. 2009. Aurora B-Mediated Abscission Checkpoint Protects against Tetraploidization. *Cell* 136:473-84.

Sudakin, V., Chan, G. K. T., and Yen, T. J. 2001. Checkpoint inhibition of the APC/C in HeLa cells is mediated by a complex of BUBR1, BUB3, CDC20, and MAD2. *Journal of Cell Biology* 154:925-36.

Sugimoto, K., Urano, T., Zushi, H., Inoue, K., Tasaka, H., Tachibana, M., and Dotsu, M. 2002. Molecular dynamics of Aurora-A kinase in living mitotic cells simultaneously visualized with histone H3 and nuclear membrane protein importinalpha. *Cell Structure and Function* 27:457-67.

Sugiyama, Sugiura, Hara, Sugimoto, Shima, Honda, Furukawa, Yamashita, and Urano. 2002. Aurora-B associated protein phosphatases as negative regulators of kinase activation. *Oncogene* 21:3103-11.

Sumara, I., Quadroni, M., Frei, C., Olma, M. H., Sumara, G., Ricci, R., and Peter, M. 2007. A Cul3-Based E3 Ligase Removes Aurora B from Mitotic Chromosomes, Regulating Mitotic Progression and Completion of Cytokinesis in Human Cells. *Developmental Cell* 12:887-900.

Syred, H. M., Welburn, J., Rappsilber, J., and Ohkura, H. 2013. Cell cycle regulation of microtubule interactomes: multi-layered regulation is critical for the interphase/mitosis transition. *Molecular & Cellular Proteomics* 12:3135-47.

Tada, K., Susumu, H., Sakuno, T., and Watanabe, Y. 2011. Condensin association with histone H2A shapes mitotic chromosomes. *Nature* 474:477-83.

Takahashi, T., Futamura, M., Yoshimi, N., Sano, J., Katada, M., Takagi, Y., Kimura, M., Yoshioka, T., Okano, Y., and Saji, S. 2000. Centrosomal Kinases, HsAIRK1 and HsAIRK3, are Overexpressed in Primary Colorectal Cancers. *Japanese Journal of Cancer Research* 91 (10):1007-14.

Takeshita, M., Koga, T., Takayama, K., Ijichi, K., Yano, T., Maehara, Y., Nakanishi, Y., and Sueishi, K. 2013. Aurora-B overexpression is correlated with aneuploidy and poor prognosis in non-small cell lung cancer. *Lung Cancer* 80 (1):85-90.

Tan, L. and Kapoor, T. M. 2011. Examining the dynamics of chromosomal passenger complex (CPC)-dependent phosphorylation during cell division. *Proc Natl Acad Sci U S A* 108 (40):16675-80.

Tanaka, T. U., Rachidi, N., Janke, C., Pereira, G., Galova, M., Schiebel, E., Stark, M. J. R., and Nasmyth, K. 2002. Evidence that the Ipl1-Sli15 (Aurora Kinase-INCENP) complex promotes chromosome bi-orientation by altering kinetochore-spindle pole connections. *Cell* 108:317-29.

Tanner, M. M., Grenman, S., Koul, A., Johannsson, O., Meltzer, P., Pejovic, T., Borg, Å., and Isola, J. J. 2000. Frequent Amplification of Chromosomal Region 20q12-q13 in Ovarian Cancer. *Clinical Cancer Research* 6 (5):1833-9.

Tanno, Y., Kitajima, T. S., Honda, T., Ando, Y., Ishiguro, K. I., and Watanabe, Y. 2010. Phosphorylation of mammalian Sgo2 by Aurora B recruits PP2A and MCAK to centromeres. *Genes and Development* 24:2169-79.

Tatsuka, M., Katayama, H., Ota, T., Tanaka, T., Odashima, S., Suzuki, F., and Terada, Y. 1998. Multinuclearity and Increased Ploidy Caused by Overexpression of the Aurora- and Ipl1-like Midbody-associated Protein Mitotic Kinase in Human Cancer Cells. *Cancer Research* 58 (21):4811-6.

Tchatchou, S., Wirtenberger, M., Hemminki, K., Sutter, C., Meindl, A., Wappenschmidt, B., Kiechle, M., Bugert, P., Schmutzler, R. K., Bartram, C. R., and Burwinkel, B. 2007. Aurora kinases A and B and familial breast cancer risk. *Cancer Letters* 247 (2):266-72.

Teixeira, L. K. and Reed, S. I. 2013. Ubiquitin Ligases and Cell Cycle Control. *Annual Review of Biochemistry* 82:387-414.

Teixidó-Travesa, N., Villén, J., Lacasa, C., Bertran, M. T., Archinti, M., Gygi, S. P., Caelles, C., Roig, J., and Lüders, J. 2010. The γTuRC Revisited: A Comparative Analysis of Interphase and Mitotic Human γTuRC Redefines the Set of Core Components and Identifies the Novel Subunit GCP8. *Molecular Biology of the Cell* 21 (22):3963-72.

Tien, A.-C., Lin, M.-H., Su, L.-J., Hong, Y.-R., Cheng, T.-S., Lee, Y.-C. G., Lin, W.-J., Still, I. H., and Huang, C.-Y. F. 2004. Identification of the substrates and interaction proteins of aurora kinases from a protein-protein interaction model. *Molecular & Cellular Proteomics* 3:93-104.

Tilney, L. G., Bryan, J., Bush, D. J., Fujiwara, K., Mooseker, M. S., Murphy, D. B., and Snyder, D. H. 1973. MICROTUBULES: EVIDENCE FOR 13 PROTOFILAMENTS. *The Journal of Cell Biology* 59 (2):267-75.

Tirnauer, J. S., Grego, S., Salmon, E. D., and Mitchison, T. J. 2002. EB1–Microtubule Interactions in Xenopus Egg Extracts: Role of EB1 in Microtubule Stabilization and Mechanisms of Targeting to Microtubules. *Molecular Biology of the Cell* 13 (10):3614-26.

Toji, S., Yabuta, N., Hosomi, T., Nishihara, S., Kobayashi, T., Suzuki, S., Tamai, K., and Nojima, H. 2004. The centrosomal protein Lats2 is a phosphorylation target of Aurora-A kinase. *Genes to Cells* 9:383-97.

Tsai, C. Y., Ngo, B., Tapadia, A., Hsu, P. H., Wu, G., and Lee, W. H. 2011. Aurora-A phosphorylates augmin complex component hice1 protein at an N-terminal

serine/threonine cluster to modulate its microtubule binding activity during spindle assembly. *Journal of Biological Chemistry* 286:30097-106.

Tsai, M.-Y., Wiese, C., Cao, K., Martin, O., Donovan, P., Ruderman, J., Prigent, C., and Zheng, Y. 2003. A Ran signalling pathway mediated by the mitotic kinase Aurora A in spindle assembly. *Nature Cell Biology* 5:242-8.

Tseng, B. S., Tan, L., Kapoor, T. M., and Funabiki, H. 2010. Dual detection of chromosomes and microtubules by the chromosomal passenger complex drives spindle assembly. *Developmental Cell* 18:903-12.

Twu, N.-F., Yuan, C.-C., Yen, M.-S., Lai, C.-R., Chao, K.-C., Wang, P.-H., Wu, H.-H., and Chen, Y.-J. 2009. Expression of Aurora kinase A and B in normal and malignant cervical tissue: High Aurora A kinase expression in squamous cervical cancer. *European Journal of Obstetrics & Gynecology and Reproductive Biology* 142 (1):57-63.

Uchida, K. S. K., Takagaki, K., Kumada, K., Hirayama, Y., Noda, T., and Hirota, T. 2009. Kinetochore stretching inactivates the spindle assembly checkpoint. *Journal of Cell Biology* 184:383-90.

Uehara, R. and Goshima, G. 2010. Functional central spindle assembly requires de novo microtubule generation in the interchromosomal region during anaphase. *Journal of Cell Biology* 191:259-67.

Uehara, R., Tsukada, Y., Kamasaki, T., Poser, I., Yoda, K., Gerlich, D. W., and Goshima, G. 2013. Aurora B and Kif2A control microtubule length for assembly of a functional central spindle during anaphase. *Journal of Cell Biology* 202:623-36.

Valenstein, Max L. and Roll-Mecak, A. 2016. Graded Control of Microtubule Severing by Tubulin Glutamylation. *Cell* 164 (5):911-21.

van den Wildenberg, S. M. J. L., Tao, L., Kapitein, L. C., Schmidt, C. F., Scholey, J. M., and Peterman, E. J. G. 2008. The Homotetrameric Kinesin-5 KLP61F Preferentially Crosslinks Microtubules into Antiparallel Orientations. *Current Biology* 18 (23):1860-4.

van Dijk, J., Miro, J., Strub, J.-M., Lacroix, B., van Dorsselaer, A., Edde, B., and Janke, C. 2008. Polyglutamylation Is a Post-translational Modification with a Broad Range of Substrates. *Journal of Biological Chemistry* 283 (7):3915-22.

van Dijk, J., Rogowski, K., Miro, J., Lacroix, B., Eddé, B., and Janke, C. 2007. A Targeted Multienzyme Mechanism for Selective Microtubule Polyglutamylation. *Molecular Cell* 26 (3):437-48.

van Heesbeen, R. G. H. P., Raaijmakers, J. A., Tanenbaum, M. E., Halim, V. A., Lelieveld, D., Lieftink, C., Heck, A. J. R., Egan, D. A., and Medema, R. H. 2017. Aurora A, MCAK, and Kif18b promote Eg5-independent spindle formation. *Chromosoma* 126:473-86.

Vasu, S., Shah, S., Orjalo, A., Park, M., Fischer, W. H., and Forbes, D. J. 2001. Novel vertebrate nucleoporins Nup133 and Nup160 play a role in mRNA export. *Journal of Cell Biology* 155:339-53.

Venoux, M., Basbous, J., Berthenet, C., Prigent, C., Fernandez, A., Lamb, N. J., and Rouquier, S. 2008. ASAP is a novel substrate of the oncogenic mitotic kinase Aurora-A: Phosphorylation on Ser625 is essential to spindle formation and mitosis. *Human Molecular Genetics* 17:215-24.

Vulprecht, J., David, A., Tibelius, A., Castiel, A., Konotop, G., Liu, F., Bestvater, F., Raab, M. S., Zentgraf, H., Izraeli, S., and Kramer, A. 2012. STIL is required for centriole duplication in human cells. *Journal of Cell Science* 125:1353-62.

Walczak, C. E., Mitchison, T. J., and Desai, A. 1996. XKCM1: A Xenopus kinesin-related protein that regulates microtubule dynamics during mitotic spindle assembly. *Cell* 84:37-47.

Walther, T. C., Alves, A., Pickersgill, H., Loïodice, I., Hetzer, M., Galy, V., Hülsmann, B. B., Köcher, T., Wilm, M., Allen, T., Mattaj, I. W., and Doye, V. 2003. The conserved Nup107-160 complex is critical for nuclear pore complex assembly. *Cell* 113:195-206.

Wandke, C., Barisic, M., Sigl, R., Rauch, V., Wolf, F., Amaro, A. C., Tan, C. H., Pereira, A. J., Kutay, U., Maiato, H., Meraldi, P., and Geley, S. 2012. Human chromokinesins promote chromosome congression and spindle microtubule dynamics during mitosis. *Journal of Cell Biology* 198:847-63.

Wang, E., Ballister, E. R., and Lampson, M. A. 2011. Aurora B dynamics at centromeres create a diffusion-based phosphorylation gradient. *Journal of Cell Biology* 194:539-49.

Wang, F., Ulyanova, N. P., Van Der Waal, M. S., Patnaik, D., Lens, S. M. A., and Higgins, J. M. G. 2011. A positive feedback loop involving haspin and aurora B promotes CPC accumulation at centromeres in mitosis. *Current Biology* 21:1061-9.

Wang, T., Lander, E. S., and Sabatini, D. M. 2016. Viral packaging and cell culture for CRISPR-based screens. *Cold Spring Harbor Protocols* 2016:289-96.

Wang, Y. and Dasso, M. 2009. SUMOylation and deSUMOylation at a glance. *Journal of Cell Science* 122:4249-52.

Wei, R. R., Al-Bassam, J., and Harrison, S. C. 2007. The Ndc80/HEC1 complex is a contact point for kinetochore-microtubule attachment. *Nature Structural & Molecular Biology* 14 (1):54-9.

Weil, C. F., Oakley, C. E., and Oakley, B. R. 1986. Isolation of mip (microtubule-interacting protein) mutations of *Aspergillus nidulans*. *Molecular and Cellular Biology* 6 (8):2963-8.

Weisenberg, R. C., Deery, W. J., and Dickinson, P. J. 1976. Tubulin-nucleotide interactions during the polymerization and depolymerization of microtubules. *Biochemistry* 15 (19):4248-54.

Welburn, J. P. I. and Cheeseman, I. M. 2008. Toward a Molecular Structure of the Eukaryotic Kinetochore. *Developmental Cell* 15:645-55.

Welburn, J. P. I., Vleugel, M., Liu, D., Yates, J. R., Lampson, M. A., Fukagawa, T., and Cheeseman, I. M. 2010. Aurora B Phosphorylates Spatially Distinct Targets to Differentially Regulate the Kinetochore-Microtubule Interface. *Molecular Cell* 38:383-92.

Westermann, S. and Weber, K. 2003. Post-translational modifications regulate microtubule function. *Nature Reviews Molecular Cell Biology* 4:938-48.

Wheatley, S. P., Henzing, A. J., Dodson, H., Khaled, W., and Earnshaw, W. C. 2004. Aurora-B Phosphorylation in Vitro Identifies a Residue of Survivin That Is Essential for Its Localization and Binding to Inner Centromere Protein (INCENP) in Vivo. *Journal of Biological Chemistry* 279:5655-60.

Wike, C. L., Graves, H. K., Hawkins, R., Gibson, M. D., Ferdinand, M. B., Zhang, T., Chen, Z., Hudson, D. F., Ottesen, J. J., Poirier, M. G., Schumacher, J., and Tyler, J. K. 2016. Aurora-A mediated histone H3 phosphorylation of threonine 118 controls condensin I and cohesin occupancy in mitosis. *Elife* 5:1-28.

Winey, M. and O'Toole, E. 2014. Centriole structure. *Philosophical Transactions of the Royal Society B: Biological Sciences* 369 (1650):20130457.

Wong, J., Lerrigo, R., Jang, C.-Y., and Fang, G. 2008. Aurora A Regulates the Activity of HURP by Controlling the Accessibility of Its Microtubule-binding Domain. *Molecular Biology of the Cell* 19 (5):2083-91.

Wood, K. W., Lad, L., Luo, L., Qian, X., Knight, S. D., Nevins, N., Brejc, K., Sutton, D., Gilmartin, A. G., Chua, P. R., Desai, R., Schauer, S. P., McNulty, D. E., Annan, R. S., Belmont, L. D., Garcia, C., Lee, Y., Diamond, M. A., Faucette, L. F., Giardiniere, M., Zhang, S., Sun, C.-M., Vidal, J. D., Lichtsteiner, S., Cornwell, W. D., Greshock, J. D., Wooster, R. F., Finer, J. T., Copeland, R. A., Huang, P. S., Morgans, D. J., Dhanak, D., Bergnes, G., Sakowicz, R., and Jackson, J. R. 2010. Antitumor activity of an allosteric inhibitor of centromere-associated protein-E. *Proc Natl Acad Sci U S A* 107:5839-44.

Wu, J. C., Chen, T. Y., Yu, C. T. R., Tsai, S. J., Hsu, J. M., Tang, M. J., Chou, C. K., Lin, W. J., Yuan, C. J., and Huang, C. Y. F. 2005. Identification of V23RalA-Ser194 as a critical mediator for Aurora-A-induced cellular motility and transformation by small pool expression screening. *Journal of Biological Chemistry* 280:9013-22.

Xu, Z., Vagnarelli, P., Ogawa, H., Samejima, K., and Earnshaw, W. C. 2010. Gradient of increasing aurora B kinase activity is required for cells to execute mitosis. *Journal of Biological Chemistry* 285:40163-70.

Yamagishi, Y., Sakuno, T., Goto, Y., and Watanabe, Y. 2014. Kinetochore composition and its function: Lessons from yeasts. *FEMS Microbiology Reviews* 38:185-200.

Yang, X. J. and Seto, E. 2008. Lysine Acetylation: Codified Crosstalk with Other Posttranslational Modifications. *Molecular Cell* 31:449-61.

Yasui, Y., Urano, T., Kawajiri, A., Nagata, K. I., Tatsuka, M., Saya, H., Furukawa, K., Takahashi, T., Izawa, I., and Inagaki, M. 2004. Autophosphorylation of a Newly Identified Site of Aurora-B Is Indispensable for Cytokinesis. *Journal of Biological Chemistry* 279:12997-3003.

Ye, A. A., Deretic, J., Hoel, Christopher M., Hinman, Albert W., Cimini, D., Welburn, Julie P., and Maresca, Thomas J. 2015. Aurora A Kinase Contributes to a Pole-Based Error Correction Pathway. *Current Biology* 25 (14):1842-51.

Ye, A. A., Torabi, J., and Maresca, T. J. 2016. Aurora A Kinase Amplifies a Midzone Phosphorylation Gradient to Promote High-Fidelity Cytokinesis. *The Biological Bulletin* 231 (1):61-72.

Yokoyama, H., Koch, B., Walczak, R., Ciray-Duygu, F., González-Sánchez, J. C., Devos, D. P., Mattaj, I. W., and Gruss, O. J. 2014. The nucleoporin MEL-28 promotes RanGTP-dependent γ-tubulin recruitment and microtubule nucleation in mitotic spindle formation. *Nature Communications* 5:3270.

Young, S., Besson, S., and Welburn, J. P. I. 2014. Length-dependent anisotropic scaling of spindle shape. *Biology Open* 3:1217-23.

Yu, C.-T. R., Hsu, J.-M., Lee, Y.-C. G., Tsou, A.-P., Chou, C.-K., and Huang, C.-Y. F. 2005. Phosphorylation and stabilization of HURP by Aurora-A: implication of HURP as a transforming target of Aurora-A. *Molecular and Cellular Biology* 25:5789-800.

Yu, C. T. R., Wu, J. C., Liao, M. C., Hsu, S. L., and Huang, C. Y. F. 2008. Identification of c-Fos as a mitotic phosphoprotein: Regulation of c-Fos by Aurora-A. *Journal of Biomedical Science* 15:79-87.

Yue, Z., Carvalho, A., Xu, Z., Yuan, X., Cardinale, S., Ribeiro, S., Lai, F., Ogawa, H., Gudmundsdottir, E., Gassmann, R., Morrison, C. G., Ruchaud, S., and Earnshaw, W. C. 2008. Deconstructing Survivin: Comprehensive genetic analysis of Survivin function by conditional knockout in a vertebrate cell line. *Journal of Cell Biology* 183:279-96.

Zaytsev, A. V., Mick, J. E., Maslennikov, E., Nikashin, B., DeLuca, J. G., and Grishchuk, E. L. 2015. Multisite phosphorylation of the NDC80 complex gradually tunes its microtubule-binding affinity. *Molecular Biology of the Cell* 26 (10):1829-44.

Zeitlin, S. G., Shelby, R. D., and Sullivan, K. F. 2001. CENP-A is phosphorylated by Aurora B kinase and plays an unexpected role in completion of cytokinesis. *Journal of Cell Biology* 155:1147-57.

Zencheck, W. D., Xiao, H., and Weiss, L. M. 2012. Lysine post-translational modifications and the cytoskeleton. *Essays In Biochemistry* 52:135-45.

Zeng, K., Bastos, R. N., Barr, F. A., and Gruneberg, U. 2010. Protein phosphatase 6 regulates mitotic spindle formation by controlling the T-loop phosphorylation state of Aurora A bound to its activator TPX2. *Journal of Cell Biology* 191:1315-32.

Zhang, X., Ems-McClung, S. C., and Walczak, C. E. 2008. Aurora A Phosphorylates MCAK to Control Ran-dependent Spindle Bipolarity. *Molecular Biology of the Cell* 19 (7):2752-65.

Zhang, X., Lan, W., Ems-McClung, S. C., Stukenberg, P. T., and Walczak, C. E. 2007. Aurora B Phosphorylates Multiple Sites on Mitotic Centromere-associated Kinesin to Spatially and Temporally Regulate Its Function. *Molecular Biology of the Cell* 18 (9):3264-76.

Zhou, H., Kuang, J., Zhong, L., Kuo, W.-l., Gray, J., Sahin, A., Brinkley, B., and Sen, S. 1998. Tumour amplified kinase STK15/BTAK induces centrosome amplification, aneuploidy and transformation. *Nature Genetics* 20 (2):189-93.

Zhou, H., Watts, J. D., and Aebersold, R. 2001. A systematic approach to the analysis of protein phosphorylation. *Nature Biotechnology* 19 (4):375-8.

Zimniak, T., Fitz, V., Zhou, H., Lampert, F., Opravil, S., Mechtler, K., Stolt-Bergner, P., and Westermann, S. 2012. Spatiotemporal regulation of Ipl1/aurora activity by direct Cdk1 phosphorylation. *Current Biology* 22:787-93.

Zorba, A., Buosi, V., Kutter, S., Kern, N., Pontiggia, F., Cho, Y.-J., and Kern, D. 2014. Molecular mechanism of Aurora A kinase autophosphorylation and its allosteric activation by TPX2. *Elife* 3:e02667.

Zuccolo, M., Alves, A., Galy, V., Bolhy, S., Formstecher, E., Racine, V., Sibarita, J.-B., Fukagawa, T., Shiekhattar, R., Yen, T., and Doye, V. 2007. The human Nup107–160 nuclear pore subcomplex contributes to proper kinetochore functions. *The EMBO Journal* 26 (7):1853-64.

Report

Current Biology

Aurora A Kinase Contributes to a Pole-Based Error Correction Pathway

Graphical Abstract

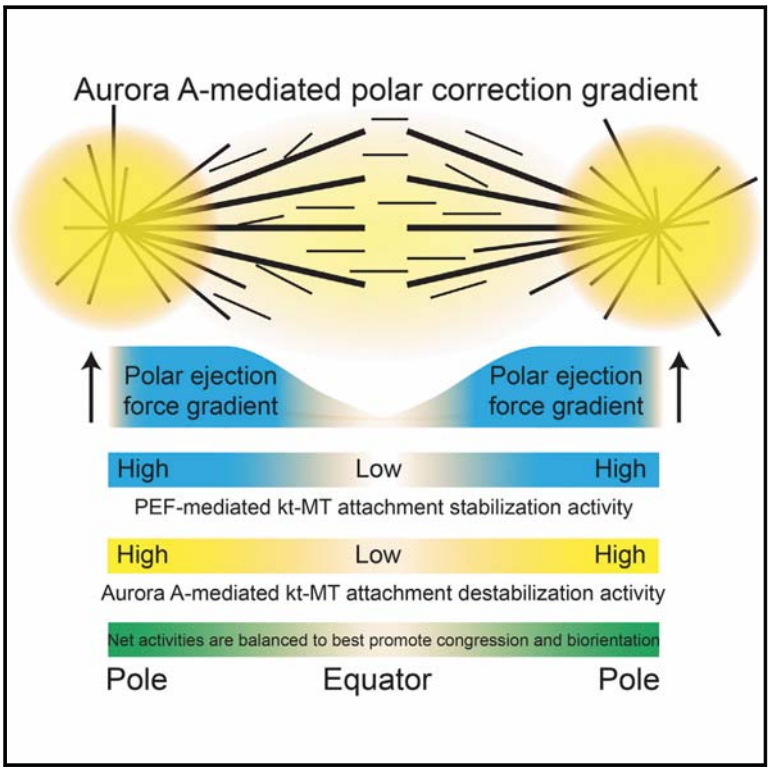

Authors

Anna A. Ye, Jovana Deretic, Christopher M. Hoel, Albert W. Hinman, Daniela Cimini, Julie P. Welburn, Thomas J. Maresca

Correspondence

tmaresca@bio.umass.edu

In Brief

Error correction, which requires the destabilization of improper kinetochore-microtubule attachments, often takes place near spindle poles, but the significance of this location was unclear. Ye et al. show that Aurora A kinase facilitates error correction through a pole-centered activity gradient that locally phosphorylates kinetochore substrates.

Highlights

- An AAK activity gradient in *Drosophila* S2 cells counters the effects of elevated PEFs
- AAK phosphorylates kinetochores and destabilizes attachments near poles in S2 cells
- AAK is required for efficient error correction in *Drosophila* and mammalian cells
- AAK phosphorylates the core kinetochore-MT attachment factor Ndc80/Hec1 in human cells

Ye et al., 2015, Current Biology *25*, 1842–1851
July 20, 2015
http://dx.doi.org/10.1016/j.cub.2015.06.021

CellPress

Current Biology
Report

Aurora A Kinase Contributes to a Pole-Based Error Correction Pathway

Anna A. Ye,[1,2] Jovana Deretic,[3] Christopher M. Hoel,[1] Albert W. Hinman,[4] Daniela Cimini,[4] Julie P. Welburn,[3] and Thomas J. Maresca[1,2,*]

[1]Biology Department, University of Massachusetts Amherst, Amherst, MA 01003, USA
[2]Molecular and Cellular Biology Graduate Program, University of Massachusetts Amherst, Amherst, MA 01003, USA
[3]Wellcome Trust Centre for Cell Biology, School of Biological Sciences, University of Edinburgh, Edinburgh EH9 3JR, UK
[4]Department of Biological Sciences and Virginia Bioinformatics Institute, Virginia Tech, Blacksburg, VA 24061, USA
*Correspondence: tmaresca@bio.umass.edu
http://dx.doi.org/10.1016/j.cub.2015.06.021

SUMMARY

Chromosome biorientation, where sister kinetochores attach to microtubules (MTs) from opposing spindle poles, is the configuration that best ensures equal partitioning of the genome during cell division. Erroneous kinetochore-MT attachments are commonplace but are often corrected prior to anaphase [1, 2]. Error correction, thought to be mediated primarily by the centromere-enriched Aurora B kinase (ABK) [3–5], typically occurs near spindle poles [6]; however, the relevance of this locale is unclear. Furthermore, polar ejection forces (PEFs), highest near poles [7], can stabilize improper attachments by pushing mal-oriented chromosome arms away from spindle poles [8, 9]. Hence, there is a conundrum: erroneous kinetochore-MT attachments are weakened where PEFs are most likely to strengthen them. Here, we report that Aurora A kinase (AAK) opposes the stabilizing effect of PEFs. AAK activity contributes to phosphorylation of kinetochore substrates near poles and its inhibition results in chromosome misalignment and an increased incidence of erroneous kinetochore-MT attachments. Furthermore, AAK directly phosphorylates a site in the N-terminal tail of Ndc80/Hec1 that has been implicated in reducing the affinity of the Ndc80 complex for MTs when phosphorylated [10–12]. We propose that an AAK activity gradient contributes to correcting mal-oriented kinetochore-MT attachments in the vicinity of spindle poles.

RESULTS

Bioriented attachments are thought to be stabilized, in part, by tension-dependent movements [13, 14] of outer kinetochore components away from ABK. The resultant spatial separation correlates with a reduction in phosphorylation of kinetochore-microtubule (MT) attachment factors [15, 16] that is proposed to increase the kinetochore's affinity for MTs [17]. Flawed attachments are weakened in favor of bioriented kinetochores through a process called error correction. Many models evoke tension-dependent inhibition of centromere (CEN)-based error correction via spatial separation [18]. The concept is reasonable if erroneous attachments are "tensionless," yet improper attachments may come under tension when mal-oriented chromosomes are opposed by polar ejection forces (PEFs) [19]. In support of this, we previously reported that elevated PEFs stabilize syntelic attachments [8], where sister kinetochores attach to the same pole, by overwhelming Aurora B kinase (ABK). Thus, while CEN-based models explain the instability of tensionless attachments, they fail to account for error correction when PEF-generated tension opposes ABK. Furthermore, recent work suggests that CEN-based Aurora kinase is dispensable for error correction in budding yeast, as mutants with Ipl1 (*S.c.* Aurora homolog) enriched on the spindle rather than the centromeres still achieved biorientation [20]. Clearly, a more comprehensive understanding of error correction requires further inquiry.

Unlike budding yeast, metazoans possess multiple Aurora kinases, most notably ABK and Aurora A kinase (AAK), which are enriched at centromeres and spindle poles/centrosomes, respectively [21]. As the kinases share nearly identical consensus target motifs [22], it is likely that the principal determinant of their substrate specificity is their respective sub-cellular localizations [23]. Here, we investigate whether a non-CEN-based pathway contributes to error correction by testing the hypothesis that AAK phosphorylates kinetochore substrates in the vicinity of poles.

We previously developed a cell-based assay in which tension can be experimentally elevated at kinetochores by manipulating PEF production [8]. In the PEF assay, inducible overexpression of the major PEF-producing kinesin-10 motor NOD [24] results in a dose-dependent increase in stable syntelic attachments in *Drosophila* S2 cells. To examine whether AAK affects the ability of PEFs to stabilize syntelic attachments, we created a cell line in which both NOD and AAK could be overexpressed simultaneously via $CuSO_4$ induction (Figure 1A and Movie S1). AAK-GFP localized to spindle MTs to varying degrees depending on the level of overexpression and was always highly enriched at centrosomes (Figures 1B and 1C). In agreement with previous observations in HeLa cells [25], the centrosome-enriched population of AAK-GFP turned over with rapid kinetics ($t_{1/2}$ of 7 s) in S2 cells (Figures S1A and S1B and Movie S2). Inducible NOD-mCherry and AAK-GFP cells co-expressing Ndc80-GFP, for assessment of attachment states, were subjected to the PEF

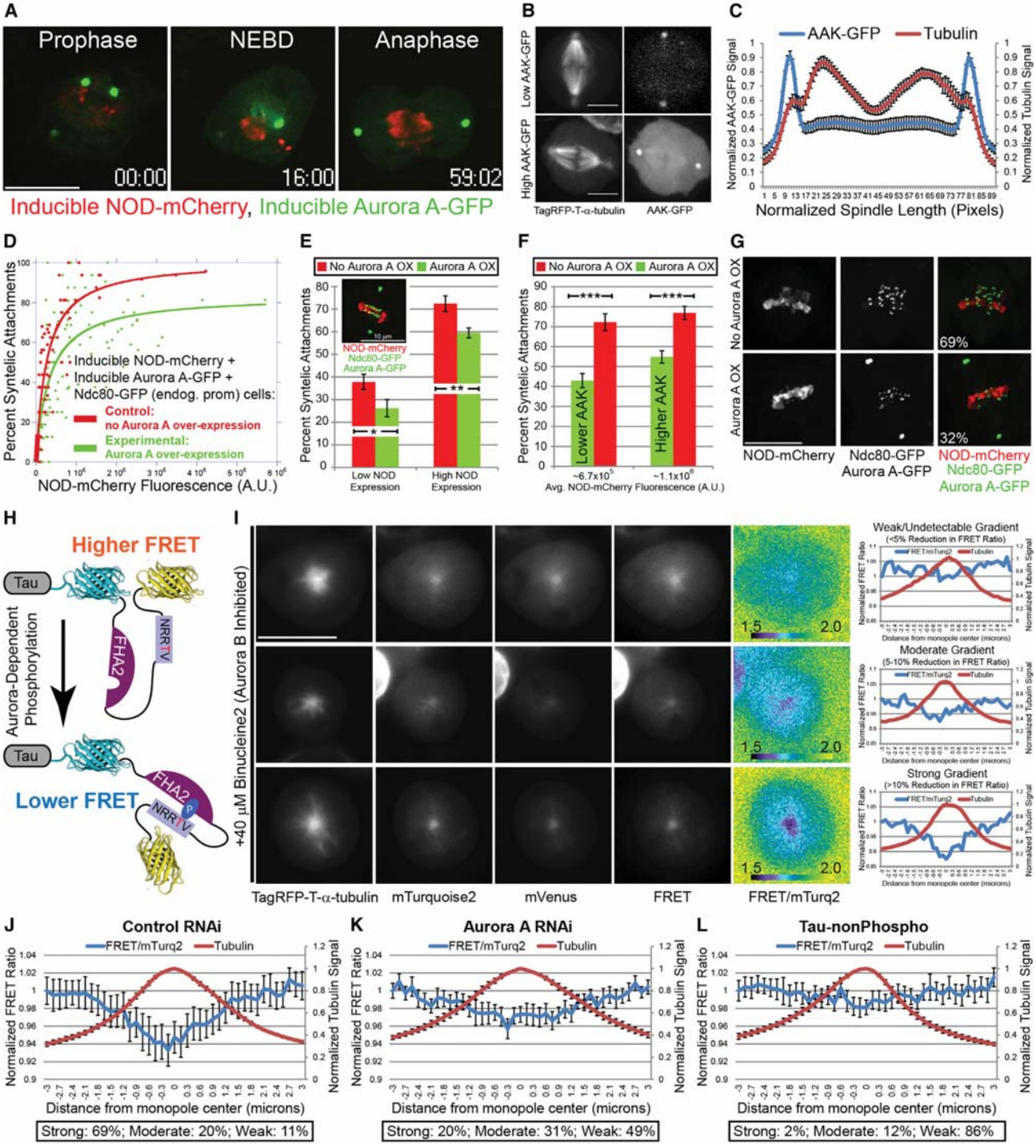

Figure 1. AAK Activity Is Highest near Spindle Poles and Counteracts the Kinetochore-MT Attachment Stabilizing Effect of Elevated PEFs

(A) Still frames from a time-lapse of a dividing S2 cell expressing inducible NOD-mCherry and inducible AAK-GFP.

(B) Spinning-disk confocal images showing examples of low (top) and high (bottom) AAK-overexpressing cells. MT localization is more evident in the higher expressing cell.

(C) Normalized fluorescence intensities of AAK-GFP and TagRFP-T-α-tubulin along the length of 14 mitotic spindles (normalized for variability in spindle length) from cells with a range of AAK-GFP overexpression. AAK-GFP is most abundant at centrosomes and its levels are slightly higher closer to the spindle poles than in the mid-spindle.

(legend continued on next page)

assay. Cells with and without AAK-GFP expression on the same coverslip could be compared due to variability in expression levels. Importantly, AAK overexpression reduced the potency of the PEF effect (Figures 1D–1G). Thus, AAK overexpression attenuates the kinetochore-MT attachment stabilizing effects of elevated PEFs in S2 cells.

The observation that centrosomal/spindle-pole-enriched AAK affected kinetochore-MT attachment stability suggested that the kinase could phosphorylate substrates at a distance through an activity gradient. A fluorescence resonance energy transfer (FRET)-based sensor that exhibits changes in intramolecular FRET upon phosphorylation [26] was used to probe this possibility. In the reporter used here, Aurora kinase phosphorylation causes a structural rearrangement such that phosphorylation leads to reduced FRET efficiency [27], and a prior strategy [28] was adapted to target the reporter to MTs in S2 cells (Figure 1H). To isolate the contribution of AAK to probe phosphorylation, we treated cells co-expressing TagRFP-T-α-tubulin and the Tau-Aurora FRET reporter with a high dose (40 μM) of the *Drosophila* ABK-specific inhibitor binucleine 2 [29, 30]. This treatment, which requires the addition of MG132 to prevent mitotic exit, results in monopolar spindle assembly in a majority of cells. Three categories of FRET emission ratios at the monopole center, as defined by TagRFP-T-α-tubulin signal, relative to ~3 μm away emerged when FRET of the MT-associated reporter was examined across monopoles (Figure 1I): weak/undetectable gradients (<5% reduction in FRET ratio), moderate gradients (5%–10% reduction), and strong gradients (>10% reduction). AAK activity was required for FRET-based visualization of the gradients, as depletion of AAK (Figures S1C–S1E) led to a reduction in the number of cells with strong gradients relative to control RNAi-treated cells (Figures 1J and 1K) and most AAK-depleted cells had weak/undetectable gradients (Figure 1K). A substantial majority of cells (86%) did not have detectable gradients in cells expressing a non-phosphorylatable (negative control) version of the reporter (Figure 1L). Thus, a pole-centered AAK phosphorylation gradient is present in mitotic *Drosophila* S2 cells.

While PEFs act on chromosome arms, it is the transmission of opposing force through the mis-attached kinetochores that leads to their stabilization. Thus, we reasoned that the AAK activity gradient counteracts the PEF effect by targeting kinetochore substrates that approach the spindle poles. To test this hypothesis, we adapted a strategy previously used to target the Aurora kinase FRET sensor to human kinetochores [15] for use in *Drosophila* S2 cells by fusing the FRET reporter to the C terminus of TagRFP-T-tagged *Drosophila* Mis12, a component of the core kinetochore-MT attachment complex [10] (Figure 2A). We confirmed earlier findings from HeLa cells [15] that the sensor is more phosphorylated (lower emission ratio) at unattached kinetochores than at bioriented kinetochores in *Drosophila* S2 cells (Figures 2B and 2C). Cells treated with binucleine 2 (Figure S1F) exhibited reduced sensor phosphorylation at unattached kinetochores (Figures 2B and 2C). The FRET measurements in binucleine 2-treated cells most likely underestimate the reduction in phosphorylation, given that a non-phosphorylatable reporter, which has equally high emission ratios at bioriented and unattached kinetochores, exhibited a 5% reduction in FRET in the presence of 40 μM binucleine 2 (Figures S2A and S2B). Taken together, the data suggest that ABK is the dominant kinase targeting the Mis12-FRET sensor at unattached kinetochores in S2 cells.

Sensor phosphorylation at aligned and polar kinetochores was evaluated next. The *Drosophila* CENP-E homolog (CENP-meta) was depleted from cells expressing the kinetochore-targeted FRET sensor to increase the number of polar chromosomes [31]. The FRET sensor was more phosphorylated at polar kinetochores than at bioriented kinetochores (Figures 2D, 2E, and S2C). Since polar chromosomes in CENP-E-depleted mouse fibroblasts have been shown to lack kinetochore-MT attachments [32], the increased phosphorylation observed at these kinetochores may have solely been a result of ABK-mediated phosphorylation of unattached kinetochores. However, this was not the case, as double depletion of CENP-meta and AAK, which did not reduce ABK activity (Figures S2D and S2E), resulted in a reduction in phosphorylation of the reporter at polar kinetochores relative to those in CENP-meta RNAi cells (Figures 2D, 2E, and Figure S2C). The data do not rule out a role for ABK in phosphorylating polar kinetochores in S2 cells, which may account for the statistically significant increase in phosphorylation of the reporter at polar versus aligned kinetochores that

(D) Plots of percent syntelic attachments versus NOD-mCherry fluorescence for cells with (green) and without (red) AAK-GFP overexpression. PEF-mediated stabilization of syntelic attachments is less potent in AAK-GFP-overexpressing cells. Data from six independent experiments were fit with a hyperbolic function. Control, n = 64 cells; AAK overexpression, n = 117 cells. R values are 0.81 (no AAK overexpression) and 0.72 (AAK overexpression).

(E) Mean percent syntelic attachments for low and high NOD-expressing cells, defined by the halfway point of the expression range in control cells, in control versus AAK-GFP-overexpressing (inset) cells. The percentage of syntelic attachments is significantly lower in AAK-overexpressing cells than in control cells at low and high NOD expression levels.

(F) AAK-GFP levels were quantified and the mean percent of syntelic attachments in cells from both the lower and upper half of the AAK-GFP overexpression range are significantly lower than groupings of control cells with comparable levels of NOD overexpression.

(G) Maximum-intensity projections of Ndc80-GFP (green)- and NOD-mCherry (red)-expressing cells with and without overexpressed AAK-GFP (green) but with comparable levels of NOD-mCherry. The percentage of syntelic attachments, which is lower in the AAK-GFP-overexpressing cell, is shown in the merged images.

(H) Schematic of the MT-targeted Tau-Aurora FRET sensor used in this study.

(I) Representative images of cells co-expressing TagRFP-T-α-tubulin and the Tau-Aurora FRET reporter treated with binucleine 2 and MG132. The FRET emission ratio images "FRET/mTurq2" are pseudo-colored, and the color wedge spans ratio values of 1.5 (black) to 2.0 (yellow). Examples of cells with "weak/undetectable" (<5% reduction), "moderate" (5%–10% reduction), and "strong" (>10% reduction) gradients as defined by the percent reduction in normalized FRET emission ratio in the monopole center relative to 3 μm away are shown.

(J–L) Normalized FRET ratios across monopoles (normalized tubulin intensity) from ten cells per condition. Each plot contains data reflecting the percentage of each type of gradient in that condition (for example, the control RNAi plot is from seven strong, two moderate, and one weak/undetectable). Control RNAi, n = 35 cells; AAK RNAi, n = 45 cells; Tau-nonPhospho, n = 41 cells.

Scale bars, 10 μm (A, E, and I) and 5 μm (B and G). Error bars indicate the SEM. Two-tailed p values of a Student's t test are reported: *p < 0.05, **p < 0.005, ***p < 0.0005. See also Figure S1 and Movie S1.

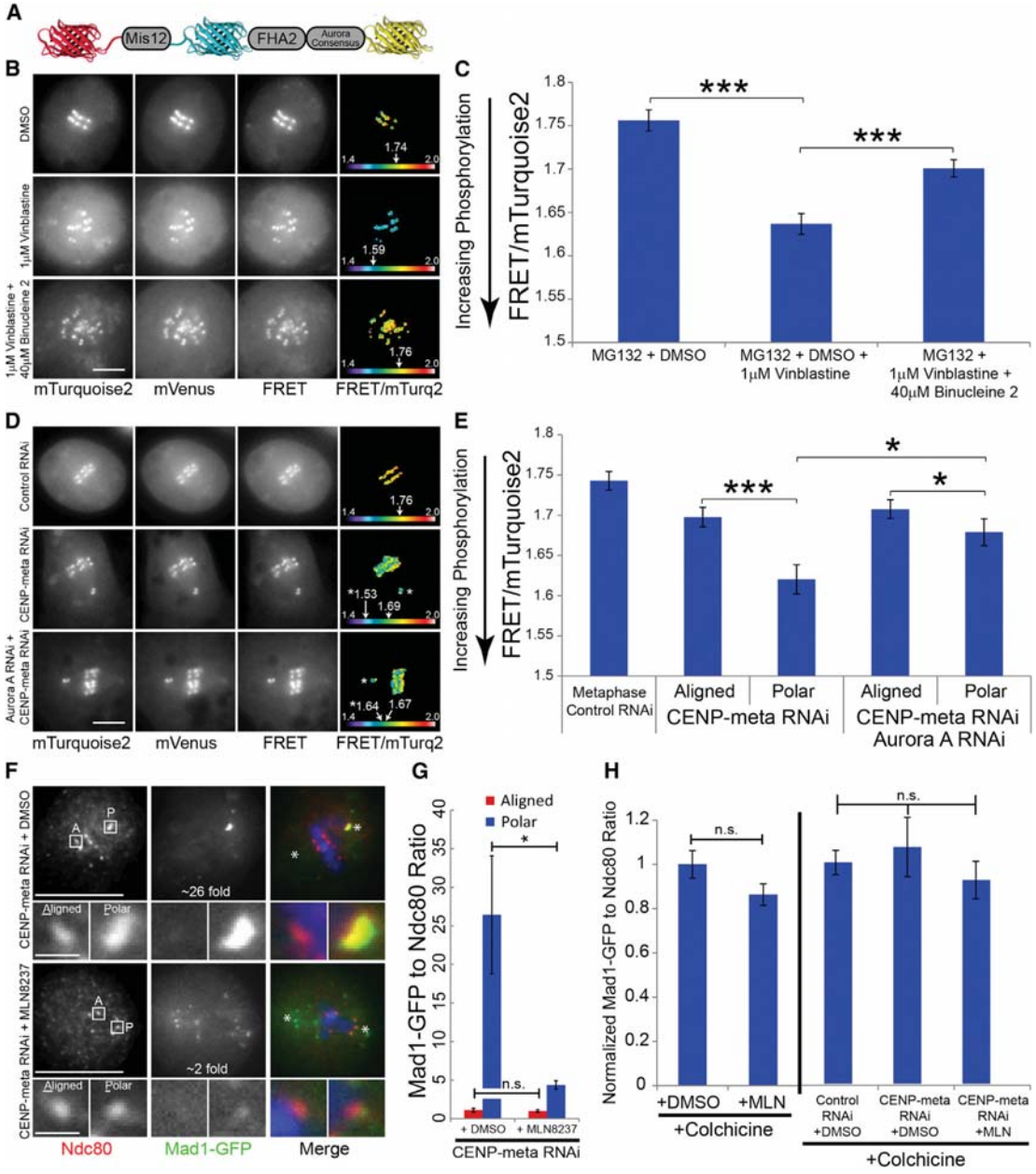

Figure 2. AAK Contributes to Elevated Levels of Kinetochore Phosphorylation and Reduced Kinetochore-MT Attachment Stability near Spindle Poles

(A) Schematic of the kinetochore-targeted Mis12-Aurora FRET sensor used in this study.

(B) Representative images of the FRET reporter in the conditions shown in (C). The FRET emission ratio images "FRET/mTurq2" are pseudo-colored and the arrows point to the position on the color wedge (spanning ratio values of 1.4 to 2.0) corresponding to the average emission ratio measured for the kinetochore-targeted sensor in that cell.

(C) Vinblastine treatment, to generate unattached kinetochores, lowers the emission ratio of the FRET reporter, indicating that it is more phosphorylated. Binucleine 2 treatment leads to an increase in the reporter FRET emission ratio at kinetochores in vinblastine-treated cells, demonstrating that ABK contributes to phosphorylation of the sensor at unattached kinetochores. Mean values from three independent experiments are shown. DMSO, n = 106 cells; vinblastine, n = 104 cells; vinblastine + binucleine 2, n = 108 cells.

(D) Representative images of the FRET reporter in the conditions shown in (E). The FRET emission ratio images "FRET/mTurq2" are pseudo-colored, and the arrows point to the position on the color wedge (spanning ratio values of 1.4 to 2.0) corresponding to the FRET emission ratios measured for the sensor at aligned and, when appropriate, polar kinetochores (asterisk) in that cell.

(E) The mean FRET emission ratio of the sensor is lower at polar kinetochores, generated by depletion of CENP-meta, than at aligned kinetochores. Co-depletion of AAK leads to an increase in the emission ratio at polar kinetochores compared to polar kinetochores in CENP-meta-depleted cells. Thus, the sensor is more phosphorylated at kinetochores near spindle poles than at bioriented kinetochores, and AAK contributes to this difference in the phosphorylation state. Mean

(legend continued on next page)

remained in AAK-depleted cells (Figure 2E). Unfortunately, the effects of binucleine 2 on FRET measurements (Figure S2B) combined with catastrophic failure in bipolar spindle assembly in ABK-inhibited S2 cells made it technically infeasible to measure FRET ratios at polar versus bioriented attachments in ABK-inhibited cells. Nonetheless, the data support the conclusion that an AAK activity gradient contributes to phosphorylation of the Mis12-FRET sensor at polar kinetochores in S2 cells.

The checkpoint protein Mad1, which is depleted from stable kinetochore-MT attachments [33], was next used to probe the attachment states of polar kinetochores in the presence and absence of AAK activity. Mad1 levels at kinetochores were examined in CENP-meta-depleted cells expressing Mad1-GFP under the control of its endogenous promoter (Figures 2F and 2G). To measure Mad1 enrichment at polar kinetochores, we compared the ratio of background corrected fluorescence intensities of Mad1-GFP to Ndc80 signals at misaligned kinetochores to the average Mad1 to Ndc80 ratio intensities of six bioriented kinetochores within the same cell. Indicative of a lack of attachment [32], polar kinetochores, on average, exhibited an ~26-fold increase in Mad1 levels relative to bioriented attachments in CENP-meta-depleted cells treated with DMSO. Treatment with 125 nM MLN8237, an AAK-specific inhibitor [34] that potently and specifically inhibits *Drosophila* AAK (Figures S3A–S3C), caused a significant reduction in Mad1 enrichment (~4-fold) at polar kinetochores. The observed differences in kinetochore-associated Mad1 levels were not due to general effects of the treatments on Mad1 localization as neither MLN-treatment, CENP-meta depletion, or the combination affected Mad1 loading at unattached kinetochores (Figure 2H). These findings along with recent work [35] suggest that polar kinetochores in CENP-meta-depleted cells establish more stable attachments when AAK is inhibited.

Chromosome alignment and kinetochore-MT attachment states were next examined in cells with compromised AAK activity. Similar to previous observations in S2 cells [36], AAK depletion resulted in ~40% of MG132-treated mitotic cells exhibiting "abnormal metaphases" with at least one misaligned chromosome (Figures 3A and 3B). Treatment with 125 nM MLN8237 mirrored the AAK RNAi depletion phenotype (Figures 3C and 3D). The attachment states of misaligned chromosomes were evaluated by careful examination of serial fluorescent z sections of chromosomes, kinetochores, and MTs in control and AAK-inhibited cells (Figures 3E–3H). The attachment states of the misaligned chromosomes fell into four categories: (1) "mono-oriented (k-fiber)" if one kinetochore was attached to a pole and the other kinetochore was nucleating a second kinetochore fiber (k-fiber) or focused spindle pole extending into the cytoplasm, (2) "mono-oriented/lateral" if one kinetochore was attached to a pole and its sister was either unattached or was laterally interacting with a nearby k-fiber (most likely in the process of CENP-E-mediated congression [37]), (3) "syntelic" if sister kinetochores were attached to the same pole, and (4) "unknown" if the attachment state could not be discerned. Once again, the MLN8237 treatment phenocopied AAK RNAi (Figures 3F and 3H). In both conditions, the majority of misaligned chromosomes (50%–60%) had syntelic attachments and 25%–30% had mono-oriented/lateral interactions, suggesting that CENP-meta is active in AAK-inhibited S2 cells. A role for AAK in error correction was further evidenced by the observation that the PEF effect was more potent in AAK-depleted cells relative to control RNAi cells (Figures S3D–S3F). The fixed cell data were corroborated by live-cell imaging of AAK depleted Ndc80-GFP expressing cells (Figure 3I and Movie S3). In an excellent example that captured the chromosome misalignment types observed in fixed AAK-inhibited cells, a syntelically attached chromosome remained "pinned" at the spindle pole for at least 40 min before congressing, most likely via a mono-oriented/lateral interaction, at a rate consistent with CENP-E-driven congression [37]. One of the sister kinetochores then became merotelically attached to both poles, laterally deformed, and briefly lagged in anaphase before properly segregating.

To investigate whether the contribution of AAK to error correction is conserved beyond *Drosophila*, we used PtK1 cells, which, due to their low chromosome number, have been an excellent model for characterizing error correction mechanisms [3, 6]. First, we identified a concentration (1 μM) of the AAK inhibitor MLN8054 [38] that affected chromosome behavior but did not alter mitotic index, distribution of mitotic stages, or spindle assembly (Figures S4A–S4C). PtK1 cells treated with 1 μM MLN8054 did not exhibit a reduction in centromere-associated phosphorylated-ABK (Figure S4D), indicating that ABK activity was not affected by this drug concentration. However, kinetochores in MLN8054-treated prometaphase cells were, on average, positioned closer to the spindle poles than in untreated cells and a significant number of kinetochores localized very close to the poles, which was never observed in control cells (Figures 4A and 4B). Moreover, MLN8054-treated PtK1 cells displayed higher frequencies of merotelic kinetochores at the metaphase plate than control cells (Figures 4C and 4D), and, as a result, significantly more anaphase

values from three independent experiments are shown. Control RNAi, metaphase n = 119 cells; CENP-meta RNAi, aligned n = 98, polar n = 107; CENP-meta, AAK double RNAi, aligned n = 106, polar n = 120.

(F) Single planes from representative images of CENP-meta-depleted Mad1-GFP (green in merged images) expressing cells treated with DMSO or 125 nM MLN8237 and stained for Ndc80 (red) and DAPI (blue). Examples of aligned (A) and polar (P) kinetochores for each condition are shown in the (5× zoom) insets. The fold enrichments of Mad1 at the polar relative to aligned kinetochores are indicated in the Mad1-GFP images for each cell. Asterisks indicate the position of the spindle poles.

(G) Quantifications of fold Mad1-GFP enrichment at polar kinetochores in CENP-meta-depleted cells treated with DMSO (control) or 125 nM MLN8237. Mean values are shown. CENP-meta RNAi + DMSO, n = 18 polar kinetochores, n = 42 aligned kinetochores; CENP-meta RNAi + MLN, n = 46 polar kinetochores, n = 48 aligned kinetochores.

(H) Levels of Mad1-GFP ratioed to Ndc80 at unattached kinetochores are unaffected by MLN treatment and CENP-meta depletion. Mean values from two independent experiments are shown. Colchicine +: DMSO, n = 255 kinetochores; MLN8237, n = 255 kinetochores; control RNAi + DMSO, n = 200 kinetochores; CENP-meta RNAi + DMSO, n = 198 kinetochores; CENP-meta RNAi + MLN8237, n = 200 kinetochores.

All error bars indicate the SEM. Scale bars, 5 μm (B and D), 10 μm (F), and 1 μm (F, insets). Two-tailed p values of a Student's t test are reported in (C), (G), and (H), and p values from a Mann-Whitney Wilcoxon t test are reported in (E): not significant (n.s.) $p > 0.05$, *$p < 0.05$, ***$p < 0.0005$. See also Figure S2.

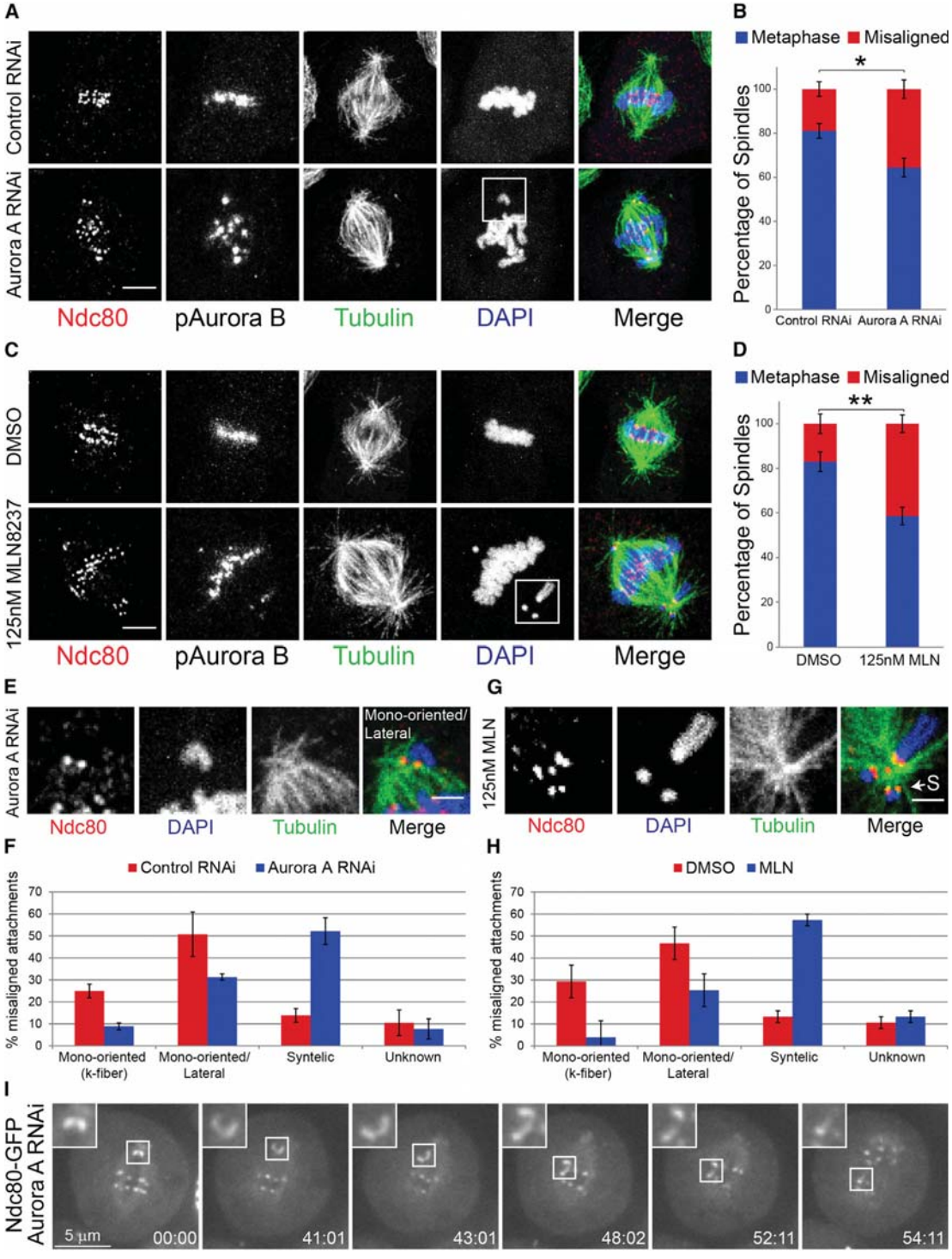

Figure 3. AAK Is Required for Efficient Error Correction in *Drosophila* S2 Cells

(A) Representative maximum-intensity projections from confocal z sections of control and AAK-depleted cells stained for Ndc80 (red in the merged image), phospho-ABK, tubulin (green), and DAPI (blue). Misaligned chromosomes with normal levels of centromere-enriched phospho-ABK are more prevalent in AAK-depleted cells than in control cells.

(B) Quantification of the percentage of MG132-treated cells with normal metaphase plates and misaligned chromosomes in control and AAK-depleted cells. Mean values from three independent experiments are shown. Control RNAi, n = 317 cells; AAK RNAi, n = 326 cells.

(C) Representative maximum-intensity projections from confocal z sections of DMSO- and MLN8237-treated cells stained for Ndc80 (red in the merged image), phospho-ABK, tubulin (green), and DAPI (blue). Treatment with 125 nM MLN8237 phenocopies AAK depletion.

(legend continued on next page)

lagging chromosomes were observed in MLN8054-treated cells (Figure 4E). These data demonstrate that inhibition of AAK compromises error correction and results in chromosome mis-segregation in mammalian PtK1 cells.

We reasoned that AAK regulates error correction by targeting many of the same substrates as ABK. A crucial target of ABK is the Ndc80 complex, which directly binds MTs [10, 11, 39, 40]. High-affinity interactions between the Ndc80 complex and MTs requires the unstructured and highly basic N-terminal tail of Ndc80/Hec1 [11, 40–42], which contains numerous ABK sites [10–12, 22] that, when phosphorylated, lower the complex's affinity for MTs [10, 11, 17]. Thus, we examined the contribution of AAK to the phosphorylation of a previously defined ABK site in Ndc80/Hec1 (Ser55) [10–12] by using a phospho-specific antibody against pSer55 in HeLa cells. Compared to control cells, treatment with 300 nM MLN8237 significantly reduced kinetochore pSer55 staining at attached (Figures 4F and 4G) and unattached kinetochores (Figures S4E and S4F). The 300 nM MLN8237 treatment caused a minor but significant reduction in Ndc80 levels relative to CENP-A (Figures S4G and S4H), which may be due to partial inhibition of ABK at this inhibitor concentration, although phospho-H3-Ser10 levels were not significantly reduced relative to control metaphase cells (Figure S4I). These data are consistent with a phospho-proteomic study that implicated AAK as the primary kinase targeting Ndc80-Ser55 [43]. Although cell-based inhibitor studies suggest that AAK contributes to phosphorylation of Ser55, they are not a direct demonstration of AAK-mediated phosphorylation. To test whether AAK directly phosphorylates Ser55, we performed an in vitro phosphorylation assay with recombinant bonsai Ndc80 complex [11] and purified AAK. When incubated with the bonsai Ndc80 complex in phosphorylation buffer, AAK efficiently phosphorylated Ser55 (Figure 4H). Finally, to examine the spatial contribution of AAK activity to phosphorylation of Ndc80-Ser55, we used the CENP-E inhibitor [44] GSK923295 to generate polar and aligned kinetochores in HeLa cells in the presence and absence of MLN8237 (Figure 4I). In agreement with the S2 cell findings, polar kinetochores were more phosphorylated than aligned/away from the pole kinetochores, and the polar bias in phosphorylation was lost when cells were treated with 300 nM MLN8237 (Figure 4J). Although these findings do not exclude a role for ABK in phosphorylating Ndc80-Ser55 or other kinetochore substrates in the vicinity of spindle poles, taken together, the data demonstrate that AAK can directly phosphorylate Ndc80-Ser55 and that AAK activity contributes to phosphorylation of this residue in HeLa cells.

DISCUSSION

While it has been postulated that AAK could create a kinetochore-MT attachment destabilizing environment near spindle poles [45], it has not been demonstrated experimentally. Here we directly test this hypothesis, and our findings support the existence of a pole-centered AAK phosphorylation gradient that contributes to error correction and counters the potential side effects of elevated PEFs. We envision that superimposed PEF and AAK gradients create a balance of activities near spindle poles that promotes error correction, congression, and biorientation resulting in a spatiotemporal path from mal- to bioriented chromosomes (Figure 4K). First, as an erroneous attachment moves poleward, it may become stabilized by progressively higher levels of opposing PEFs. Second, at some distance from the pole, the PEF effect is countered by an AAK gradient that phosphorylates attachment factors such as the Ndc80 complex. Third, AAK facilitates congression by biasing CENP-E activity, which has been shown to be phospho-regulated near spindle poles by Aurora kinases [46], toward the mid-spindle and by allowing PEFs to push chromosomes away from poles. Note that in this model, production of an unattached kinetochore(s) by AAK is not only a prerequisite for biorientation, but also permits PEFs to congress chromosomes without generating unwanted tension at incorrect attachments.

Both the CEN- and pole-based pathways are spatial positioning phenomena, with the CEN-based system depending on positioning of kinetochore targets relative to ABK and the pole-based pathway relying on spatial positioning of kinetochores relative to spindle poles and AAK. Although both error correction pathways are likely to share common targets (e.g., Ndc80/Hec1), we view the CEN-based pathway as kinetochore intrinsic because the correction machinery (ABK) localizes to the kinetochore region, whereas the pole-based pathway is kinetochore extrinsic since the correction machinery is primarily enriched outside the kinetochore region at the spindle poles/centrosomes. There may be orders of magnitude difference in the working distances of the CEN- and pole-based systems, as changes in spatial separation occur on the nanometer [13–17, 47] and micrometer scale [6], respectively. It will be worthwhile to characterize how the working distance of the pole-based AAK gradient is defined. Although *Drosophila* TPX2 does not regulate AAK [48], in other organisms, TPX2, which localizes AAK to spindle microtubules [49] and activates its kinase activity [50, 51], may help delineate and amplify an AAK gradient [52].

(D) Quantification of the percentage of MG132-treated cells with normal metaphase plates and misaligned chromosomes in DMSO- and MLN8237-treated cells. Mean values from three independent experiments are shown. DMSO, n = 318 cells; 125 nM MLN8237, n = 322 cells.
(E) Zoomed views of the insets highlighted in the DAPI channel in (A). In the merged image, Ndc80 is red, tubulin is green, and DAPI is blue.
(F) Mean values of each type of attachment at misaligned chromosomes in control and AAK-depleted cells from three independent experiments. Control RNAi, n = 71 kinetochore pairs; AAK RNAi, n = 80 kinetochore pairs.
(G) Zoomed views of the insets highlighted in the DAPI channel in (C). In the merged image, Ndc80 is red, tubulin is green, and DAPI is blue. The arrow points to a syntelic (S) attachment.
(H) Mean values of each type of attachment at misaligned chromosomes in DMSO- and MLN8237-treated cells from three independent experiments. n = 75 kinetochore pairs each for the DMSO and MLN conditions.
(I) Still frames from a spinning disk confocal time-lapse of an Ndc80-GFP-expressing S2 cell depleted of AAK. Insets show an 8× zoom of the highlighted regions.
Error bars indicate the SEM. Scale bars, 5 μm (A and C) and 2 μm (E and G). Two-tailed p values of a Student's t test are reported: *$p < 0.05$, **$p < 0.005$. See also Figure S3 and Movie S3.

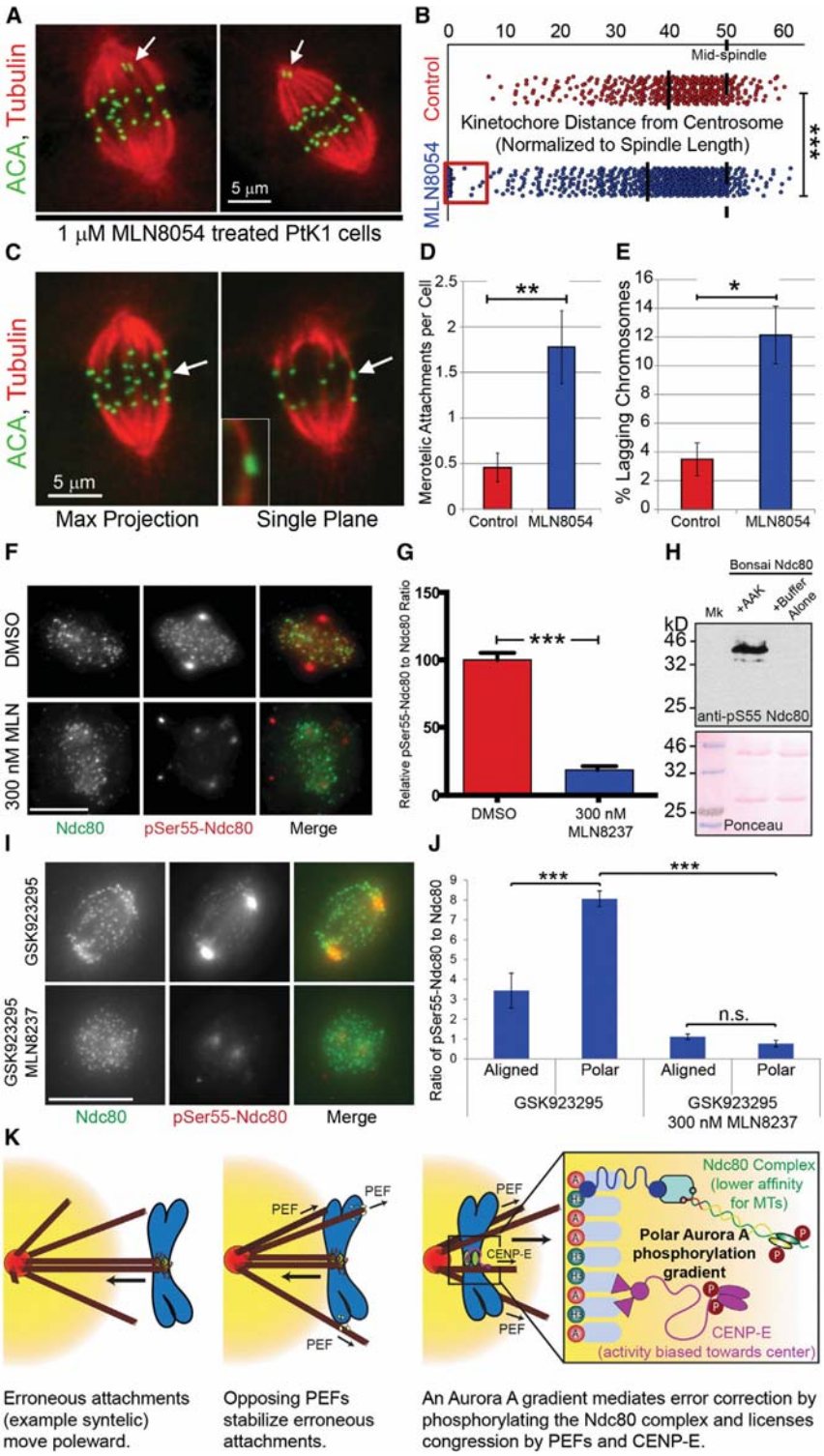

Figure 4. AAK Contributes to Error Correction in Mammalian Cells and Phosphorylates the N-Terminal Tail of Ndc80/Hec1 in Human Cells

(A) Representative maximum-intensity projections of confocal z sections of PtK1 cells treated with 1 μM MLN8054 and stained for tubulin (red) and centromeres (green). Arrows point to polar, misaligned chromosomes.

(B) Scatter plots of relative kinetochore positions normalized to the spindle length in control and MLN8054-treated PtK1 cells. The "0" position represents the spindle pole, and the "50" position marks the mid-spindle (dashed black line). The average centromere position (black bar) is closer to the spindle poles in MLN8054-treated cells than in control cells, and a significant population of kinetochores are "pinned" to the poles (near 0) in MLN8054-treated cells (red box). Control, n = 406 kinetochores; 1 μM MLN8054, n = 642 kinetochores.

(C) Representative images (left, maximum-intensity projection; right, single focal plane) of a PtK1 cell treated with 1 μM MLN8054 and stained for tubulin (red) and centromeres (green). Arrows point to a merotelic kinetochore at the metaphase plate that is attached to both spindle poles.

(D) MLN8054 treatment leads to a significant increase in the average number of merotelic attachments per cell relative to control cells. Control, n = 191 kinetochores from 11 cells; 1 μM MLN8054, n = 144 kinetochores from nine cells.

(E) MLN8054 treatment leads to a significant increase in the percentage of lagging chromosomes in anaphase cells relative to control cells. Mean values of lagging chromosomes from three independent experiments are shown. Control, n = 270 anaphase chromosomes; 1 μM MLN8054, n = 268 anaphase chromosomes.

(F) Representative images of control (DMSO) and AAK-inhibited (300 nM MLN8237) HeLa cells stained for pSer55-Ndc80 (red) and Ndc80 (green).

(G) Mean values of pSer55-Ndc80 to Ndc80 ratios. DMSO, n = 280 kinetochores from 14 cells; 300 nM MLN, n = 275 kinetochores from 12 cells.

(H) An in vitro phosphorylation assay with purified Ndc80 bonsai complex plus and minus purified AAK blotted for anti-pSer55. AAK directly phosphorylates Ndc80 in vitro.

(I) Representative images of GSK923295-treated HeLa cells with and without MLN8237 stained for pSer55-Ndc80 (red) and Ndc80 (green).

(J) Polar kinetochores are more phosphorylated than aligned kinetochores in GSK923295-treated cells, and the polar bias in Ser55 phosphorylation is lost in the presence of MLN8237. Mean values are shown. pSer55-Ndc80 to Ndc80 ratios from four independent experiments for GSK923295, aligned n = 408 kinetochores from 68 cells, polar n = 239 kinetochores from 68 cells; three independent experiments for GSK923295 + MLN 8237, aligned n = 465 kinetochores from 55 cells, polar n = 207 kinetochores from 55 cells.

(K) A spatiotemporal model for the path from mal- to bioriented chromosomes. As a syntelic attachment moves poleward, it becomes stabilized as it encounters increasing PEFs, until encountering the AAK phosphorylation gradient. AAK mediates error correction by phosphorylating kinetochore-MT attachment factors such as Ndc80/Hec1 at Ser55. The AAK gradient also facilitates congression by biasing CENP-E activity toward the mid-spindle and by allowing PEFs to push chromosome arms away from the poles without stabilizing syntelic attachments.

Error bars indicate the SEM. Scale bars, 5 μm (A and C) and 10 μm (F and I). Two-tailed p values of a Student's t test are reported: not significant (n.s.) $p > 0.05$, *$p < 0.05$, **$p < 0.005$, ***$p < 0.0005$. See also Figure S4.

Regardless of the effective range of AAK activity, we propose that a key difference between the two pathways is that tension opposes CEN-based error correction, whereas the pole-based pathway is regulated not by tension, but by positioning kinetochores within the spindle relative to the poles. The pole-based error correction pathway appears to be conserved in meiotic cells as a concurrent study using mouse oocytes found that AAK activity contributes to destabilizing kinetochore-MT attachments near spindle poles [53].

It is imperative that mal-oriented chromosomes near spindle poles are corrected, because whereas only a fraction of merotelic kinetochores at the metaphase plate result in chromosome mis-segregation [54], mitotic progression in the presence of polar chromosomes would inevitably lead to aneuploidy. Furthermore, we view the consequences of inhibiting AAK-mediated error correction not merely as more subtle than the effects of ABK inhibition, but as more insidious. Although catastrophic failure in error correction, like that seen after potent ABK inhibition, would lead to massive and most likely lethal aneuploidy, the presence of comparatively low numbers of "pinned" polar chromosomes when the AAK pathway is compromised would increase the frequency of single chromosome mis-segregation events and be more likely to yield viable aneuploid cells. Our findings support the conclusion that an AAK phosphorylation gradient contributes to correcting such hazardous polar attachments before cells divide.

EXPERIMENTAL PROCEDURES

Experimental procedures are described in the Supplemental Information.

SUPPLEMENTAL INFORMATION

Supplemental Information includes Supplemental Experimental Procedures, four figures, one table, and three movies and can be found with this article online at http://dx.doi.org/10.1016/j.cub.2015.06.021.

AUTHOR CONTRIBUTIONS

T.J.M. conceived of the project, carried out experiments and analyses, and wrote the paper. A.A.Y. conducted and analyzed most of the *Drosophila* cell experiments. C.M.H. performed experiments examining Mad1 localization and characterizing the specificity of MLN8237 in *Drosophila* cells. D.C. and A.W.H. designed and performed experiments and analyses with PtK1 cells. J.P.W. and J.D. performed all HeLa cell experiments and analyses. Text was contributed by D.C., J.P.W., C.M.H., and A.A.Y. The manuscript was edited by T.J.M., D.C., J.P.W., A.A.Y., and C.M.H.

ACKNOWLEDGMENTS

We thank Marcin Przewloka and David Glover for the generous gift of the *Drosophila* anti-Aurora A, Iain Cheeseman for anti-bonsai-Ndc80, and Jennifer DeLuca for the phospho-ABK antibody. We are grateful to Michael Lampson, Jennifer DeLuca, and Iain Cheeseman for communicating unpublished findings. We also acknowledge Ted Salmon and members of the J.P.W., D.C., Lee, Wadsworth, and T.J.M. labs for thoughtful scientific discussions. We thank Julia Torabi for generating the Tau-FRET sensors. This work was supported by an NIH grant (5 R01 GM107026) to T.J.M and by Research Grant No. 5-FY13-205 from the March of Dimes Foundation to T.J.M, as well as by the Charles H. Hood Foundation (T.J.M.). The work was also partly funded by NSF grant MCB-0842551 to D.C. A.W.H was the recipient of a VT-IMSD Undergraduate Research Apprenticeship. J.P.W. is supported by a CRUK Career Development Fellowship (C40377/A12840). J.D. is supported by a Darwin Trust Studentship.

Received: April 1, 2015
Revised: June 8, 2015
Accepted: June 9, 2015
Published: July 9, 2015

REFERENCES

1. Cimini, D., Moree, B., Canman, J.C., and Salmon, E.D. (2003). Merotelic kinetochore orientation occurs frequently during early mitosis in mammalian tissue cells and error correction is achieved by two different mechanisms. J. Cell Sci. *116*, 4213–4225.
2. Kitajima, T.S., Ohsugi, M., and Ellenberg, J. (2011). Complete kinetochore tracking reveals error-prone homologous chromosome biorientation in mammalian oocytes. Cell *146*, 568–581.
3. Cimini, D., Wan, X., Hirel, C.B., and Salmon, E.D. (2006). Aurora kinase promotes turnover of kinetochore microtubules to reduce chromosome segregation errors. Curr. Biol. *16*, 1711–1718.
4. Kelly, A.E., and Funabiki, H. (2009). Correcting aberrant kinetochore microtubule attachments: an Aurora B-centric view. Curr. Opin. Cell Biol. *21*, 51–58.
5. Tanaka, T.U., Rachidi, N., Janke, C., Pereira, G., Galova, M., Schiebel, E., Stark, M.J., and Nasmyth, K. (2002). Evidence that the Ipl1-Sli15 (Aurora kinase-INCENP) complex promotes chromosome bi-orientation by altering kinetochore-spindle pole connections. Cell *108*, 317–329.
6. Lampson, M.A., Renduchitala, K., Khodjakov, A., and Kapoor, T.M. (2004). Correcting improper chromosome-spindle attachments during cell division. Nat. Cell Biol. *6*, 232–237.
7. Ke, K., Cheng, J., and Hunt, A.J. (2009). The distribution of polar ejection forces determines the amplitude of chromosome directional instability. Curr. Biol. *19*, 807–815.
8. Cane, S., Ye, A.A., Luks-Morgan, S.J., and Maresca, T.J. (2013). Elevated polar ejection forces stabilize kinetochore-microtubule attachments. J. Cell Biol. *200*, 203–218.
9. Nicklas, R.B., and Koch, C.A. (1969). Chromosome micromanipulation. 3. Spindle fiber tension and the reorientation of mal-oriented chromosomes. J. Cell Biol. *43*, 40–50.
10. Cheeseman, I.M., Chappie, J.S., Wilson-Kubalek, E.M., and Desai, A. (2006). The conserved KMN network constitutes the core microtubule-binding site of the kinetochore. Cell *127*, 983–997.
11. Ciferri, C., Pasqualato, S., Screpanti, E., Varetti, G., Santaguida, S., Dos Reis, G., Maiolica, A., Polka, J., De Luca, J.G., De Wulf, P., et al. (2008). Implications for kinetochore-microtubule attachment from the structure of an engineered Ndc80 complex. Cell *133*, 427–439.
12. DeLuca, J.G., Gall, W.E., Ciferri, C., Cimini, D., Musacchio, A., and Salmon, E.D. (2006). Kinetochore microtubule dynamics and attachment stability are regulated by Hec1. Cell *127*, 969–982.
13. Maresca, T.J., and Salmon, E.D. (2009). Intrakinetochore stretch is associated with changes in kinetochore phosphorylation and spindle assembly checkpoint activity. J. Cell Biol. *184*, 373–381.
14. Uchida, K.S., Takagaki, K., Kumada, K., Hirayama, Y., Noda, T., and Hirota, T. (2009). Kinetochore stretching inactivates the spindle assembly checkpoint. J. Cell Biol. *184*, 383–390.
15. Liu, D., Vader, G., Vromans, M.J., Lampson, M.A., and Lens, S.M. (2009). Sensing chromosome bi-orientation by spatial separation of aurora B kinase from kinetochore substrates. Science *323*, 1350–1353.
16. Suzuki, A., Badger, B.L., Wan, X., DeLuca, J.G., and Salmon, E.D. (2014). The architecture of CCAN proteins creates a structural integrity to resist spindle forces and achieve proper Intrakinetochore stretch. Dev. Cell *30*, 717–730.
17. Welburn, J.P., Vleugel, M., Liu, D., Yates, J.R., 3rd, Lampson, M.A., Fukagawa, T., and Cheeseman, I.M. (2010). Aurora B phosphorylates spatially distinct targets to differentially regulate the kinetochore-microtubule interface. Mol. Cell *38*, 383–392.

18. Maresca, T.J., and Salmon, E.D. (2010). Welcome to a new kind of tension: translating kinetochore mechanics into a wait-anaphase signal. J. Cell Sci. *123*, 825–835.
19. Cassimeris, L., Rieder, C.L., and Salmon, E.D. (1994). Microtubule assembly and kinetochore directional instability in vertebrate monopolar spindles: implications for the mechanism of chromosome congression. J. Cell Sci. *107*, 285–297.
20. Campbell, C.S., and Desai, A. (2013). Tension sensing by Aurora B kinase is independent of survivin-based centromere localization. Nature *497*, 118–121.
21. Carmena, M., and Earnshaw, W.C. (2003). The cellular geography of aurora kinases. Nat. Rev. Mol. Cell Biol. *4*, 842–854.
22. Cheeseman, I.M., Anderson, S., Jwa, M., Green, E.M., Kang, Js., Yates, J.R., 3rd, Chan, C.S., Drubin, D.G., and Barnes, G. (2002). Phospho-regulation of kinetochore-microtubule attachments by the Aurora kinase Ipl1p. Cell *111*, 163–172.
23. Li, S., Deng, Z., Fu, J., Xu, C., Xin, G., Wu, Z., Luo, J., Wang, G., Zhang, S., Zhang, B., et al. (2015). Spatial compartmentalization specializes function of Aurora-A and Aurora-B. J. Biol. Chem. Published online May 18, 2015. http://dx.doi.org/10.1074/jbc.M115.652453.
24. Theurkauf, W.E., and Hawley, R.S. (1992). Meiotic spindle assembly in Drosophila females: behavior of nonexchange chromosomes and the effects of mutations in the nod kinesin-like protein. J. Cell Biol. *116*, 1167–1180.
25. Stenoien, D.L., Sen, S., Mancini, M.A., and Brinkley, B.R. (2003). Dynamic association of a tumor amplified kinase, Aurora-A, with the centrosome and mitotic spindle. Cell Motil. Cytoskeleton *55*, 134–146.
26. Violin, J.D., Zhang, J., Tsien, R.Y., and Newton, A.C. (2003). A genetically encoded fluorescent reporter reveals oscillatory phosphorylation by protein kinase C. J. Cell Biol. *161*, 899–909.
27. Fuller, B.G., Lampson, M.A., Foley, E.A., Rosasco-Nitcher, S., Le, K.V., Tobelmann, P., Brautigan, D.L., Stukenberg, P.T., and Kapoor, T.M. (2008). Midzone activation of aurora B in anaphase produces an intracellular phosphorylation gradient. Nature *453*, 1132–1136.
28. Tseng, B.S., Tan, L., Kapoor, T.M., and Funabiki, H. (2010). Dual detection of chromosomes and microtubules by the chromosomal passenger complex drives spindle assembly. Dev. Cell *18*, 903–912.
29. Eggert, U.S., Kiger, A.A., Richter, C., Perlman, Z.E., Perrimon, N., Mitchison, T.J., and Field, C.M. (2004). Parallel chemical genetic and genome-wide RNAi screens identify cytokinesis inhibitors and targets. PLoS Biol. *2*, e379.
30. Smurnyy, Y., Toms, A.V., Hickson, G.R., Eck, M.J., and Eggert, U.S. (2010). Binucleine 2, an isoform-specific inhibitor of Drosophila Aurora B kinase, provides insights into the mechanism of cytokinesis. ACS Chem. Biol. *5*, 1015–1020.
31. Yucel, J.K., Marszalek, J.D., McIntosh, J.R., Goldstein, L.S., Cleveland, D.W., and Philp, A.V. (2000). CENP-meta, an essential kinetochore kinesin required for the maintenance of metaphase chromosome alignment in Drosophila. J. Cell Biol. *150*, 1–11.
32. Putkey, F.R., Cramer, T., Morphew, M.K., Silk, A.D., Johnson, R.S., McIntosh, J.R., and Cleveland, D.W. (2002). Unstable kinetochore-microtubule capture and chromosomal instability following deletion of CENP-E. Dev. Cell *3*, 351–365.
33. Shah, J.V., Botvinick, E., Bonday, Z., Furnari, F., Berns, M., and Cleveland, D.W. (2004). Dynamics of centromere and kinetochore proteins; implications for checkpoint signaling and silencing. Curr. Biol. *14*, 942–952.
34. Pollard, J.R., and Mortimore, M. (2009). Discovery and development of aurora kinase inhibitors as anticancer agents. J. Med. Chem. *52*, 2629–2651.
35. Barisic, M., Aguiar, P., Geley, S., and Maiato, H. (2014). Kinetochore motors drive congression of peripheral polar chromosomes by overcoming random arm-ejection forces. Nat. Cell Biol. *16*, 1249–1256.
36. Giet, R., McLean, D., Descamps, S., Lee, M.J., Raff, J.W., Prigent, C., and Glover, D.M. (2002). Drosophila Aurora A kinase is required to localize D-TACC to centrosomes and to regulate astral microtubules. J. Cell Biol. *156*, 437–451.
37. Kapoor, T.M., Lampson, M.A., Hergert, P., Cameron, L., Cimini, D., Salmon, E.D., McEwen, B.F., and Khodjakov, A. (2006). Chromosomes can congress to the metaphase plate before biorientation. Science *311*, 388–391.
38. Manfredi, M.G., Ecsedy, J.A., Meetze, K.A., Balani, S.K., Burenkova, O., Chen, W., Galvin, K.M., Hoar, K.M., Huck, J.J., LeRoy, P.J., et al. (2007). Antitumor activity of MLN8054, an orally active small-molecule inhibitor of Aurora A kinase. Proc. Natl. Acad. Sci. USA *104*, 4106–4111.
39. Alushin, G.M., Ramey, V.H., Pasqualato, S., Ball, D.A., Grigorieff, N., Musacchio, A., and Nogales, E. (2010). The Ndc80 kinetochore complex forms oligomeric arrays along microtubules. Nature *467*, 805–810.
40. Wei, R.R., Al-Bassam, J., and Harrison, S.C. (2007). The Ndc80/HEC1 complex is a contact point for kinetochore-microtubule attachment. Nat. Struct. Mol. Biol. *14*, 54–59.
41. Guimaraes, G.J., Dong, Y., McEwen, B.F., and Deluca, J.G. (2008). Kinetochore-microtubule attachment relies on the disordered N-terminal tail domain of Hec1. Curr. Biol. *18*, 1778–1784.
42. Miller, S.A., Johnson, M.L., and Stukenberg, P.T. (2008). Kinetochore attachments require an interaction between unstructured tails on microtubules and Ndc80(Hec1). Curr. Biol. *18*, 1785–1791.
43. Kettenbach, A.N., Schweppe, D.K., Faherty, B.K., Pechenick, D., Pletnev, A.A., and Gerber, S.A. (2011). Quantitative phosphoproteomics identifies substrates and functional modules of Aurora and Polo-like kinase activities in mitotic cells. Sci. Signal. *4*, rs5.
44. Wood, K.W., Lad, L., Luo, L., Qian, X., Knight, S.D., Nevins, N., Brejc, K., Sutton, D., Gilmartin, A.G., Chua, P.R., et al. (2010). Antitumor activity of an allosteric inhibitor of centromere-associated protein-E. Proc. Natl. Acad. Sci. USA *107*, 5839–5844.
45. Godek, K.M., Kabeche, L., and Compton, D.A. (2015). Regulation of kinetochore-microtubule attachments through homeostatic control during mitosis. Nat. Rev. Mol. Cell Biol. *16*, 57–64.
46. Kim, Y., Holland, A.J., Lan, W., and Cleveland, D.W. (2010). Aurora kinases and protein phosphatase 1 mediate chromosome congression through regulation of CENP-E. Cell *142*, 444–455.
47. Wan, X., O'Quinn, R.P., Pierce, H.L., Joglekar, A.P., Gall, W.E., DeLuca, J.G., Carroll, C.W., Liu, S.T., Yen, T.J., McEwen, B.F., et al. (2009). Protein architecture of the human kinetochore microtubule attachment site. Cell *137*, 672–684.
48. Goshima, G. (2011). Identification of a TPX2-like microtubule-associated protein in Drosophila. PLoS ONE *6*, e28120.
49. Kufer, T.A., Silljé, H.H., Körner, R., Gruss, O.J., Meraldi, P., and Nigg, E.A. (2002). Human TPX2 is required for targeting Aurora-A kinase to the spindle. J. Cell Biol. *158*, 617–623.
50. Eyers, P.A., Erikson, E., Chen, L.G., and Maller, J.L. (2003). A novel mechanism for activation of the protein kinase Aurora A. Curr. Biol. *13*, 691–697.
51. Tsai, M.Y., Wiese, C., Cao, K., Martin, O., Donovan, P., Ruderman, J., Prigent, C., and Zheng, Y. (2003). A Ran signalling pathway mediated by the mitotic kinase Aurora A in spindle assembly. Nat. Cell Biol. *5*, 242–248.
52. Greenan, G., Brangwynne, C.P., Jaensch, S., Gharakhani, J., Jülicher, F., and Hyman, A.A. (2010). Centrosome size sets mitotic spindle length in Caenorhabditis elegans embryos. Curr. Biol. *20*, 353–358.
53. Chmátal, L., Yang, K., Schultz, R.M., and Lampson, M.A. (2015). Spatial regulation of kinetochore microtubule attachments by destabilization at spindle poles in meiosis I. Curr. Biol. *25*, this issue, 1835–1841.
54. Thompson, S.L., and Compton, D.A. (2011). Chromosome missegregation in human cells arises through specific types of kinetochore-microtubule attachment errors. Proc. Natl. Acad. Sci. USA *108*, 17974–17978.